Organisation for Economic Co-operation and Development

ENV/CBC/MONO(2022)7

Unclassified

English - Or. English

17 October 2022

ENVIRONMENT DIRECTORATE
CHEMICALS AND BIOTECHNOLOGY COMMITTEE

Validation Report on Particle and Fibre Size Distribution Measurements of Nanomaterials. Supporting TG 125 on Particle Size and Particle Size Distribution of Nanomaterials

Series on Testing and Assessment
No. 352

JT03505121

OECD Environment, Health and Safety Publications
Series on Testing & Assessment
No. 352

Validation Report on Particle and Fibre Size Distribution Measurements of Nanomaterials. Supporting TG 125 on Particle Size and Particle Size Distribution of Nanomaterials

IOMC
INTER-ORGANIZATION PROGRAMME FOR THE SOUND MANAGEMENT OF CHEMICALS
A cooperative agreement among FAO, ILO, UNDP, UNEP, UNIDO, UNITAR, WHO, World Bank and OECD

Environment Directorate
ORGANISATION FOR ECONOMIC COOPERATION AND DEVELOPMENT
Paris 2022

About the OECD

The Organisation for Economic Co-operation and Development (OECD) is an intergovernmental organisation in which representatives of 38 industrialised countries in North and South America, Europe and the Asia and Pacific region, as well as the European Commission, meet to co-ordinate and harmonise policies, discuss issues of mutual concern, and work together to respond to international problems. Most of the OECD's work is carried out by more than 200 specialised committees and working groups composed of member country delegates. Observers from several countries with special status at the OECD, and from interested international organisations, attend many of the OECD's workshops and other meetings. Committees and working groups are served by the OECD Secretariat, located in Paris, France, which is organised into directorates and divisions.

The Environment, Health and Safety Division publishes free-of-charge documents in eleven different series: **Testing and Assessment; Good Laboratory Practice and Compliance Monitoring; Pesticides; Biocides; Risk Management; Harmonisation of Regulatory Oversight in Biotechnology; Safety of Novel Foods and Feeds; Chemical Accidents; Pollutant Release and Transfer Registers; Emission Scenario Documents;** and **Safety of Manufactured Nanomaterials.** More information about the Environment, Health and Safety Programme and EHS publications is available on the OECD's World Wide Web site (www.oecd.org/chemicalsafety/).

This publication was developed in the IOMC context. The contents do not necessarily reflect the views or stated policies of individual IOMC Participating Organizations.

The Inter-Organisation Programme for the Sound Management of Chemicals (IOMC) was established in 1995 following recommendations made by the 1992 UN Conference on Environment and Development to strengthen co-operation and increase international co-ordination in the field of chemical safety. The Participating Organisations are FAO, ILO, UNDP, UNEP, UNIDO, UNITAR, WHO, World Bank and OECD. The purpose of the IOMC is to promote co-ordination of the policies and activities pursued by the Participating Organisations, jointly or separately, to achieve the sound management of chemicals in relation to human health and the environment.

This publication is available electronically, at no charge.

Also published in the Series on Testing and Assessment: link

For this and many other Environment,

Health and Safety publications, consult the OECD's

World Wide Web site (www.oecd.org/chemicalsafety/)

or contact:

OECD Environment Directorate,

Environment, Health and Safety Division

2 rue André-Pascal

75775 Paris Cedex 16

France

Fax: (33-1) 44 30 61 80

E-mail: ehscont@oecd.org

Validation Report on Particle and Fibre Size Distribution Measurements of Nanomaterials

Report prepared by Volker Bachmann[2], Harald Bresch[1], Kerstin Kämpf[2], Torben Peters[2], Thomas Kuhlbusch[2] and Alexandra Schmidt[1].

1Federal Institute for Materials Research and Testing (BAM), Unter den Eichen 87, 12205 Berlin

2 Federal Institute of Occupational Safety and Health (BAuA), Nöldnerstraße 40-42, 10317 Berlin

Foreword

The validation report presents the basic scientific information and data gathered in support of the Test Guideline (TG) 125 Nanomaterial Particle Size Distribution and Size Distribution of Nanomaterials[1]. The scope of this TG is to specify methods to determine the size and size distributions of nanoscale particles and fibres (1-1000 nm). Like the TG, the validation report is subdivided into two parts: the first part addresses particles and the second part fibres. More than 15 international participants were taking part in the interlaboratory comparison comprising 10 different measurement methods and 12 different tested Nanomaterials.

Following methods were tested for particle size distribution measurements in the first section: Atomic Force Microscopy (AFM), Centrifugal Liquid Sedimentation coupled Analytical Ultracentrifugation (CLS-AUC), Differential Mobility Analysis System (DMAS), Dynamic Light Scattering (DLS), Electron Microscopy (EM), Particle Tracking Analysis (PTA), Small Angle X-ray Scattering (SAXS) as well as Single Particle - Inductively Coupled Plasma – Mass Spectrometry (sp-ICP-MS). Details on the test materials used, test results and conclusions on the usability of the methods are given in this validation report. All mentioned methods but sp-ICP-MS were found to be suitable to be included in a TG. The latter method needs some further investigations due to the limited number of tests, which could be conducted during the interlaboratory comparison.

Fibres by definition have at least a three times larger length than their diameter. Only transmission electron microscopy (TEM) or scanning electron microscopy (SEM) were identified as practicable methods, which can identify and measure fibre length and diameter. The fibre diameter and length distributions are obtained as number-based distributions of the geometric size. The tested measurement method allows the determination of length x_l and diameter x_d for each fibre and hence enables the differentiation of mixtures of fibres if they differ in length and diameter. This method covers the size range in fibre diameter of 1 nm to 1000 nm and in fibre length up to 20 µm in general. Details on the test materials used, test results and conclusions can be found in the validation report. Both tested methods were found to be suitable for the measurement of size distributions of fibres with the limitation that TEM could only be validated up to a fibre length if 5 µm. For longer fibre lengths, SEM is recommended.

[1] OECD (2022), Test No. 125: Nanomaterial Particle Size and Size Distribution of Nanomaterials, OECD Guidelines for the Testing of Chemicals, Section 1, OECD Publishing, Paris, https://doi.org/10.1787/af5f9bda-en .

Table of contents

Foreword 7

1 Particle size determination 10
- Participating laboratories 10
- AFM: Silica particles (50 nm) 18
- AFM: Polystyrene particles (90/125 nm) 20
- AFM: Zinc oxide 22
- DLS: Silver particles 63

2 Fibre size determination 131
- Time schedule 133
- Study design 133
- Materials and test 133
- Evaluation of results 135
- Results of each test material 135

3 List of references 171

4 Appendix 173
- Application of different regulations 173
- Example images (one from each institute and method) 174
- Sonication procedures for ZnO and TiO_2 particles 193

Annex A. Questions raised and answered during the interlaboratory comparison 196

Annex B. Inter-laboratory validation plan of the test guideline on particle size and size distribution of nanomaterials - Fibres 198
- Introduction 198
- Scope of the interlaboratory comparison 198
- Materials, reagents and analysis 199
- Rationale for the choice of test materials in the interlaboratory comparison: 199
- Annex: Examples of the samples, additional information for sample preparation 201
- FAQ answered in the telephone conferences: 210

Annex C. Inter-laboratory validation plan of the test guideline on particle size and size distribution of manufactured nanomaterials – Particles 213
- Distribution: 213

Introduction	213
Scope of the round robin test	213
Rationale for the choice of particle test materials in the round robin	214
General dispersion protocol and information about the materials	214
Experimental procedures	217
Evaluation and representation of obtained results, test report	223
Validation of the results from the participating laboratories	223

Introduction

The OECD"s Sponsorship Programme for the Testing of Manufactured Nanomaterials (further referred to as "the Testing Programme") was concluded in March 2013, and the publication of the dossiers via the OECD website (www.oecd.org/science/nanosafety) started in June 2015. The evaluation process of the results of the Sponsorship Programme started in spring of 2014 and the results were published in 2016 [1]. Parallel to concluding the final stages of the Testing Programme, a series of workshops took place [2-5], in which for different topics the applicability of existing OECD Test Guidelines for nanomaterials were discussed and the need for new ones was analysed.

Some Test Guidelines (TG) were given a high priority in the need for an update. One of these was the TG110 (adopted in 1981) for the "Particle Size Distribution/Fibre Length and Diameter" which is only valid for particles and fibres with sizes above 250 nm.

To this extend, Germany 2017 volunteered to lead the development of a new Guidance Document or TG for "Particle size and particle size distribution of nanomaterials". The project started in 2017 with the establishment of an international advisory expert group. This group concluded that a new Test Guideline would be of better suitability than a Guidance Document to the TG110. One important reason was that the TG110 might be updated in the next future.

The decision was that the new TG does though connect to the TG 110 in terms of an overlap in size ranges, 1-1000 nm this TG, > 250 nm the TG110. The separate considerations in TG 110 of methods suitable for particles and fibres were kept as well. There is a common understanding among WPMN Experts that by the time this TG is drafted the TG110 in its current form needs revision und adaptation to the technical state of the art.

The current document reports the efforts taken during the international interlaboratory comparison (ILC) for approval of the TG on particle size and particle size distribution (PSD) of nanomaterials. The ILC was designed to learn about the applicability and reproducibility of the proposed experimental methods, to identify the factors that can affect the result variability and to perform the analysis of the statistical variability.

The validation test of the TG has been performed in two separate Inter-laboratory comparison (ILCs). One ILC was organised to test the methods for the determination of particle size and size distribution by BAM, the second one was performed to test the methods for the determination of fibre length and width and their distributions by BAuA. The study design, performance and results are described separately for each ILC.

We thank every laboratory that participated in the ILC. Fortunately, a lot of laboratories have contributed useful results. In some cases, we had to exclude reported measurements, but these reported results reviled the problems with the Draft OECD Test Guideline on PSD of nanomaterials. Especially these problematic results were very helpful and lead to additions and corrections in the draft TG.

1 Particle size determination

Participating laboratories

On the ILC on PSD on nanomaterials determination 31 laboratories were participating. The participating laboratories are listed in the following Table 1.

Table 1. Participating laboratories in particle size determination, their abbreviation and country code in alphabetical order.

Laboratories	Abbreviation	Country code
BASF	BASF	DE
Bundesanstalt für Materialforschung und -prüfung (lead)	BAM	DE
Bundesinstitut für Risikobewertung	BfR	DE
Chemours		US
CIDITEC	CID	ES
Environmental and Radiation Health Sciences Directorate	EHSRB/ERHSD	CA
Federal Institute of Occupational Safety and Health	BAuA	DE
Fraunhofer Institute for Ceramic Technologies and Systems	IKTS	DE
Fraunhofer Institute for Microengineering and Microsystems	IMM	DE
Fraunhofer Institute for Molecular Biology and applied Ecology	IME	DE
French Institute of Metrology	LNE	FR
French National Institute for Industrial Environment and Risks	INERIS	FR
Institute for Medical Research and Occupational Health	IMI	HR
Iran Nanotechnology Innovation Council	INIC	IR
Joint Research Centre	JRC	EC
Korea Research Institute of Standards and Science	KRISS	KR
Laboratoire Interdisciplinaire sur l'Organisation Nanométrique et Supramoléculaire	LIONS/ CEA	FR
Luxembourg Institute of Science and Technology	LIST	LU
Microtrac		DE
National Institute for Occupational Safety and Health	NIOSH	US
National Institute of Standards and Technologies	NIST	US
National Measurement Institute	NMI	AU
National Nanotechnology Center	NANOTEC	TH
National Research Council of Canada	NRC CNRC	CA
Norwegian Institute of Air Research	NILU	NO
Physikalisch-Technische Bundesanstalt	PTB	DE
Scientific and Technological Centers of the University of Barcelona and Spanish National Research Council	CCiTUB-CSIC	ES
Solvay		FR
Superior Council of Scientific Investigations	CSIC	ES

University of Venice – Ca' Foscari	Unive	IT
Xenocs		FR

Methods:

1) Atomic Force Microscopy (AFM)
   Participating Laboratories: 6
2) Centrifugal Liquid Sedimentation (CLS)
   Participating Laboratories: 5
3) Differential Mobility Analysis System (DMAS)
   Participating Laboratories: 6
4) Dynamic Light Scattering (DLS)
5) Participating Laboratories: 21
6) Particle Tracking Analysis (PTA)
   Participating Laboratories: 6
7) Scanning Electron Microscopy (SEM)
   Participating Laboratories: 9
8) Single particle Inductively Coupled Plasma - Mass Spectrometry (sp ICP-MS)
   Participating Laboratories: 4
9) Small Angle X-ray Scattering (SAXS)
   Participating Laboratories: 5
10) Transmission Electron Microscopy (TEM)
    Participating Laboratories: 11

Time schedule

Activity	Schedule date
Meeting on interlaboratory comparison	19th of February 2019
Start of the interlaboratory comparison	2nd of Mai 2019
Completion of the interlaboratory comparison	30th of September 2019
Discussion of interlaboratory comparison	June/July 2020
Delivery of the validation report to OECD	July 2021

Study design

This interlaboratory comparison was designed to measure the particles size distribution of particles in the range of 1-1000 nm.

The methods that were considered in the study are Atomic Force Microscopy (AFM), Centrifugal Liquid Sedimentation (CLS/AUC), Differential Mobility Analysis System (DMAS), Dynamic Light Scattering (DLS), Particle Tracking Analysis (PTA), Scanning Electron Microscopy (SEM), single particle Inductively Coupled Plasma – Mass Spectroscopy (sp ICP-MS), Small Angle X-Ray Scattering (SAXS) and Transmission Electron Microscopy (TEM). All selected methods were validated in previous studies for their specific applicability to nanomaterials. These validations were not repeated in this study. This ILC validates the comparability of the methods and the applicability of the *Draft OECD-TG on PSD of nanomaterials*.

The validity of the methods was proven to deliver reasonable uncertainties with comparability to size determination in several ILC:

- AFM for example for PSL, Au and SiO_2 particles [6, 7] [8]
- CLS for example for SiO_2, PSL, TiO_2 and $BaSO_4$ [6, 9, 10]
- DMAS for example for PSL, $BaSO_4$ and SiO_2 particles [9, 11]
- DLS for example for SiO_2, PSL TiO_2 (not primary particles) and Au [6, 9, 11, 12]
- PTA for example for SiO_2, PSL and Au [6, 9, 13]
- SEM for example for SiO_2, PSL TiO_2 and Au [6, 8, 9, 11, 14]
- sp ICP-MS for example for Au, Ag, TiO^2 [15] [16] [9]
- SAXS for example for SiO_2, PSL and Au [6, 8]
- TEM for example for SiO_2, TiO_2, PSL and Au [7-9, 11, 17, 18].

Sample preparation was not scope of the ILC and is not scope of the draft TG. All samples for microscopic analysis were prepared by the lead laboratory and were provided fully prepared to the participants. For all other methods the particles were sent out with a standard operation protocol for the sample preparation.

All experimental procedures to follow were described in the former draft “TG on particle size and particle size distribution of nanomaterials” TG PSD (Version July 2021). Experimental procedures regarding the sample preparation were described in the document “Interlaboratory validation plan” (see appendix p.213).

Test materials

The materials were chosen to cover a broad range of sizes within the range of validity of the Test Guideline of 1-1000 nm. The materials contain ideal spherical particles as well as more irregularly shaped real-world materials. The physico-chemical properties of the materials vary in a wider range (density, scattering, atomic number, refractive index). Thus, not all materials can be measured with every method. A matrix of which material was to be measured with which method in this ILC is given in the Table 2.

Table 2. Overview of the materials tested with the respective method.

Method	Ag (BAM) 17 nm	SiO_2 (KRISS) 20 nm	SiO_2 (KRISS) 50 nm	ZnO (JRC) ~100 nm	PSL Mix (NTRM) 90/125 nm	TiO_2 (JRC) ~250 nm	PSL Mix (NTRM) 80/800 nm
DLS	X	X	X	X	X	X	
CLS	X	X*	X*	X	X	X	X
PTA	X			X	X	X	
SAXS	X	X	X		X		
sp ICP-MS						X	
AFM			X	X	X		
TEM	X	X	X	X	X	X	X
SEM	X	X		X	X	X	X
DMAS	X	X	X		X	X	X

The silver particles are nearly spherical particles with a wide size distribution with a size at around 10-30 nm with a bimodal character. For the microscopic methods the specimens were sent out prepared. For SEM, the specimens were prepared by drop-on method of particles dispersed in water on a silicon wafer (40 µl of pure Ag dispersion). For TEM the specimens were prepared on a TEM copper grid by the drop-on method (7.7 µl of pure Ag dispersion). For all other methods, measuring the particles in dispersion or aerosol concentrations for the analysis were recommended to use. As the useful concentrations depends also on the measurement setup, the labs slightly adjusted the concentrations for their measurement. For the sample preparation sonication of the particles was not advised.

The silica particles are nearly spherical particles with small monomodal size distribution. Two different particle sizes, at around 20 nm and at around 50 nm, were sent out. For the microscopic methods the specimens were sent out prepared. For AFM and SEM, the specimens were prepared by spin-coating (40 rps for 60 s) of particles dispersed in ethanol (7.7 µl of 0.5 g/L SiO_2) on a silicon wafer. Spin-coating was chosen to keep the number of agglomerates low and have a homogeneous distribution of the particles all over the specimen. For TEM the specimens were prepared on a TEM copper grid by the drop-on method (7.7 µl of 0.5 g/L SiO_2 dispersed in ethanol). For all other methods, measuring the particles in dispersion or aerosol concentrations for the analysis were recommended to use. As the useful concentrations depends also on the measurement setup, the labs slightly adjusted the concentrations for their measurement. For the sample preparation sonication of the particles was not advised.

The zinc oxide particles are a real-life material, where the particles have no uniform shape and tend to agglomerate. The particles have a wide size distribution around 100 nm. For the microscopic methods

the specimens were sent out prepared. For AFM and SEM, the specimens were prepared by spin-coating (40 rps for 60 s) of particles dispersed in ethanol (7.7 µl of 0.6 mg/mL ZnO) on a silicon wafer. Spin-coating was chosen to keep the number of agglomerates low and have a homogeneous distribution of the particles all over the specimen. For TEM the specimens were prepared on a TEM copper grid by the drop-on method (7.7 µl of 1.5 g/L ZnO dispersed in ethanol). For all other methods, measuring the particles in dispersion or aerosol concentrations for the analysis were recommended to use. As the useful concentrations depends also on the measurement setup, the labs slightly adjusted the concentrations for their measurement. For the sample preparation a sonication procedure of the particles was given. Sonication of the particles should be performed directly before the measurement.

The polystyrene particles are a size mixture of spherical particles with a size at around 90 and 125 nm with a number-based ratio of 1:1. For the microscopic methods the specimens were sent out prepared. For AFM and SEM, the specimens were prepared by spin-coating (40 rps for 60 s) of particles dispersed in ethanol (7.7 µl of 0.5 g/L PSL) on a silicon wafer. Spin-coating was chosen to keep the number of agglomerates low and have a homogeneous distribution of the particles all over the specimen. For TEM the specimens were prepared on a TEM copper grid by the drop-on method (7.7 µl of 0.5 g/L PSL dispersed in ethanol). For all other methods, measuring the particles in dispersion or aerosol concentrations for the analysis were recommended to use. As the useful concentrations depends also on the measurement setup, the labs slightly adjusted the concentrations for their measurement. For the sample preparation sonication of the particles was not advised.

The titanium oxide particles are a real-life material, where the particles have no uniform shape and tend to agglomerate. The particles have a wide size distribution around 200-300 nm. For the microscopic methods the specimens were sent out prepared. For SEM, the specimens were prepared by spin-coating (40 rps for 60 s) of particles dispersed in ethanol (7.7 µl of 0.8 mg/mL TiO_2) on a silicon wafer. Spin-coating was chosen to keep the number of agglomerates low and have a homogeneous distribution of the particles all over the specimen. For TEM the specimens were prepared on a TEM copper grid by the drop-on method (7.7 µl of 1.6 mg/mL TiO_2 dispersed in ethanol). For all other methods, measuring the particles in dispersion or aerosol concentrations for the analysis were recommended to use. As the useful concentrations depends also on the measurement setup, the labs slightly adjusted the concentrations for their measurement. For the sample preparation a sonication procedure of the particles was given. Sonication of the particles should be performed directly before the measurement.

The polystyrene particles are a size mixture of spherical particles with a size at around 80 and 800 nm with a number-based ratio of 2:1. For the microscopic methods the specimens were sent out prepared. For SEM, the specimens were prepared by spin-coating (40 rps for 60 s) of particles dispersed in ethanol (7.7 µl of 0.5 g/L PSL) on a silicon wafer. Spin-coating was chosen to keep the number of agglomerates low and have a homogeneous distribution of the particles all over the specimen. For TEM the specimens were prepared on a TEM copper grid by the drop-on method (7.7 µl of 0.5 g/L PSL dispersed in ethanol). For all other methods, measuring the particles in dispersion or aerosol concentrations for the analysis were recommended to use. As the useful concentrations depends also on the measurement setup, the labs slightly adjusted the concentrations for their measurement. For the sample preparation sonication of the particles was not advised.

Validation of results

During the validation of the results the normalized size distributions and the cumulated distribution functions (CDF) for each material were compared for all labs in a common plot to visually assess the similarity of the obtained data. The variation of the parameters mean median modal and geometric standard deviation of the distributions was then assessed in a statistical analysis.

This statistical analysis comprised the test of the mean, median and modal diameter of the particle size distribution on Gaussianity and the calculation of the standard deviation for mean, median and modal diameter for the cleaned data set. Within this document we used the terms “repeatability standard deviation” for the repeated experiments from one lab and the term “reproducibility standard deviation” for the deviations between different labs. The term “expanded reproducibility standard deviation” is used for the reproducibility standard deviation with a coverage factor of 2.

Further influencing factors were analysed for their statistical significance in hypothesis testing with respect to different instrumentals factors or evaluations processes, which could influence the obtained size distribution.

Results of each method

Atomic force microscopy – AFM

For analysis with AFM the materials silica (50 nm), polystyrene particles 90/125 nm and zinc oxide were sent out readily prepared on silicon wafer.

We received AFM measurements from six laboratories. 14 results were handed in. In Table 3 an overview for the obtained diameters is given. The results of the AFM measurements are presented for each particle system and individual data set.

Table 3. Overview of the results for the mean, median and modal diameter determined via AFM measurement. The reported standard deviation is the between laboratory deviation by a factor of 2.

Particle system	# labs	$d_{0,hgt,mean}$ (nm)	$d_{0,hgt,median}$ (nm)	$d_{0,hgt,modal}$ (nm)
SiO_2 (50 nm)	5	50.5 ± 8	50.9 ± 8.2	50.6 ± 7.8
PSL (90/125 nm)	6	110.1 ± 1.1	113.6 ± 2.8	94.2 ± 1.7/123.2 ± 0.6
ZnO	3	154.9 ± 40	122.2 ± 33.8	64.8 ± 41

AFM: Silica particles (50 nm)

We received AFM measurements from five laboratories. All laboratories measured with the in the TG recommended intermittent contact mode and used a tip <10 nm. The pixel sizes of the recordings of four labs varied between 1.95 to 3 nm/px. Lab 01 measured with a pixel size of 6 nm/px but ensured with close-up measurements at a higher pixel size that the obtained height is not influenced by using the higher pixel size. All other AFM measurements were performed with the minimal required pixel size or better. For background correction plane and/or line levelling were used. Particle size was determined from the maximum height of a particle. All labs used a semi-automatic evaluation mode, the particles are masked to count the sizes automatically. Agglomerates and aggregates are removed manually before the automatic evaluation. The laboratories were advised to count at least 300 particles for a reliable size distribution. The obtained normalized size distributions and the cumulative size distributions are shown in Figure 1.

Table 4. Used instrument setup and settings for the measurement of silica particles with AFM

Lab	Instrument	Software	Tip	Pixel size
1	JPK Nanowizard 4	Gwyddion v. 2.53	Multi75 Gd-g, 75KHz, 3 N/m	6 nm/px
9	Asylum Research Inc. MFP3D-SA	SPIPTM v. 6.5.1	TAP150Al-G, 150 kHz, 5.94 N/m	1.95 nm/px
12	JPK Nanowizard® II	JPK Data Processing v. 5.1.8; Gwyddion v. 2.52	HQ:XSC11/Al BS, D, 350 kHz, 42 N/m	3 nm/px
18	Agilent 5420	PicoView v. 1.16.0; Gwyddion v. 2.53	Tap190Al-G, 190 kHz, 48 N/m	2.9 nm/px
26	MFP-3D Origin+	Igor Pro v. 6.37	SSS-NCH-10, 330kHz, 42 N/m	2.9 nm/px

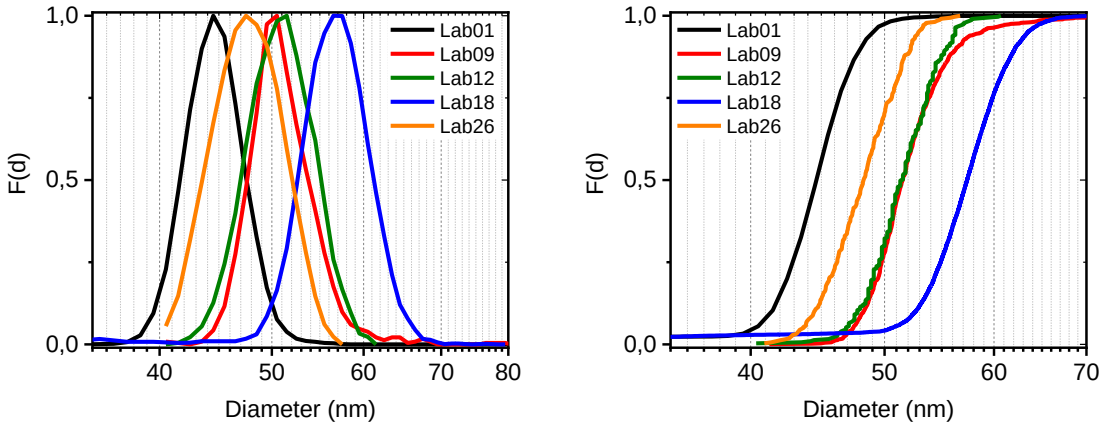

Figure 1: normalized (left) and cumulated (right) size distribution functions of the diameter of silica nanoparticles (50 nm). All reported results are shown.

From the distributions of the selected datasets the mean, median and modal diameters are calculated and plotted in Figure 2. The error bars are calculated using the bootstrap method.

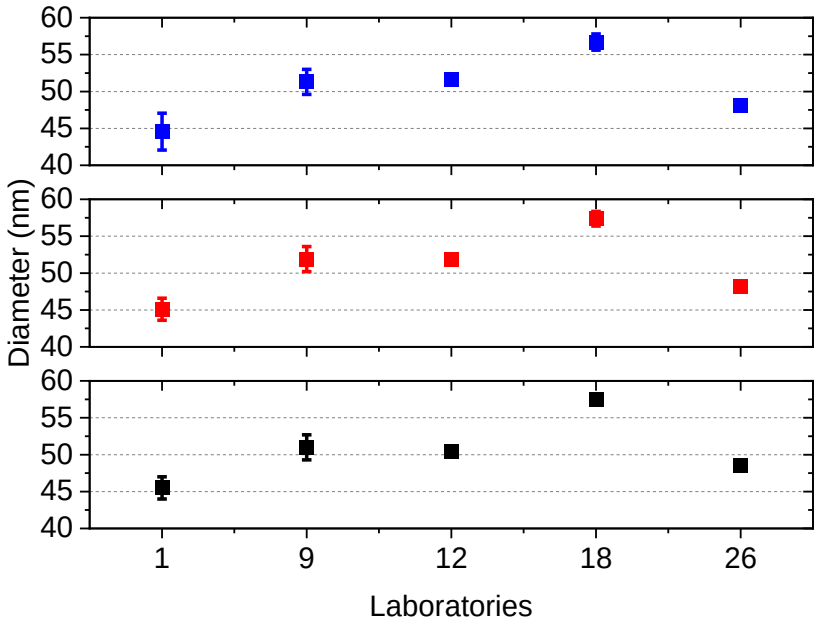

Figure 2: mean (blue), median (red) and modal (black) diameter with bootstrap error of silica nanoparticles analysed with AFM.

To evaluate the precision of the results of the ILC obtained on SiO_2 (50 nm) particles, the average values of the mean and median diameters of the selected datasets were calculated as well as the standard deviation between the laboratories σ_L of the mean, median and modal values and the relative standard deviation σ_{rel} (=standard deviation/average diameter). The values are given in Table 5

Table 5. Statistics of SiO_2 (50 nm) particles datasets

	$d_{0,hgt}$ (nm)	σ_L	σ_{rel}
average (**mean**(diameter))	50.5	4.0	0.08
average (**median**(diameter))	50.9	4.1	0.08
average (**modal**(diameter))	50.6	3.9	0.08
average geometric standard deviation (diameter)	1.12	0.1	0.07

The standard deviation is multiplied by a factor of 2 in order to yield a coverage probability of 95% and additionally the percentage is given. Thus, the mean diameter of the SiO_2 (50 nm) particles is obtained as 50.5 ± 8 nm (16%), the median diameter is given by 50.9 ± 8.2 nm (16%) and the modal diameter is given by 50.6 ± 7.8 nm (15.5%).

AFM: Polystyrene particles (90/125 nm)

We received AFM measurements from five laboratories. All laboratories measured with the recommended intermittent contact mode and used a tip <10 nm. The pixel sizes of the recordings varied between 2.93 to 12.2 nm/px. That means that not all AFM measurements were performed with the minimal recommended pixel size. Lab 01, Lab 12 and Lab 18 used a pixel size of 6, 10 and 12.2 nm/px for image acquisition. For background correction plane and/or line levelling were used. Particle size was determined from the maximum height of a particle. All labs used a semi-automatic evaluation mode, the particles were masked to count the sizes automatic. Agglomerates and aggregates were removed manually before the automatic evaluation. The laboratories were advised to count at least 700 particles for a reliable size distribution. The obtained normalized size distributions and the cumulative size distributions are shown in

Figure 3.

Table 6. Used instrument setup and settings for the measurement of the polystyrene particles (90/125 nm) with AFM

Lab	Instrument	Software	Tip	Pixel size (nm/px)
1	JPK Nanowizard 4	Gwyddion v. 2.53	Multi75 Gd-g, 75KHz, 3 N/m	6
4	Veeco Dimension V	Platypus v.2.2.4	OTESPA - R3, 300 kHz, 26 N/m	2.93 / 4.88
9	Asylum Research Inc. MFP3D-SA	SPIPTM v. 6.5.1	TAP150Al-G, 150 kHz, 5.94 N/m	3.9
12	JPK Nanowizard® II	JPK Data Processing v. 5.1.8; Gwyddion v. 2.52	HQ:XSC11/Al BS, D, 350 kHz, 42 N/m	10
18	Agilent 5420	PicoView v. 1.16.0; Gwyddion v. 2.53	Tap190Al-G, 190 kHz, 48 N/m	12.2

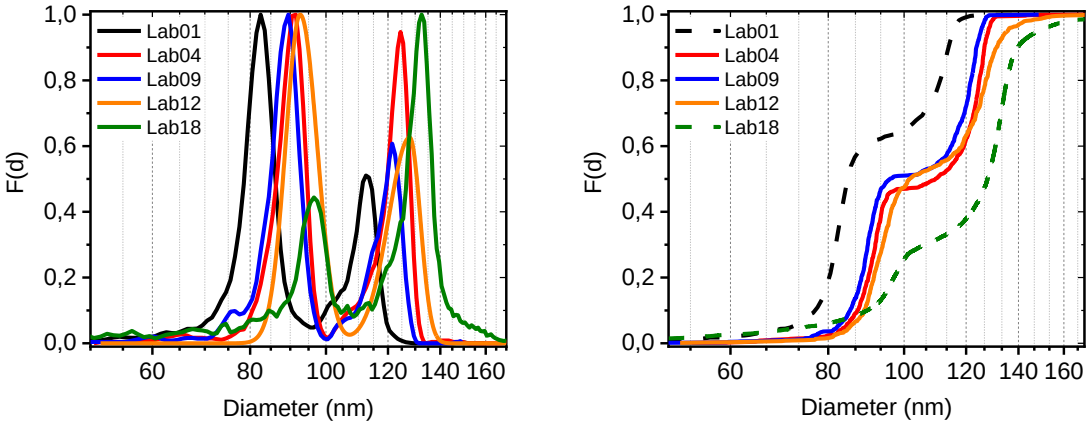

Figure 3: normalized (left) and cumulated (right) size distribution functions of the diameter of polystyrene nanoparticles (90/125 nm). All reported results are shown.

The size distribution of Lab 01 and 18 show deviating size distributions. Lab 01 included smaller agglomerates in the image evaluation, but nearly yields the same particles sizes when they excluded the agglomerates. There might be an influence in the yielded ratio of the different size population, but this cannot be the cause for the generally too low particle size determination. Also, for the 50 nm silica particles Lab 01 yielded the smallest size distribution, so that this might be a systematic error, which could rise from wrong calibration of the instrument, background levelling or an influence from the used tip. Lab 18 used the highest pixel size for image evaluation. Agglomerates are included in the measurement, but they used watershed segmentation and artefacts were excluded. An influence from the high pixel size and the measurement of agglomerates cannot be excluded here. For the further evaluation of the average diameters the results from Lab 01 and 18 are excluded, but for the completeness are still shown in Figure 4.

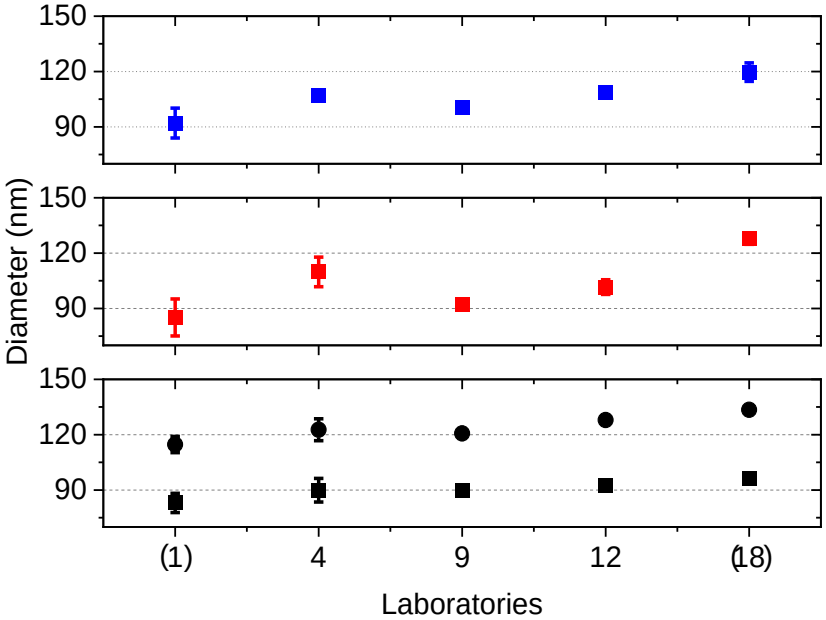

Figure 4: mean (blue), median (red) and modal (black) diameter with bootstrap error of polystyrene nanoparticles analysed with AFM.

From the distributions of the selected datasets the mean, median and modal diameters are calculated and plotted in Figure 4. The error bars are calculated using the bootstrap method.

To further evaluate the precision of the results of the ILC obtained on PSL (90/125 nm) particles, the average values of the mean and median diameters of the selected datasets were calculated as well as the standard deviation between the laboratories σ_L of the mean, median and modal values and the relative standard deviation σ_{rel} (=standard deviation/average diameter). These values are given in Table 7.

Table 7. Statistics of polystyrene (90/125 nm) particles datasets

	$d_{0,hgt}$ (nm)	σ_L	σ_{rel}
average (**mean**(diameter))	110.1	1.1	0.01
Average (**median** (diameter))	113.6	2.8	0.03
average (**modal(1)**(diameter))	94.2	1.7	0.02
average (**modal(2)**(diameter))	123.2	0.6	0.02
average geometric standard deviation (diameter)	1.18	0.02	0.02

The standard deviation is multiplied by a factor of 2 in order to yield a coverage probability of 95% and additionally the percentage is given. Thus, the mean diameter of the PSL (90/125 nm) particles is obtained as 110.1 ± 1.1 nm (1%) and the median diameter is given by 113.6 ± 2.8 nm (3%). The modal diameters are for mode 1 94.2 ± 1.7 nm (2%) and for mode 2 123.2 ± 0.6 nm (1%).

AFM: Zinc oxide

We received AFM measurements from three laboratories. All laboratories measured with the recommended intermittent contact mode and used a tip <10 nm. The pixel sizes varied between 7.81 to 20 nm/px. That means that no AFM measurements were performed with the minimal recommended pixel size. The quality of the prepared specimen is also under optimized preparation condition low. To keep the number of agglomerates low, a low concentration of the particle dispersion was chosen, resulting in a low allocation of particles on the specimen. Resulting from the low occupancy of particles on the specimen, where agglomerates are still present, the recommended pixel size was not practicable to measure in an appropriate time, so that the labs had to adjust the measurement conditions. For background correction plane and/or line levelling was used. Particle size was determined from the maximum height of a particle. All labs used a semi-automatic evaluation mode, the particles are masked to count the sizes automatic. Agglomerates and aggregates were removed manually before the automatic evaluation. The laboratories were advised to count at least 700 particles for a reliable size distribution. The obtained normalized size distributions and the cumulative size distributions are shown in Figure 5.

Table 8. Used instrument setup and settings for the measurement of the zinc oxide particles with AFM

Lab	Instrument	Software	Tip	Pixel size
1	JPK Nanowizard 4	Gwyddion v. 2.53	Multi75 Gd-g, 75KHz, 3 N/m	6 nm/px
9	Asylum Research Inc. MFP3D-SA	SPIPTM v. 6.5.1	TAP150Al-G, 150 kHz, 5.94 N/m	7.81 nm/px
12	JPK Nanowizard® II	JPK Data Processing v. 5.1.8; Gwyddion v. 2.52	HQ:XSC11/Al BS, D, 350 kHz, 42 N/m	20 nm/px

18	Agilent 5420	PicoView v. 1.16.0; Gwyddion v. 2.53	Tap190Al-G, 190 kHz, 48 N/m	19.5 nm/px

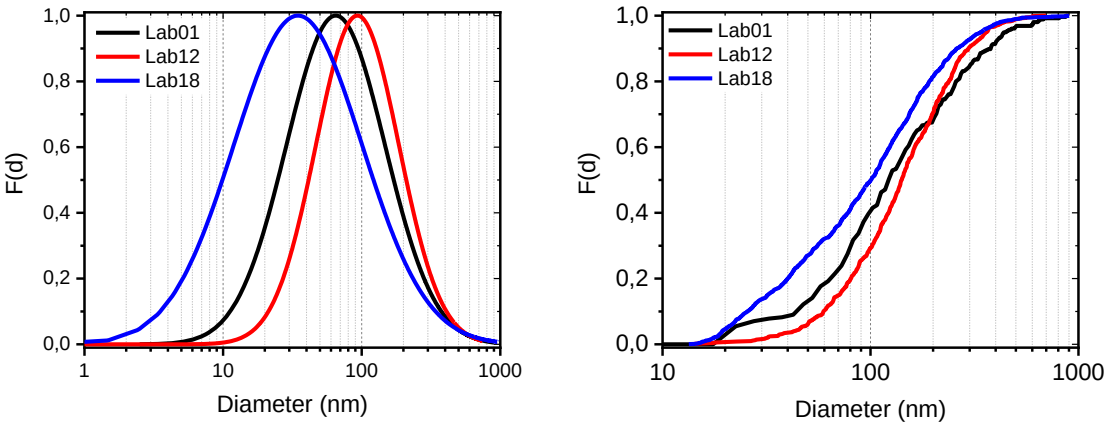

Figure 5: normalized (left) and cumulated (right) size distribution functions of the diameter of zinc oxide nanoparticles. All reported results are shown.

From the distributions of the selected datasets the mean, median and modal diameters are calculated and plotted in Figure 6. The error bars are calculated using the bootstrap method.

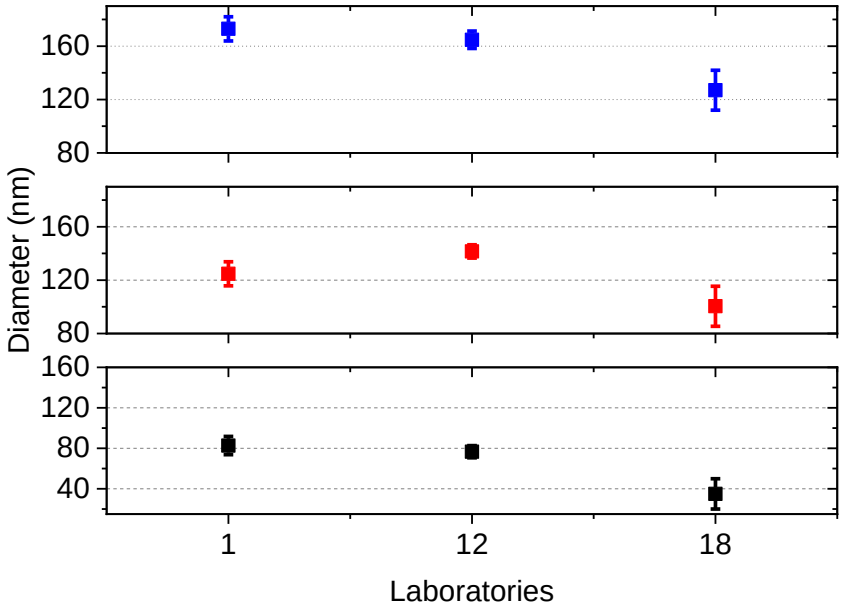

Figure 6: mean (blue), median (red) and modal (black) diameter with bootstrap error of zinc oxide nanoparticles analysed with AFM.

To evaluate the precision of the results of the ILC obtained on ZnO particles, the average values of the mean and median diameters of the selected datasets were calculated as well as the standard deviation between the laboratories σ_L of the mean, median and modal values and the relative standard deviation σ_{rel} (=standard deviation/average diameter). These values are given in Table 9.

Table 9. statistics of zinc oxide nanoparticles datasets

	$d_{0,hgt}$ (nm)	σ_L	σ_{rel}
average (**mean**(diameter))	154.9	20	0.13
average (**median**(diameter))	122.2	16.9	0.14
average (**modal**(diameter))	64.8	20.2	0.33
average geometric standard deviation (diameter)	2.15	0,19	0,09

The standard deviation is multiplied by a factor of 2 in order to yield a coverage probability of 95% and additionally the percentage is given. Thus, the mean diameter of the ZnO particles is obtained as 154.9 ± 40 nm (26%) and the median diameter is given by 122.2 ± 33.7 nm (28%) and the modal diameter is given by 64.8 ± 41.4 nm (64%).

Centrifugal liquid sedimentation CLS/Analytical ultracentrifugation AUC

For analysis with CLS/AUC silica particles (20 nm and 50 nm), polystyrene particles (90/125 nm and 80/800 nm), zinc oxide, titanium oxide and silver particles were sent out as powder or suspension. For the preparation of the measurement suspension a standard operating procedure (SOP) was given. It was recommended to measure two different concentration of each material. The shown size distribution is the average distribution of both concentrations. If a consistent concentration dependency between the both concentrations was found it is mentioned in the respective paragraph to the size distribution of the material.

We received CLS/AUC measurements from five laboratories. 25 results were handed in. In Table 3 an overview for the obtained diameters is given. The results of the CLS and AUC measurements are presented for each particle system and individual data.

Table 10. Overview of the results for the mean, median and modal diameter determined via CLS measurement. The reported expanded reproducibility standard deviation is calculated using a coverage factor of 2.

Particle system	# labs	$d_{3,St,mean}$ (nm)	$d_{3,St,median}$ (nm)	$d_{3,St,modal}$ (nm)
Ag	4	15.7 ± 10.6	13.8 ± 3.5	13.1 ± 3.9
SiO_2 (20 nm)	4	18.5 ± 7.7	17 ± 4.2	17.2 ± 4.2
SiO_2 (50 nm)	5	44.7 ± 8.7	44.7 ± 8.5	44.8 ± 8.1
PSL (90/125 nm)	3	No reliable validation possible		
ZnO	3	190.5 ± 50.2	196.5 ± 14.9	188.2 ± 38.3
TiO_2	4	284 ± 86.6	276.4 ± 110.8	307 ± 51.8
PSL (80/800 nm)	4	No reliable validation possible		911 ± 112

CLS: Silica particles (20 nm)

We received centrifugal measurements from four laboratories using three different kinds of centrifuges. An AUC was used from one lab and two labs used a disc CLS and one lab a cuvette CLS. With the cuvette CLS no evaluable measurements could be obtained. The obtained size distributions from the different centrifuges might not be comparable as a different instrument setup with other detection systems was used. The laboratories were advised to measure two different concentration of the particle dispersion. It was recommended to use concentrations of 10 mg/ml and 5 mg/ml. The obtained normalized size distributions and the cumulative size distributions are shown in Figure 7. In the graphs the average size distribution of both concentrations is shown.

Table 11. Used concentrations and measurement conditions

Lab	Instrument	Centrifuge speed (rpm)	Concentration (mg/ml)	Gradient (wt%)
1	Lumisizer 6512-72	4000	5 + 10	-
3	CPS DC 24000 UHR	22000	5 + 10	0-8
5	Beckman XLI-80	55000 ramped	5 + 10	-
7	CPS DC 24000 UHR	22000	5 + 10	0-8

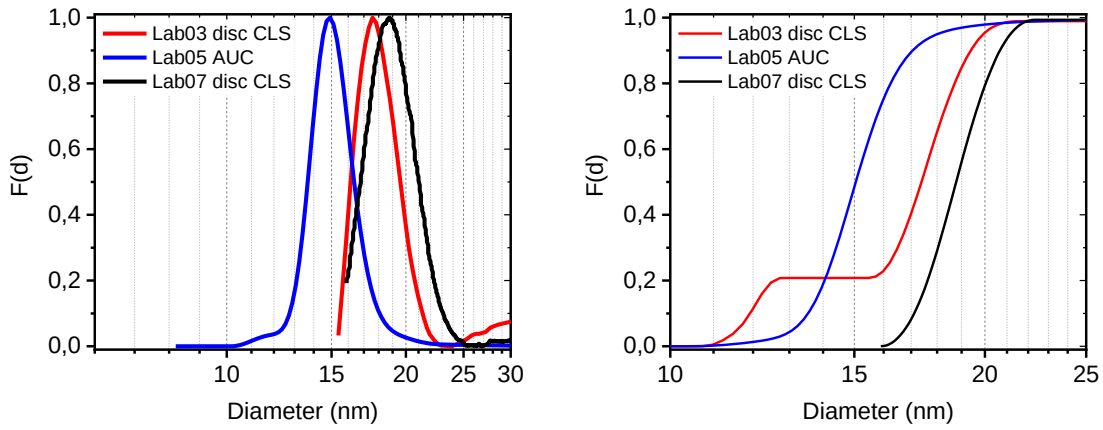

Figure 7: normalized (left) and cumulated (right) size distribution functions of the diameter of silica nanoparticles (20 nm). All reported results are shown.

The size distribution between the different used centrifuges clearly differ. Generally, a very small particle size is determined, and some measurement showed artefacts at size ranges below 15 nm. The silica particles are a boundary material due to the low difference of the refractive index of the particles from the one of the measurement medium. This might lead to an underestimation of the particle size.

From the distributions of the selected datasets the mean, median and modal diameters of the different concentration measured with repeatability standard deviation are determined from the measurement of the two different concentrations and plotted in Figure 8. In case only one concentration was measured by a lab, only one diameter is depicted in the figure.

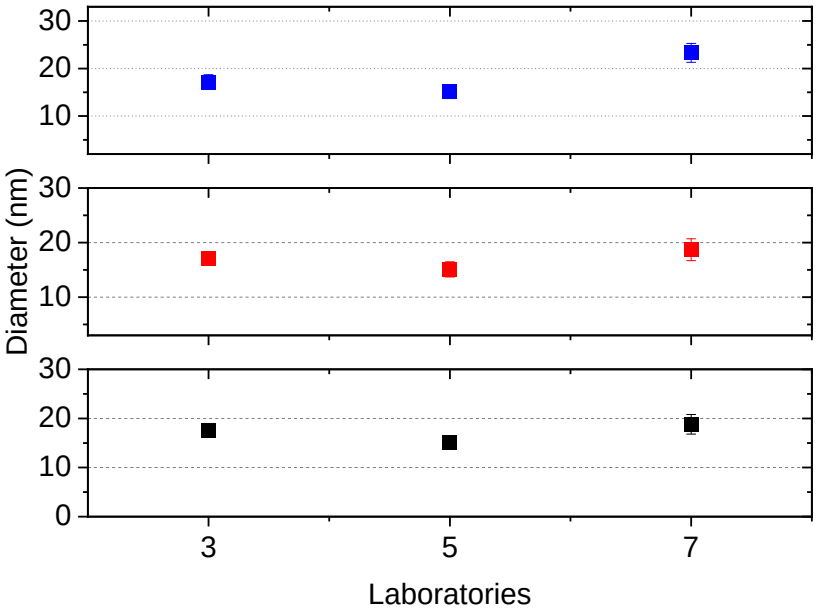

Figure 8: mean (blue), median (red) and modal (black) diameter with repeatability standard deviation of silica nanoparticles (20 nm) analysed with CLS.

To further evaluate the precision of the results of the ILC obtained on SiO_2 (20 nm) particles, the average values of the mean, median and modal diameters of the selected datasets were calculated as well as the reproducibility standard deviation σ_R of the mean, median and mode values and the relative standard deviation σ_r (=standard deviation/mean). These values are given in Table 12.

Table 12. Statistics of silica (20 nm) nanoparticles datasets

	$d_{3,St}$ (nm)	σ_R	σ_r
average (**mean**(diameter))	18.5	3.8	0.21
average (**median**(diameter))	17	2.1	0.12
average (**modal**(diameter))	17.2	2.1	0.12

The expanded reproducibility standard deviation is calculated by multiplying it with the coverage factor, k=2. Thus, the mean diameter of the SiO_2 (20 nm) particles is obtained as 18.5 ± 7.6 nm (41%), the median diameter is given by 17 ± 4.2 nm (24%) and the mode diameter is given by 17.2 ± 4.2 nm (25%).

CLS: Silica particles (50 nm)

We received centrifugal measurements from five laboratories using three different kinds of centrifuges. An AUC was used from one lab, three labs used a disc CLS and one lab used a cuvette CLS. The obtained size distributions from the different centrifuges might not be comparable as a different instrument setup with other detection systems was used. The laboratories were advised to measure two different concentration of the particle dispersion. It was recommended to use concentrations of 10

mg/ml and 5 mg/ml. The obtained normalized size distributions and the cumulative size distributions are shown in Figure 9. In the graphs the average size distribution of both concentrations is shown.

Table 13. Used concentrations and measurement conditions

Lab	Instrument	Centrifuge speed (rpm)	Concentration (mg/ml)	Gradient (wt%)
1	Lumisizer 6512-72	4000	5 + 10	-
3	CPS DC 24000 UHR	22000	5 + 10	0-8
5	Beckman XLI-80	55000 ramped	5 + 10	-
7	CPS DC 24000 UHR	22000	5 + 10	0-8
9	CPS DC 24000 UHR	22000	0.5 + 1	4-18

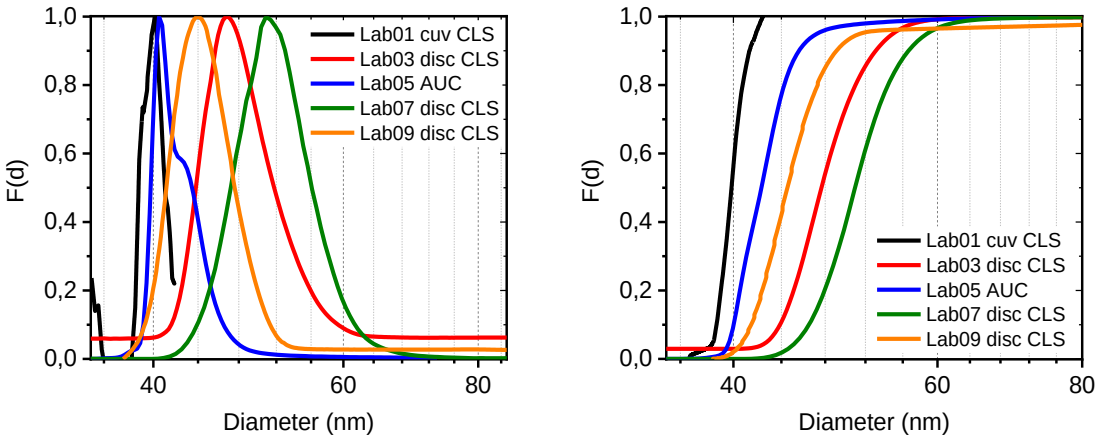

Figure 9: normalized (left) and cumulated (right) size distribution functions of the diameter of silica nanoparticles (50 nm). All reported results are shown.

The size distribution between the different used centrifuges clearly differ. Generally, a very small particle size is determined. The silica particles are a boundary material due to the low difference of the refractive index of the particles from the one of the measurement medium. This might lead to an underestimation of the particle size. Lab 01 was only able to measure the dispersion as received with a concentration of 10 mg/ml the measurement of the diluted particle dispersion could not be evaluated.

From the distributions of the selected datasets the mean, median and modal diameters of the different concentration measured with repeatability standard deviation are determined from the measurement of the two different concentrations and plotted in Figure 10. In case only one concentration was measured by a lab, only one diameter is depicted in the figure.

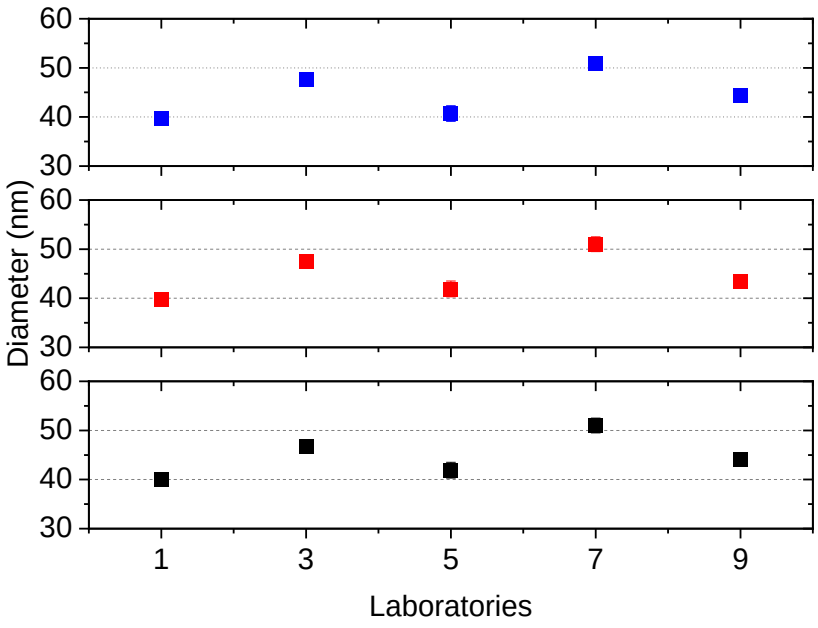

Figure 10: mean (blue), median (red) and modal (black) diameter for the silica nanoparticles analysed with CLS.

To further evaluate the precision of the results of the ILC obtained on SiO_2 (50 nm) particles, the average values of the mean, median and modal diameters of the selected datasets were calculated as well as the reproducibility standard deviation σ_R of the mean, median and modal values and the relative standard deviation σ_r (=standard deviation/mean). These values are given Table 14.

Table 14. Statistics of silica (50 nm) nanoparticles datasets

	$d_{3,St}$ (nm)	σ_R	σ_r
average (**mean**(diameter))	44.7	4.4	0.10
average (**median**(diameter))	44.7	4.2	0.09
average (**modal**(diameter))	44.8	4	0.09

The expanded reproducibility standard deviation is calculated by multiplying it with the coverage factor, k=2. Thus, the mean diameter of the SiO_2 (50 nm) particles is obtained as 44.7 ± 8.7 nm (19%), the median diameter is given by 44.7 ± 8.4 nm (19%) and the mode diameter is given by 44.8 ± 8 nm (18%).

CLS: Titanium oxide particles

We received CLS measurements from four laboratories using three different kinds of centrifuges. An analytical ultracentrifuge was used from one lab, two labs used a disc CLS and one lab used a cuvette CLS. The obtained size distributions from the different centrifuges might not be comparable as a different instrument setup with other detection systems is used. The laboratories were advised to measure two different concentration of the particle dispersion. It was recommended to use concentrations of 0.2 mg/ml and 0.1 mg/ml. The obtained normalized size distributions and the

cumulative size distributions are shown in Figure 11. In the graphs the average size distribution of both concentrations is shown. Details of the sonication procedure can be found in the appendix Table 82.

Table 15. Used concentrations and measurement conditions

Lab	Instrument	Centrifuge speed (rpm)	Concentration (mg/ml)	Gradient (wt%)
1	Lumisizer 6512-72	4000	0.1 + 0.2	-
3	CPS DC 24000 UHR	22000	0.1 + 0.2	8-24
5	Beckman XLI-80	55000 ramped	0.1 + 0.2	-
7	CPS DC 24000 UHR	22000	0.1 + 0.2	8-24

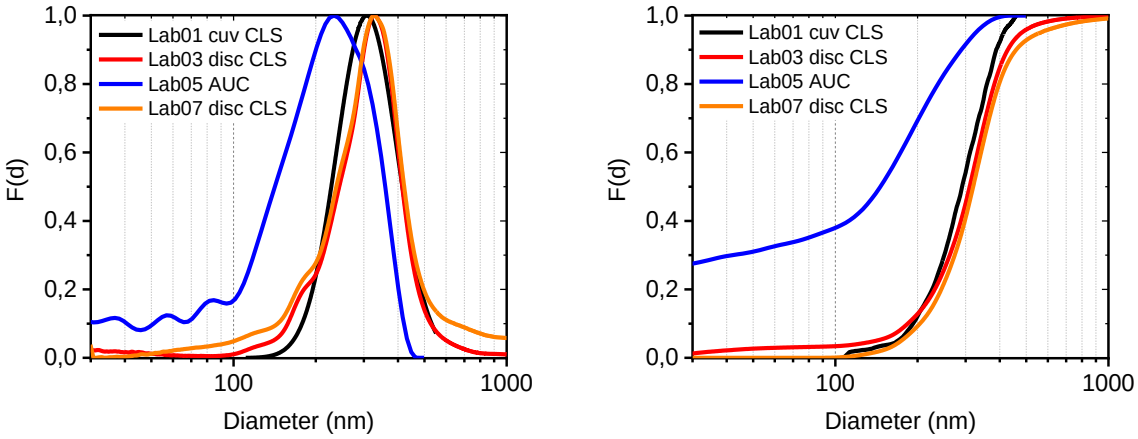

Figure 11: normalized (left) and cumulated (right) size distribution functions of the diameter of titanium oxide particles. All reported results are shown.

The size distribution from cuvette CLS and disc CLS are in good agreement. The size distribution derived from the AUC clearly differs and show presence of particles below 100 nm, which partly arises from measurement artefacts in the size region below 20 nm.

From the distributions of the selected datasets the mean, median and modal diameters of the different concentration measured with repeatability standard deviation are determined from the measurement of the two different concentrations and plotted in Figure 12.

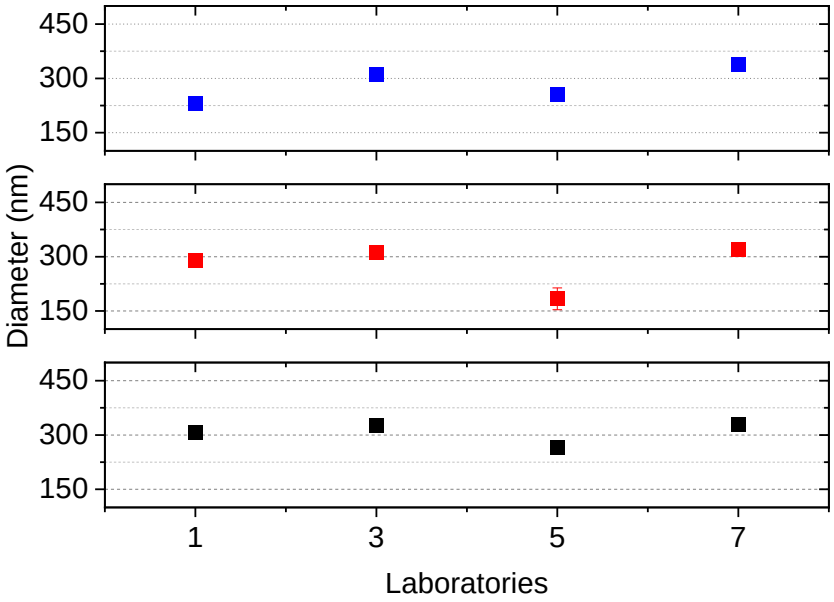

Figure 12: mean (blue), median (red) and modal (black) diameter with standard deviation of titanium oxide particles analysed with CLS.

To further evaluate the precision of the results of the ILC obtained on TiO_2 particles, the average values of the mean, median and modal diameters of the selected datasets were calculated as well as the reproducibility standard deviation σ_R of the mean, median and modal values and the relative standard deviation σ_r (=standard deviation/mean). These values are given in Table 16.

Table 16. Statistics of titanium oxide particles datasets

	$d_{3,St}$ (nm)	σ_R	σ_r
average (**mean**(diameter))	284	43.3	0.15
average (**median**(diameter))	276.4	55.4	0.2
average (**modal**(diameter))	307	25.9	0.08

The expanded reproducibility standard deviation is calculated by multiplying it with the coverage factor, k=2. Thus, the mean diameter of the TiO_2 particles is obtained as 284 ± 86.6 nm (30%), the median diameter is given by 276.4 ± 110.8 nm (40%) and the mode diameter is given by 307 ± 52 nm (17%).

CLS: Polystyrene particles (90/125 nm)

We received CLS measurements from three laboratories using three different kinds of centrifuges. An analytical ultracentrifuge was used from one lab, one lab used a disc CLS and one lab used a cuvette CLS. The obtained size distributions from the different centrifuges might not be comparable as different instrument setups with other detection systems were used. The laboratories were advised to measure two different concentration of the particle dispersion. It was recommended to use concentrations of 5 mg/ml and 2 mg/ml. The obtained normalized size distributions and the cumulative size distributions are shown in Figure 13. In the graphs the average size distribution of both concentrations is shown.

Table 17. Used concentrations and measurement conditions

Lab	Instrument	Centrifuge speed (rpm)	Concentration (mg/ml)	Gradient (wt%)
1	Lumisizer 6512-72	4000	1 + 2	-
5	Beckman XLI-80	55000 ramped	1 + 2	-
7	CPS DC 24000 UHR	22000	2 + 5	0-8

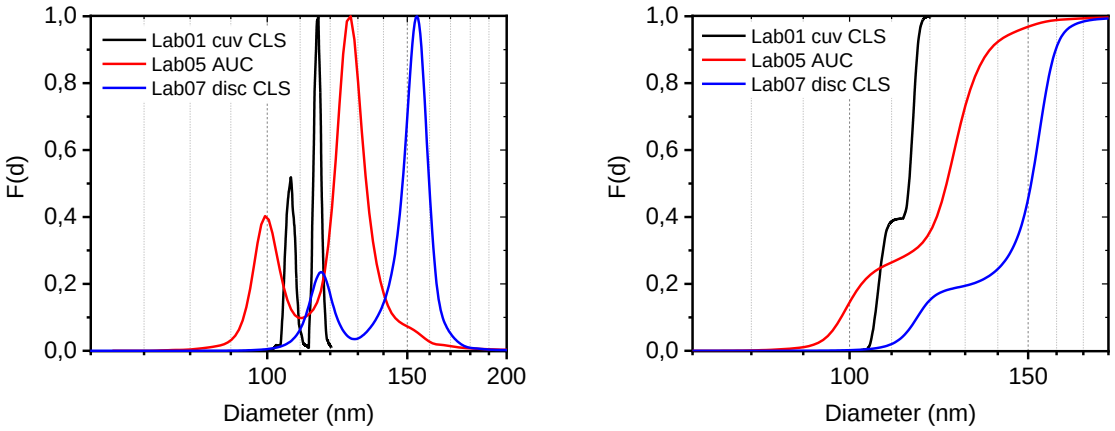

Figure 13: normalized (left) and cumulated (right) size distribution functions of the diameter of polystyrene nanoparticles (90/125 nm). All reported results are shown.

The size distribution between the different used centrifuges clearly differ. A reliable comparison of the size distributions cannot be done here. The data can only be compared to the expected size distribution for this particle system. From the measurement of Lab 01 with the cuvette CLS the derived mean and median diameters are as expected but the modal diameters are too high for the small particle population and too low for the bigger particle population. Low difference of the refractive index of the particles compared to the one of the measurement medium might be a cause. The particle system only yielded an evaluable measurement for the higher concentration. The measurement with the disc CLS delivers a generally too high particle diameter. The density difference of the particles compared to the measurement medium or the measurement gradient is rather low and leads in a higher uncertainty than usual here. The measurement from Lab 05 with the AUC delivers a size distribution, which is a little bit

too high but is still in the expected size range. The measured ratio of the particle populations differs for all measurements from the number based 1:1 ratio.

From the distributions of the selected datasets the mean, median and modal diameters of the different concentration measured with repeatability standard deviation are determined from the measurement of the two different concentrations and plotted in Figure 14. In case only one concentration was measured by a lab, only one diameter is depicted in the figure.

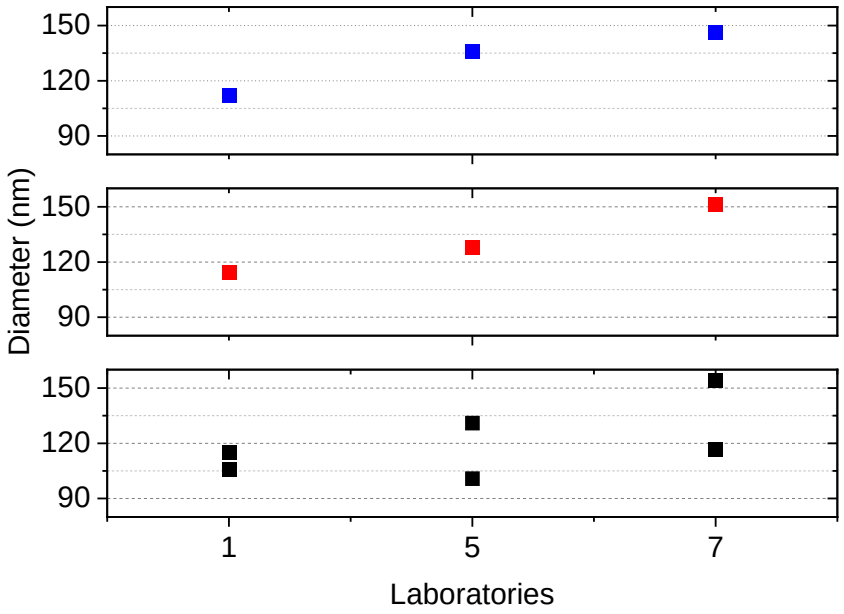

Figure 14: mean (blue), median (red) and modal (black) diameter with standard deviation of PSL particles (90/125 nm) analysed with CLS.

No further evaluation of the precision of the particles results obtained on PSL (90/125 nm) particles was done.

CLS: Polystyrene particles (80/800 nm)

We received CLS measurements from four laboratories using three different kinds of centrifuges. An AUC was used from one lab and two labs used a disc CLS. With the cuvette CLS no evaluable measurements could be obtained. The obtained size distributions from the different centrifuges might not be comparable as different instrument setups with other detection systems were used. The laboratories were advised to measure two different concentration of the particle dispersion. It was recommended to use concentrations of 5 mg/ml and 2 mg/ml. The obtained normalized size distributions and the cumulative size distributions are shown in Figure 15. In the graphs the average size distribution of both concentrations is shown.

Table 18. Used concentrations and measurement conditions

Lab	Instrument	Centrifuge speed (rpm)	Concentration (mg/ml)	Gradient (wt%)
1	Lumisizer 6512-72	4000	1 + 2	-
3	CPS DC 24000 UHR	22000	5 + 10	0-8
5	Beckman XLI-80	55000 ramped	0.1 + 0.2 + 0.5	-
7	CPS DC 24000 UHR	22000	2	0-8

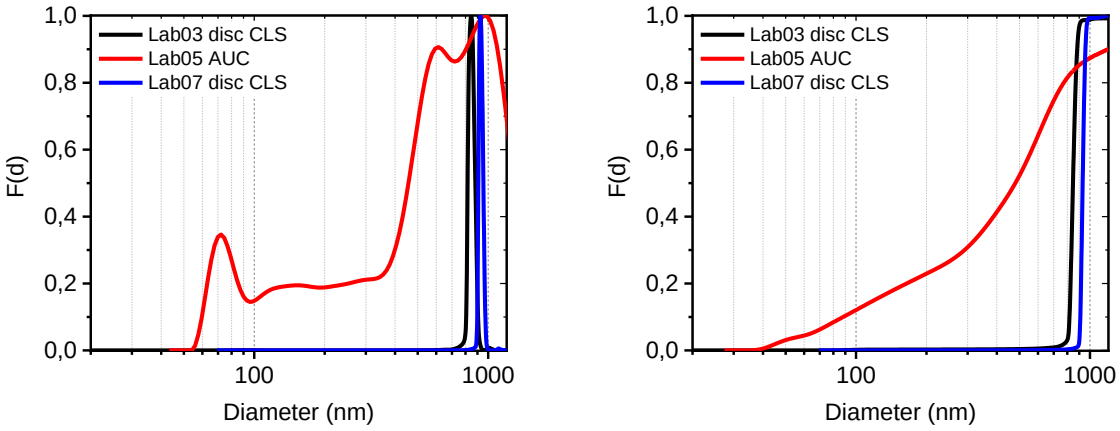

Figure 15: normalized (left) and cumulated (right) size distribution functions of the diameter of polystyrene particles (80/800 nm). All reported results are shown.

The size distribution from disc CLS and AUC clearly differ and also the measurement with disc CLS slightly differ from each other. Generally, the 80 nm particle population is not determined. With the AUC smaller particle populations below 800 nm are detected but all over the measurement range, which does not lead to a reliable determination of one particle population, the differing particle populations might arise due to agglomerated particles. Lab 07 just reported data for one particle concentration. Lab 03 and 07 only detected the 800 nm particle population, which differ from each other but are in the range of the standard deviation. The density difference of the particles and the measurement gradient is rather low and leads in a higher uncertainty than usual here.

From the distributions of the selected datasets the mean, median and modal diameters of the different concentration measured with repeatability standard deviation are determined from the measurement of

the two different concentrations and plotted in Figure 16. In case only one concentration was measured by a lab, only one diameter is depicted in the figure.

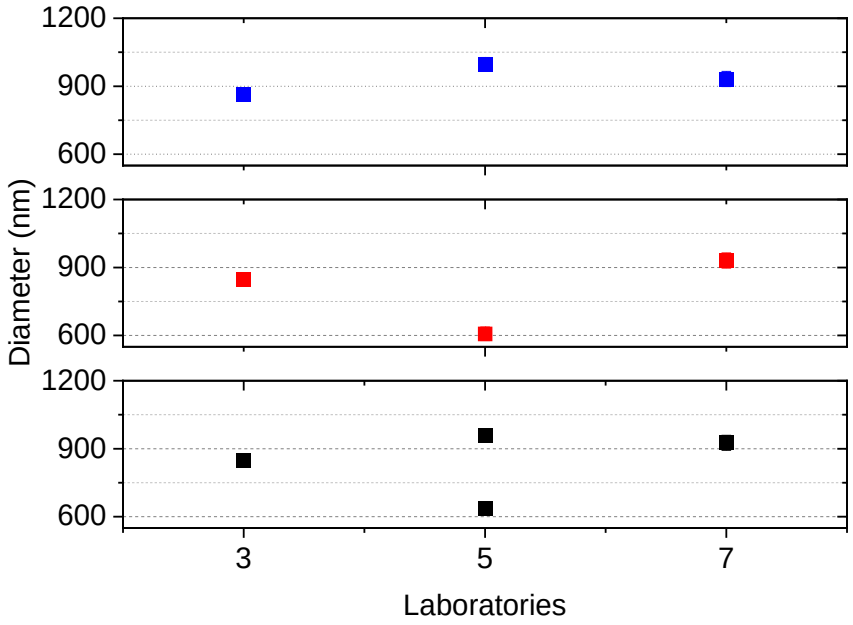

Figure 16: mean (blue), median (red) and modal (black) diameter of PSL particles (80/800 nm) analysed with CLS.

No reliable evaluation of the precision of the particles results obtained on PSL (80/800 nm) particles can be done as only few reported results with high variance are available. For the disc CLS the two available results for the 800 nm particles a modal diameter of 911 ± 56 nm is derived from all available results.

The expanded reproducibility standard deviation is calculated by multiplying reproducibility standard deviation with the coverage factor, k=2. This results in 911 ± 112 nm (12%).

CLS: Silver particles

We received CLS measurements from four laboratories using three different kinds of centrifuges. An AUC was used from one lab; two labs used a disc CLS and one lab used a cuvette CLS. The obtained size distributions from the different centrifuges might not be comparable as different instrument setups with other detection systems were used. The laboratories were advised to measure two different concentration of the particle dispersion. It was recommended to use concentrations of 100 µg/ml and 50 µg/ml. The obtained normalized size distributions and the cumulative size distributions are shown in Figure 17. In the graphs the average size distribution of both concentrations is shown.

Table 19. Used concentration and measurement conditions

Lab	Instrument	Centrifuge speed (rpm)	Concentration (µg/ml)	Gradient (wt%)
1	Lumisizer 6512-72	4000	50 + 60	-
3	CPS DC 24000 UHR	22000	50 + 100	8-24
5	Beckman XLI-80	55000 ramped	50 + 100	-
9	CPS DC 24000 UHR	22000	5 + 10	8-24

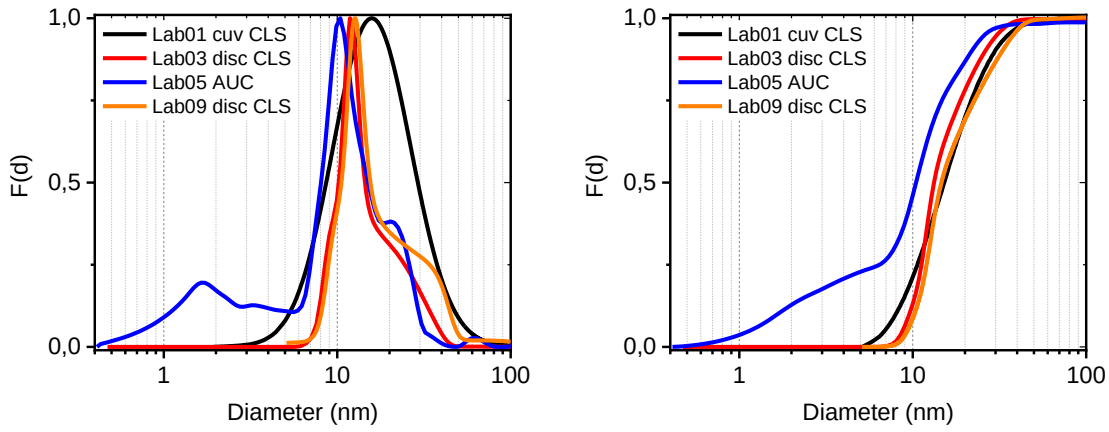

Figure 17: normalized (left) and cumulated (right) size distribution functions of the diameter of silver nanoparticles. All reported results are shown.

The size distribution from cuvette CLS, disc CLS and AUC show differences. The size distribution obtained by the cuvette CLS does not resolve the bimodal character of silver particles and the size distribution from AUC show an additional particle population in the range from 1-5 nm. The differences are small and might arise from the different instrumental setup, but generally the size distributions are comparable.

From the distributions of the selected datasets the mean, median and modal diameters of the different concentration measured with repeatability standard deviation are determined from the measurement of the two different concentrations and plotted in Figure 18.

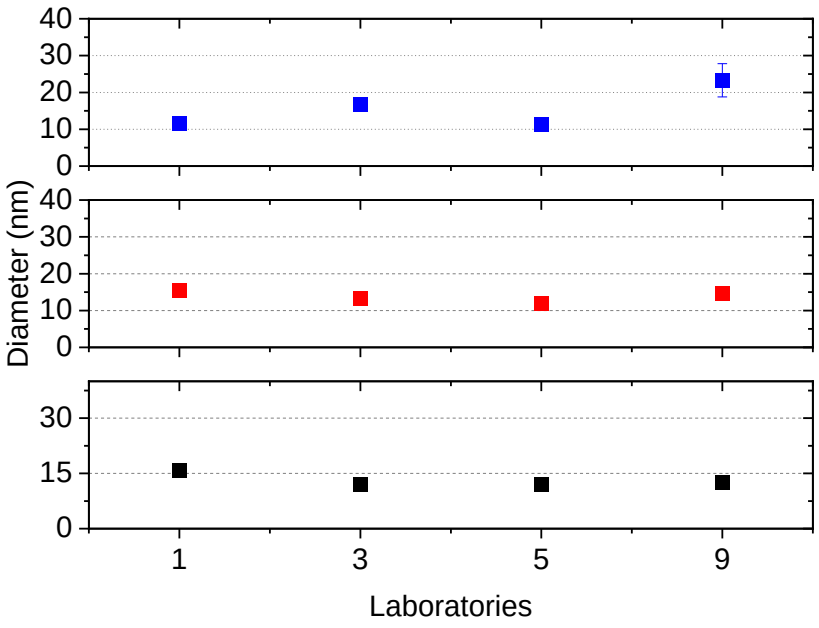

Figure 18: mean (blue), median (red) and modal (black) diameter of silver nanoparticles analysed with CLS.

To further evaluate the precision of the results of the ILC obtained on Ag particles, the average values of the mean, median and modal diameters of the selected datasets were calculated as well as the reproducibility standard deviation σ_R of the mean, median and modal values and the relative standard deviation σ_r (=standard deviation/mean). These values are given in Table 20.

Table 20. Statistics of silver nanoparticles datasets

	$d_{3,St}$ (nm)	σ_R	σ_r
average (**mean**(diameter))	15.7	5.3	0.34
average (**median**(diameter))	13.8	1.7	0.13
average (**modal**(diameter))	13.1	1.96	0.15

The expanded reproducibility standard deviation is calculated by multiplying it with the coverage factor, k=2. Thus, the mean diameter of the Ag particles is obtained as 15.7 ± 10.6 nm (67%), the median diameter is given by 13.8 ± 3.5 nm (25%) and the mode diameter is given by 13.1 ± 3.9 nm (30%).

CLS: Zinc oxide particles

We received CLS measurements from three laboratories using three different kinds of centrifuges. An AUC was used from one lab, one lab used a disc CLS and one lab used a cuvette CLS. Although the size distributions are obtained from the different centrifuges with a different instrument setup using other detection systems, the size distributions are generally good comparable. The laboratories were advised

to measure two different concentration of the particle dispersion. It was recommended to use concentrations of 2 mg/ml and 1 mg/ml. The obtained normalized size distributions and the cumulative size distributions are shown in Figure 19. In the graphs the average size distribution of both concentrations is shown. Details of the sonication procedure can be found in the appendix Table 83.

Table 21. Used concentrations and measurement conditions

Lab	Instrument	Centrifuge speed (rpm)	Concentration (mg/ml)	Gradient (wt%)
1	Lumisizer 6512-72	4000	0.5 + 0.75	-
3	CPS DC 24000 UHR	22000	1 + 2	8-24
5	Beckman XLI-80	55000 ramped	1 + 2	-

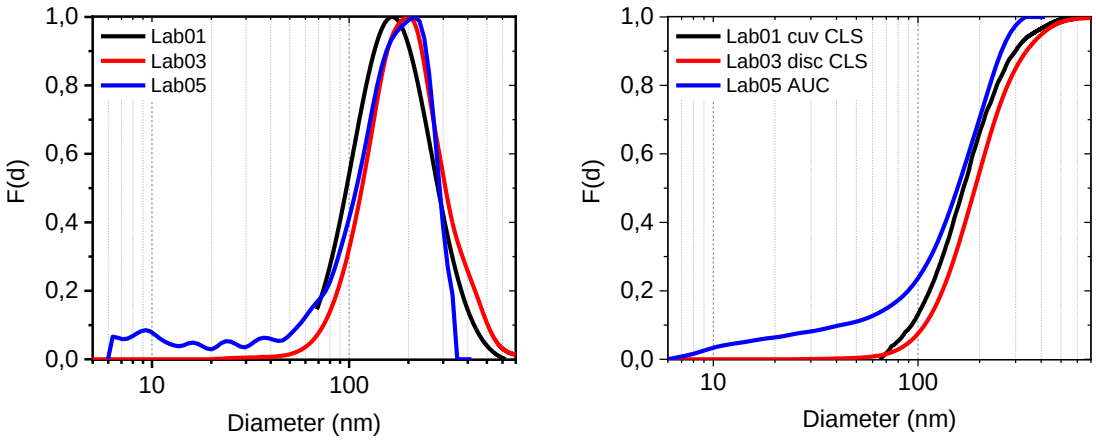

Figure 19: normalized (left) and cumulated (right) size distribution functions of the diameter of zinc oxide nanoparticles. All reported results are shown.

From the distributions of the selected datasets the mean, median and modal diameters of the different concentration measured with repeatability standard deviation are determined from the measurement of the two different concentrations and plotted in Figure 20.

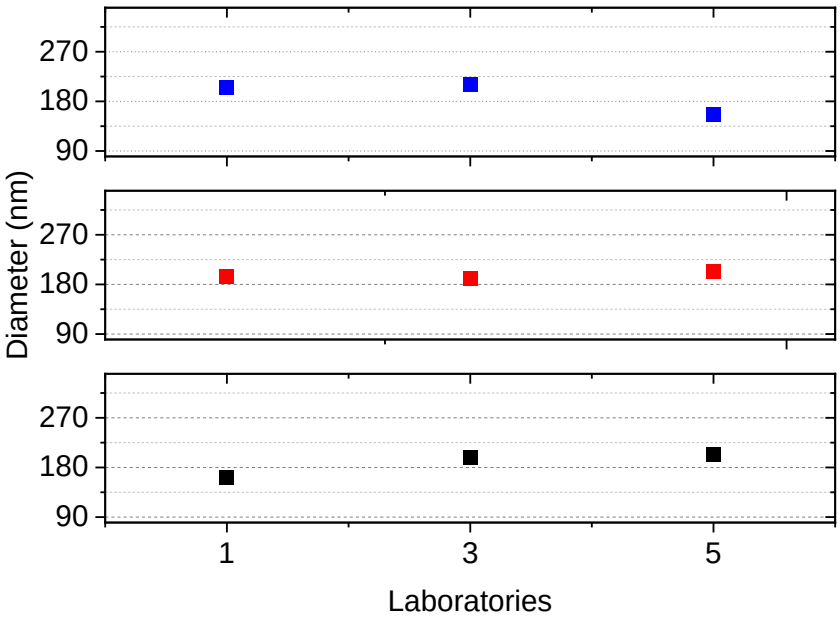

Figure 20: mean (blue), median (red) and modal (black) diameter of zinc oxide particles analysed with CLS.

To further evaluate the precision of the results of the ILC obtained on ZnO particles, the average values of the mean, median and modal diameters of the selected datasets were calculated as well as the reproducibility standard deviation σ_R of the mean, median and modal values and the relative standard deviation σ_r (=standard deviation/mean). These values are given in Table 22.

Table 22. Statistics of zinc oxide nanoparticles datasets

	$d_{3,St}$ (nm)	σ_R	σ_r
average (**mean**(diameter))	190.5	25.1	0.13
average (**median**(diameter))	196.5	7.5	0.04
average (**modal**(diameter))	188.2	19.1	0.1

The expanded reproducibility standard deviation is calculated by multiplying it with the coverage factor, k=2. Thus, the mean diameter of the ZnO particles is obtained as 190.5 ± 50.2 nm (26%), the median diameter is given by 196.5 ± 14.9 nm (8%) and the mode diameter is given by 188.2 ± 38.2 nm (20%).

Differential mobility analysis system - DMAS

For analysis with DMAS silica particles (20 nm and 50 nm), polystyrene particles (90/125 nm and 80/800 nm), titanium oxide and silver particles were sent out as powder or suspension. For the preparation of the measurement suspension a SOP was given. It was recommended to measure two different concentrations of each material. The shown size distribution is the average distribution of both concentrations. If a consistent concentration dependency between both concentrations was found it is mentioned in the respective paragraph to the size distribution of the material.

We received DMAS measurements from six laboratories. 24 results were handed in. In Table 23 an overview for the obtained diameters is given. The results of the DMAS measurements are presented for each particle system.

Table 23. Overview of the results for the mean, median and modal diameter determined via DMAS measurement. The reported expanded reproducibility standard deviation is calculated using a coverage factor of 2.

Particle system	# labs	$d_{0,emob,mean}$ (nm)	$d_{0,emob,median}$ (nm)	$d_{0,emob,modal}$ (nm)
Ag	6	19.1 ± 3.9	19.5 ± 4.7	22 ± 7.8
SiO_2 (20 nm)	5	21.6 ± 2.6	21.6 ± 2.8	21.9 ± 2.6
SiO_2 (50 nm)	5	57.7 ± 8	55.9 ± 4.5	55.6 ± 3.6
PSL (90/125 nm)	2	No reliable validation possible		94.7 ± 2/125.3 ± 7.5
TiO_2	3	238 ± 38.3	221.3 ± 40	243 ± 43.5
PSL (80/800 nm)	3	No reliable validation possible		774 ± 35

DMAS: Silica particles (20 nm)

We received DMAS measurements from five laboratories. For particle generation all laboratories used an electrospray device. The laboratories were advised to measure two different concentrations of the particle dispersion. It was recommended to use concentrations of 1 mg/ml and 0.5 mg/ml with electrospray particle generation and 0.1 mg/ml and 0.05 mg/ml with an atomizer for particle generation. The obtained normalized size distributions and the cumulative size distributions are shown in Figure 21. In the graphs the average size distribution of both concentrations is shown.

Table 24. Used concentration and flow rates for particle generation

Lab	concentration (mg/ml)	sheath flow (L/min)	aerosol flow (L/min)	particle generation
1	1 + 0.5	15	1.5	electrospray
5	1 + 0.5	15	1.5	electrospray
10	1 + 0.5	15	1.5	electrospray
19	1 + 0.5	10	1.2	electrospray
26	1 + 0.5	10	1.2	electrospray

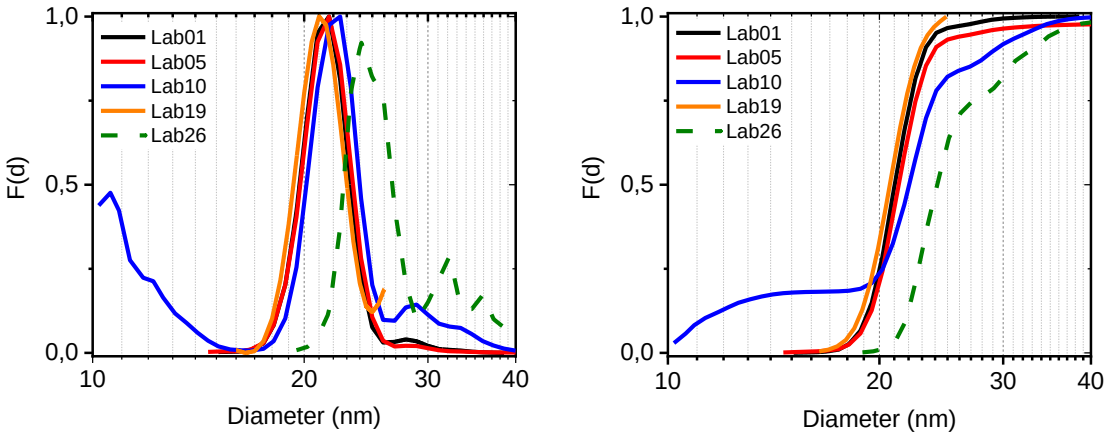

Figure 21 normalized (left) and cumulated (right) size distribution functions of the diameter of silica nanoparticles (20 nm). All reported results are shown.

Lab 10 reported the measurement data as received from the measurement. No correction of the background was done. In the distribution of Lab 10 the contribution of the stabilizing material is seen in the size range of 10-15 nm. For the determination of the mean, median and modal diameter this contribution was corrected. Furthermore, another contribution is seen in the particle range over 20 nm. There is another broad peak, which is typical when the concentration was chosen too high and agglomerates are present.

The size distribution from lab 26 clearly differs from the other reported distribution. It shows also a contribution from agglomerates and the curve is generally shifted to a higher particle size. The laboratory measured the particles with the recommended particle concentration. As the practicable useful concentration depends on the used instrument and settings it was furthermore recommended to adjust the concentration to own instrument. As this has not been done here for the further evaluation this measurement was excluded.

Lab 05 reported a mean diameter for one concentration which is clearly an outlier, which might arise from present agglomerates, although no big contribution is seen in the size distribution of the measurement. The mean diameter of this measurement is excluded from further evaluation.

From the distributions of the selected datasets the mean, median and modal diameters of the different concentration measured with repeatability standard deviation are determined from the measurement of the two different concentrations and plotted in Figure 22.

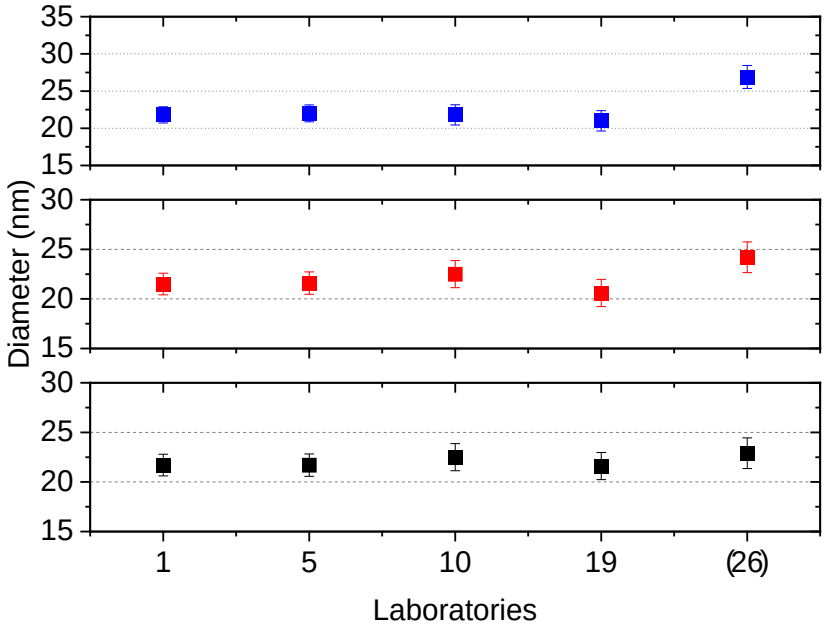

Figure 22: mean (blue), median (red) and modal (black) diameter with standard deviation of silica particles analysed with DMAS.

To further evaluate the precision of the results of the ILC obtained on SiO_2 (20 nm) particles, the average values of the mean and median diameters of the selected datasets were calculated as well as the reproducibility standard deviation σ_R of the mean and median values and the relative standard deviation σ_r (=standard deviation/mean). These values are given in Table 25.

Table 25. Statistics of silica (20 nm) nanoparticles datasets

	$d_{0,emob}$ (nm)	σ_R	σ_r
average(**mean**(diameter))	21.6	1.3	0.06
average(**median**(diameter))	21.6	1.4	0.07
average(**modal**(diameter))	21.9	1.3	0.06
average geometric standard deviation(diameter)	1.35	0.18	0.13

The expanded reproducibility standard deviation is calculated by multiplying it with the coverage factor, k=2. Thus, the mean diameter of the SiO_2 (20 nm) particles is obtained as 21.6 ± 2.6 nm (12%), the median diameter is given by 21.6 ± 2.8 nm (13%) and the mode diameter is given by 21.9 ± 2.6 nm (12%).

DMAS: Silica particles (50 nm)

We received DMAS measurements from five laboratories. The laboratories were advised to measure two different concentrations of the particle dispersion. It was recommended to use concentrations of 1 mg/ml and 0.5 mg/ml with electrospray particle generation and 0.1 mg/ml and 0.05 mg/ml with an atomizer for particle generation. The obtained normalized size distributions and the cumulative size distributions are shown in Figure 23. In the graphs the average size distribution of both concentrations is shown.

Table 26. Used concentrations and flowrates for particle generation

Lab	concentration (mg/ml)	sheath flow (L/min)	aerosol flow (L/min)	particle generation
1	1 + 0.5	15	1.5	electrospray
4	3	6	0.6	electrospray
5	1 + 0.5	10	1.5	electrospray
10	1 + 0.5	15	1.5	electrospray
19	1 + 0.5	10	1.2	electrospray
26	0.1 + 0.05	2	0.3	atomizer

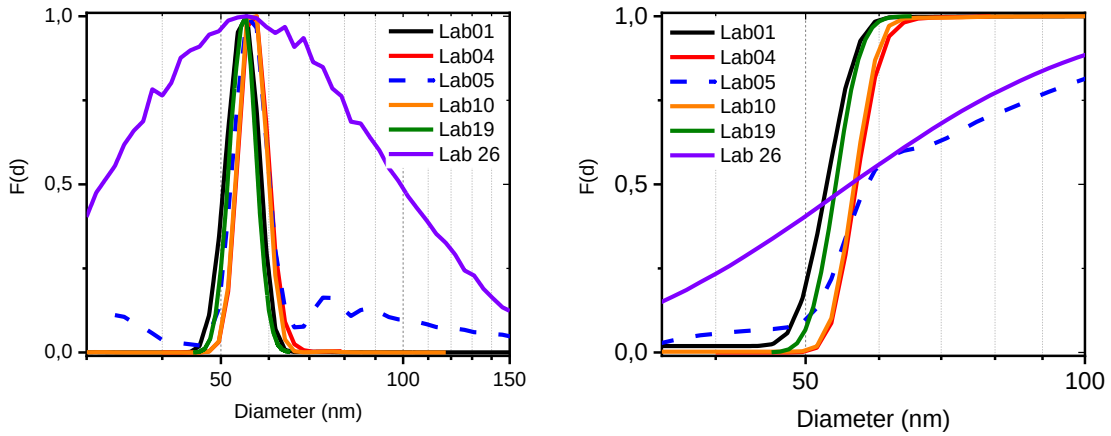

Figure 23: normalized (left) and cumulated (right) size distribution functions of the diameter of silica nanoparticles (50 nm). All reported results are shown.

The reported size distribution from Lab 05 shows the presence of particles in the size range over 60 nm. The broad peaks are normally seen when the concentration was chosen too high and agglomerates are present. Looking at the received particle size for the two different concentration measurement a concentration dependency is seen. For the further evaluation the average diameters of this measurement was excluded, but for the completeness it is still shown in Figure 24.

From the distributions of the selected datasets the mean, median and modal diameters of the different concentration measured with repeatability standard deviation are determined from the measurement of the two different concentrations and plotted in Figure 24.

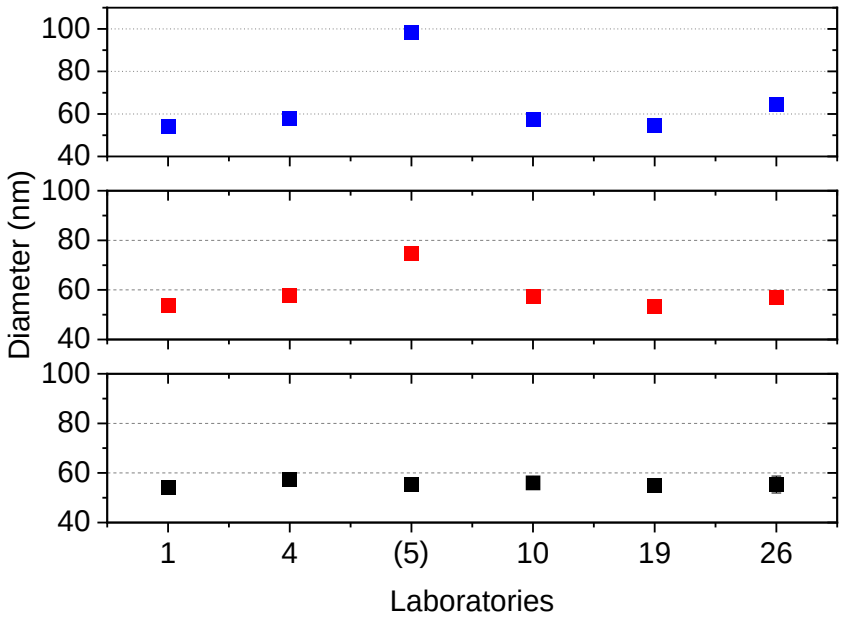

Figure 24: mean (blue), median (red) and modal (black) diameter of silica particles analysed with DMAS.

To further evaluate the precision of the results of the ILC obtained on SiO_2 (50 nm) particles, the average values of the mean and median diameters of the selected datasets were calculated as well as the reproducibility standard deviation σ_R of the mean and median values and the relative standard deviation σ_r (=standard deviation/mean). These values are given in Table 27.

Table 27. Statistics of silica (50 nm) nanoparticles datasets

	$d_{0,emob}$ (nm)	σ_R	σ_r
average(**mean**(diameter))	57.6	4.03	0.07
average(**median**(diameter))	55.9	2.26	0.04
average(**modal**(diameter))	55.6	1.8	0.03
average geometric standard deviation(diameter)	1.33	0.23	0.17

The expanded reproducibility standard deviation is calculated by multiplying it with the coverage factor, k=2.. Thus, the mean diameter of the SiO_2 (50 nm) particles is obtained as 57.6 ± 8 nm (14%), the median diameter is given by 55.9 ± 4.5 nm (8%) and the mode diameter is given by 55.6 ± 3.6 nm (6%).

DMAS: Titanium oxide particles

We received DMAS measurements from three laboratories. All labs used an Atomizer. The laboratories were advised to measure two different concentrations of the particle dispersion. It was recommended to use concentrations of 0.1 mg/ml and 0.05 mg/ml. The obtained normalized size distributions and the cumulative size distributions are shown in Figure 25. In the graphs the average size distribution of both concentrations is shown. Details of the sonication procedure can be found in the appendix Table 84.

Table 28. Used concentration and flow rates for particle generation

Lab	concentration (mg/ml)	sheath flow (L/min)	aerosol flow (L/min)	particle generation
1	18 + 13	3	0.3	atomizer
4	0.06	1.8	0.3	atomizer
26	6 + 3	2	0.3	atomizer

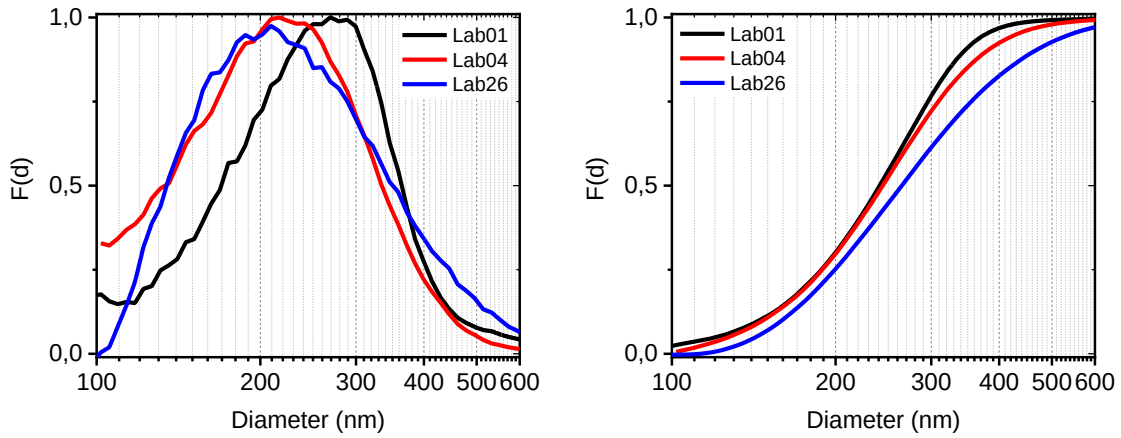

Figure 25 normalized (left) and cumulated (right) size distribution functions of the diameter of titanium oxide particles. All reported results are shown.

The obtained size distributions are generally in good comparison. For the evaluation of the particle size lab 26 subtracted the background. Lab 01 and 04 just cut off the received measurement. An overlap of the peak of the used stabilizer, ranging from abt. 10 to 50, with the particle peak cannot be fully excluded here, but as there is only a small overlap of the peaks the influence on the received size distribution isn´t high. In the draft TG the measurement of the background only is advised to be done before the measurement, but no advice for background is given and was added after the ILC.

From the distributions of the selected datasets the mean, median and modal diameters of the different concentration measured with repeatability standard deviation are determined from the measurement of the two different concentrations and plotted in Figure 26. In case only one concentration was measured by a lab, only one diameter is depicted in the figure.

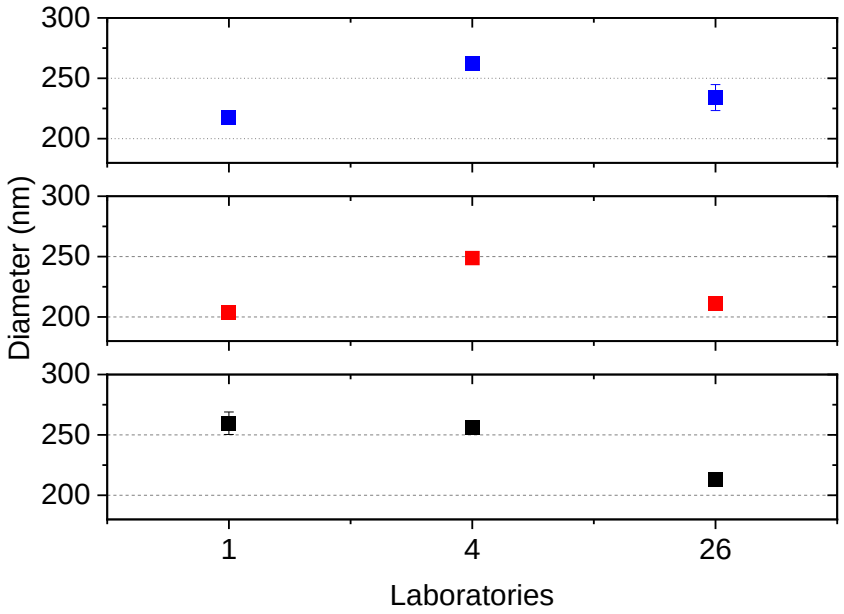

Figure 26: mean (blue), median (red) and modal (black) diameter of titanium oxide particles analysed with DMAS.

To further evaluate the precision of the results of the ILC obtained on TiO_2 particles, the average values of the mean and median diameters of the selected datasets were calculated as well as the reproducibility standard deviation σ_R of the mean and median values and the relative standard deviation σ_r (=standard deviation/mean). These values are given in Table 29.

Table 29. Statistics of titanium oxide particles datasets

	$d_{0,emob}$ (nm)	σ_R	σ_r
average(**mean**(diameter))	238	19.1	0.08
average(**median**(diameter))	221.3	19.8	0.09
average(**modal**(diameter))	243	21.8	0.09
average geometric standard deviation(diameter)	1.47	0.04	0.03

The expanded reproducibility standard deviation is calculated by multiplying it with the coverage factor, k=2. Thus, the mean diameter of the TiO_2 particles is obtained as 238 ± 38.3 nm (16%), the median diameter is given by 221.3 ± 40 nm (18%) and the mode diameter is given by 243 ± 44 nm (18%).

DMAS: Polystyrene particles (90/125 nm)

We received DMAS measurements from two laboratories. For particle generation Lab 01 used an atomizer and Lab 05 used an electrospray aerosol generator. The laboratories were advised to measure two different concentrations of the particle dispersion. It was recommended to use concentrations of 0.1 mg/ml and 0.05 mg/ml with an atomizer for particle generation. The obtained normalized size distributions and the cumulative size distributions are shown in Figure 27. In the graphs the average size distribution of both concentrations is shown.

Table 30. Used concentration and flow rates for particle generation

Lab	concentration (mg/ml)	sheath flow (L/min)	aerosol flow (L/min)	particle generation
1	1 + 0.5	15	1.5	atomizer
5	1 + 0.5	5	1.5	electrospray

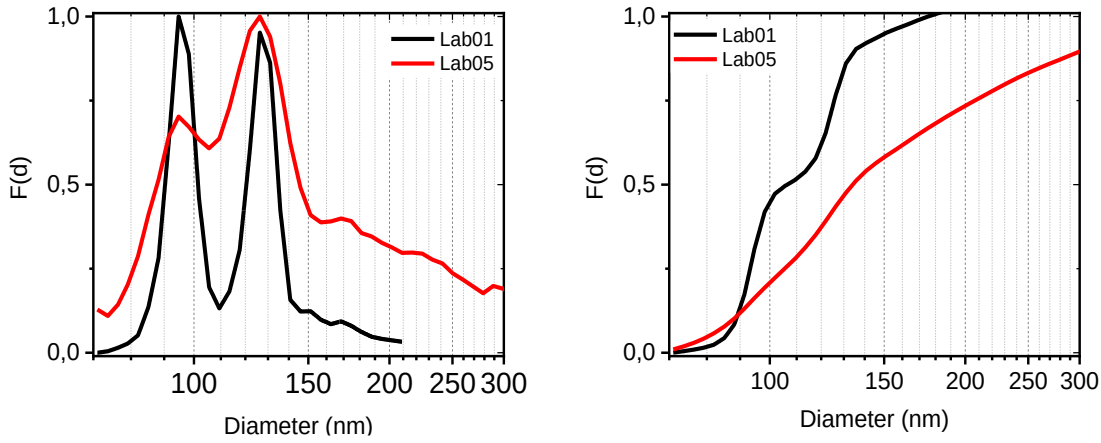

Figure 27: normalized (left) and cumulated (right) size distribution functions of the diameter of polystyrene particle (90/125 nm). All reported results are shown.

In both size distributions the two size populations of the particles are resolved. And the modal diameters are in good accordance. The mean and median diameter differ from each other, which might be due to contribution of agglomerates and/or contribution of the stabilizer to the size distribution by the measurement of Lab 05.

From the distributions of the selected datasets the mean, median and modal diameters of the different concentration measured with repeatability standard deviation are determined from the measurement of the two different concentrations and plotted in Figure 28.

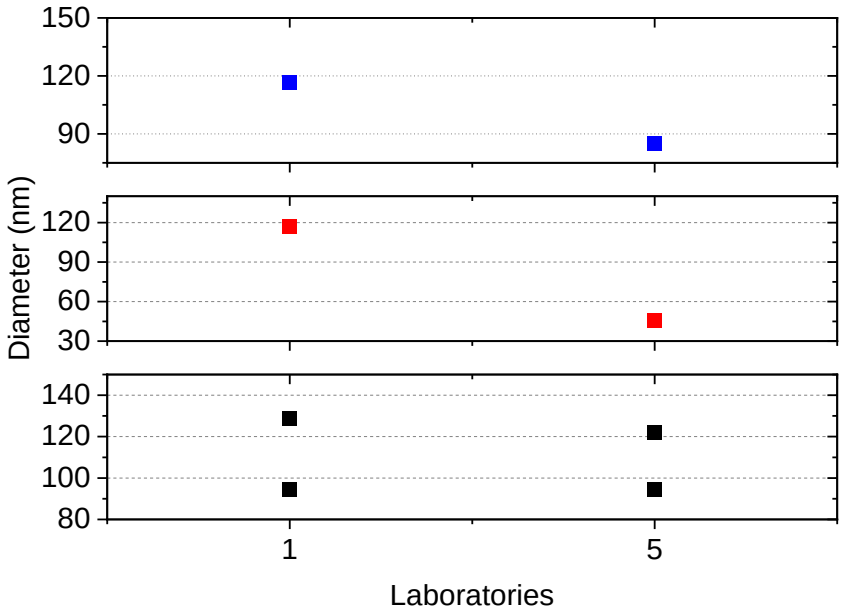

Figure 28: mean (blue), median (red) and modal (black) diameter of polystyrene particles (90/125 nm) analysed with DMAS.

No further evaluation of the precision of the results of the ILC obtained on polystyrene (90/125 nm) particles has been done as only rare data is available. Nevertheless, the derived modal diameters are in good comparison and with mode 1 given by 94.7 ± 1 nm and 125.3 ± 3.7 nm are in accordance with the expected diameters.

The expanded reproducibility standard deviation is calculated by multiplying reproducibility standard deviation with the coverage factor, k=2. This results in modal diameter of by 94.7 ± 2 nm (2%) and 125.3 ± 7.5 nm (6%).

DMAS: Polystyrene particles (80/800 nm)

We received DMAS measurements from three laboratories. All three labs used an atomizer for the particle generation. The laboratories were advised to measure two different concentrations of the particle dispersion. It was recommended to use concentrations of 0.1 mg/ml and 0.05 mg/ml with an atomizer for particle generation. The obtained normalized size distributions and the cumulative size distributions are shown in Figure 29. In the graphs the average size distribution of both concentrations is shown.

Table 31. Used concentration and flow rates for particle generation

Lab	concentration (mg/ml)	sheath flow (L/min)	aerosol flow (L/min)	particle generation
1	0.1 + 0.05	4.2	0.9	atomizer
4	0.03	1.8	0.3	atomizer
10	0.1 + 0.05	1.5	0.3	atomizer

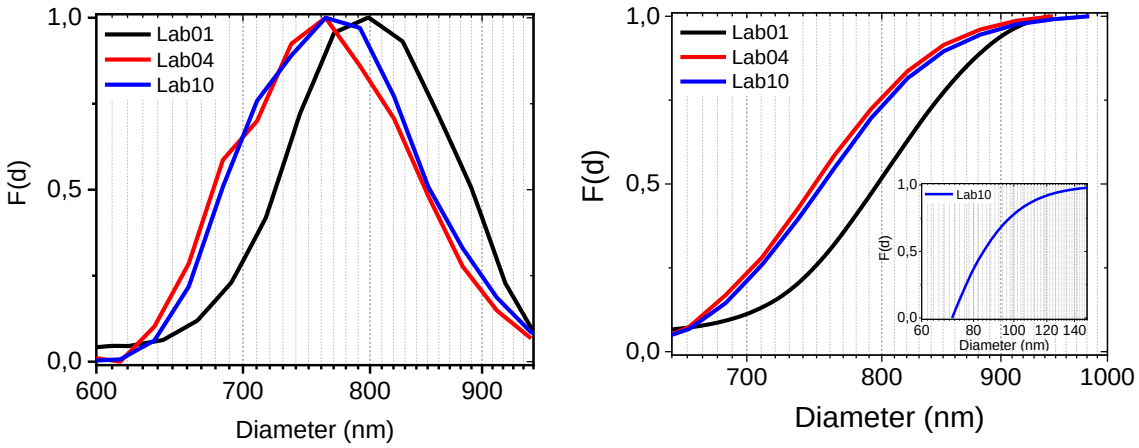

Figure 29: normalized (left) and cumulated (right) size distribution functions of the diameter of polystyrene particle (80/800 nm) for the 800 nm particle population. All reported results are shown.

Only Lab 10 was able to detect the 80 nm particle population. They measured the respective size range for each size population of the size mixture with different setting. Lab 01 and Lab 04 measured over the whole size range but were only able to detect the 800 nm fraction. A high peak ranging from 50 to 200 nm was removed from the size distribution from Lab 01, which originated from stabilizing material used for the dispersion. Lab 04 adjusted their measurement range for reporting to the 800 nm particle size population.

From the distributions of the selected datasets the mean, median and modal diameters of the different concentration measured with repeatability standard deviation are determined from the measurement of the two different concentrations and plotted in Figure 22.

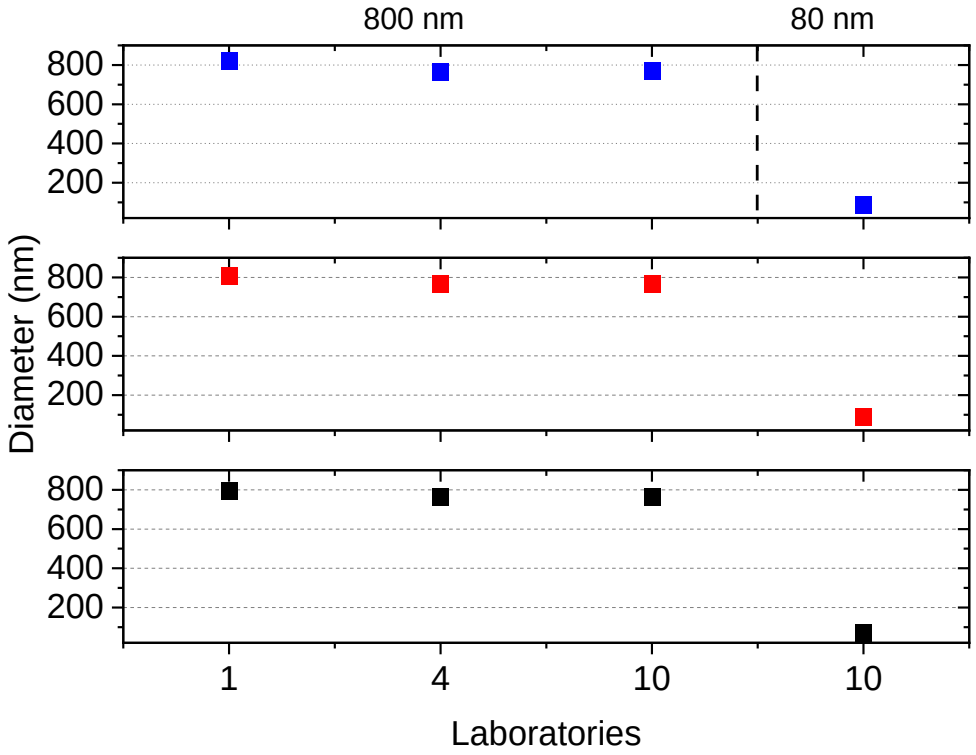

Figure 30: mean (blue), median (red) and modal (black) diameter of polystyrene particles (80/800 nm) analysed with DMAS. Lab 10 is shown twice because it was able to detect the 80 nm particles

No further evaluation of the particle size mixture has been done, as only one lab was able to detect the 80 nm particle size population. Nevertheless, the derived modal diameters for the 800 nm particles are in good comparison and with mode given by 774 ± 18 nm a good comparison to the expected diameter is given and shows a comparable and valid use of DMAS for particles with higher diameter up to 1000 nm.

The expanded reproducibility standard deviation is calculated by multiplying reproducibility standard deviation with the coverage factor, k=2. This results in a modal diameter of 774 ± 35 nm (5%).

DMAS: Silver particles

We received DMAS measurements from six laboratories. For particle generation all labs used an electrospray device. The laboratories were advised to measure two different concentrations of the particle dispersion. It was recommended to use concentrations of 100 µg/ml and 50 µg/ml with an Atomizer for particle generation. The obtained normalized size distributions and the cumulative size distributions are shown in Figure 31. In the graphs the average size distribution of both concentrations is shown.

Table 32. Used concentration and flow rates for particle generation

Lab	concentration (mg/ml)	sheath flow (L/min)	aerosol flow (L/min)	particle generation
1	100 + 50	15	1.5	electrospray
4	30	6	0.6	electrospray
5	50	5	1.5	electrospray
10	100 + 50	15	1.5	electrospray
19	100 + 50	10	1.2	electrospray
26	100 + 50	10	1.5	electrospray

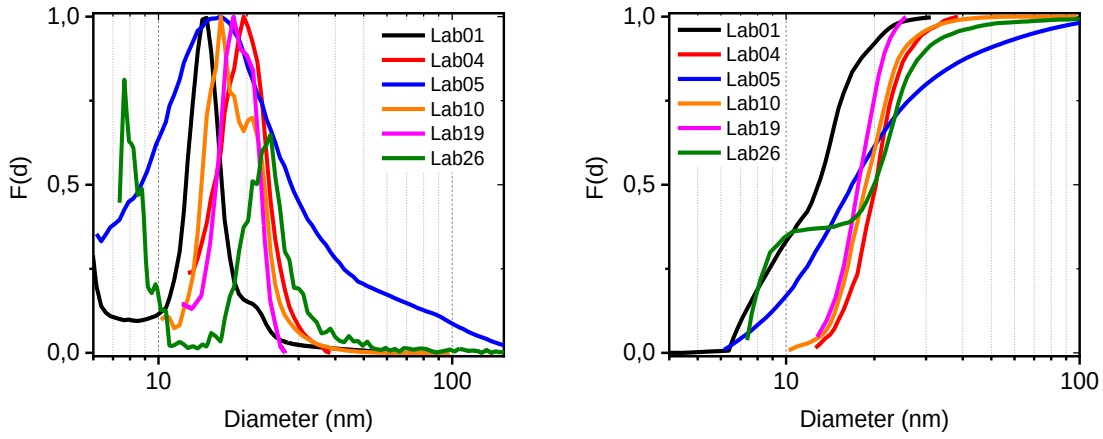

Figure 31: normalized (left) and cumulated (right) size distribution functions of the diameter of silver particles. All reported results are shown

An influence of a particle fraction below 10 nm is seen in the distribution of lab 01, 05 and 26. The other labs didn´t measure below 10 nm. So, the difference of the obtained size distributions for the labs that measured below 10 nm and those that do not is explainable.

From the distributions of the selected datasets the mean, median and modal diameters of the different concentration measured with repeatability standard deviation are determined from the measurement of the two different concentrations and plotted in Figure 32. In case only one concentration was measured by a lab, only one diameter is depicted in the figure.

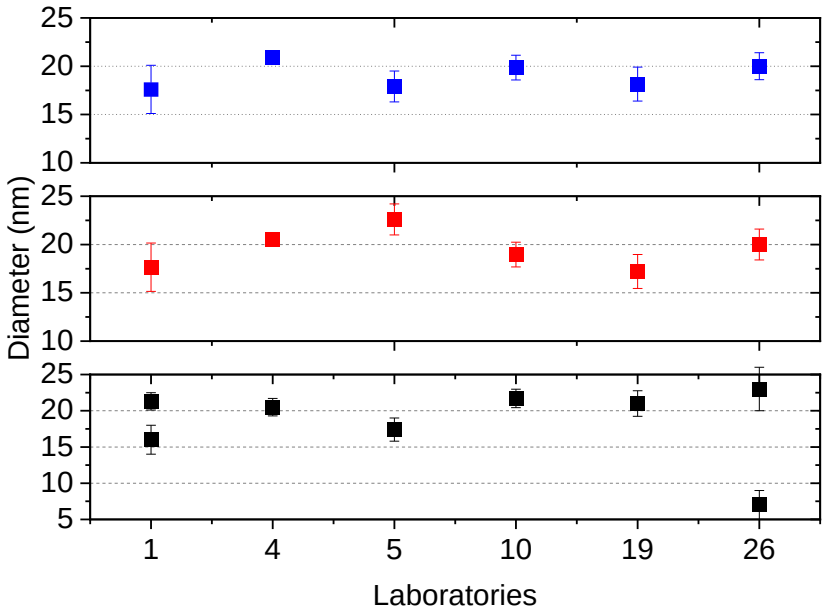

Figure 32: mean (blue), median (red) and modal (black) diameter of silver analysed with DMAS.

To further evaluate the precision of the results of the ILC obtained on Ag particles, the average values of the mean and median diameters of the selected datasets were calculated as well as the reproducibility standard deviation σ_R of the mean and median values and the relative standard deviation σ_r (=standard deviation/mean). These values are given in Table 33.

Table 33. Statistics of silver nanoparticles datasets

	$d_{0,emob}$ (nm)	σ_R	σ_r
average(**mean**(diameter))	19.1	1.9	0.1
average(**median**(diameter))	19.5	2.4	0.12
average(**modal**(diameter))	22	3.9	0.17
average geometric standard deviation(diameter)	1.5	0.25	0.17

The expanded reproducibility standard deviation is calculated by multiplying it with the coverage factor, k=2. Thus, the mean diameter of the Ag particles is obtained as 19.1 ± 3.9 nm (20%), the median diameter is given by 19.5 ± 4.7 nm (24%) and the mode diameter is given by 22 ± 7.7 nm (35%).

Dynamic Light Scattering – DLS

For analysis with DLS silica particles (20 nm and 50 nm), polystyrene particles (90/125 nm and 80/800 nm), zinc oxide, titanium oxide and silver particles were sent out as powder or suspension. For the preparation of the measurement suspension a SOP was given. It was recommended to measure two different concentrations of each material. The shown size distribution is the average distribution of both concentrations. If a concentration dependency between both concentrations was found it is mentioned in the respective paragraph to the size distribution of the material.

We received DLS measurements from 21 laboratories. 88 results were handed in. In Table 34 an overview for the obtained diameters is given. The results of the DLS measurements are presented for each particle system.

Table 34. Overview of the results for the mean, median and modal diameter determined via DLS measurement. The reported expanded reproducibility standard deviation is calculated using a coverage factor of 2.

Particle system	# labs	$d_{i,hyd,mean}$ (nm)	$d_{i,hyd,median}$ (nm)	$d_{i,hyd,modal}$ (nm)
Ag	15	34.8 ± 17.5	40.8 ± 18.2	6.2 ± 7 / 48 ± 21.3
SiO_2 (20 nm)	13	20.2 ± 2.2	19.4 ± 1.7	20.5 ± 3
SiO_2 (50 nm)	15	56.4 ± 7	55.2 ± 6.2	57.1 ± 10.9
PSL (90/125 nm)	7	119.8 ± 7.4	116.1 ± 8.1	120.5 ± 12
ZnO	15	260 ± 112	255 ± 90	252 ± 98
TiO_2	13	314 ± 132	301 ± 123	312 ± 139
PSL (80/800 nm)	10	805 ± 53	781 ± 80	808 ± 73

DLS: Silica particles (20 nm)

We received DLS measurements from 13 laboratories. The laboratories were advised to measure two different concentrations of the particle dispersion. It was recommended to use concentrations of 10 mg/ml and 5 mg/ml. The obtained normalized size distributions (intensity) and the cumulative size distributions (intensity) are shown in Figure 33. In the graphs the average size distribution of both concentrations is shown.

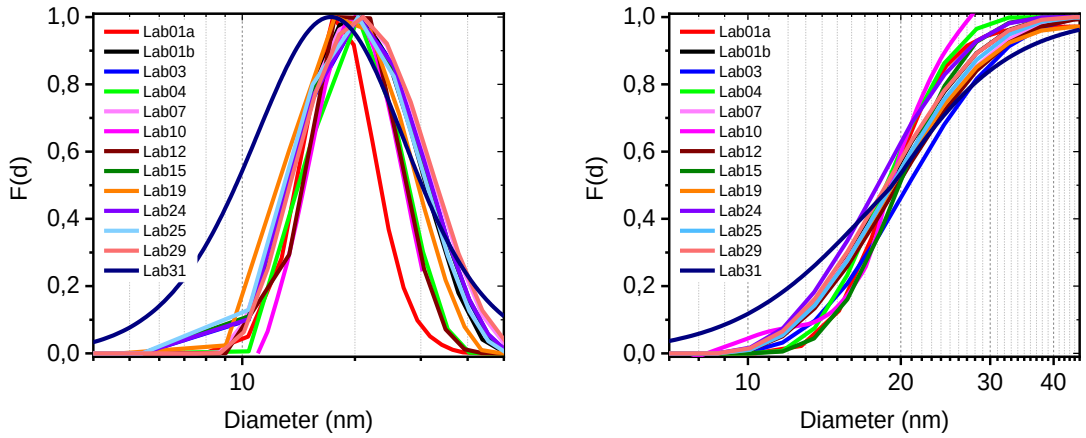

Figure 33: normalized (left) and cumulated (right) size distribution functions (intensity) of the diameter of silica nanoparticles (20 nm). All reported results are shown.

The particle size distribution of lab 31 slightly differs according to the measurements of the other labs. For data evaluation NICOMP algorithm was used. One lab used the frequency method and all other labs used NNLS, CONTIN algorithm or the cumulants method. As the measurement of Lab 31 was done without any deviation from the given protocol the deviation of the size distribution might arise from the used algorithm for data evaluation.

From the distributions of the selected datasets the mean, median and modal diameters of the different concentration measured with repeatability standard deviation are determined from the measurement of the two different concentrations and plotted in Figure 34.

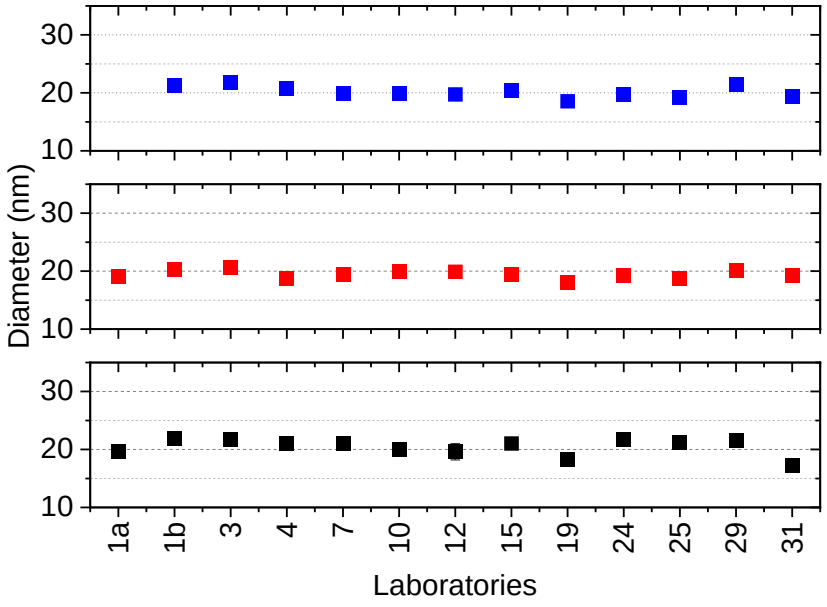

Figure 34: mean (blue), median (red) and modal (black) diameter of silica nanoparticles (20 nm) analysed with DLS. Lab 01a no mean diameter determined.

To further evaluate the precision of the results of the ILC obtained on SiO_2 (20 nm) particles, the average values of the mean, median and modal diameters of the selected datasets were calculated as well as the reproducibility standard deviation σ_R of the mean, median and mode values and the relative standard deviation σ_r (=standard deviation/mean). These values are given in Table 35.

Table 35. Statistics of silica (20 nm) nanoparticles datasets

	$d_{i,hyd}$ (nm)	σ_R	σ_r
average(**mean**(diameter))	20.2	1.1	0.05
average(**median**(diameter))	19.4	0.8	0.04
average(**modal**(diameter))	20.5	1.5	0.07

The expanded reproducibility standard deviation is calculated by multiplying it with the coverage factor, k=2. Thus, the mean diameter of the SiO_2 (20 nm) particles is obtained as 20.2 ± 2.2 nm (11%), the median diameter is given by 19.4 ± 1.7 nm (9%) and the modal diameter is given by 20.5 ± 3 nm (15%).

DLS: Silica particles (50 nm)

We received DLS measurements from 15 laboratories. The laboratories were advised to measure two different concentrations of the particle dispersion. It was recommended to use concentrations of 10 mg/ml and 5 mg/ml. The obtained normalized size distributions (intensity) and the cumulative size distributions (intensity) are shown in Figure 52. In the graphs the average size distribution of both concentrations is shown.

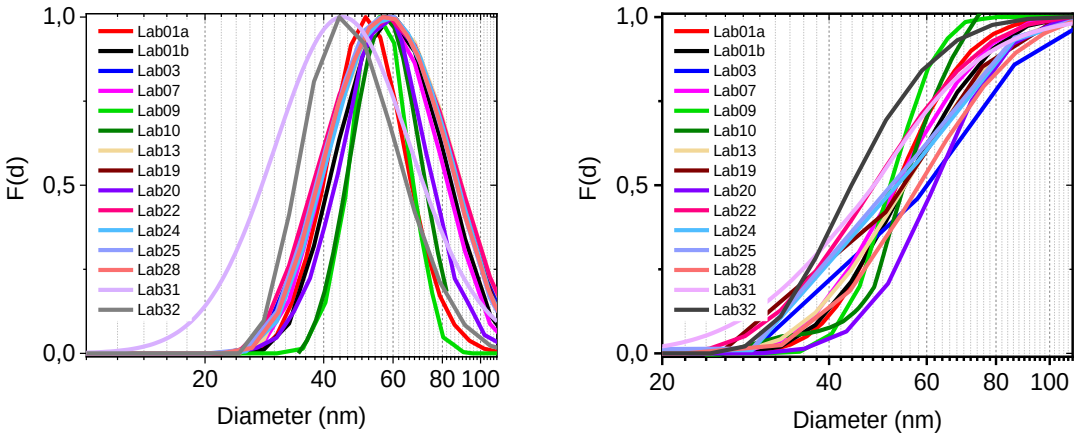

Figure 35: normalized (left) and cumulated (right) size distribution functions (intensity) of the diameter of silica nanoparticles (50 nm). All reported results are shown.

The particle size distribution of Lab 31 slightly differs according to the other measurements. For data evaluation NICOMP algorithm was used. Two labs used the frequency method and all other labs used NNLS, CONTIN algorithm or cumulants method. As the measurement of Lab 31 was done without any deviation from the given protocol the deviation of the size distribution might arise from the used algorithm for data evaluation.

From the distributions of the selected datasets the mean, median and modal diameters of the different concentration measured with repeatability standard deviation are determined from the measurement of the two different concentrations and plotted in Figure 36.

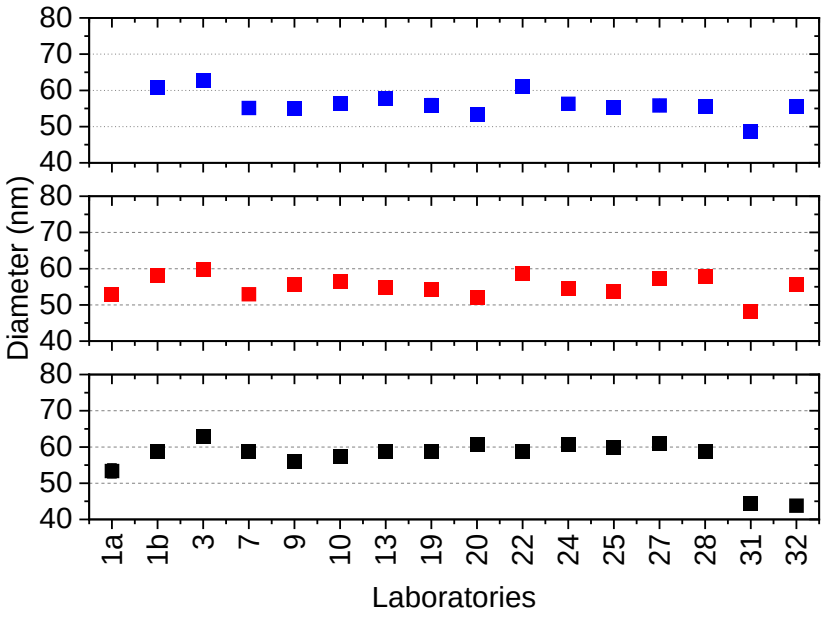

Figure 36: mean (blue), median (red) and modal (black) diameter of silica nanoparticles analysed with DLS. Lab 01a no mean diameter determined.

To further evaluate the precision of the results of the ILC obtained on SiO_2 (50 nm) particles, the average values of the mean, median and modal diameters of the selected datasets were calculated as well as the reproducibility standard deviation σ_R of the mean, median and modal values and the relative standard deviation σ_r (=standard deviation/mean). These values are given in Table 36.

Table 36. Statistics of silica (50 nm) nanoparticles datasets

	$d_{i,hyd}$ (nm)	σ_R	σ_r
average (**mean**(diameter))	56.4	3.5	0.07
average (**median**(diameter))	55.2	3.1	0.06
average (**modal**(diameter))	57.1	5.4	0.1

The expanded reproducibility standard deviation is calculated by multiplying it with the coverage factor, k=2.Thus, the mean diameter of the SiO_2 (50 nm) particles is obtained as 56.4 ± 7 nm (12%), the median diameter is given by 55.2 ± 6.1 nm (11%) and the modal diameter is given by 57.1 ± 11 nm (19%).

Titanium oxide particles

We received DLS measurements from 14 laboratories. The laboratories were advised to measure two different concentrations of the particle dispersion. It was recommended to use concentrations of 0.2 mg/ml and 0.1 mg/ml. The obtained normalized size distributions (intensity) and the cumulative size distributions (intensity) are shown in Figure 37. In the graphs the average size distribution of both concentrations is shown. Details of the sonication procedure can be found in the appendix Table 85.

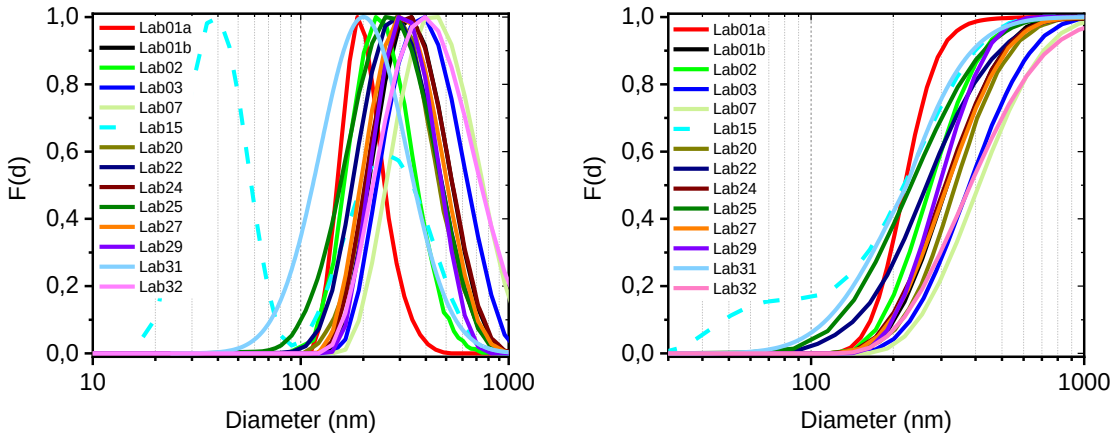

Figure 37: normalized (left) and cumulated (right) size distribution functions (intensity) of the diameter of titanium oxide particles. All reported results are shown.

Lab 15 detected a particle size fraction in the size range below 100 nm. From electron microscopic analyses it is known that just some very rare particles below 100 nm are present in the titanium oxide sample. The here obtained high particle fraction seems to be a contamination. For the further evaluation of the average diameters the measurement is excluded, but for the completeness is still shown in Figure 38.

Different algorithms were used for data evaluation: Two labs used the frequency method, one lab NICOMP, one lab Histogram, 8 labs used NNLS and two labs used cumulants. The use for cumulants method was not recommended, as the particles have a wide size distribution and cumulants is only for particles with a narrow size distribution.

From the distributions of the selected datasets the mean, median and modal diameters of the different concentration measured with repeatability standard deviation are determined from the measurement of the two different concentrations and plotted in Figure 38.

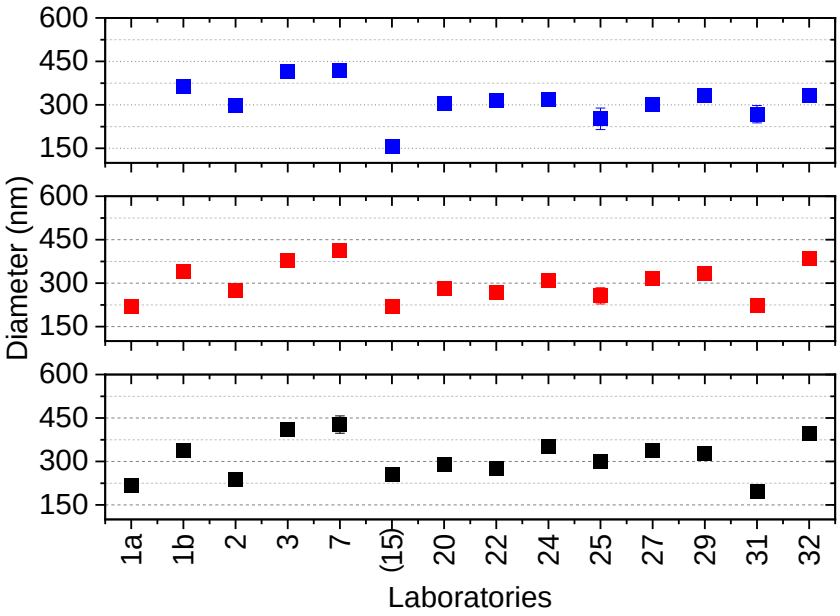

Figure 38: mean (blue), median (red) and modal (black) diameter of titanium oxide particles analysed with DLS. Lab 01a no mean diameter determined.

To further evaluate the precision of the results of the ILC obtained on TiO_2 particles, the average values of the mean, median and modal diameters of the selected datasets were calculated as well as the reproducibility standard deviation σ_R of the mean, median and modal values and the relative standard deviation σ_r (=standard deviation/mean). These values are given in Table 37.

Table 37. Statistics of titanium oxide articles datasets

	$d_{i,hyd}$ (nm)	σ_R	σ_r
average (**mean**(diameter))	314	66	0.21
average (**median**(diameter))	301	62	0.2
average (**modal**(diameter))	312	70	0.22

The expanded reproducibility standard deviation is calculated by multiplying it with the coverage factor, k=2.Thus, the mean diameter of the TiO_2 is obtained as 314 ± 134 nm (42%), the median diameter is given by 301 ± 123 nm (41%) and the modal diameter is given by 312 ± 139 nm (45%).

DLS: Polystyrene particles (90/125 nm)

We received DLS measurements from eight laboratories. The laboratories were advised to measure two different concentrations of the particle dispersion. It was recommended to use concentrations of 1 mg/ml and 0.5 mg/ml. The obtained normalized size distributions (intensity) and the cumulative size distributions (intensity) are shown in Figure 39. In the graphs the average size distribution of both concentrations is shown.

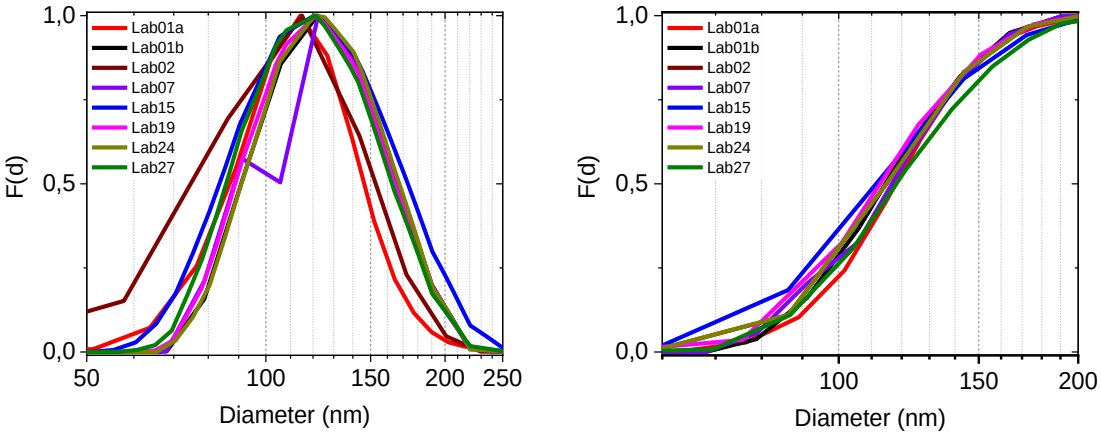

Figure 39: normalized (left) and cumulated (right) size distribution functions (intensity) of the diameter of polystyrene particles (90/125 nm). All reported results are shown.

For data evaluation NNLS algorithm, cumulants and the frequency method was used. The obtained size distributions are in good accordance. As expected, the different size populations of the particle size mixture could not be resolved with DLS.

From the distributions of the selected datasets the mean, median and modal diameters of the different concentration measured with repeatability standard deviation are determined from the measurement of the two different concentrations and plotted in Figure 40. Lab 01a reported no mean diameter.

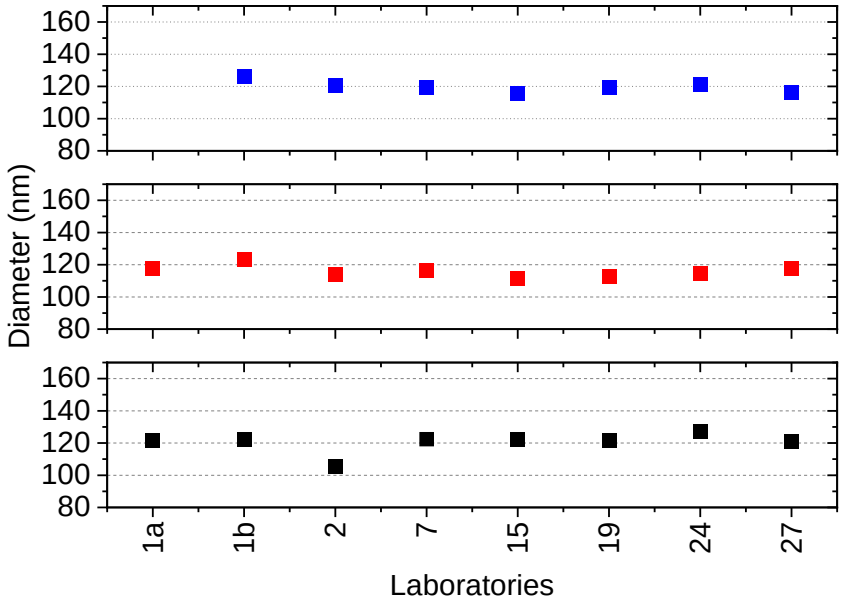

Figure 40: mean (blue), median (red) and modal (black) diameter of PSL particles (90/125 nm) analysed with DLS. Lab 01a no mean diameter determined.

To further evaluate the precision of the results of the ILC obtained on PSL (90/125 nm) particles, the average values of the mean, median and modal diameters of the selected datasets were calculated as well as the reproducibility standard deviation σ_R of the mean, median and modal values and the relative standard deviation σ_r (=standard deviation/mean). These values are given in Table 38.

Table 38. Statistics of polystyrene (90/125 nm) particles datasets

	$d_{i,hyd}$ (nm)	σ_R	σ_r
average (**mean**(diameter))	119.8	3.7	0.03
average (**median**(diameter))	116.1	4	0.03
average (**modal**(diameter))	120.4	6	0.05

The expanded reproducibility standard deviation is calculated by multiplying it with the coverage factor, k=2.Thus, the mean diameter of the PSL (90/125 nm) particles is obtained as 119.8 ± 7.4 nm (6%), the median diameter is given by 116.1 ± 8.1 nm (7%) and the modal diameter is given by 120.4 ± 12 nm (10%).

DLS: Polystyrene particles (80/800 nm)

The polystyrene particles are a size mixture of spherical particles with a size at around 80 and 800 nm with a ratio of 2:1. The particles were sent out as dispersion with a concentration of 10 mg/ml. The laboratories were advised to measure two different concentrations of the particle dispersion. It was recommended to use concentrations of 1 mg/ml and 0.5 mg/ml.

We received DLS measurements from eleven laboratories. The obtained normalized size distributions (intensity) and the cumulative size distributions (intensity) are shown in Figure 41. In the graphs the average size distribution of both concentrations is shown.

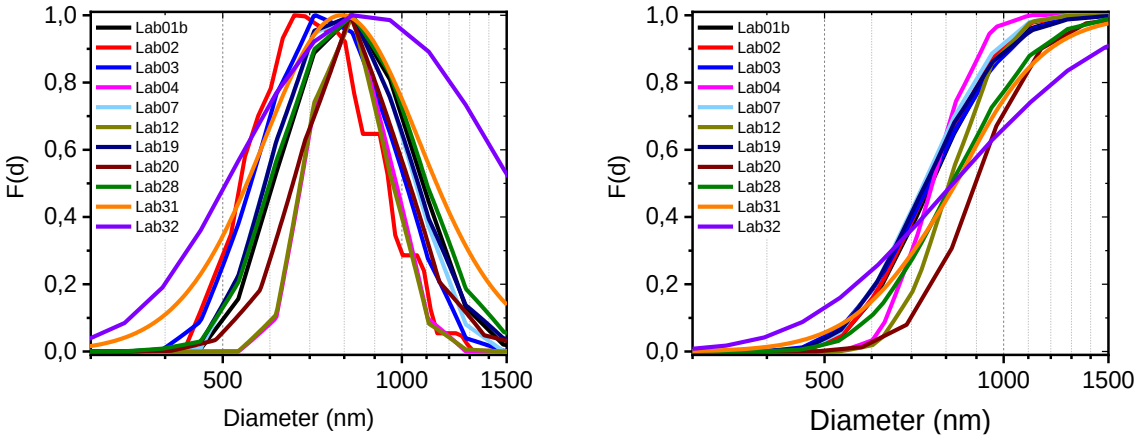

Figure 41: normalized (left) and cumulated (right) size distribution functions (intensity) of the diameter of polystyrene particles (80/800 nm). All reported results are shown.

For data evaluation NICOMP, CONTIN and NNLS algorithm, cumulants and the frequency method was used. The obtained size distributions are in good accordance. No lab was able to detect the 80 nm particle fraction. When preparing the PSL size mixture 80/800 nm freshly before the measurement, in principle, the 80 nm particles could be detected with DLS. Unfortunately, the particle dispersion was highly prone to agglomeration and only an evaluation of the 800 nm particles can be done.

From the distributions of the selected datasets the mean, median and modal diameters of the different concentration measured with repeatability standard deviation are determined from the measurement of the two different concentrations and plotted in Figure 42.

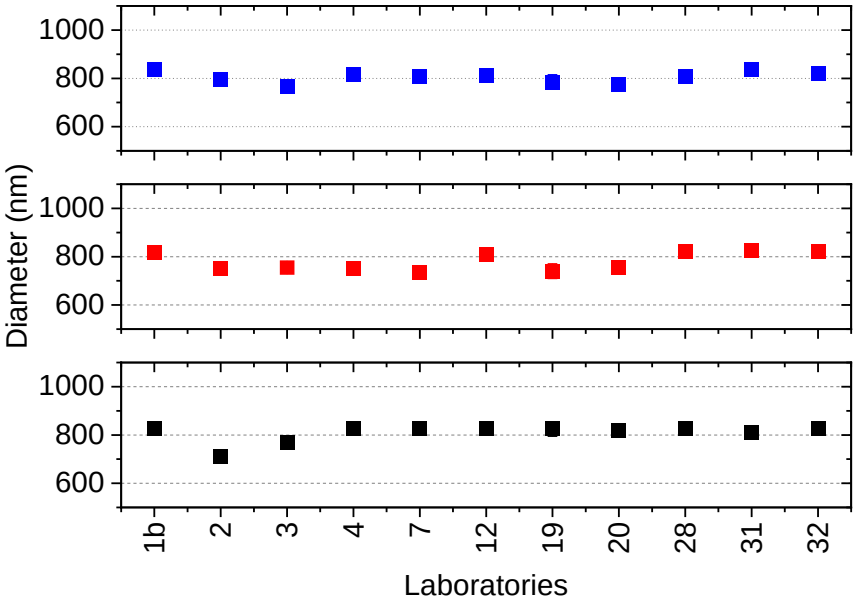

Figure 42: mean (blue), median (red) and modal (black) diameter of PSL particles (80/800 nm) analysed with DLS.

To further evaluate the precision of the results of the ILC obtained on PSL (80/800 nm) particles, the average values of the mean, median and modal diameters of the selected datasets were calculated as well as the reproducibility standard deviation σ_R of the mean, median and modal values and the relative standard deviation σ_r (=standard deviation/mean). These values are given in Table 39.

Table 39. Statistics of polystyrene (80/800 nm) particles datasets

	$d_{i,hyd}$ (nm)	σ_R	σ_r
average (**mean**(diameter))	805	26.5	0.03
average (**median**(diameter))	781	40	0.05
average (**modal**(diameter))	808	37	0.05

The expanded reproducibility standard deviation is calculated by multiplying it with the coverage factor, k=2. Thus, the mean diameter of the PSL (80/800 nm) particles is obtained as 805 ± 53 nm (7%), the median diameter is given by 782 ± 80 nm (10%) and the modal diameter is given by 808 ± 73 nm (9%).

DLS: Silver particles

We received DLS measurements from 16 laboratories. The laboratories were advised to measure two different concentrations of the particle dispersion. It was recommended to use concentrations of 100 µg/ml and 50 µg/ml. The obtained normalized size distributions (intensity) and the cumulative size distributions (intensity) are shown in Figure 43. In the graphs the average size distribution of both concentrations is shown.

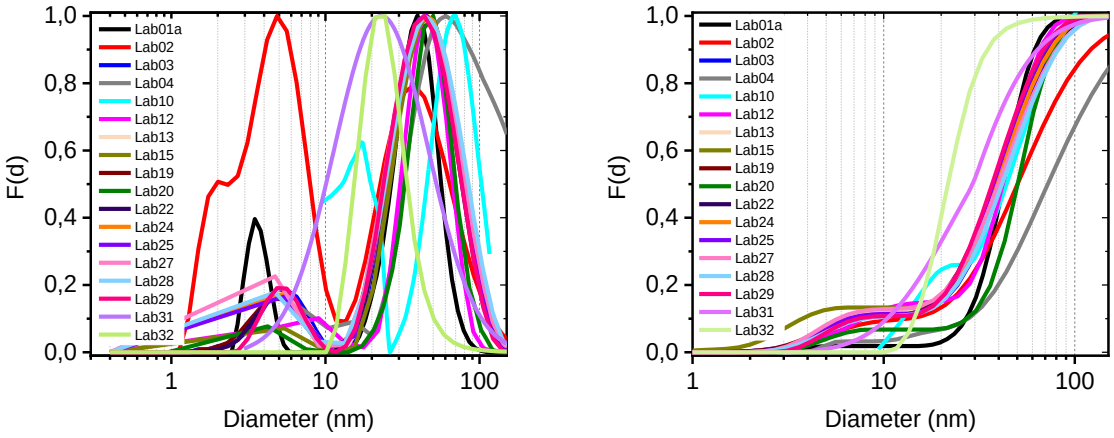

Figure 43: normalized (left) and cumulated (right) size distribution functions (intensity) of the diameter of silver nanoparticles. All reported results are shown.

For data evaluation NICOMP, CONTIN and NNLS algorithm, cumulants and the frequency method was used. The use of cumulants method was not recommended, as the particles have a wide size distribution and cumulants is only for particles with a narrow size distribution. Except lab 15 the size distribution shows a small size fraction in the range from 3-10 nm and a high size fraction in the range of 30-50 nm. For measurements of Lab 4 an inconsistency is seen in between the measurements for different concentrations. As the obtained diameters are outliers, the measurement is excluded for the further evaluation of the average diameters, but for completeness the diameters are still shown in Figure 44.

From the distributions of the selected datasets the mean, median and modal diameters of the different concentration measured with repeatability standard deviation are determined from the measurement of the two different concentrations and plotted in Figure 44.

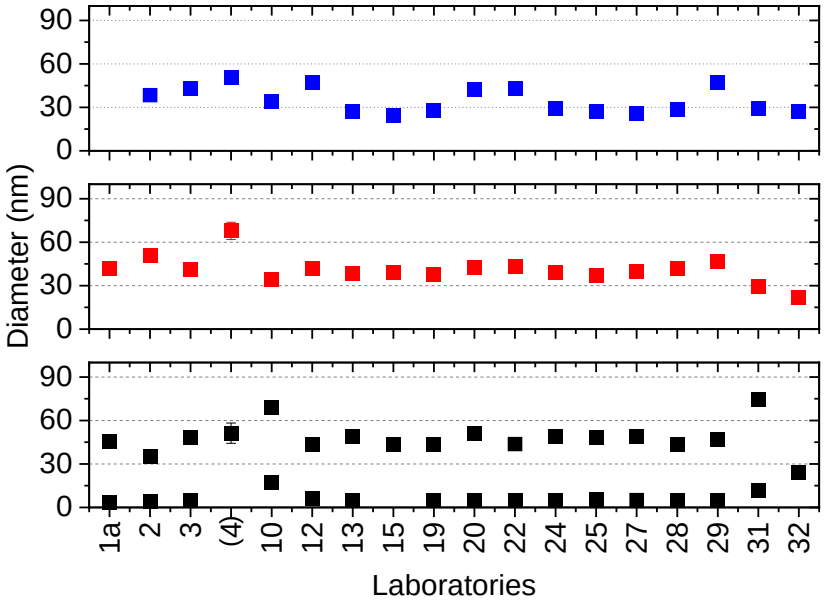

Figure 44: mean (blue), median (red) and modal (black) diameter of silver nanoparticles analysed with DLS. Lab 01a no mean diameter determined.

To further evaluate the precision of the results of the ILC obtained on Ag particles, the average values of the mean, median and modal diameters of the selected datasets were calculated as well as the reproducibility standard deviation σ_R of the mean, median and modal values and the relative standard deviation σ_r (=standard deviation/mean). These values are given in Table 40.

Table 40. Statistics of silver nanoparticles datasets

	$d_{i,hyd}$ (nm)	σ_R	σ_r
average (**mean**(diameter))	34.8	8.8	0.25
average (**median**(diameter))	40.8	9.1	0.22
average (**modal 1**(diameter))	6.2	3.5	0.5
average (**modal 2**(diameter))	48	10.7	0.22

The expanded reproducibility standard deviation is calculated by multiplying it with the coverage factor, k=2. Thus, the mean diameter of the Ag particles is obtained as 34.8 ± 17.5 nm (50%), the median diameter is given by 40.8 ± 18.2 nm (44%) and the modal diameters are given as 1: 6.2 ± 7 nm (113%) and 2: 48 ± 21.3 nm (45%).

DLS: Zinc oxide particles

We received DLS measurements from 16 laboratories. The laboratories were advised to measure two different concentrations of the particle dispersion. It was recommended to use concentrations of 1 mg/ml and 0.5 mg/ml. The obtained normalized size distributions (intensity) and the cumulative size distributions (intensity) are shown in Figure 45. In the graphs the average size distribution of both concentrations is shown. Details of the sonication procedure can be found in the appendix Table 86.

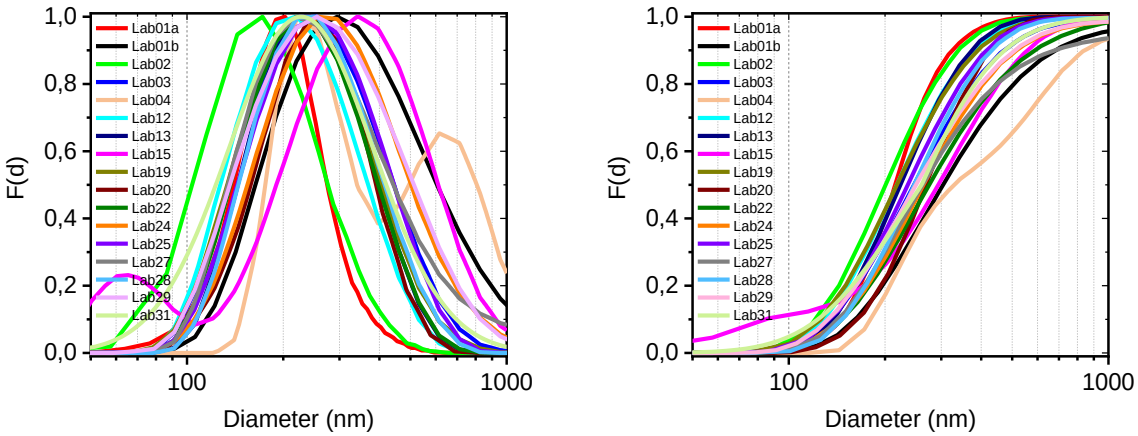

Figure 45: normalized (left) and cumulated (right) size distribution functions (intensity) of the diameter of zinc oxide particles. All reported results are shown.

For data evaluation Histogram, NICOMP, CONTIN and NNLS algorithm, cumulants and the frequency method was used. The use of the cumulants method was not recommended, as the particles have a wide size distribution and cumulants is only for particles with a narrow size distribution.

From the distributions of the selected datasets the mean, median and modal diameters of the different concentration measured with repeatability standard deviation are determined from the measurement of the two different concentrations and plotted in Figure 46.

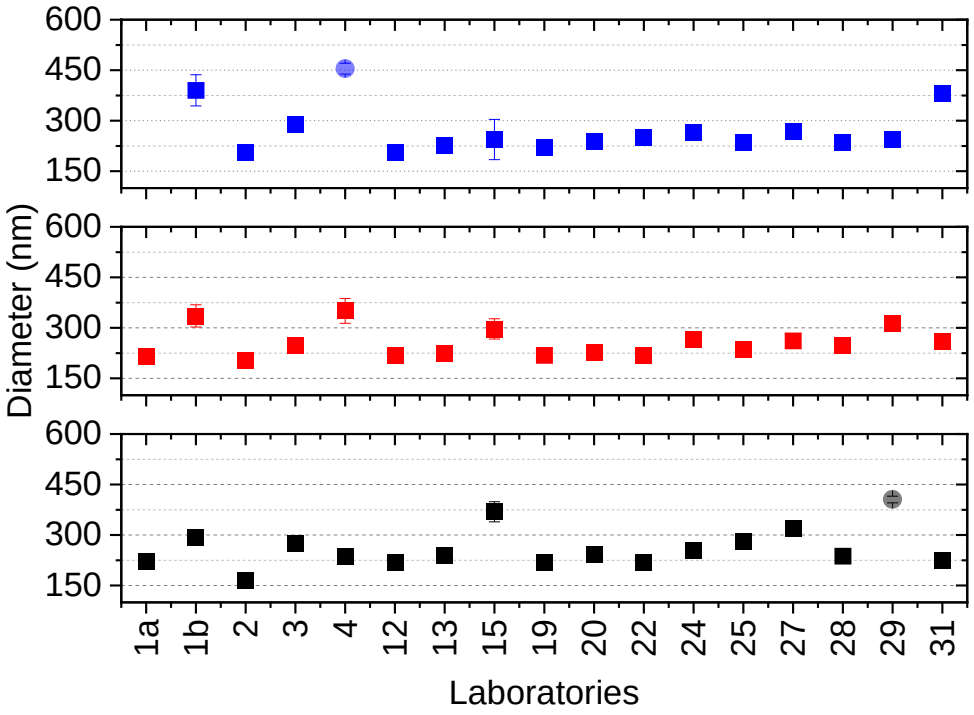

Figure 46: mean (blue), median (red) and modal (black) diameter with repeatability standard deviation of zinc oxide particles analysed with DLS. Lab 01a no mean diameter determined. Lab 04 only reported the mean diameter for a higher concentration sample, Lab 29 reported a modal diameter which was not in accordance with the reported distribution. Both values were excluded from the further evaluation.

To further evaluate the precision of the results of the ILC obtained on ZnO particles, the average values of the mean, median and modal diameters of the selected datasets were calculated as well as the reproducibility standard deviation σ_R of the mean, median and modal values and the relative standard deviation σ_r (=standard deviation/mean). These values are given in Table 41.

Table 41. Statistics of zinc oxide nanoparticles datasets

	$d_{i,hyd}$ (nm)	σ_R	σ_r
average (**mean**(diameter))	260	56	0.22
average (**median**(diameter))	255	45	0.18
average (**modal**(diameter))	252	48	0.19

The expanded reproducibility standard deviation is calculated by multiplying it with the coverage factor, k=2. Thus, the mean diameter of the ZnO is obtained as 260 ± 112 nm (46%), the median diameter is given by 255 ± 90 nm (35%) and the modal diameter is given by 252 ± 96 nm (38%).

Particle Tracking Analysis - PTA

For analysis with polystyrene particles (90/125 nm), zinc oxide, titanium oxide and silver particles were sent out as powder or suspension. For the preparation of the measurement suspension a SOP was given. It was recommended to measure two different concentrations of each material. The shown size distribution is the average distribution of both concentrations. If a concentration dependency between both concentrations was found it is mentioned in the respective paragraph to the size distribution of the material.

We received PTA measurements from six different laboratories. For the four particle systems overall 17 results were handed in. In Table 42 an overview for the obtained diameters is given. The results of the AFM measurements are presented for each particle system and individual data set.

Table 42. Overview of the results for the mean, median and modal diameter determined via PTA measurement. The reported expanded reproducibility standard deviation is calculated using a coverage factor of 2.

Particle system	# labs	$d_{0,hyd,mean}$ (nm)	$d_{0,hyd,median}$ (nm)	$d_{0,hyd,modal}$ (nm)
Ag	5	52 ± 24	41.3 ± 12.6	39.9 ± 15.8
PSL (90/125 nm)	3	122.7 ± 27	115.2 ± 16	93.3 ± 4/117.8 ± 17.5
ZnO	4	No reliable validation possible		
TiO_2	5	No reliable validation possible		

PTA: Titanium oxide particles

We received PTA measurements from six laboratories. The laboratories were advised to measure two different concentrations of the particle dispersion. It was recommended to use a dilution to 10^6 to 10^9 particles/ml. The obtained normalized size distributions and the cumulative size distributions are shown in Figure 47 for both concentrations. Lab 15 just measured one concentration. Details of the sonication procedure can be found in the appendix Table 87.

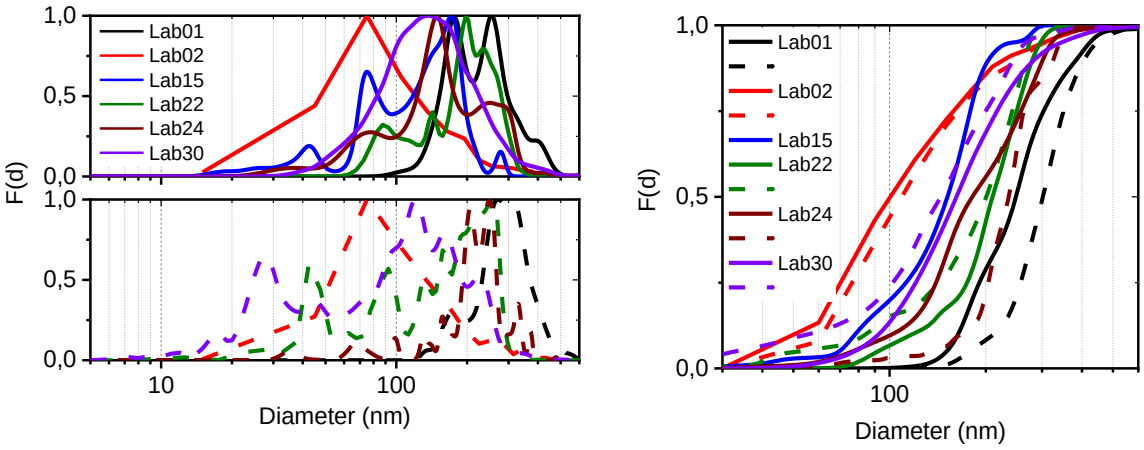

Figure 47: normalized (left) and cumulated (right) size distribution functions of the diameter of titanium oxide particles. All reported results are shown. Dashed line lower concentration.

High variance in the obtained particle size distributions is observed. The protocol was fulfilled by all the participants.

From the distributions of the selected datasets the mean, median and modal diameters of the different concentration measured with repeatability standard deviation are determined from the measurement of the two different concentrations and plotted in Figure 48.

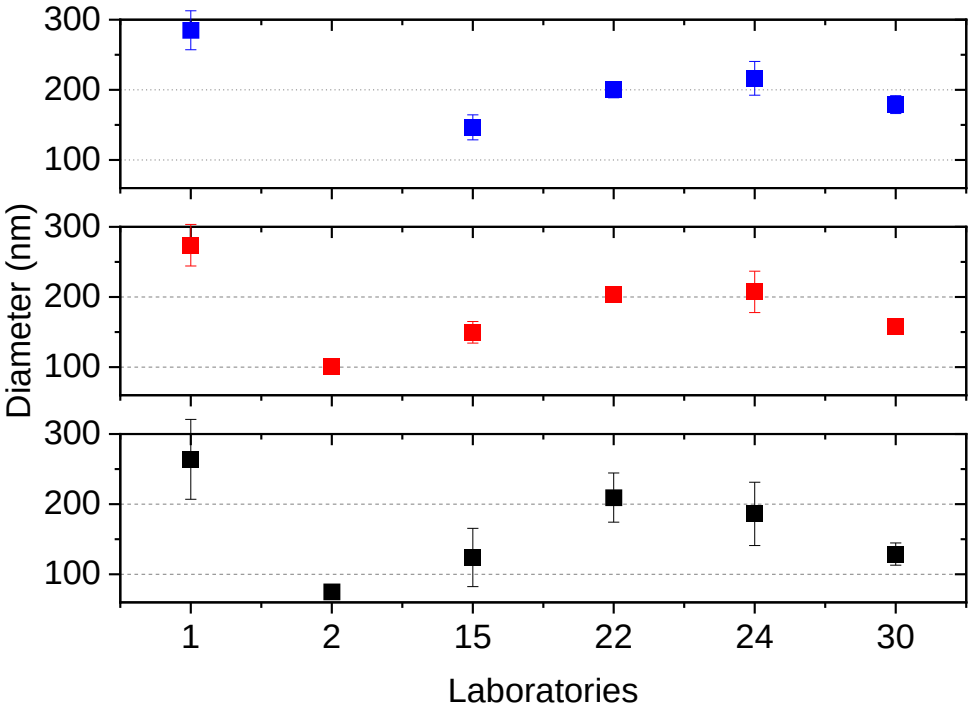

Figure 48: mean (blue), median (red) and modal (black) diameter with repeatability standard deviation of titanium oxide particles analysed with PTA. No mean diameter reported for Lab 02.

No further evaluation of the precision of the results of the ILC obtained on titanium oxide particles has been done as the obtained particle size distribution from the labs are not in comparison with each other and deviate from the results of other methods.

PTA: Polystyrene particles (90/125 nm)

We received PTA measurements from four laboratories. The laboratories were advised to measure two different concentrations of the particle dispersion. It was recommended to use a dilution to 10^6 to 10^9 particles/ml. The obtained normalized size distributions and the cumulative size distributions are shown in Figure 49 for both concentrations. Lab 15 just measured one concentration.

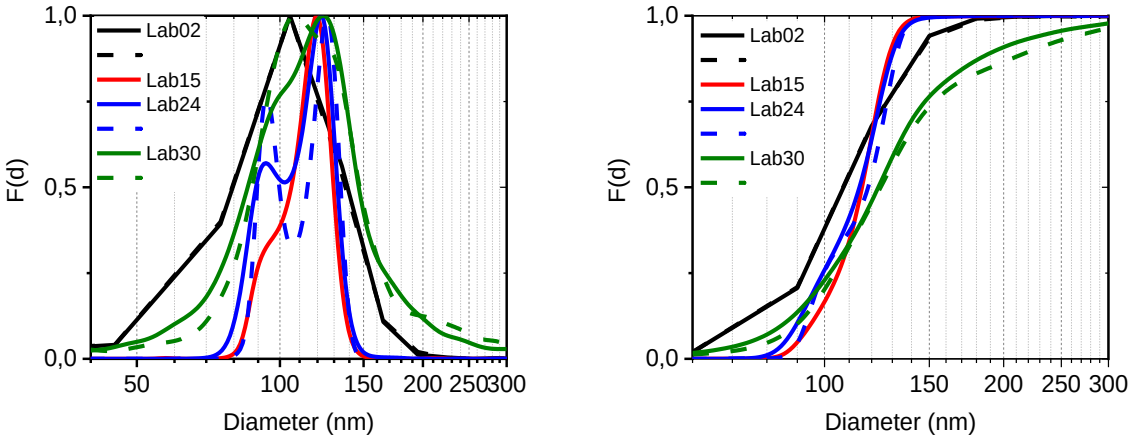

Figure 49: normalized (left) and cumulated (right) size distribution functions of the diameter of polystyrene particles (90/125 nm). All reported results are shown. Dashed line lower concentration.

The different size population of the particle fraction are only partly resolved. A reliable differentiation is not possible. The size distribution from Lab 30 is reproducible in the lab with a different concentration but slightly differs from the distributions of the other labs. Nevertheless, the obtained mean, median and modal diameter are in accordance to those of the other labs.

From the distributions of the selected datasets the mean, median and modal diameters of the different concentration measured with repeatability standard deviation are determined from the measurement of the two different concentrations and plotted in Figure 50.

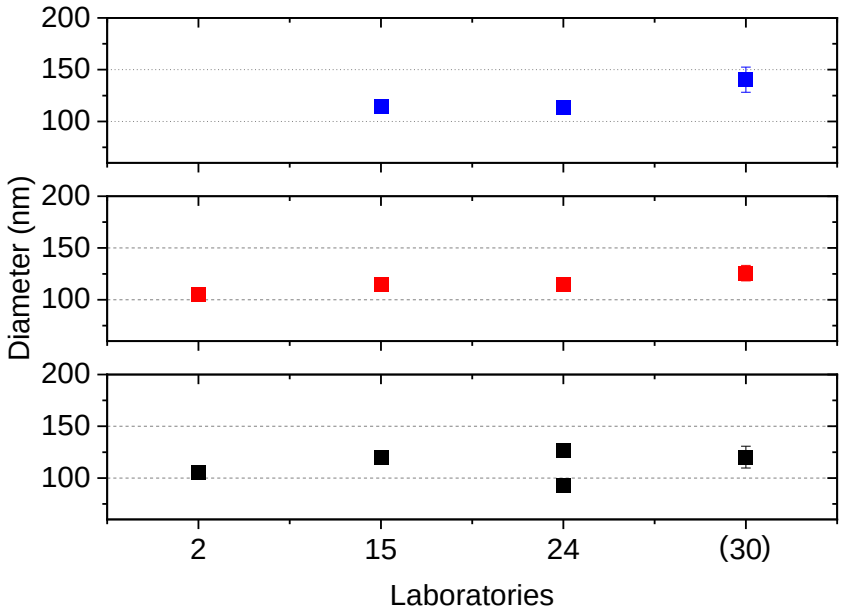

Figure 50: mean (blue), median (red) and modal (black) diameter with repeatability standard deviation of polystyrene particles (90/125 nm) analysed with PTA. No mean diameter reported for Lab 02.

To further evaluate the precision of the results of the ILC obtained on polystyrene (90/125 nm) particles, the average values of the mean and median diameters of the selected datasets were calculated as well as the reproducibility standard deviation σ_R of the mean and median values and the relative standard deviation σ_r (=standard deviation/mean). These values are given in Table 43.

Table 43. Statistics of polystyrene (90/125 nm) nanoparticles datasets

	$d_{0,hyd}$ (nm)	σ_R	σ_r
average(**mean**(diameter))	122.8	13.4	0.11
average(**median**(diameter))	115	7.9	0.11
average(**modal(1)**(diameter))	93.3	2	0.03
average(**modal(2)**(diameter))	117.8	8.8	0.08

The expanded reproducibility standard deviation is calculated by multiplying it with the coverage factor, k=2. Thus, the mean diameter of the PSL (90/125 nm) particles is obtained as 122.8 ± 26.8 nm (22%) and the median diameter is given by 115 ± 15.9 nm (14%). The modal diameters are for mode 1 93.3 ± 4 nm (4%) and for mode 2 117.8 ± 17.6 nm (15%).

PTA: Silver particles

We received PTA measurements from six laboratories. The laboratories were advised to measure two different concentrations of the particle dispersion. It was recommended to use a dilution to 10^6 to 10^9 particles/ml. The obtained normalized size distributions and the cumulative size distributions are shown in Figure 51 for both concentrations. Lab 1 and 15 just measured one concentration.

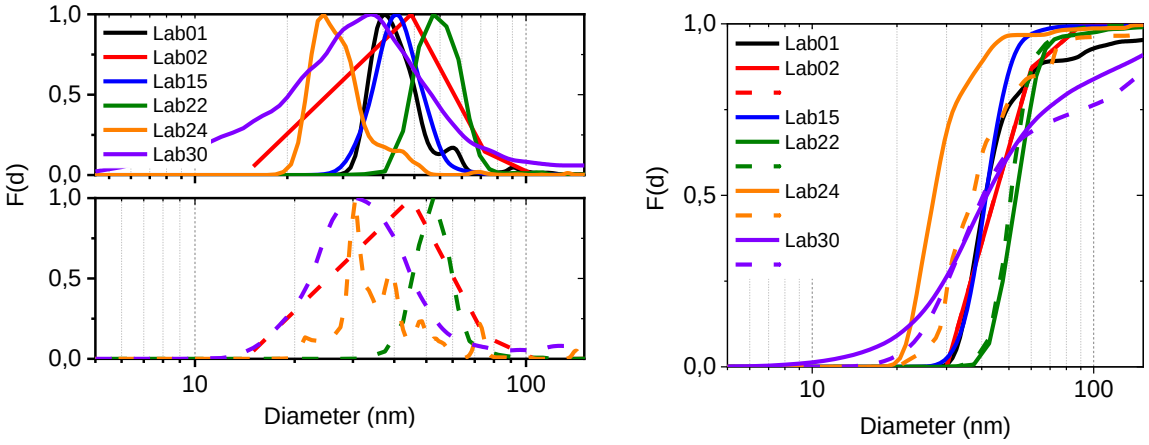

Figure 51: normalized (left) and cumulated (right) size distribution functions of the diameter of silver particles. All reported results are shown. Dashed line lower concentration.

For Lab 24 the reported size distributions are concentration depended. For the PSL (90/125 nm) particles the size distribution measured by Lab 30 also slightly differs with the particle concentration. A higher fraction of big particles is measured here, which show a slight dependency on the used particle concentration. For further evaluation both concentrations dependent size distributions were excluded.

From the distributions of the selected datasets the mean, median and modal diameters of the different concentration measured with repeatability standard deviation are determined from the measurement of the two different concentrations and plotted in Figure 52.

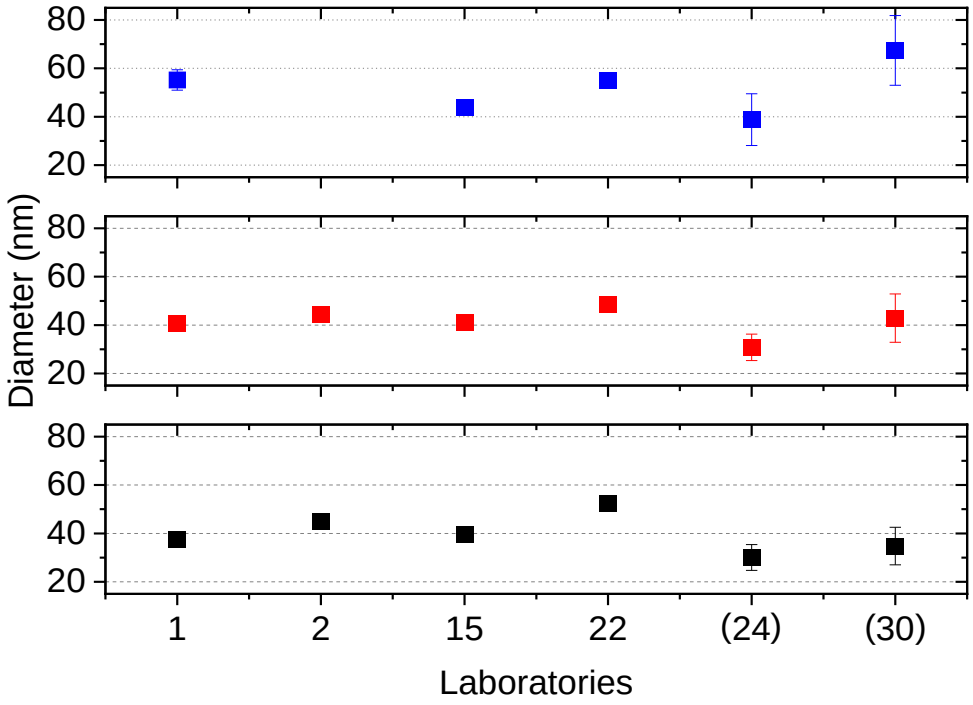

Figure 52: mean (blue), median (red) and modal (black) diameter with standard deviation of silver particles analysed with PTA. No mean diameter reported for Lab 02.

To further evaluate the precision of the results of the ILC obtained on Ag particles, the average values of the mean and median diameters of the selected datasets were calculated as well as the reproducibility standard deviation σ_R of the mean and median values and the relative standard deviation σ_r (=standard deviation/mean). These values are given Table 44.

Table 44. Statistics of silver nanoparticles datasets

	$d_{0,hyd}$ (nm)	σ_R	σ_r
average(**mean**(diameter))	52	11.9	0.23
average(**median**(diameter))	41.3	6.3	0.15
average(**modal**(diameter))	39.9	7.9	0.20

The expanded reproducibility standard deviation is calculated by multiplying it with the coverage factor, k=2. Thus, the mean diameter of the Ag particles is obtained as 52 ± 23.8 nm (45%) and the median diameter is given by 41.3 ± 12.6 nm (30%). The modal diameter is given by 39.9 ± 15.8 nm (40%).

PTA: Zinc oxide particles

We received PTA measurements from five laboratories. The laboratories were advised to measure two different concentrations of the particle dispersion. It was recommended to use a dilution to 10^6 to 10^9 particles/ml. The obtained normalized size distributions and the cumulative size distributions are shown

in Figure 53 for both concentrations. Lab 1 just measured one concentration. Details of the sonication procedure can be found in the appendix **Error! Reference source not found.**

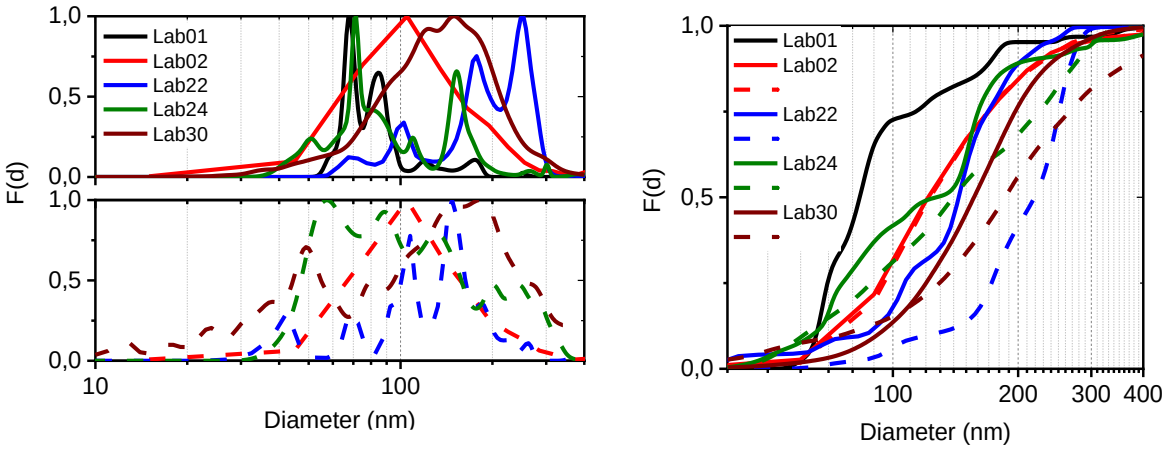

Figure 53: normalized (left) and cumulated (right) size distribution functions of the diameter of zinc oxide particles. All reported results are shown. Dashed line lower concentration.

High variance in the obtained particle size distributions is observed.

The protocol was fulfilled by all the participants.

From the distributions of the selected datasets the mean, median and modal diameters of the different concentration measured with repeatability standard deviation are determined from the measurement of the two different concentrations and plotted in Figure 54.

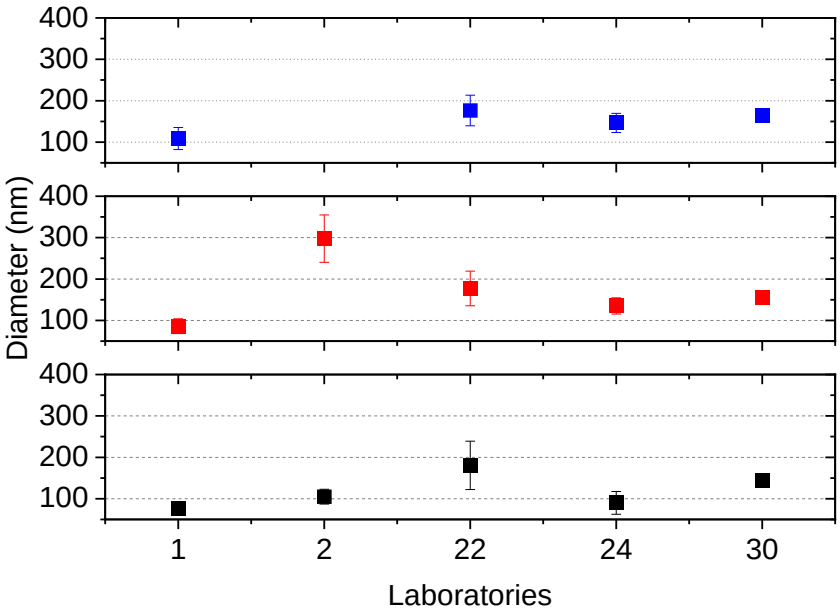

Figure 54: mean (blue), median (red) and modal (black) diameter with repeatability standard deviation of zinc oxide particles analysed with PTA. No mean diameter reported for Lab 02.

No further evaluation of the precision of the results of the ILC obtained on titanium oxide particles has been done as the obtained particle size distribution from the labs are not in comparison.

Scanning electron microscopy – SEM

For analysis with SEM the test materials silica (20 nm), polystyrene particles 90/125 nm and 80/800 nm, titanium oxide, zinc oxide and silver particles were sent out readily prepared on silicon wafers. Except of silver, the specimens were prepared via spin-coating. Silver particles were prepared with drop on method.

We received SEM measurements from nine different laboratories. 26 results were handed in. An overview of the results is given in Table 45. The results of the SEM measurements are presented for each particle system.

Table 45. Overview of the results for the mean, median and modal diameter determined via SEM measurement. The reported standard deviation is the between laboratory deviation by a factor of 2.

Particle system	# labs	d	$d_{0,\,mean}$ (nm)	$d_{0,\,median}$ (nm)	$d_{0,\,modal}$ (nm)
Ag	5	Max. Feret	43.1 ± 10.6	40.2 ± 10.6	39.8 ± 14.4
		Min. Feret	34.8 ± 11	33.2 ± 10	31.2 ± 16
		Eq. circular	38.3 ± 13.8	35.3 ± 11.8	32.2 ± 4.2
SiO_2 (20 nm)	6	Max. Feret	20.4 ± 1.96	20.3 ± 1.88	20.1 ± 2.58
		Min. Feret	17.1 ± 1.94	17.1 ± 1.98	17.2 ± 1.42
		Eq. circular	17.9 ± 1.94	17.9 ± 1.9	17.6 ± 1.88
PSL (90/125 nm)	6	Max. Feret	111.5 ± 9.4	114.8 ± 10.6	97.8 ± 9.4/128.7 ± 13.8
		Min. Feret	106.6 ± 9	111.6 ± 9.8	89.8 ± 10.4/124.2 ± 9.4
		Eq. circular	109.3 ± 10.8	113.6 ± 9.8	93.5 ± 8.6/126.2 ± 12.6
ZnO	2		No reliable validation possible		
TiO_2	3	Max. Feret	271.2 ± 6.2	269.9 ± 6.5	257.5 ± 31.8
		Min. Feret	200.4 ± 7.8	195.9 ± 9.2	150.5 ± 79
		Eq. circular	224.4 ± 5.6	222.4 ± 8	237 ± 14
PSL (80/800 nm)	4	Eq. circular	No reliable validation possible		790 ± 60

SEM: Silica particles (20 nm)

We received SEM measurements from six laboratories. One further laboratory measured the particles, but received non-evaluable images, as the particle size was below the instrument resolution. The pixel sizes used in image acquisition were in a range of 0.32 nm/px to 2 nm/px on average. Lab 34 used a pixel size of 3.7 nm/px. That means that except of one measurement the SEM measurements were performed with the minimal required pixel size or better. The laboratories were advised to count at least 300 particles for a reliable size distribution. The obtained normalized size distributions and the cumulative size distributions of the max. Feret diameter are shown in Figure 55. For the minimum Feret diameter and the equivalent circular diameter the results are given in Table 46.

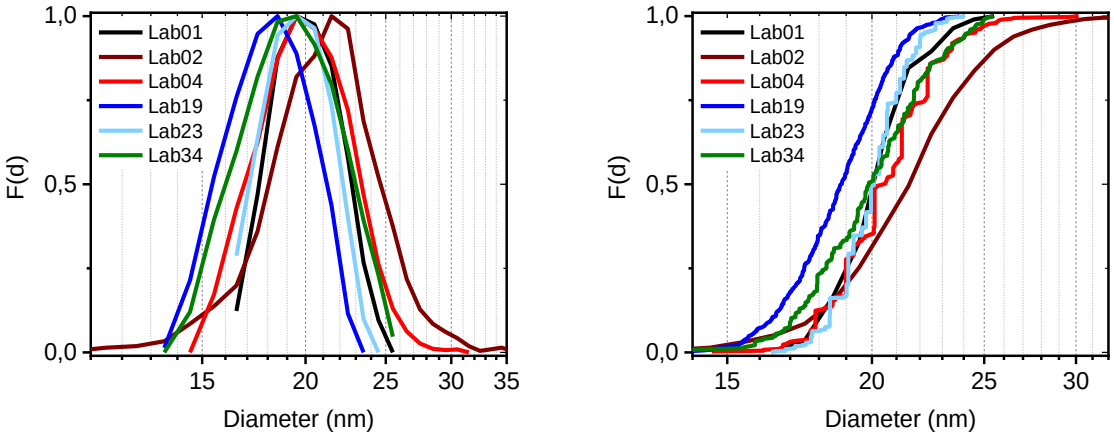

Figure 55: normalized (left) and cumulated (right) size distribution functions of the max. Feret diameter of silica particles (20 nm). All reported results are shown.

The obtained size distribution and diameters show slight variations but are in the expected variance for SEM analysis. All measurements are used for the further data evaluation.

From the distributions of the selected datasets the mean, median and modal diameters are calculated and plotted in Figure 56. The error bars are calculated using the bootstrap method.

To further evaluate the precision of the results of the ILC obtained on SiO_2 (20 nm) particles, the average values of the mean and median diameters of the selected datasets were calculated as well as the standard deviation between the laboratories σ_L of the mean, median and modal values and the relative standard deviation σ_{rel} (=standard deviation/average diameter). These values are given in Table 46.

The standard deviation is multiplied by a factor of 2 in order to yield a coverage probability of 95% and additionally the percentage is given. Thus, the mean equivalent circular diameter of the SiO_2 (20 nm) particles is obtained as 17.9 ± 1.94 nm (11%) and the median equivalent circular diameter is given by 17.9 ± 1.9 nm (11%) and the modal equivalent circular diameter is given by 17.6 ± 1.88 nm (11%).

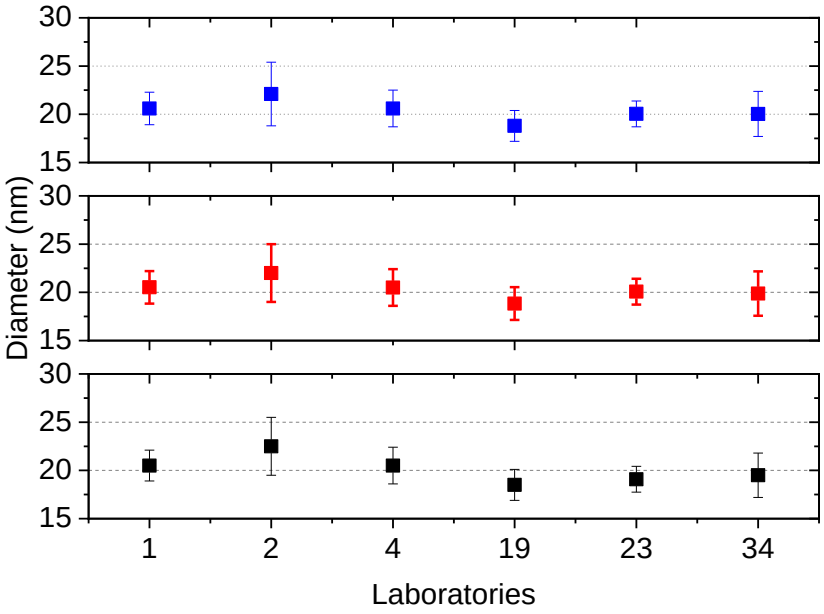

Figure 56: mean (blue), median (red) and modal (black) max. Feret diameter with bootstrap error of silica nanoparticles analysed with SEM.

Table 46. Statistics of silica (20 nm) nanoparticles datasets

	d_0(nm)	σ_L	σ_{rel}
max. Feret diameter			
average (**mean**(diameter))	20.4	0.98	0.05
average (**median**(diameter))	20.3	0.94	0.05
average (**modal**(diameter))	20.1	1.29	0.06
min. Feret diameter			
average (**mean**(diameter))	17.1	0.92	0.05
average (**median**(diameter))	17.1	0.94	0.06
average (**modal**(diameter))	17.2	0.71	0.04
equivalent circular diameter			
average (**mean**(diameter))	17.9	0.92	0.05
average (**median**(diameter))	17.9	0.85	0.05
average (**modal**(diameter))	17.6	0.94	0.05
average geometric standard deviation (diameter)	1.1	0.03	0.03

SEM: Titanium oxide particles

We received SEM measurements from three laboratories. The pixel sizes used in image acquisition were in a range of 4.67 nm/px to 10.2 nm/px on average. That means that all SEM measurements were performed with the minimal required pixel size or better. The laboratories were advised to count at least 700 particles for a reliable size distribution. The obtained normalized size distributions and the cumulative size distributions of the max. Feret diameter are shown in Figure 57. For the minimum Feret diameter and the equivalent circular diameter the results are given in Table 47.

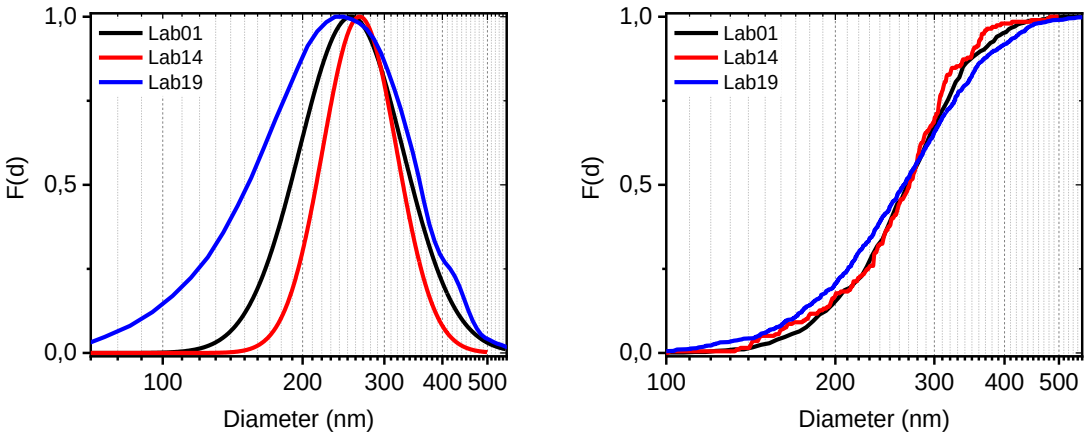

Figure 57: normalized (left) and cumulated (right) size distribution functions of the max. Feret diameter of titanium oxide particles. All reported results are shown.

The determined size distributions are in comparison and are all used for further data evaluation.

From the distributions of the selected datasets the mean, median and modal diameters are calculated and plotted in Figure 58. The error bars are calculated using the bootstrap method.

To further evaluate the precision of the results of the ILC obtained on TiO_2 particles, the average values of the mean, median and modal diameters of the selected datasets were calculated as well as the standard deviation between the laboratories σ_L of the mean, median and modal values and the relative standard deviation σ_{rel} (=standard deviation/average diameter). These values are given in Table 47..

The standard deviation is multiplied by a factor of 2 in order to yield a coverage probability of 95% and additionally the percentage is given. Thus, the mean equivalent circular diameter of the TiO_2 particles is obtained as 224.4 ± 5.6 nm (2.5%) and the median equivalent circular diameter is given by 222.4 ± 8 nm (3.6%) and the modal equivalent circular diameter is given by 237 ± 14 nm (6%).

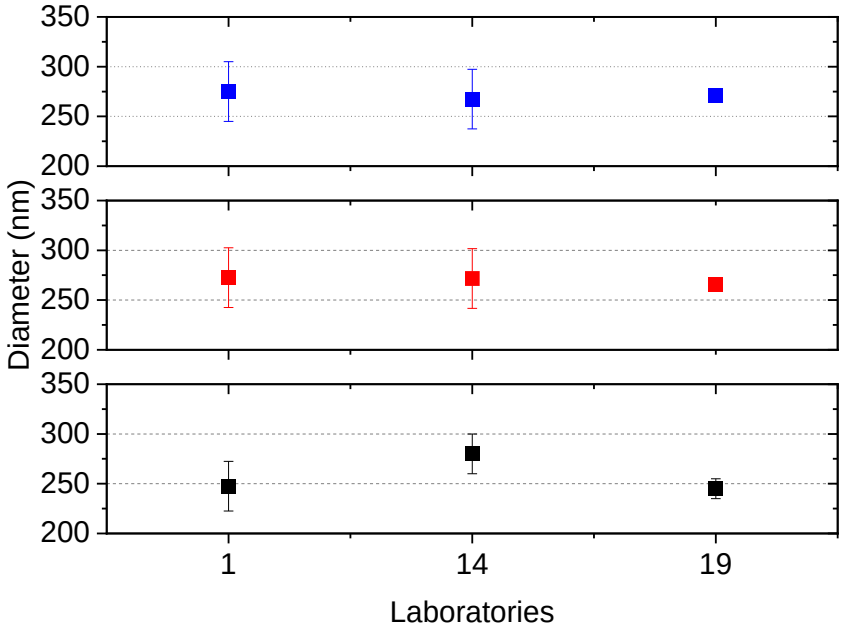

Figure 58: mean (blue), median (red) and modal (black) max. Feret diameter of titanium oxide particles analysed with SEM.

Table 47. Statistics of titanium oxide particles datasets

	d_0 (nm)	σ_L	σ_{rel}
max. Feret diameter			
average (**mean**(diameter))	271.2	3.09	0.01
average (**median**(diameter))	269.9	3.25	0.01
average (**modal**(diameter))	257.5	15.9	0.06
min. Feret diameter			
average (**mean**(diameter))	200.4	3.9	0.02
average (**median**(diameter))	195.9	4.6	0.02
average (**modal**(diameter))	150.5	39.5	0.26
equivalent circular diameter			
average (**mean**(diameter))	224.4	2.8	0.01
average (**median**(diameter))	222.4	4	0.02
average (**modal**(diameter))	237	7	0.03
average geometric standard deviation (diameter)	1.34	0.07	0.05

SEM: Polystyrene particles (90/125 nm)

We received SEM measurements from five laboratories. The pixel sizes used in image acquisition were in a range of 1.38 nm/px to 5.3 nm/px on average. That means that all SEM measurements were performed with the minimal required pixel size or better. The laboratories were advised to count at least 700 particles for a reliable size distribution. The obtained normalized size distributions and the cumulative size distributions for the max. Feret diameter are shown in Figure 59. For the minimum Feret diameter and the equivalent circular diameter the results are given in Table 48.

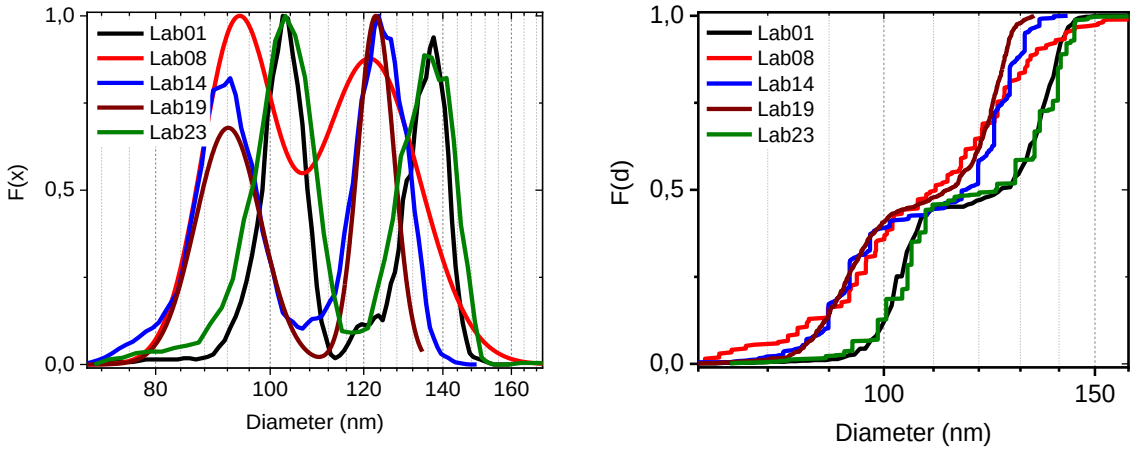

Figure 59: normalized (left) and cumulated (right) size distribution functions of the max. Feret diameter of polystyrene particles (90/125 nm). All reported results are shown.

The determined size distribution from Lab 23 and Lab 01 differ from those from the other labs. A dependency on the used pixel size or a general influence of the image quality was checked and can be excluded. Both labs made a manual image evaluation as recommended in the draft TG and counted the given particle number. The mean and median diameters obtained from the size distribution are in the range of the error of those from the other labs. The modal diameters are slightly out of the range.

Lab 08 provided a size distribution including the particle fraction at 20 nm which is present in the suspension coming of the preparation process. This submission was not taken into account for the size distribution in this ILC. This fraction has been removed in the here shown data.

From the distributions of the selected datasets the mean, median and modal diameters are calculated and plotted in Figure 60. The error bars are calculated using the bootstrap method.

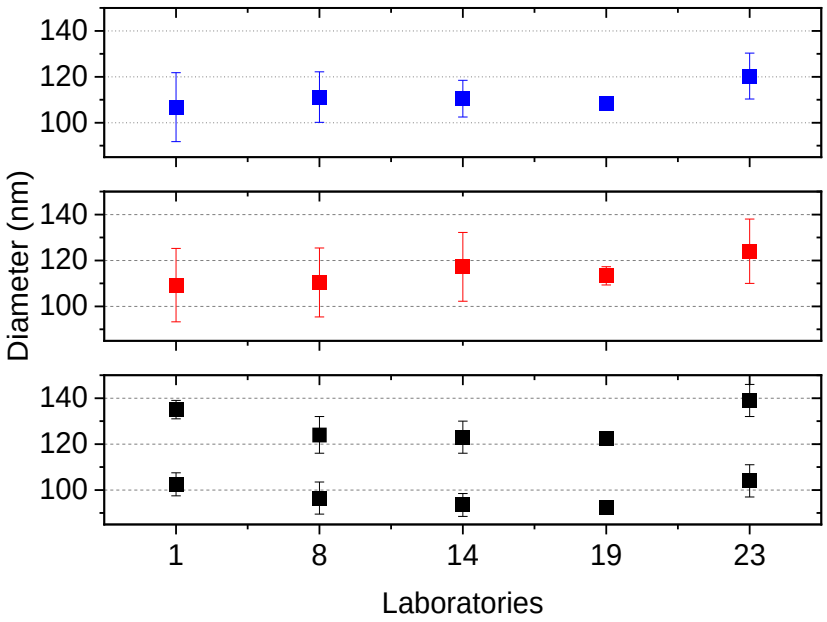

Figure 60: mean (blue), median (red) and modal (black) max. Feret diameter with bootstrap error of PSL particles (90/125 nm) analysed with SEM.

To further evaluate the precision of the results of the ILC obtained on polystyrene (90/125 nm) particles, the average values of the mean, median and modal diameters of the selected datasets were calculated as well as the standard deviation between the laboratories σ_L of the mean, median and modal values and the relative standard deviation σ_{rel} (=standard deviation/average diameter). These values are given in Table 48.

The standard deviation is multiplied by a factor of 2 in order to yield a coverage probability of 95% and additionally the percentage is given. Thus, the mean equivalent circular diameter of the PSL (90/125 nm) particles is obtained as 109.3 ± 10.8 nm (10%) and the median equivalent circular diameter is given by 113.6 ± 9.8 nm (9%). The modal equivalent circular diameters are for mode1 93.5 ± 8.6 nm (9%) and for mode 2 126.2 ± 12.6 nm (10%).

Table 48. Statistics of polystyrene (90/125 nm) nanoparticles datasets

	d_0 (nm)	σ_L	σ_{rel}
max. Feret diameter			
average (**mean**(diameter))	111.5	4.7	0.04
average (**median**(diameter))	114.8	5.3	0.05
average(**modal(1)**(diameter))	97.8	4.7	0.05
average(**modal(2)**(diameter))	128.7	6.9	0.05
min. Feret diameter			
average (**mean**(diameter))	106.6	4.5	0.04
average (**median**(diameter))	111.6	4.9	0.04
average(**modal(1)**(diameter))	89.8	5.2	0.05
average(**modal(2)**(diameter))	124.2	4.7	0.04
equivalent circular diameter			
average (**mean**(diameter))	109.3	5.4	0.05

average (**median**(diameter))	113.6	4.9	0.04
average (**modal(1)**(diameter))	93.5	4.3	0.04
average (**modal(2)**(diameter))	126.2	6.3	0.05
average geometric standard deviation (diameter)	1.18	0.02	0.02

SEM: Polystyrene particles (80/800 nm)

We received SEM measurements from four laboratories. The pixel sizes used in image acquisition were in a range of 2.54 nm/px to 14.65 nm/px for the 80 nm particle fraction and in a range of 3.7-18.61 nm/px for the 800 nm particle fraction. That means that except one measurement of the 80 nm particle fraction all SEM measurements were performed with the minimal required pixel size or better. The laboratories were advised to count at least 700 particles for a reliable size distribution. The cumulative size distributions for the max. Feret diameter is shown in Figure 61.

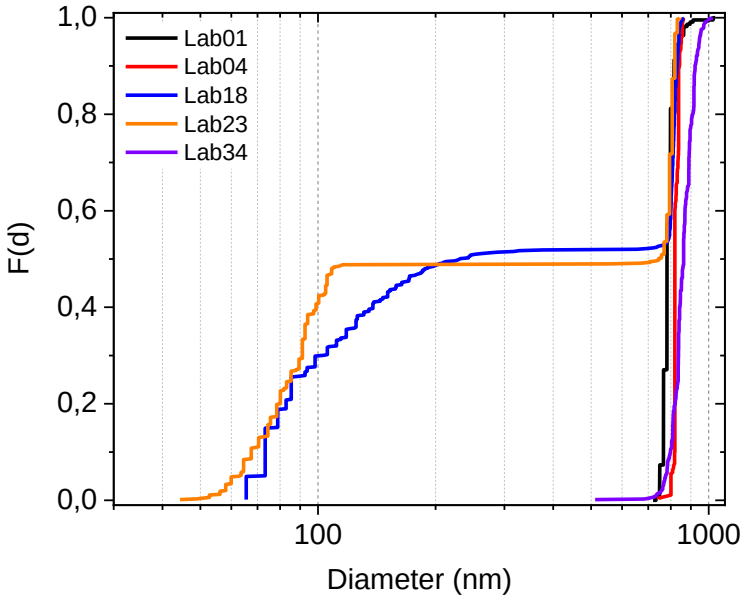

Figure 61: cumulated distribution functions of the max. Feret diameter of polystyrene nanoparticles (80/800 nm). All reported results are shown.

From four labs only two detected the 80 nm particle fraction. A reliable determination of the ratio of the two particle size populations is not possible, as also the labs who were able to detect 80 nm didn´t proceed as recommended in the draft TG and evaluated the same area for 80 and 800 nm particles.

From the distributions of the selected datasets the mean, median and modal diameters are calculated and plotted in Figure 62. The error bars are calculated using the bootstrap method.

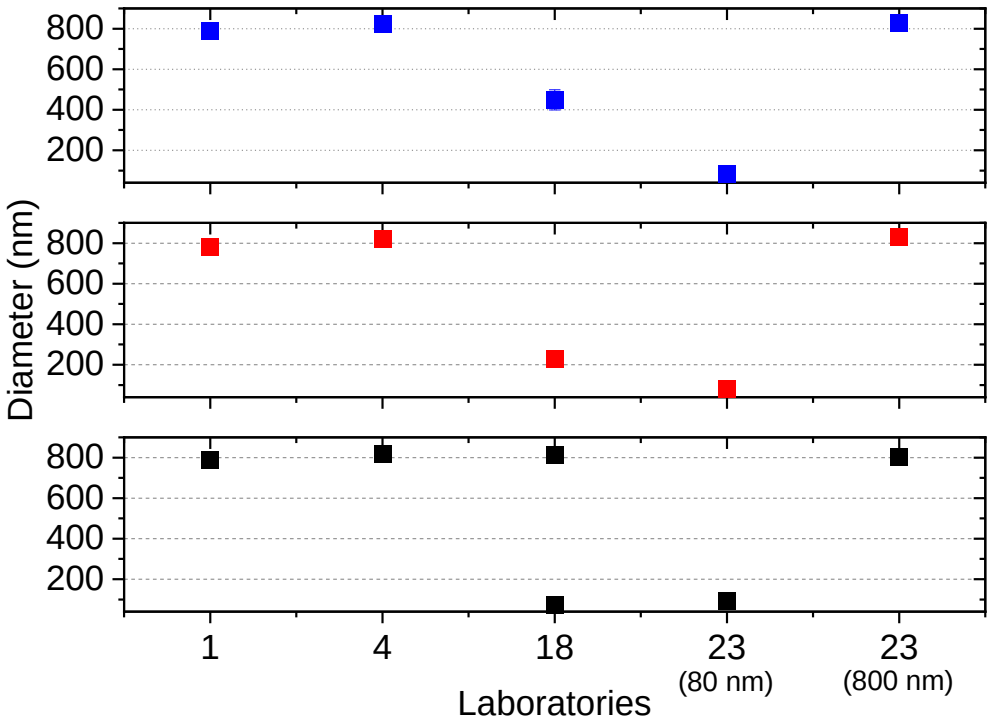

Figure 62: mean (blue), median (red) and modal (black) max. Feret diameter with bootstrap error of PSL particles (80/800 nm) analysed with SEM.

No further evaluation the precision of the results of the ILC obtained on polystyrene (80/800 nm) particles are done as no reliable determination of both particle population is possible. Nevertheless, the derived modal diameters for the 800 nm particles are in good comparison and with mode equivalent circular diameter given by 790 ± 30 nm a good comparison to the expected diameter is given.

The expanded reproducibility standard deviation is calculated by multiplying reproducibility standard deviation with the coverage factor, k=2. A modal diameter of 790 ± 60 nm (8%).

SEM: Silver nanoparticles

We received SEM measurements from five laboratories. The pixel sizes used in image acquisition were in a range of 1.117 nm/px to 14.65 nm/px. That means that not all SEM measurements were performed with the minimal required pixel size. Lab 01 and 02 were with 1.117 and 2.1 nm/px in the required pixel size range. Lab 18, 23 and 34 measured with pixel sizes of 14.65, 4.96 and 3.7 nm/px. The laboratories were advised to count at least 700 particles for a reliable size distribution. The obtained normalized size distributions and the cumulative size distributions of the max. Feret diameter are shown in Figure 63. For the minimum Feret diameter and the equivalent circular diameter the results are given in Table 49.

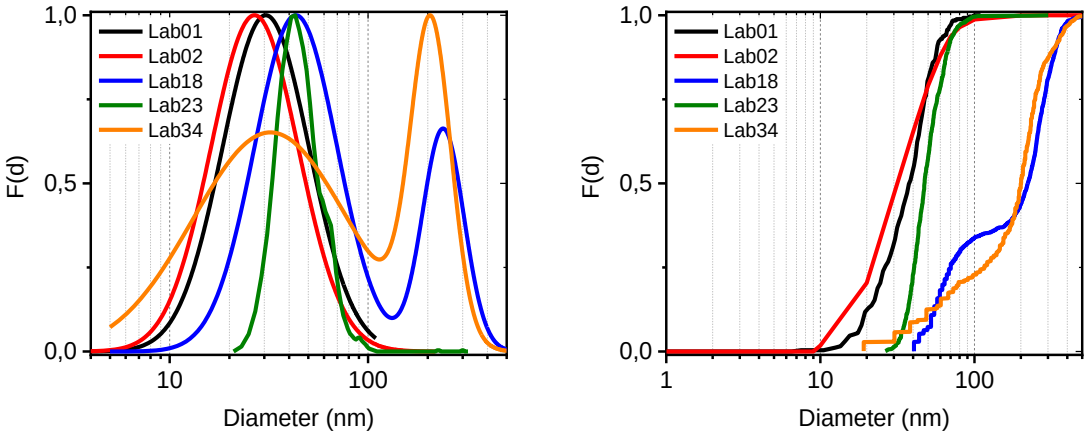

Figure 63: normalized (left) and cumulated (right) size distribution functions of the max. Feret diameter of silver nanoparticles. All reported results are shown.

The cumulative distributions of Lab 18 and 34 significantly differ from the obtained size distribution of the other labs. Both labs made an automatic image evaluation. Lab 02 also used automatic image evaluation, but the results are comparable to the manual image evaluation. As seen in the normalized size distribution two particle fraction are present. The first mode of the size distribution of both labs is comparable to the obtained size distribution of the other labs. A second mode is at around 200 nm. Images of all labs show that 200 nm silver particles are present but only in low amount, which does not explain the high percentage in the size distribution of Lab 18 and 34. For the further evaluation only the first modal diameter is considered from Lab 18 and 34 but for the completeness are still shown in Figure 64. The size distribution from Lab 01 and 02, which measured in the required pixel size range, are in a slightly smaller size region as the ones of the labs who used a too high pixel size.

From the distributions of the selected datasets the mean, median and modal diameters are calculated and plotted in Figure 64. The error bars are calculated using the bootstrap method.

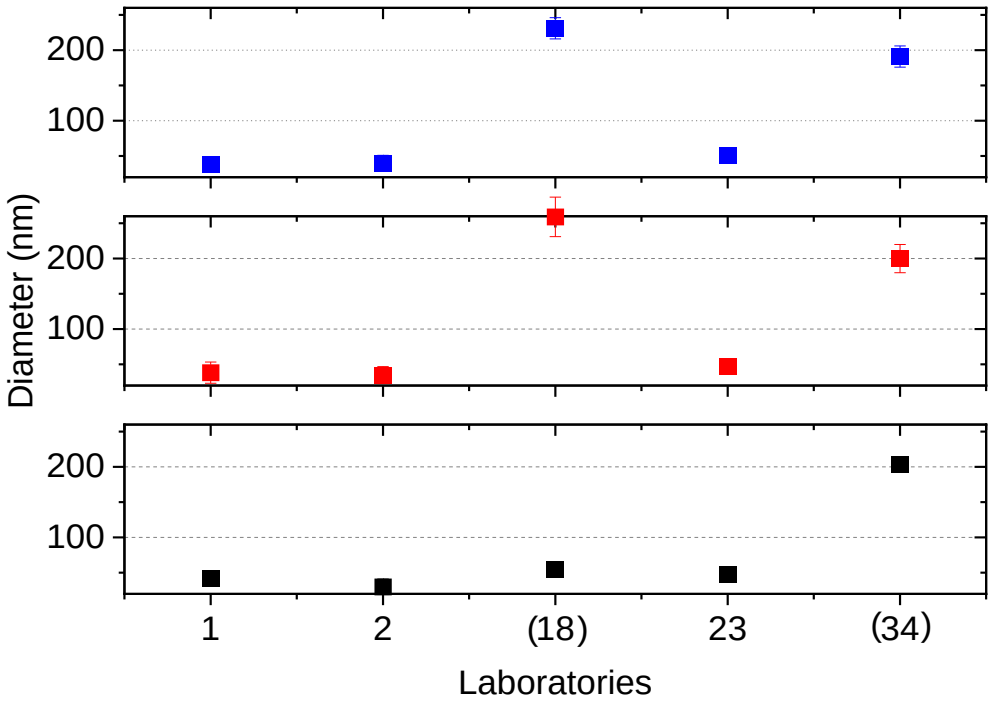

Figure 64: mean (blue), median (red) and modal (black) max. Feret diameter of silver nanoparticles analysed with SEM.

To further evaluate the precision of the results of the ILC obtained on Ag particles, the average values of the mean, median and modal diameters of the selected datasets were calculated as well as the standard deviation between the laboratories σ_L of the mean, median and modal values and the relative standard deviation σ_{rel} (=standard deviation/average diameter). These values are given in Table 49.

Table 49. Statistics of silver nanoparticles datasets

	d_0 (nm)	σ_L	$\sigma_{rel.}$
max. Feret diameter			
average (**mean**(diameter))	43.1	5.3	0.12
average (**median**(diameter))	40.2	5.3	0.13
average (**modal**(diameter))	39.8	7.2	0.18
min. Feret diameter			
average (**mean**(diameter))	34.8	5.5	0.16
average (**median**(diameter))	33.2	5	0.15
average (**modal**(diameter))	31.2	8	0.26
equivalent circular diameter			
average (**mean**(diameter))	38.3	6.9	0.18
average (**median**(diameter))	35.3	5.9	0.17
average (**modal**(diameter))	32.2	2.1	0.06
average geometric standard deviation (diameter)	1.5	0.12	0.09

The standard deviation is multiplied by a factor of 2 in order to yield a coverage probability of 95% and additionally the percentage is given. Thus, the mean equivalent circular diameter of the Ag particles is obtained 38.3 ± 13.8 nm (36%) and the median equivalent circular diameter is given by 35.3 ± 11.8 nm (33%) and the modal equivalent circular diameter is given by 32.2 ± 4.2 nm (4%).

SEM: Zinc oxide particles

We received SEM measurements from three laboratories. The pixel sizes used in image acquisition were in a range of 3.7 nm/px to 4.9 to 14.65 nm/px on average. The SEM measurement of Lab18 was not performed with the minimal required pixel size. The laboratories were advised to count at least 700 particles for a reliable size distribution. The obtained normalized size distributions and the cumulative size distributions of the max. Feret diameter are shown in Figure 65.

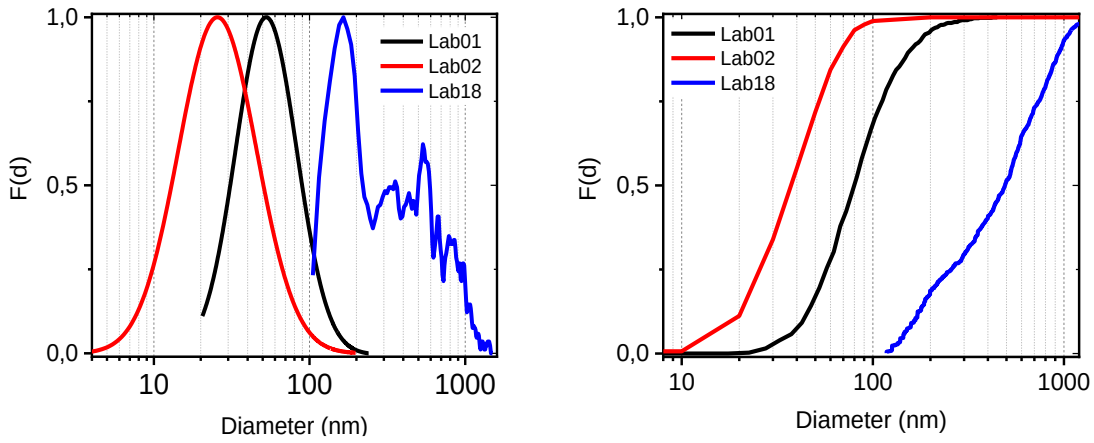

Figure 65: normalized (left) and cumulated (right) size distribution functions of the max. Feret diameter of zinc oxide particles. All reported results are shown.

The obtained size distribution differs significantly from each other. The pixel size used from Lab 18 was over the minimal requirement and. Due to the fact that zinc oxide has a high tendency to agglomerate the obtained high size distribution could arise from that. The measurement was excluded for further evaluation. From remaining two size distribution, which also show a high variance no reliable evaluation can be done.

Single particle ICP-MS

For analysis with sp ICP-MS the test material titanium oxide was sent out as powder. For the preparation of the measurement suspension an SOP was given. It was recommended to measure two different concentrations of the material. The shown size distribution is the average distribution of both concentrations. If a concentration dependency between the both concentrations was found it is mentioned in the respective paragraph to the size distribution of the material.

We received sp ICP-MS measurements from four laboratories. For one particle system. An overview of the results is given in Table 50. The results of the sp ICP-MS measurements of titanium oxide are presented.

Table 50. Results for the mean, median and modal diameter determined via sp ICP-MS measurement. The reported expanded reproducibility standard deviation is calculated using a coverage factor of 2.

Particle system	# labs	$d_{0,mass,mean}$ (nm)	$d_{0,mass,median}$ (nm)	$d_{0,mass,modal}$ (nm)
TiO_2	4	217 ± 65	206 ± 55	171 ± 114

sp ICP-MS: Titanium oxide particles

We received sp ICP-MS measurements from four laboratories. The obtained normalized size distributions and the cumulative size distributions are shown in Figure 66 for both concentrations, as there is a high variance of the curves through the variance of different bin the log-normal fit of the size distributions is shown. The laboratories were advised to measure two different concentration of the particle dispersion. As concentration it was proposed to use 100 ng/L and 500 ng/L for the analyses, but with the possibility to adapt the concentration to used instrument setting. Lab 04 and 05 adjusted the concentration for their measurement to a higher concentration. Lab 22 and 25 used the proposed concentrations. All labs measured with a recommended dwell time below 10 ms. Details of the sonication procedure can be found in the appendix Table 89.

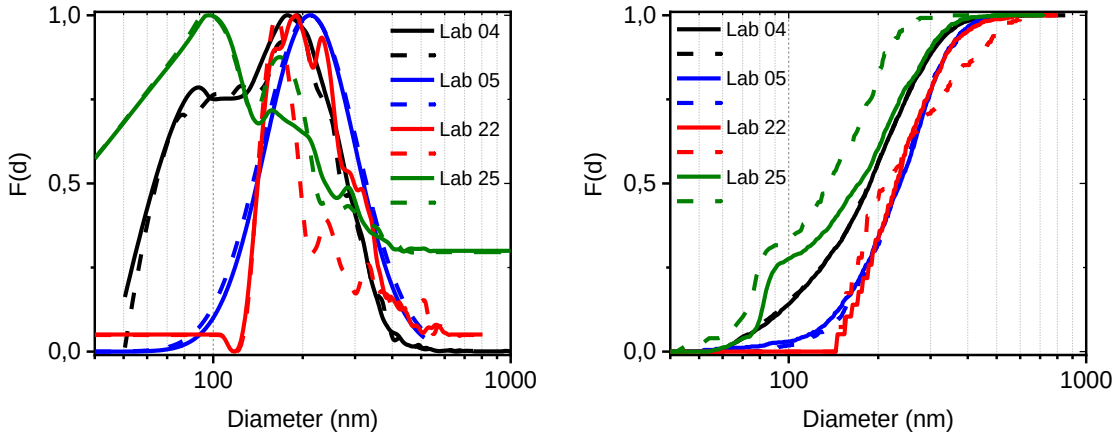

Figure 66: normalized (left) and cumulated (right) size distribution functions of the diameter of titanium oxide particles. All reported results are shown. Dashed line is the lower concentration.

The obtained size distributions of Lab 25 show a small variance dependent on the used concentration, with a shift to smaller particle size with lower concentration. For both, a high contribution of particles at around 100 nm is observed in the size distributions, which was not detected by the other labs. For the concentration of 100 ng/L the number of particles is below the recommendation of 700 particles and it is therefore not considered in the further data evaluation but for the completeness the diameter are still shown in Figure 67.

From the distributions of the selected datasets the mean, median and modal diameters with repeatability standard deviation are determined and plotted in Figure 67.

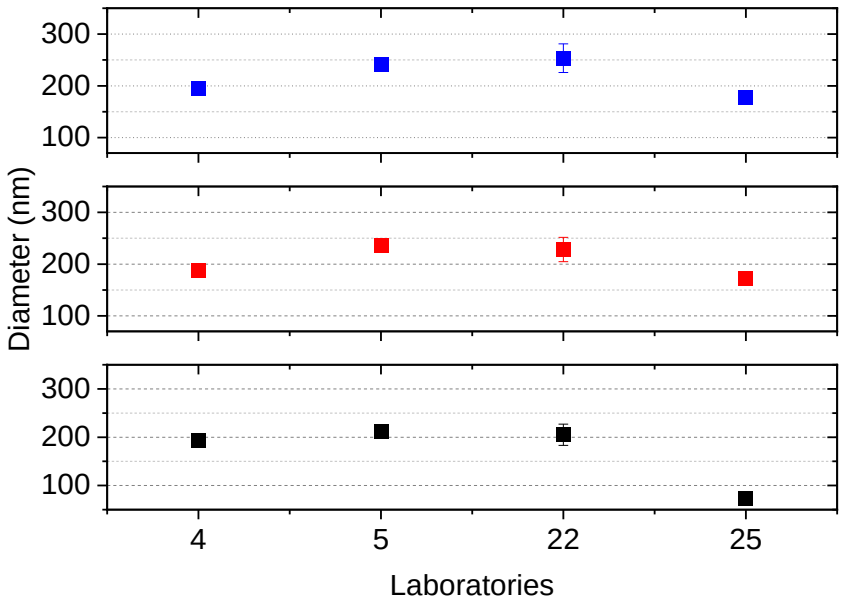

Figure 67: mean (blue), median (red) and modal (black) diameter with repeatability standard deviation of titanium oxide particles analysed with sp ICP-MS.

To further evaluate the precision of the results of the ILC obtained on TiO_2 particles, the average values of the mean, median and modal diameters of the selected datasets were calculated as well as the reproducibility standard deviation σ_R of the mean, median and modal values and the relative standard deviation σ_r (=standard deviation/mean). These values are given in Table 51.

Table 51. Statistics of titanium oxide particles datasets

	$d_{0,mass}$ (nm)	σ_R	σ_r
average(**mean**(diameter))	217	32.5	0.15
average(**median**(diameter))	206	27.6	0.13
average(**modal**(diameter))	171	57	0.33

The expanded reproducibility standard deviation is calculated by multiplying it with the coverage factor, k=2. Thus, the mean diameter of the TiO_2 is obtained as 217 ± 65 nm (30%), the median diameter is given by 206 ± 55 nm (27%) and the modal diameter is given by 170 ± 114 nm (66%).

Small angle X-Ray Scattering – SAXS

For analysis with SAXS the nanomaterials silica (20 and 50 nm), polystyrene particles 90/125 nm and silver particles were sent out as dispersion. For the preparation of the measurement suspension a SOP was given. It was recommended to measure two different concentrations of each material. The shown size distribution is the average distribution of both concentrations. If a concentration dependency between both concentrations was found it is mentioned in the respective paragraph to the size distribution of the material.

We received SAXS measurements from five different laboratories. 16 results were handed in. An overview of the results is given in Table 52. The results of the SAXS measurements are presented for each particle system.

Table 52. Overview of the results for the mean, median and modal diameter determined via SAXS measurement. The reported expanded reproducibility standard deviation is calculated using a coverage factor of 2.

Particle system	# labs	$d_{3,IScat,mean}$ (nm)	$d_{3,IScat,median}$ (nm)	$d_{3,IScat,modal}$ (nm)
Ag	4	19.2 ± 2.4	17.1 ± 2.9	14 ± 1.4
SiO_2 (20 nm)	5	18.3 ± 0.9	18.4 ± 0.9	18.2 ± 0.75
SiO_2 (50 nm)	5	49.7 ± 1.2	49.6 ± 1.8	49.4 ± 1.7
PSL (90/125 nm)	2	Not applicable		95 ± 1.9/126.6 ± 0.84

SAXS: Silica particles (20 nm)

We received SAXS measurements from five laboratories. The laboratories were advised to measure two different concentration of the particle dispersion. The dispersion as received with 10 mg/ml and diluted 1:1 to 5 mg/ml. The obtained normalized size distributions and the cumulative size distributions are shown in Figure 68. The labs applied different models for the determination of the size distribution.

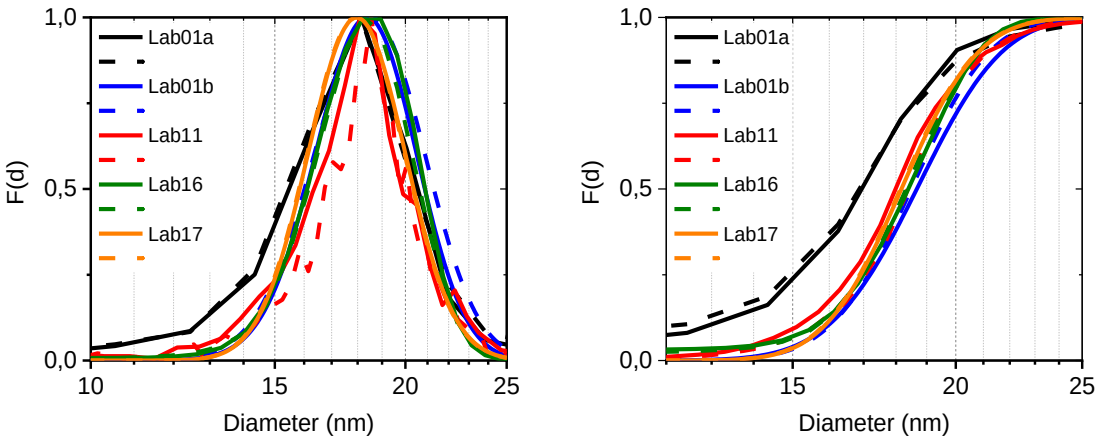

Figure 68: normalized (left) and cumulated (right) size distribution functions of the diameter of silica nanoparticles (20 nm). All reported results are shown. Dashed line lower concentration.

The obtained size distributions show a good comparability for different concentrations and in between the laboratories. The distribution from Lab 01a slightly differs from the others but the therefrom derived diameters are in good comparison.

From the distributions of the selected datasets the mean, median and modal diameters with repeatability standard deviation are determined and plotted in Figure 69.

To further evaluate the precision of the results of the ILC obtained on SiO_2 (20 nm) particles, the average values of the mean, median and modal diameters of the selected datasets were calculated as well as the reproducibility standard deviation σ_R of the mean, median and mode values and the relative standard deviation σ_r (=standard deviation/mean). These values are given Table 53.

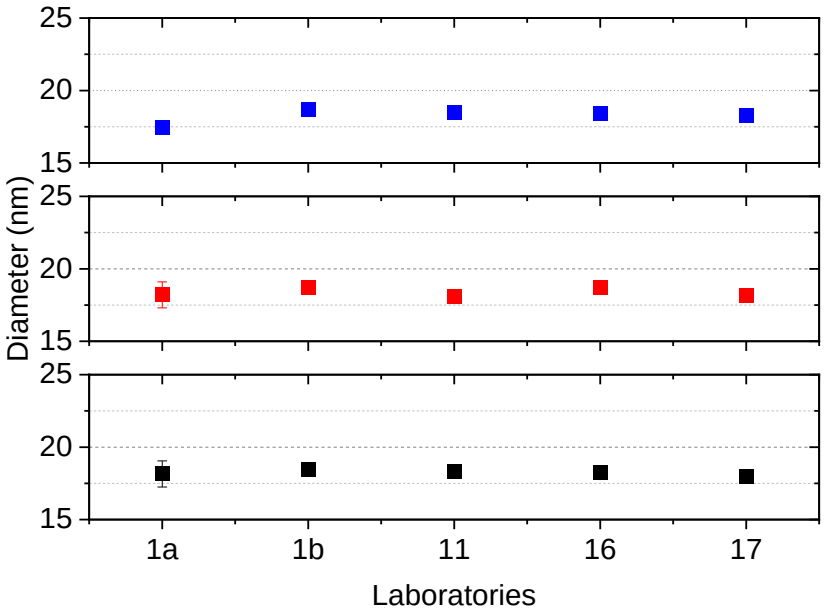

Figure 69: mean (blue), median (red) and modal (black) diameter with repeatability standard deviation of silica nanoparticles (20 nm) analysed with SAXS.

Table 53. Statistics of silica (20 nm) nanoparticles datasets

	$d_{3,lScat}$ (nm)	σ_R	σ_r
average (**mean**(diameter))	18.3	0.46	0.03
average (**median**(diameter))	18.4	0.45	0.02
average (**modal**(diameter))	18.2	0.38	0.02

The **expanded reproducibility standard deviation** is calculated by multiplying it with the **coverage factor**, k=2. Thus, the mean diameter of the SiO_2 (20 nm) particles is obtained as 18.3 ± 0.92 nm (5%), the median diameter is given by 18.4 ± 0.9 nm (5%) and the modal diameter is given by 18.2 ± 0.75 nm (4%).

SAXS: Silica particles (50 nm)

We received SAXS measurements from five laboratories. The laboratories were advised to measure two different concentrations of the particle dispersion. The dispersion as received with 10 mg/ml and diluted 1:1 to 5 mg/ml. The obtained normalized size distributions and the cumulative size distributions are shown in Figure 70.

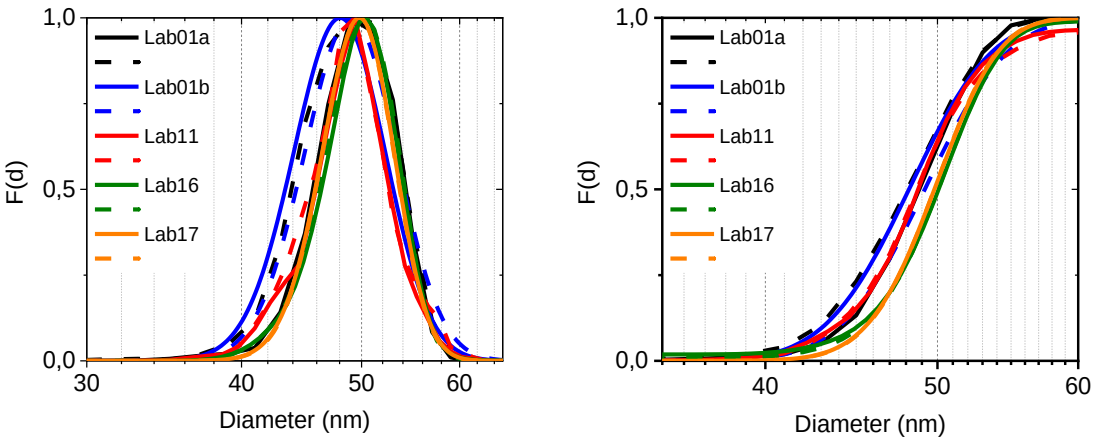

Figure 70: normalized (left) and cumulated (right) size distribution functions of the diameter of silica nanoparticles (50 nm). All reported results are shown. Dashed line lower concentration.

The obtained size distributions show a good comparability for different concentrations and in between the laboratories. From the distributions of the selected datasets the mean, median and modal diameters with repeatability standard deviation are determined and plotted in Figure 71.

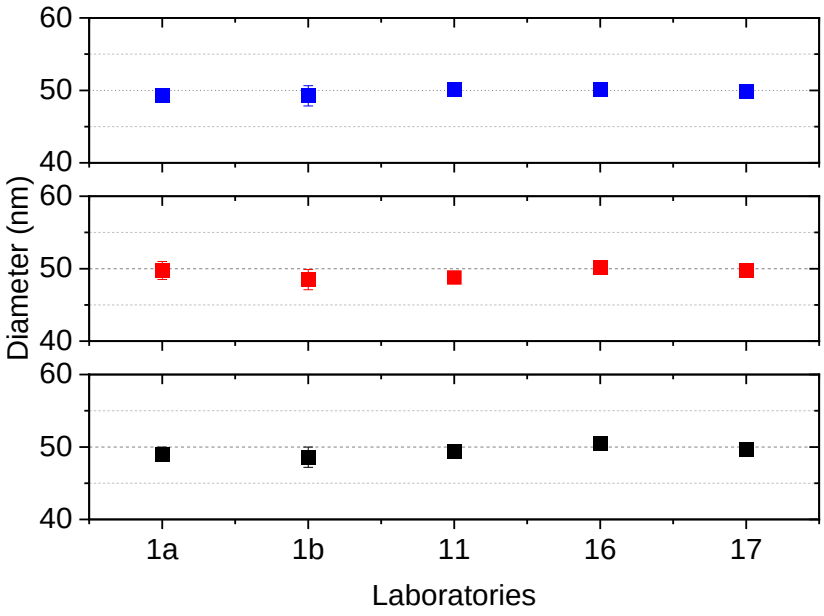

Figure 71: mean (blue), median (red) and modal (black) diameter with repeatability standard deviation of silica nanoparticles (50 nm) analysed with SAXS.

To further evaluate the precision of the results of the ILC obtained on SiO_2 (50 nm) particles, the average values of the mean, median and modal diameters of the selected datasets were calculated as well as the reproducibility standard deviation σ_R of the mean, median and modal values and the relative standard deviation σ_r (=standard deviation/mean). These values are given in Table 54.

Table 54. Statistics of silica (50 nm) nanoparticles datasets

	$d_{3,IScat}$ (nm)	σ_R	σ_r
average (**mean**(diameter))	49.7	0.58	0.01
average (**median**(diameter))	49.6	0.89	0.02
average (**modal**(diameter))	49.44	0.85	0.02

The expanded reproducibility standard deviation is calculated by multiplying it with the coverage factor, k=2.Thus, the mean diameter of the SiO_2 (50 nm) particles is obtained as 49.7 ± 1.16 nm (2%), the median diameter is given by 49.6 ± 1.79 nm (4%) and the modal diameter is given by 49.44 ± 1.7 nm (4%).

SAXS: Silver particles

We received SAXS measurements from four laboratories. The laboratories were advised to measure two different concentrations of the particle dispersion. The dispersion as received with 100 µg/ml and diluted 1:1 with 50 µg/ml. The obtained normalized size distributions and the cumulative size distributions are shown in Figure 72.

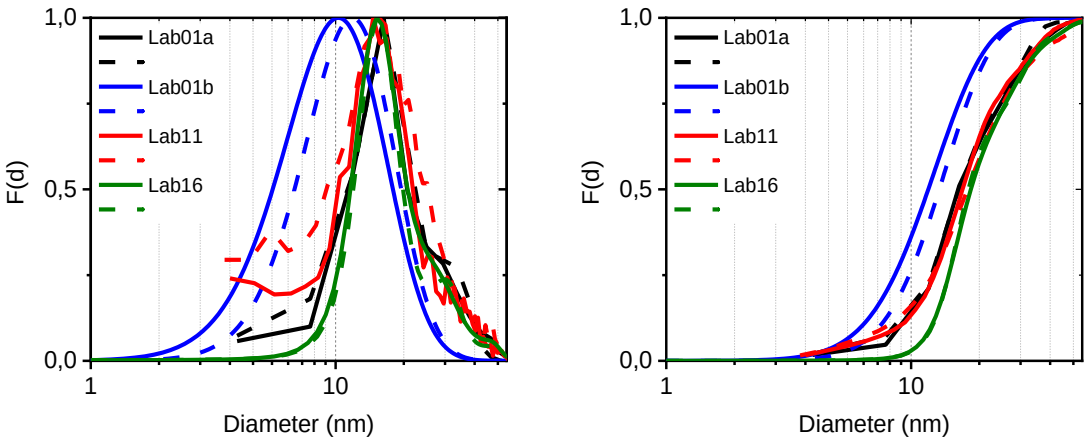

Figure 72: normalized (left) and cumulated (right) size distribution functions of the diameter of silver nanoparticles. All reported results are shown. Dashed line lower concentration.

Lab 01b determined a significantly smaller size distribution compared to the other labs. Only minor corrections of the raw data have been done by Lab 01b. Just desmearing of the curve and subtraction of the water and capillary background was performed and could explain the difference of the obtained size distribution.

From the distributions of the selected datasets the mean, median and modal diameters with repeatability standard deviation are determined and plotted in Figure 73.

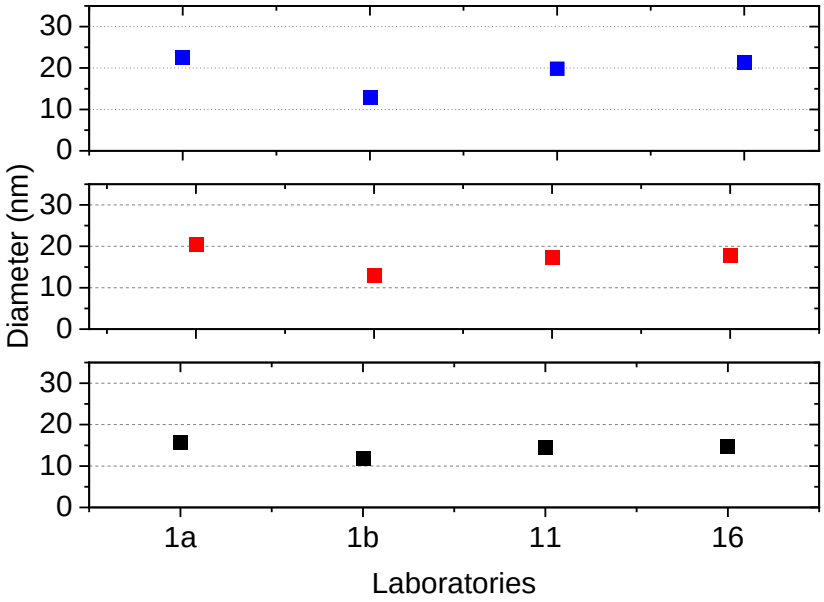

Figure 73: mean (blue), median (red) and modal (black) diameter with repeatability standard deviation of silver nanoparticles analysed with SAXS.

To further evaluate the precision of the results of the ILC obtained on Ag particles, the average values of the mean, median and modal diameters of the selected datasets were calculated as well as the reproducibility standard deviation σ_R of the mean, median and modal values and the relative standard deviation σ_r (=standard deviation/mean). These values are given in Table 55.

Table 55. Statistics of silver nanoparticles datasets

	$d_{3,IScat}$ (nm)	σ_R	σ_r
average (**mean**(diameter))	19.2	3.7	0.19
average (**median**(diameter))	17.1	2.7	0.16
average (**modal**(diameter))	14	1.5	0.11

The expanded reproducibility standard deviation is calculated by multiplying it with the coverage factor, k=2. Thus, the mean diameter of the Ag particles is obtained as 19.2 ± 7.5 nm (39%), the median diameter is given by 17.1 ± 5.4 nm (31%) and the modal diameter is given by 14 ± 3.1 nm (22%)). (Without the results from Lab 01b diameter would be mean diameter 21.2 ± 2.4 nm (11%), median diameter 18.5 ± 2.9 nm (16%) and the modal diameter 15 ± 1.4 nm (9%))

SAXS: Polystyrene particles (90/125 nm)

We received SAXS measurements from two laboratories. The laboratories were advised to measure two different concentrations of the particle dispersion. The dispersion as received with 10 mg/ml and diluted 1:1 to 5 mg/ml. For one laboratory it was not possible to measure the diluted sample due to lack of contrast. The obtained normalized size distributions and the cumulative size distributions are shown in Figure 74.

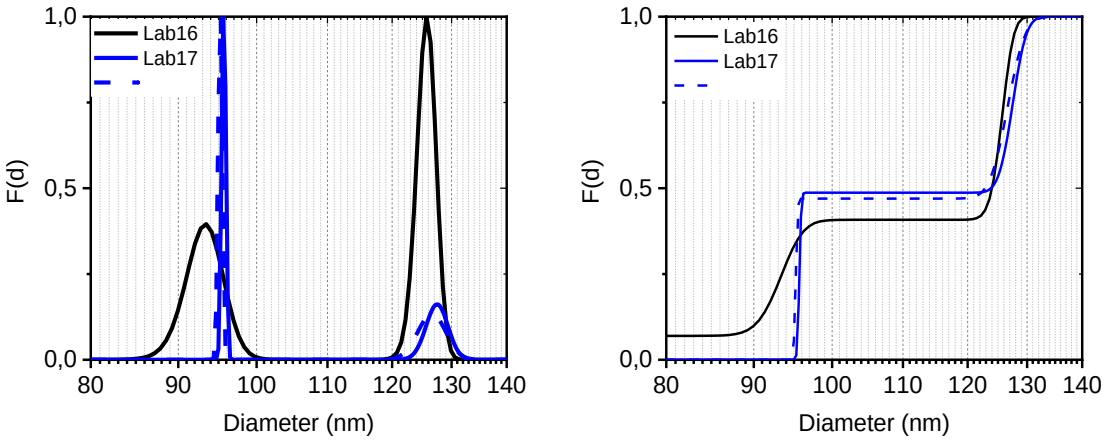

Figure 74: normalized (left) and cumulated (right) size distribution functions of the diameter of polystyrene particles (90/125 nm). All reported results are shown. Dashed line lower concentration.

From the distributions of the selected datasets the mean, median and modal diameters with repeatability standard deviation are determined and plotted in Figure 75.

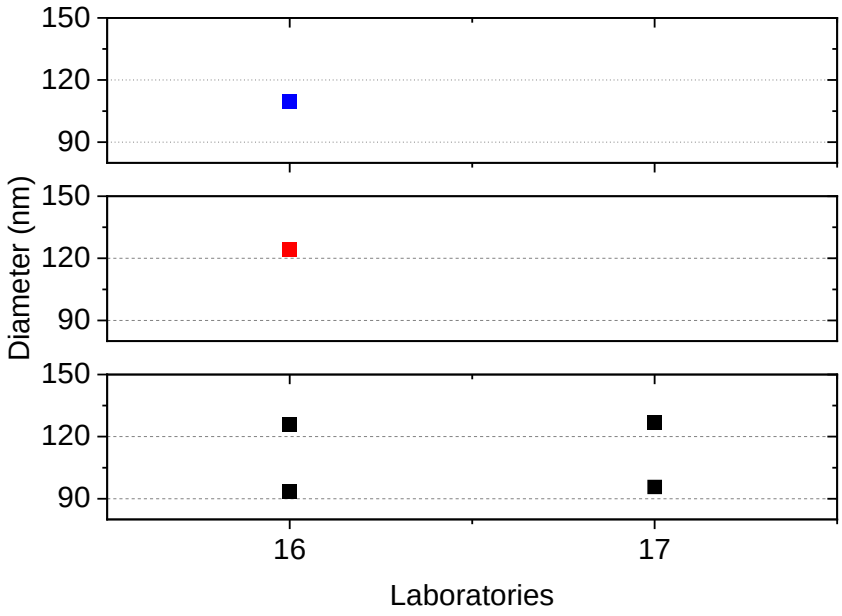

Figure 75: mean (blue), median (red) and modal (black) diameter of PSL particles (90/125 nm) analysed with SAXS.

The obtained particles size population are in the expected range and are comparable in between the laboratories. As only two labs were able to measure the PSL particles, a further evaluation of the results has not been done for the mean and median diameter. The modal diameter is given by 95 ± 1.9 nm (2%) for mode 1 and 126.6 ± 0.8 nm (1%) for mode 2.

Transmission electron microscopy – TEM

For analysis with TEM the test materials silica (20 nm and 50 nm), polystyrene particles 90/125 nm and 80/800 nm, titanium oxide, zinc oxide and silver particles were sent out readily prepared on copper TEM grids. The samples were prepared by drop on method.

We received TEM measurements from eleven different laboratories. Thirty-three results were handed in. An Overview of the received results is given in Table 56. The results of the TEM measurements are presented for each particle system.

Table 56. Overview of the results for the mean, median and modal diameter determined via TEM measurement. The reported standard deviation is the between laboratory deviation by a factor of 2.

Particle system	# labs	d	$d_{0,\,mean}$ (nm)	$d_{0,median}$ (nm)	$d_{0,modal}$ (nm)
Ag	6	Max. Feret	12.5 ± 10.2	11.4 ± 10	10.5 ± 10.2
		Min. Feret	9.5 ± 8.4	8.8 ± 7.9	8.2 ± 8.4
		Eq. circular	10.9 ± 9.8	10.1 ± 8	9.5 ± 9.4
SiO2 (20 nm)	5	Max. Feret	19.9 ± 2.6	19.5 ± 3.2	18.9 ± 3.6
		Min. Feret	17.5 ± 0.8	17.5 ± 1	17.5 ± 1.2
		Eq. circular	17.1 ± 2.6	17.2 ± 2.6	17.8 ± 2
SiO2 (50 nm)	6	Max. Feret	52.1 ± 4	52.6 ± 5	51 ± 6.4
		Min. Feret	46.5 ± 1.6	46.3 ± 2.2	47 ± 1.4
		Eq. circular	48.5 ± 2.2	48 ± 2.4	47.8 ± 2.4
PSL (90/125 nm)	7	Max. Feret	106.2 ± 14.2	105.3 ± 24.2	88.5 ± 12.4/121.9 ± 9.8
		Min. Feret	101 ± 12	96.1 ± 20.4	83.9 ± 7.6/119.8 ± 7.6
		Eq. circular	103.5 ± 15.6	99.8 ± 21.2	85.2 ± 9/121.1 ± 8.2
ZnO	2		No reliable validation possible		
TiO_2	4	Max. Feret	242.2 ± 56	236.2 ± 50	217.5 ± 25.6
		Min. Feret	175 ± 42	170 ± 40	175 ± 14
		Eq. circular	198 ± 46	189 ± 60	171 ± 50
PSL (80/800 nm)	3	Eq. circular	No reliable validation possible		783 ± 72

TEM: Silica particles (20 nm)

We received TEM measurements from five laboratories. One further laboratory measured the particles but received non-evaluable images. The pixel sizes used in image acquisition were in a range of 0.158 nm/px to 0.554 nm/px on average. That means that all TEM measurements were performed with a better pixel size than the minimal requirement. The laboratories were advised to count at least 300 particles for a reliable size distribution. The obtained normalized size distributions and the cumulative size distributions of the max. Feret diameter are shown in Figure 76.

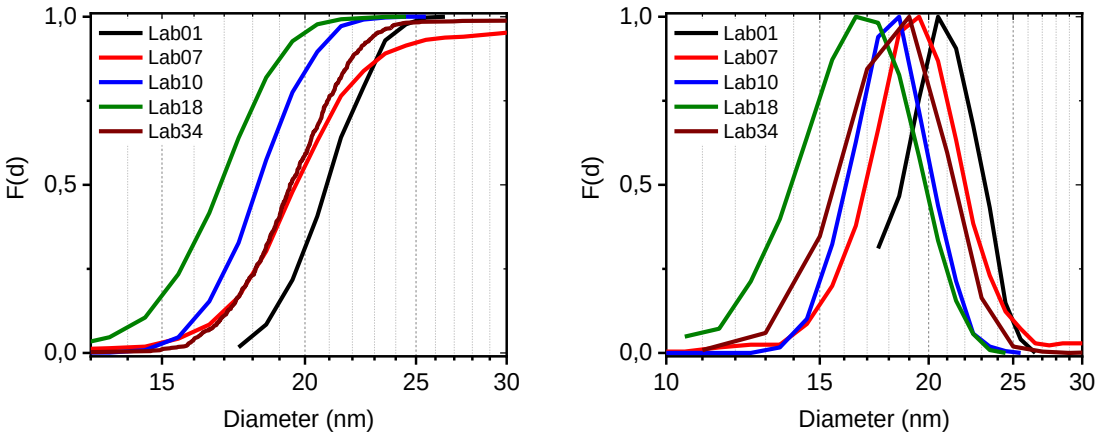

Figure 76: normalized (left) and cumulated (right) size distribution functions of the max. Feret diameter of silica particles (20 nm). All reported results are shown.

The obtained size distribution and diameters show slight variations but are in the expected variance for TEM analysis. All measurements are used for the further data evaluation.

From the distributions of the selected datasets the mean, median and modal diameters are calculated and plotted in Figure 77. The error bars are calculated using the bootstrap method.

To further evaluate the precision of the results of the ILC obtained on SiO_2 (20 nm) particles, the average values of the mean, median and modal diameters of the selected datasets were calculated as well as the standard deviation between the laboratories σ_L of the mean, median and modal values and the relative standard deviation σ_{rel} (=standard deviation/average diameter). These values are given in Table 57.

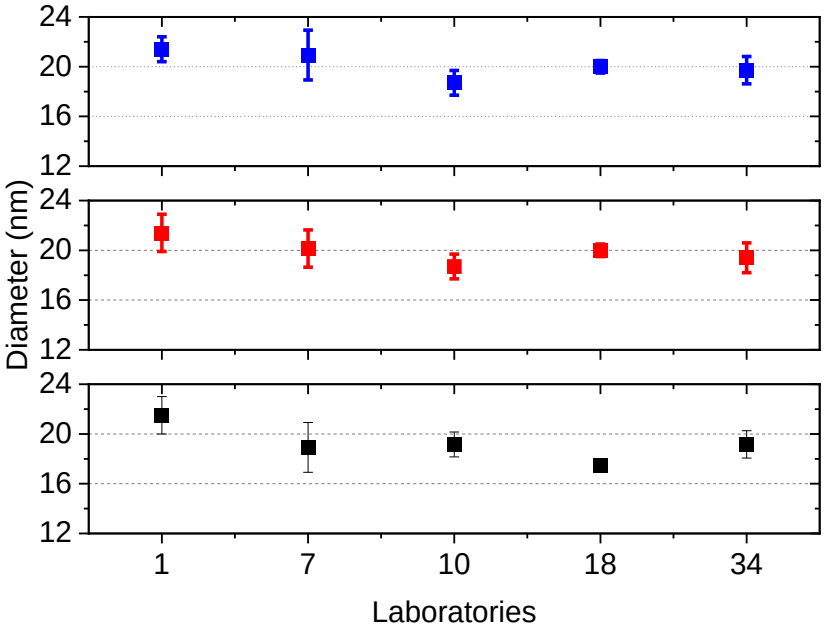

Figure 77: mean (blue), median (red) and modal (black) max. Feret diameter of silica nanoparticles analysed with TEM.

Table 57. Statistics of silica (20 nm) nanoparticles datasets

	d_0 (nm)	σ_L	σ_{rel}
max. Feret diameter			
average (**mean**(diameter))	19.9	1.3	0.07
average (**median**(diameter))	19.5	1.6	0.08
average (**modal**(diameter))	18.9	1.8	0.09
min. Feret diameter			
average (**mean**(diameter))	17.5	0.4	0.02
average (**median**(diameter))	17.5	0.5	0.03
average (**modal**(diameter))	17.5	0.6	0.03
equivalent circular diameter			
average (**mean**(diameter))	17.1	1.3	0.07
average (**median**(diameter))	17.2	1.3	0.07
average (**modal**(diameter))	17.8	1	0.06
average geometric standard deviation (diameter)	1.16	0.07	0.06

The standard deviation is multiplied by a factor of 2 in order to yield a coverage probability of 95% and additionally the percentage is given. Thus, the mean equivalent circular diameter of the SiO_2 (50 nm) particles is obtained as 17.1 ± 2.6 nm (15%), the median equivalent circular diameter is given by 17.2 ± 2.6 nm (15%) and the modal equivalent circular diameter is given by 17.8 ± 2 nm (11%).

TEM: Silica particles (50 nm)

We received TEM measurements from six laboratories. The pixel sizes used in image acquisition were in a range of 0.28 nm/px to 4.35 nm/px on average. That means that all TEM measurements were performed with the minimal required pixel size or better. The laboratories were advised to count at least 300 particles for a reliable size distribution. The obtained normalized size distributions and the cumulative size distributions of the max. Feret diameter are shown in Figure 78.

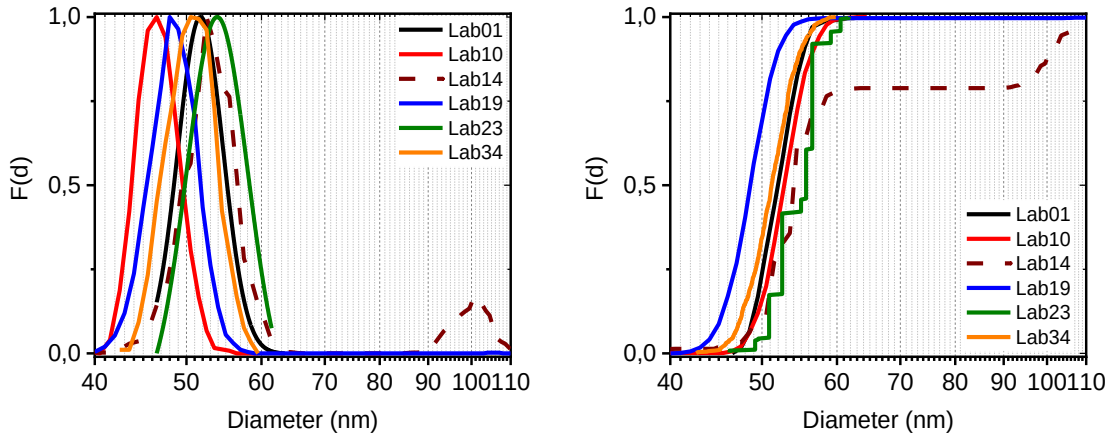

Figure 78: normalized (left) and cumulated (right) size distribution functions of the max. Feret diameter of silica particles (50 nm). All reported results are shown.

The obtained size distribution and diameters show slight variations but are not out of the expected variance for TEM analysis. For Lab 14 a contribution from agglomerates is seen at around 100 nm, for the further evaluation of diameters the measurement was excluded.

From the distributions of the selected datasets the mean, median and modal diameters are calculated and plotted in Figure 79. The error bars are calculated using the bootstrap method.

To further evaluate the precision of the results of the ILC obtained on SiO_2 (50 nm) particles, the average values of the mean and median diameters of the selected datasets were calculated as well as the standard deviation between the laboratories σ_L of the mean, median and modal values and the relative standard deviation σ_{rel} (=standard deviation/average diameter). These values are given in Table 58.

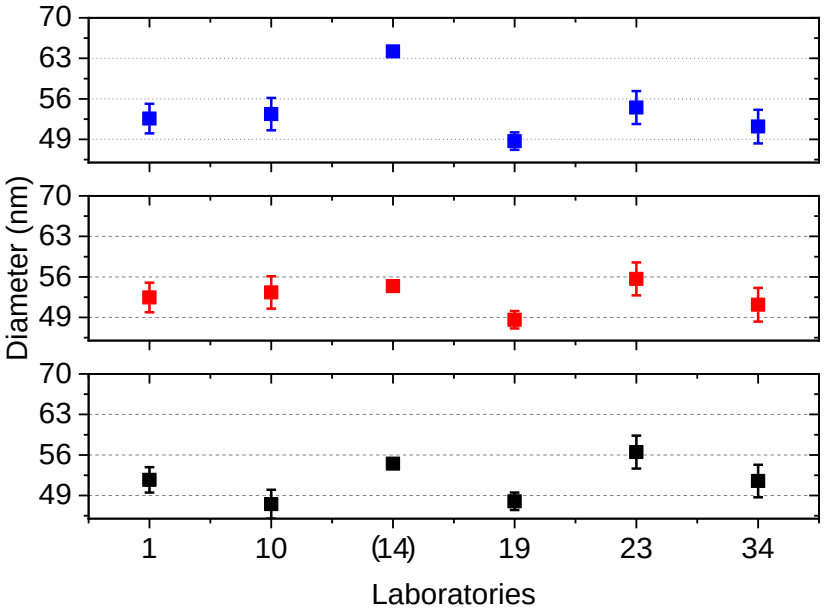

Figure 79: mean (blue), median (red) and modal (black) max. Feret diameter with bootstrap error of silica nanoparticles analysed with TEM.

Table 58. Statistics of silica (50 nm) nanoparticles datasets

	d_0 (nm)	σ_L	σ_{rel}
max. Feret diameter			
average (**mean**(diameter))	52.1	2	0.04
average (**median**(diameter))	52.6	2.5	0.05
average (**modal**(diameter))	51	3.2	0.06
min. Feret diameter			
average (**mean**(diameter))	46.5	0.8	0.02
average (**median**(diameter))	46.3	1.1	0.03
average (**modal**(diameter))	47	0.7	0.01
equivalent circular diameter			
average (**mean**(diameter))	48.5	1.1	0.02
average (**median**(diameter))	48	1.2	0.03
average (**modal**(diameter))	47.8	1.2	0.03
average geometric standard deviation (diameter)	1.1	0.06	0.05

The standard deviation is multiplied by a factor of 2 in order to yield a coverage probability of 95% and additionally the percentage is given. Thus. the mean equivalent circular diameter of the SiO_2 (50 nm) particles is obtained as 48.5 ± 2.2 nm (4.5%), the median equivalent circular diameter is given by 48 ± 2.4 nm (5%) and the modal equivalent circular diameter is given by 47.8 ± 2.4 nm (5%).

TEM: Titanium oxide particles

We received TEM measurements from four laboratories. Lab 18 also measured the particles, but the images were not evaluable due to a high agglomeration state of the particles. The pixel sizes used in image acquisition were in a range of 0.28 nm/px to 8.05 nm/px on average. That means that all TEM measurements were performed with the minimal required pixel size or better. The laboratories were advised to count at least 700 particles for a reliable size distribution. The obtained normalized size distributions and the cumulative size distributions of the max. Feret diameter are shown in Figure 80.

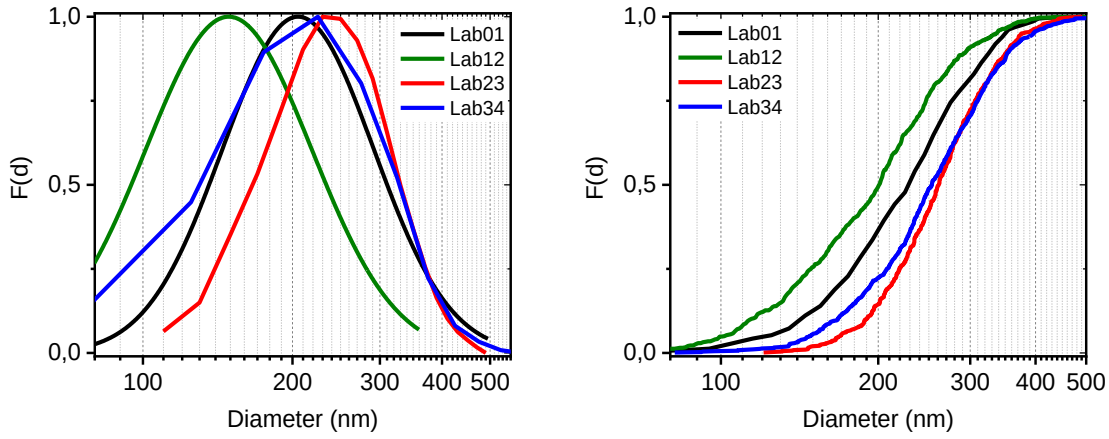

Figure 80: normalized (left) and cumulated (right) size distribution functions of the max. Feret diameter of titanium oxide particles. All reported results are shown.

The obtained size distributions are in good comparison. From the distributions of the selected datasets the mean, median and modal diameters are calculated and plotted in Figure 81. The error bars are calculated using the bootstrap method.

To further evaluate the precision of the results of the ILC obtained on TiO_2 particles, the average values of the mean and median diameters of the selected datasets were calculated as well as the standard deviation between the laboratories σ_L of the mean, median and modal values and the relative standard deviation σ_{rel} (=standard deviation/average diameter). These values are given in Table 59.

The standard deviation is multiplied by a factor of 2 in order to yield a coverage probability of 95% and additionally the percentage is given. Thus, the mean equivalent circular diameter of the TiO_2 particles is obtained as 198 ± 46 nm (32%), the median equivalent circular diameter is given by 189 ± 60 nm (23%) and the modal equivalent circular diameter is given by 171 ± 50 nm (29%).

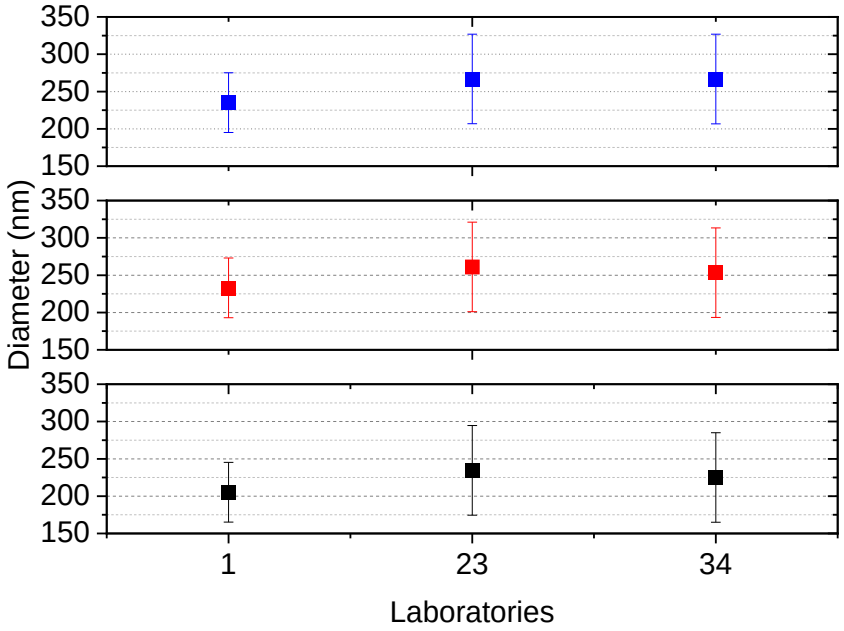

Figure 81: mean (blue), median (red) and modal (black) max. Feret diameter with bootstrap error of titanium oxide particles analysed with TEM.

Table 59. Statistics of titanium oxide nanoparticles datasets

	d_0 (nm)	σ_L	σ_{rel}
max. Feret diameter			
average (**mean**(diameter))	242.2	28	0.11
average (**median**(diameter))	236.2	25	0.10
average (**modal**(diameter))	217.5	12.8	0.06
min. Feret diameter			
average (**mean**(diameter))	175	21	0.12
average (**median**(diameter))	170	20	0.12
average (**modal**(diameter))	175	7	0.04
equivalent circular diameter			
average (**mean**(diameter))	198	23	0.12
average (**median**(diameter))	189	30	0.16
average (**modal**(diameter))	171	25	0.14
average geometric standard deviation (diameter)	1.37	0.05	0.03

TEM: Polystyrene particles (90/125 nm)

We received TEM measurements from seven laboratories. The pixel sizes used in image acquisition were in a range of 0.662 nm/px to 8.05 nm/px on average. That means that all TEM measurements were performed with the minimal required pixel size or better. The laboratories were advised to count at least 700 particles for a reliable size distribution. The obtained normalized size distributions and the cumulative size distributions of the max. Feret diameter are shown in Figure 82.

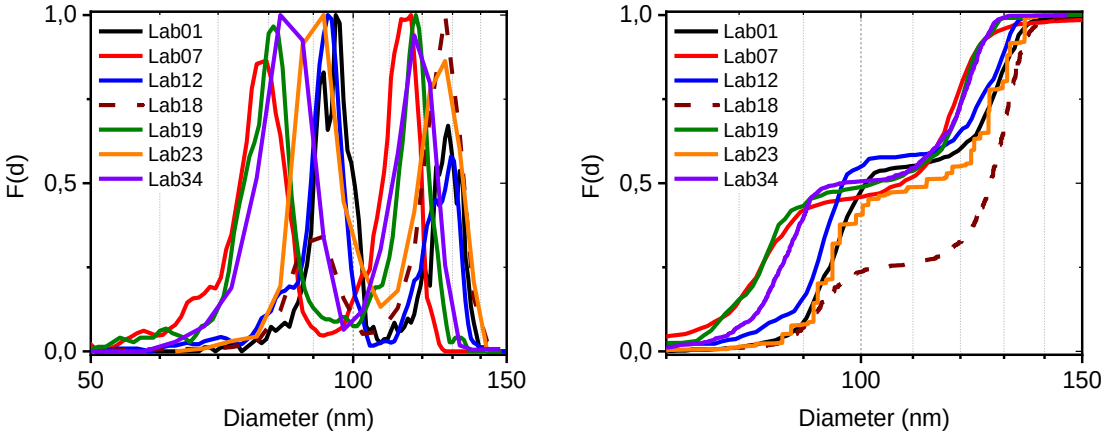

Figure 82: normalized (left) and cumulated (right) size distribution functions of the max. Feret diameter of polystyrene particles (90/125 nm). All reported results are shown.

Image evaluation was done semi-automatic by Lab 07, 18, 19 and 34. The submitted size distribution of Lab 18 shows a higher ratio of particles in the size range 125 nm. The distribution has a 2:1 ratio while a 1:1 ratio was expected. The segmentation of the particles in the image seems to be good but it cannot be excluded that the automatic counting of the particles is cause for obtained wrong ratio of the size populations for Lab 18.

From the distributions of the selected datasets the mean, median and modal diameters are calculated and plotted in Figure 83. The error bars are calculated using the bootstrap method.

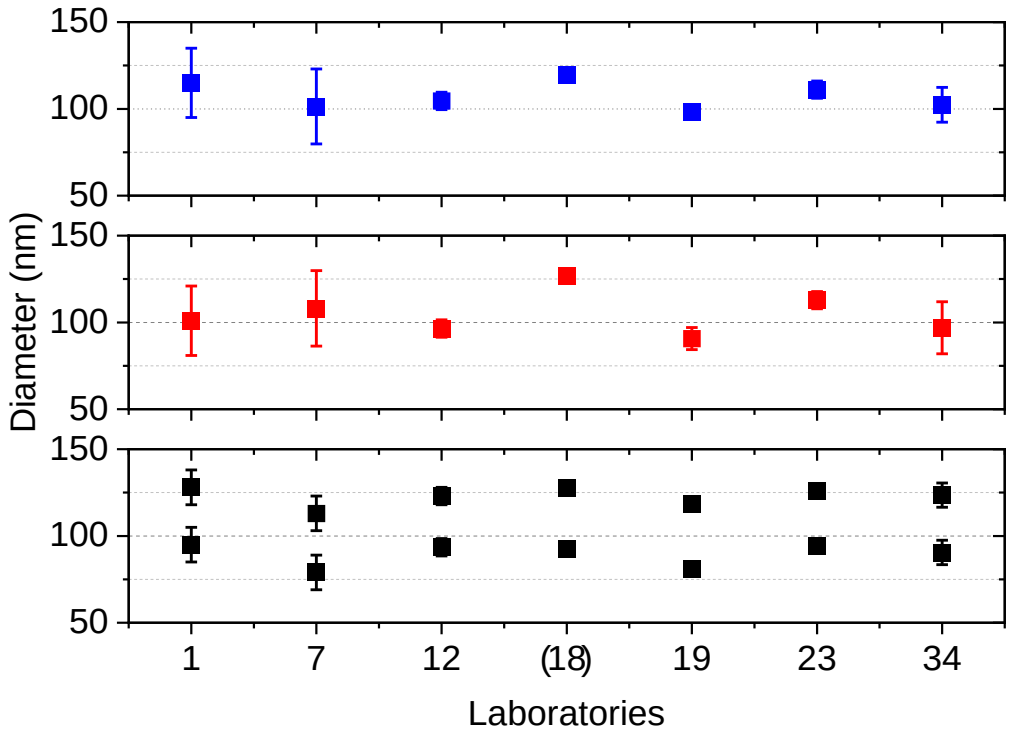

Figure 83: mean (blue), median (red) and modal (black) max. Feret diameter with bootstrap error of polystyrene particles analysed with TEM.

To further evaluate the precision of the results of the ILC obtained on polystyrene (90/125 nm) particles, the average values of the mean, median and modal diameters of the selected datasets were calculated as well as the standard deviation between the laboratories σ_L of the mean, median and modal values and the relative standard deviation σ_{rel} (=standard deviation/average diameter). These values are given in Table 60.

Table 60: Statistics of polystyrene (90/125 nm) particles datasets

	d_0 (nm)	σ_L	σ_{rel}
max. Feret diameter			
average (**mean**(diameter))	106.2	7.1	0.07
average (**median**(diameter))	105.3	12.1	0.11
average(**modal(1)**(diameter))	88.5	6.2	0.07
average(**modal(2)**(diameter))	121.9	4.9	0.04
min. Feret diameter			
average (**mean**(diameter))	101	6	0.06
average (**median**(diameter))	96.1	10.2	0.11
average(**modal(1)**(diameter))	83.9	3.8	0.05
average(**modal(2)**(diameter))	119.8	3.8	0.03
equivalent circular diameter			
average (**mean**(diameter))	103.5	7.8	0.08
average (**median**(diameter))	99.8	10.6	0.11
average (**modal(1)**(diameter))	85.2	4.5	0.05
average (**modal(2)**(diameter))	121.1	4.1	0.03
average geometric standard deviation	1.2	0.08	0.07

(diameter)			

The standard deviation is multiplied by a factor of 2 in order to yield a coverage probability of 95% and additionally the percentage is given. Thus, the mean equivalent circular diameter of the PSL (90/125 nm) particles is obtained as 103.5 ± 15.6 nm (15%) and the median equivalent circular diameter is given by 99.8 ± 21.2 nm (21%). The modal equivalent circular diameters are for mode 1 85.2 ± 9 nm (11%) and for mode 2 121.1 ± 8.2 nm (7%).

TEM: Polystyrene particles (80/800 nm)

We received TEM measurements from three laboratories. The pixel sizes used in image acquisition were in a range of 0.28 nm/px to 11.05 nm/px on average. That means that all TEM measurements were performed with the minimal required pixel size or better. The laboratories were advised to count at least 700 particles for a reliable size distribution. The obtained normalized size distributions and the cumulative size distributions of the max. Feret diameter are shown in Figure 84.

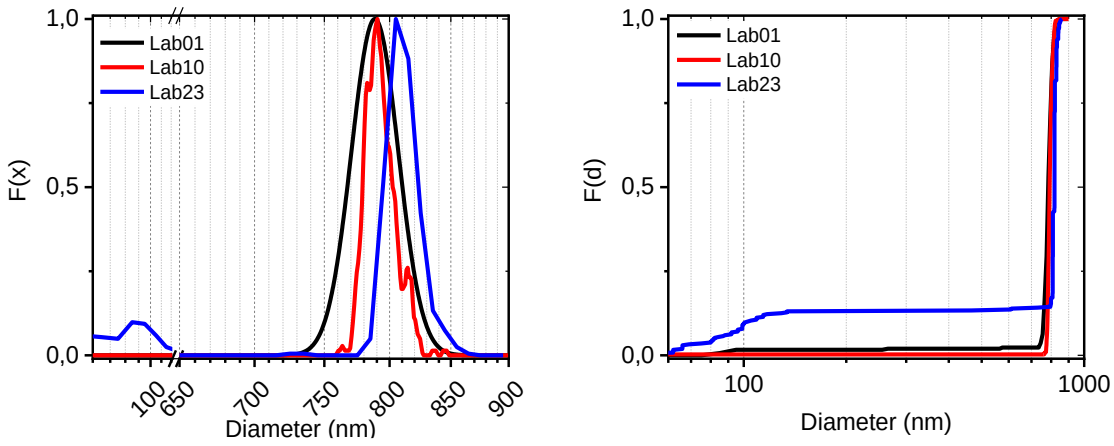

Figure 84: normalized (left) and cumulated (right) size distribution functions of the max. Feret diameter of polystyrene particles (80/800 nm). All reported results are shown.

The 80 nm particles are prone to agglomerate with the 800 nm particles. Only Lab 23 detected the 80 nm size fraction of the particle mixture. No homogeneous distribution of the different size fraction was achieved. Overlay of the small 80 nm particle fraction by 800 nm particles is an additional problem.

From the distributions of the selected datasets the mean, median and modal diameters are calculated and plotted in Figure 85. The error bars are calculated using the bootstrap method.

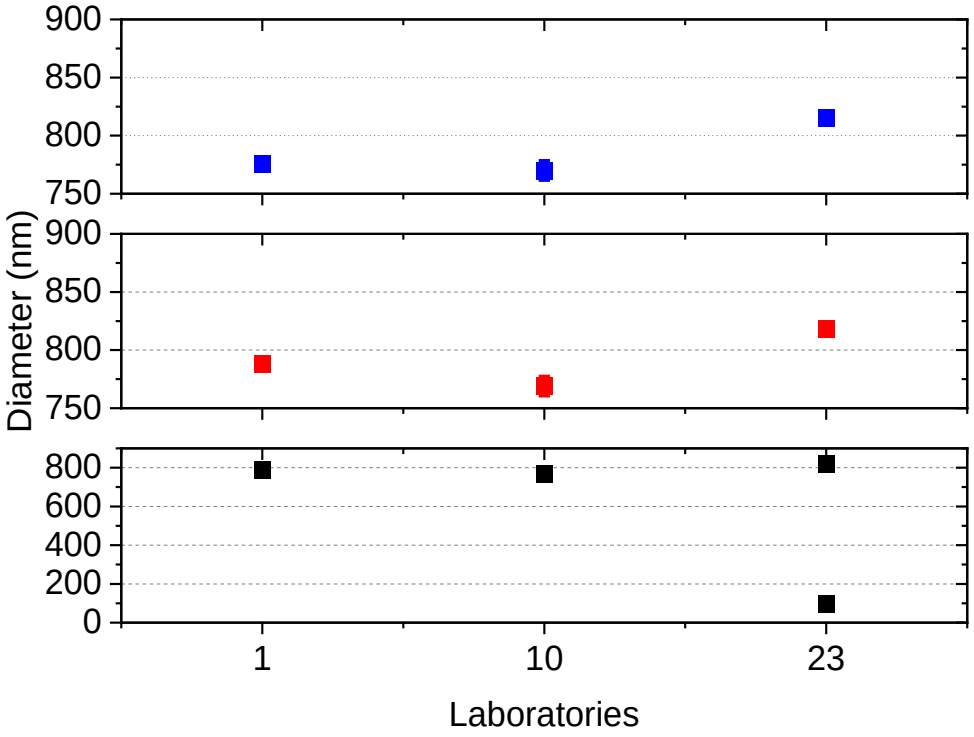

Figure 85: mean (blue), median (red) and modal (black) max. Feret diameter with bootstrap error of polystyrene particles (80/800 nm) analysed with TEM.

No further evaluation of the precision of the results of the ILC obtained on polystyrene (80/800 nm) particles for the size mixture are done as the different particles size populations are not detected reliable. Nevertheless, the 800 nm particles could be detected well and for the modal equivalent circular diameter 783 ± 36 nm is derived.

The expanded reproducibility standard deviation is calculated by multiplying reproducibility standard deviation with the coverage factor, k=2. A modal diameter of 783 ± 72 nm (9%).

TEM: Silver particles

We received TEM measurements from six laboratories. The pixel sizes used in image acquisition were in a range of 0.19 nm/px to 2.64 nm/px on average. That means that all TEM measurements were performed with the minimal required pixel size or better. The laboratories were advised to count at least 700 particles for a reliable size distribution. The obtained normalized size distributions and the cumulative size distributions of the max. Feret diameter are shown in Figure 80.

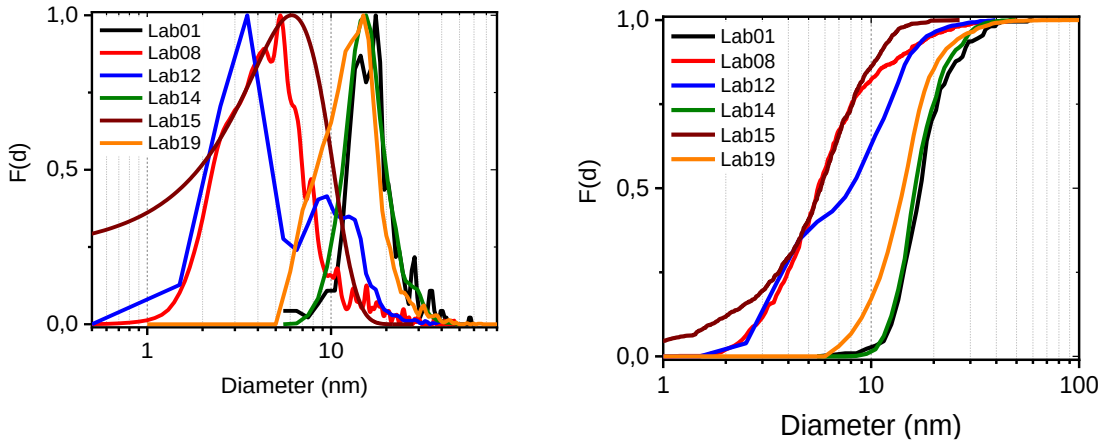

Figure 86: normalized (left) and cumulated (right) size distribution functions of the max. Feret diameter of silver particles. All reported results are shown.

Size distributions in two different fractions at around 5 nm and 15-20 nm are obtained. The therefrom obtained diameters are compared to SEM data very low. Degeneration of the silver particles on the TEM was discussed. TEM measurement of freshly prepared silver particles and the ones stored for several months show no significant differences in the obtained size distributions. Degeneration of the particles would then happen very rapidly, because of the small particle size or due to radiation damage. Compared to the obtained particle size with SAXS or DMAS the size of the 15-20 nm fraction would fit. The fraction of 5 nm particles would not fit. For both fractions the pixel size for image acquisition was comparable. An evaluator influence can be discussed but seems to be unlikely for such a significant difference.

From the distributions of the selected datasets the mean, median and modal diameters are calculated and plotted in Figure 87. The error bars are calculated using the bootstrap method.

To further evaluate the precision of the results of the ILC obtained on Ag particles, the average values of the mean and median diameters of the selected datasets were calculated as well as the standard deviation between the laboratories σ_L of the mean, median and modal values and the relative standard deviation σ_{rel} (=standard deviation/average diameter). These values are given in Table 61.

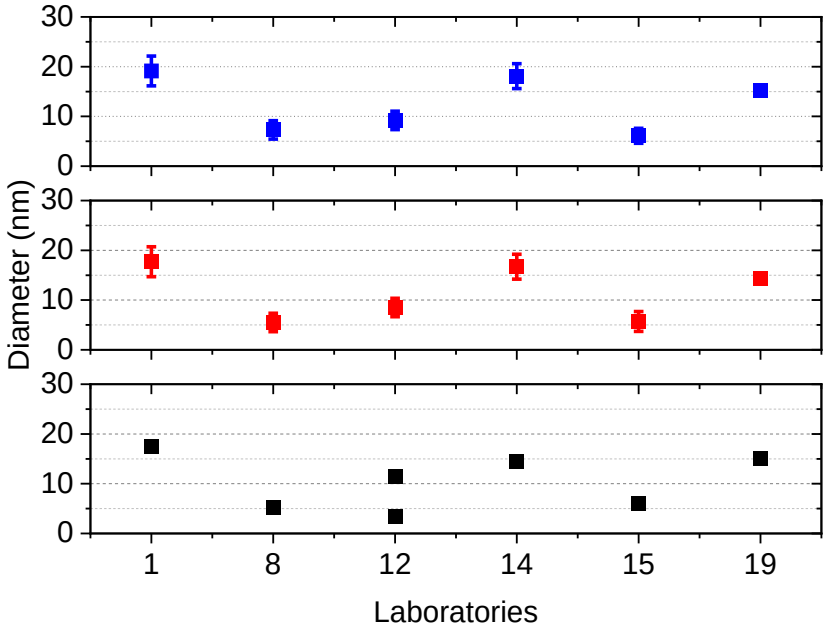

Figure 87: mean (blue), median (red) and modal (black) max. Feret diameter with bootstrap error of silver particles analysed with TEM.

Table 61. Statistics of silver nanoparticles datasets

	d_0 (nm)	σ_L	σ_{rel}
max. Feret diameter			
average (**mean**(diameter))	12.5	5.2	0.42
average (**median**(diameter))	11.4	5.0	0.44
average (**modal**(diameter))	10.5	5.1	0.49
min. Feret diameter			
average (**mean**(diameter))	9.5	4.3	0.45
average (**median**(diameter))	8.8	4.0	0.45
average (**modal**(diameter))	8.2	4.3	0.52
equivalent circular diameter			
average (**mean**(diameter))	10.9	4.4	0.40
average (**median**(diameter))	10.1	4.1	0.40
average (**modal**(diameter))	9.5	4.8	0.50
average geometric standard deviation (diameter)	1.67	0.32	0.19

The standard deviation is multiplied by a factor of 2 in order to yield a coverage probability of 95% and additionally the percentage is given. Thus, the mean equivalent circular diameter of the Ag particles is obtained as 10.9 ± 9.8 nm (90%), the median equivalent circular diameter is given by 10.1 ± 8 nm (80%) and the modal equivalent circular diameter is given by 9.5 ± 9.4 nm (99%). The obtained deviation between the laboratories of the silver particles is too high for a validation of the particle system for TEM.

TEM: Zinc oxide particles

We received TEM measurements from two laboratories. The pixel sizes used in image acquisition were in a range of 0.28 nm/px to 11.05 nm/px on average. That means that all TEM measurements were performed with the minimal required pixel size or better. The laboratories were advised to count at least 700 particles for a reliable size distribution. The obtained normalized size distributions and the cumulative size distributions of the max. Feret diameter are shown in Figure 88.

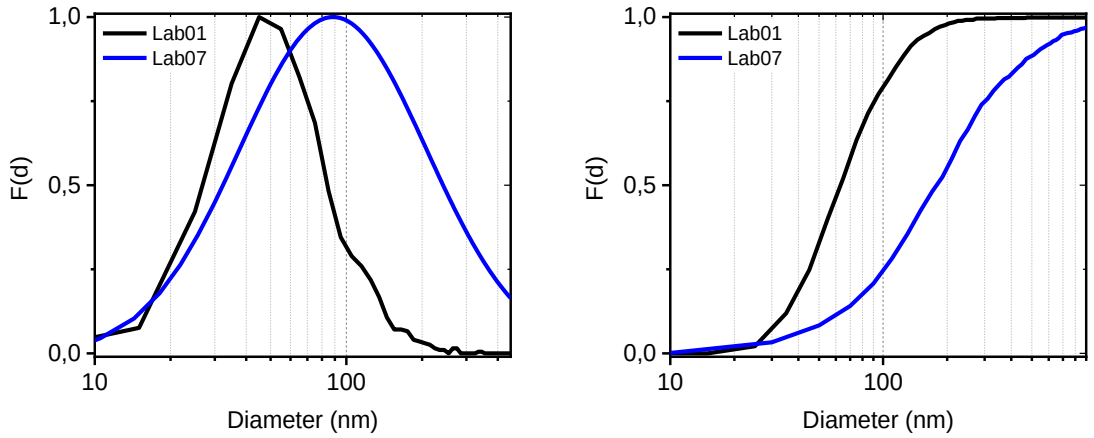

Figure 88: normalized (left) and cumulated (right) size distribution functions of the max. Feret diameter of zinc oxide particles. All reported results are shown.

The size distributions differ significantly from each other. Zinc oxide is a real-life nanomaterial with wide distribution, which tends to agglomerate. A preparation of the specimen for TEM without any agglomerates cannot be achieved. Lab 07 stated that also agglomerates were counted in the image evaluation. Agglomerate counting could explain the high variance in between the laboratories and is not in accordance with the draft TG. Lab 01 and Lab 02 made a complete manual date evaluation and only measured single particles or particles in agglomerates which could be clearly separated from the neighbouring particles. Though, the obtained particle size distributions vary significantly. Due to the low number of contributing laboratories and high variance of the results no further evaluation of the precision of the results of the ILC obtained on zinc oxide particles was done.

Analysis of integral components of agglomerates and aggregates in EM images

When particles are touching each other and are not overlapping, individual particles with a spherical shape, like polystyrene particles, may be easily visually distinguished and counted. The influence of the touching particles on the resulting size distribution is of minor importance for the resulting size distribution (see Figure 89, a) without touching particles, b) with touching particles). For individual particles with an irregular shape the difference may become significant.

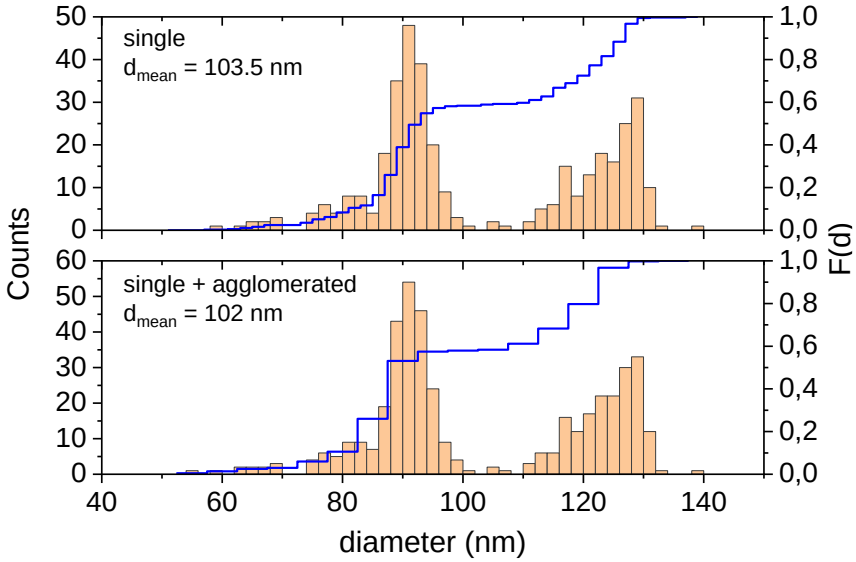

Figure 89: Histogram of polystyrene particles (90/125 nm)

In contrast to touching particles, integral components of an agglomerate or aggregate might be overlapping or fused, and the boundaries are difficult or impossible to identify. The resulting size distribution can be influenced by the selection of the integral components and the accuracy of the segmentation (threshold) of the selected integral compounds.

The identification of particles as integral component of agglomerates and aggregates is strongly material dependent. The measurement of an integral component within an agglomerate/aggregate might be possible on the surface of the agglomerates/aggregate if the complete physical boundaries of the integral component are clearly visible in the imaging plane.

Figure 90 shows some exemplary images of agglomerated and aggregated particles. Only particles can be measured where the complete physical boundaries of the integral components can be clearly identified (examples marked in yellow). Particles that are fused or are overlaying such that the particles cannot be clearly separated should not be measured as individual particle (examples marked in red).

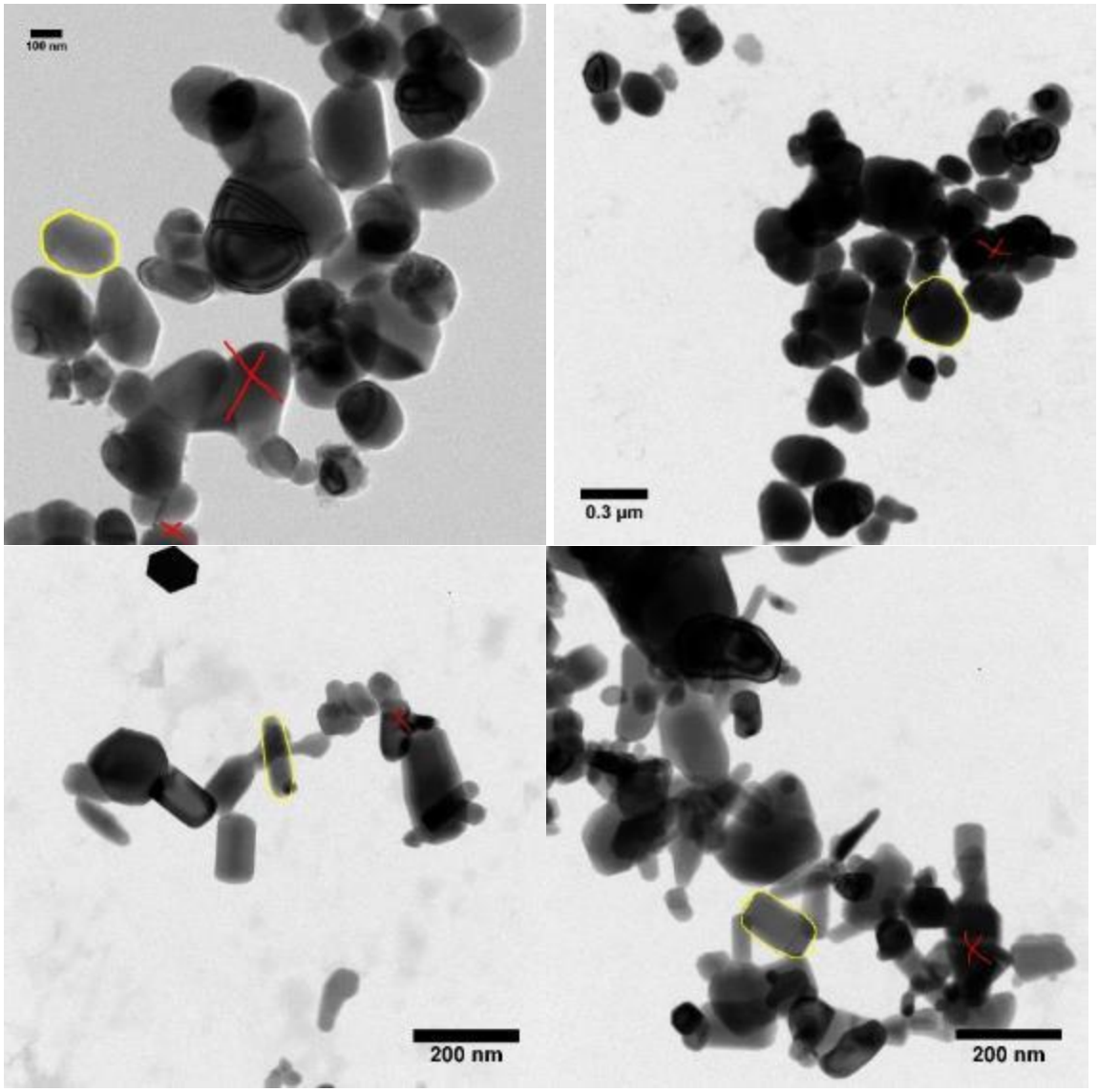

Figure 90: Exemplary TEM-images of titanium oxide particles (top) and zinc oxide particles (bottom).

The possibility to identify the borders of touching particles in electron microscopic images strongly depends on the image quality. The image quality can be influenced by many factors, e.g. the chosen settings, the subjective perception of the operator, sample preparation quality or material properties. Generally, the performance of the electron microscopes used may vary between instruments. Each instrument has its own technical limits which influences the attained image resolution. In a TEM normally a much better image resolution can be obtained as in a SEM. In order to have the best possibility to identify the integral components of an agglomerate or aggregate it is recommended to use a TEM to [19, 20].

Conclusion for the test materials

The sorting of the methods in the following graphs is done with respect to the delivered resulting diameter: A) Equivalent circular diameter (AFM, SEM, TEM); B) Hydrodynamic equivalent diameter (DLS, PTA); C) Aerodynamic/Mobility equivalent diameter (DMAS); D) Specific methods (SAXS, CLS, sp ICP-MS). The methods DLS, CLS and SAXS deliver intensity / volume-based PSDs. For non-spherical particles or wide distributions this results in non-comparable values for the mean, median and modal diameters. In this ILC this is important for TiO_2 and ZnO. For all other test materials the results for the mean, median and modal diameters are within the expected size rage.

Silica particles (20 nm)

Figure 91 and Table 62 shows the intermethod comparison for the ~20 nm silica particles. All determined diameters are in the range of 20 ± 3 nm. Deviation is obtained by CLS, here the measurement of the nanomaterial does not perform well, due to a lack of contrast of the nanomaterial to the measurement medium. In general, the diameters obtained by different methods show a good comparability, with slight variances since different methods determine a different diameter e.g. equivalent circular diameter vs. hydrodynamic diameter and aerodynamic diameter.

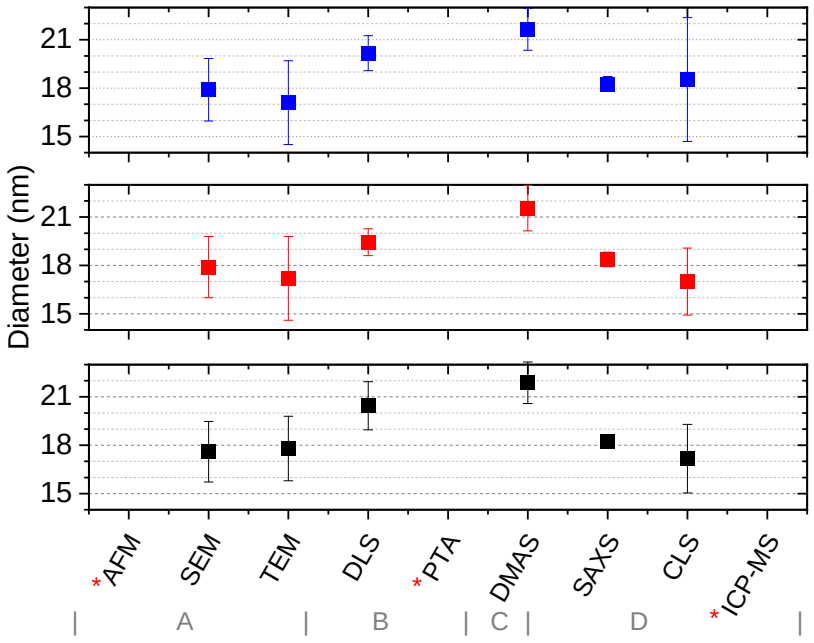

Figure 91: Intermethod comparison of mean (blue), median (red) and modal (black) diameters of silica particles (20 nm). The reproducibility standard deviation (k=1) is included. Methods marked with * were not used in the ILC with this nanomaterial. (equivalent circular diameter for TEM and SEM)

Table 62. Overview of the average mean, median and modal diameters of silica particles (20 nm) obtained by the different methods. Methods marked with * were not used in the ILC with this nanomaterial. The expanded reproducibility standard deviation (k=2) is included.

Method	d	d_{mean} (nm)	d_{median} (nm)	d_{modal} (nm)
AFM*	$d_{0,hgt}$	-	-	-
SEM	$d_{0,ecd}$	17.9 ± 1.94	17.9 ± 1.9	17.6 ± 1.88
TEM	$d_{0,ecd}$	17.1 ± 2.6	17.2 ± 2.6	17.8 ± 2
DLS	$d_{i,hyd}$	20.2 ± 2.2	19.4 ± 1.7	20.5 ± 3
PTA*	$d_{0,hyd}$	-	-	-
DMAS	$d_{0,emob}$	21.6 ± 2.6	21.6 ± 2.8	21.9 ± 2.6
SAXS	$d_{3,Iscat}$	18.3 ± 0.9	18.4 ± 0.9	18.2 ± 0.75
CLS	$d_{3,St}$	18.5 ± 7.7	17 ± 4.2	17.2 ± 4.2
sp ICP-MS*	$d_{0,mass}$	-	-	-

Silica particles (50 nm)

Figure 92 and Table 63 shows the intermethod comparison for the ~50 nm silica particles. All determined diameters are in the range of 50 ± 5 nm. Deviation is obtained by CLS, here the measurement of the nanomaterial does not perform well, due to a lack of contrast of the nanomaterial to the measurement medium. In general, the diameters obtained by different methods show a good comparability, with slight variances due to the fact that different methods determine a different diameter e.g. equivalent circular diameter vs. hydrodynamic diameter and aerodynamic diameter.

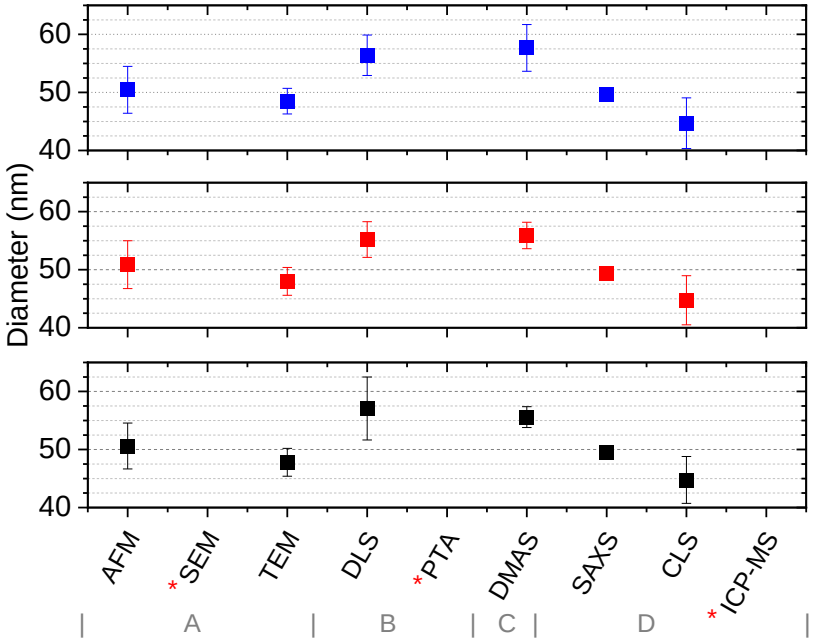

Figure 92: Intermethod comparison of mean (blue), median (red) and modal (black) diameters of silica particles (50 nm). The reproducibility standard deviation (k=1) is included. Methods marked with * were not used in the ILC with this nanomaterial. The reproducibility standard deviation is included. (Equivalent circular diameter for TEM and SEM)

Table 63. Overview of the average mean, median and modal diameters of silica particles (50 nm) obtained by the different methods. Methods marked with * were not used in the ILC with this material. The expanded reproducibility standard deviation (k=2) is included.

Method	d	d_{mean} (nm)	d_{median} (nm)	d_{modal} (nm)
AFM	$d_{0,hgt}$	50.5 ± 8	50.9 ± 8.2	50.6 ± 7.8
SEM*	$d_{0,ecd}$	-	-	-
TEM	$d_{0,ecd}$	48.5 ± 2.2	48 ± 2.4	47.8 ± 2.4
DLS	$d_{i,hyd}$	56.4 ± 7	55.2 ± 6.2	57.1 ± 10.9
PTA*	$d_{0,hyd}$	-	-	-
DMAS	$d_{0,emob}$	57.7 ± 8	55.9 ± 4.5	55.6 ± 3.6
SAXS	$d_{3,Iscat}$	49.7 ± 1.2	49.6 ± 1.8	49.4 ± 1.7
CLS	$d_{3,St}$	44.7 ± 8.7	44.7 ± 8.5	44.8 ± 8.1
sp ICP-MS*	$d_{0,mass}$	-	-	-

Titanium oxide particles

Figure 93 and Table 64 shows the intermethod comparison for the titanium oxide particles. Titanium oxide is a real-life material with unregular shaped particles with a wide size distribution which tend to agglomerate. A higher uncertainty is usually expected for the size determination of a real-life material. Only in the case of PTA the uncertainty was higher than 50% and led to an exclusion. All determined diameters by other methods are in the range of 250 ± 65 nm. Variances are due to the fact that different methods determine a different diameter e.g. equivalent circular diameter vs. hydrodynamic diameter. The values for DLS and CLS are retrieved from intensity / volume-based PSDs. Intensity/volume-based PSDs lead to higher values for the mean, median and modal diameters.

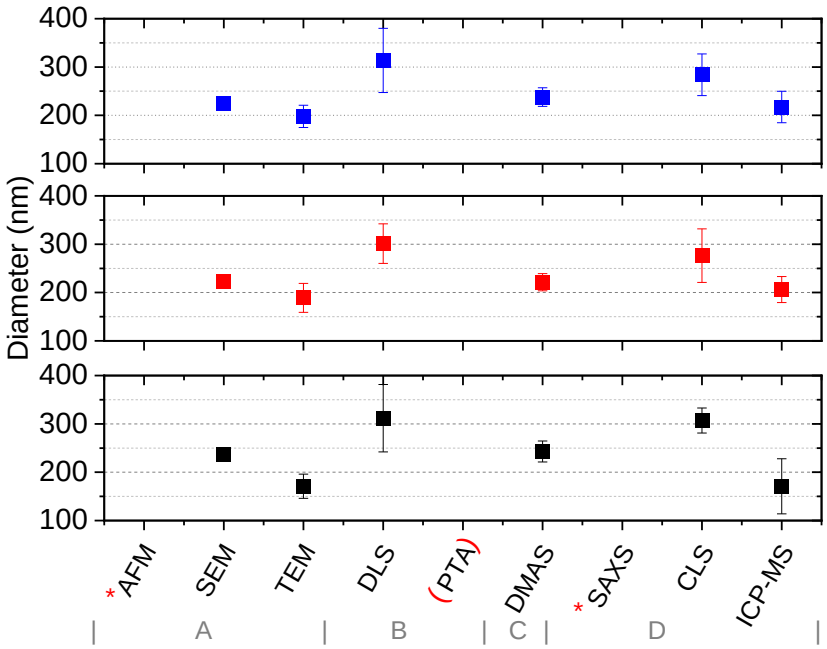

Figure 93: Intermethod comparison of mean (blue), median (red) and modal (black) diameters of titanium oxide particles. The reproducibility standard deviation (k=1) is included. Methods marked with * were not used in the ILC with this material. Methods in brackets delivered no valid results due to an uncertainty > 50%. (equivalent circular diameter for TEM and SEM)

Table 64. Overview of the average mean, median and modal diameters of titanium oxide particles obtained by the different methods. Methods marked with * were not used in the ILC with this nanomaterial. The expanded reproducibility standard deviation (k=2) is included.

Method	d	d_{mean} (nm)	d_{median} (nm)	d_{modal} (nm)
AFM*	$d_{0,hgt}$	-	-	-
SEM	$d_{0,ecd}$	224.4 ± 5.6	222.4 ± 8	237 ± 14
TEM	$d_{0,ecd}$	198 ± 46	189 ± 60	171 ± 50
DLS	$d_{i,hyd}$	314 ± 134	301 ± 123	312 ± 139
PTA	$d_{0,hyd}$	No reliable validation possible		
DMAS	$d_{0,emob}$	238 ± 38.3	221.3 ± 40	243 ± 43.5
SAXS*	$d_{3,Iscat}$	-	-	-
CLS	$d_{3,St}$	284 ± 86.6	276.4 ± 110.8	307 ± 51.8
sp ICP-MS	$d_{0,mass}$	217 ± 65	206 ± 55	171 ± 114

Polystyrene particles (90/125 nm)

Figure 94 and Table 65 shows the intermethod comparison for the polystyrene particle mixture with 90 and 125 nm particles with a ratio of 1:1. Except with spICP-MS the particles were be measured and delivered reasonable uncertainties with all methods. For DMAS only few data was available, which led to a high variance for the median diameter, but the mean and modal diameters were obtained in good comparison to the results from other methods. The separation of the two different modes was not possible to detect with DLS and the modes were only indicated when using PTA. The ratio could not be determined reliable with SAXS and CLS. For CLS the labs that used the disc CLS had no disc available for low density nanomaterial and only adjusted the gradient, which has in this case a higher uncertainty. Microscopic methods determine well comparable diameters. In the case of SEM, a slightly higher diameter was determined, due to a less high resolution compared to TEM and AFM. The derived mean/median hydrodynamic diameter from DLS and PTA is usually higher than the equivalent circular diameter but comparable in between the methods.

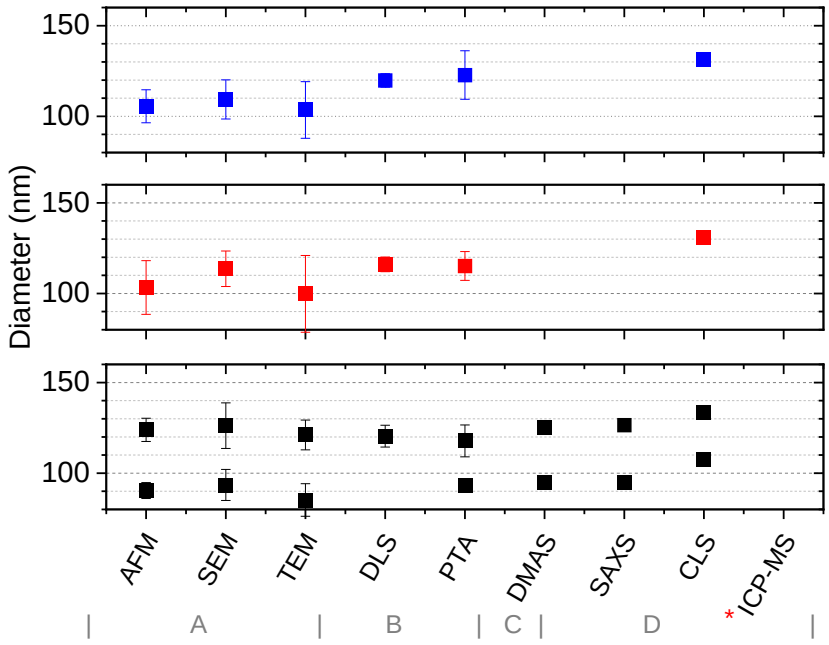

Figure 94: Intermethod comparison of mean (blue), median (red) and modal (black) diameters of polystyrene particles (90/125 nm). The reproducibility standard deviation (k=1) is included. Methods marked with * were not used in the ILC with this nanomaterial. (equivalent circular diameter for TEM and SEM)

Table 65. Overview of the average mean, median and modal diameters of polystyrene particles (90/125 nm) obtained by the different methods. Methods marked with * were not used in the ILC with this nanomaterial. The expanded reproducibility standard deviation (k=2) is included.

Method	d	d_{mean} (nm)	d_{median} (nm)	d_{modal} (nm)
AFM	$d_{0,hgt}$	110.1 ± 1.1	113.6 ± 2.8	94.2 ± 1.7/123.2 ± 0.6
SEM	$d_{0,ecd}$	109.3 ± 10.8	113.6 ± 9.8	93.5 ± 8.6/126.2 ± 12.6
TEM	$d_{0,ecd}$	103.5 ± 15.6	99.8 ± 21.2	85.2 ± 9/121.1 ± 8.2
DLS	$d_{i,hyd}$	119.8 ± 7.4	116.1 ± 8.1	120.5 ± 12
PTA	$d_{0,hyd}$	122.7 ± 27	115.2 ± 16	93.3 ± 4/117.8 ± 17.5
DMAS	$d_{0,emob}$	No reliable validation possible		94.7 ± 2/125.3 ± 7.5
SAXS	$d_{3,Iscat}$	Not applicable		95 ± 2/126.6 ± 1.7
CLS	$d_{3,St}$	No reliable validation possible d_{mean} = 131 nm, d_{median} = 131 nm, d_{modal1} = 108 nm, d_{modal2} = 133 nm		
sp ICP-MS*	$d_{0,mass}$	-	-	-

Polystyrene particles (80/800 nm)

Figure 95 and Table 66. Overview of the average mean, median and modal diameters of polystyrene particles (80/800 nm) obtained by the different methods. Methods marked with * were not used in the ILC with this material. The expanded reproducibility standard deviation (k=2) is included.

Method	d	d_{modal} (nm)
AFM*	$d_{0,hgt}$	-
SEM	$d_{0,ecd}$	790 ± 60
TEM	$d_{0,ecd}$	783 ± 72
DLS	$d_{i,hyd}$	808 ± 73
PTA*	$d_{0,hyd}$	-
DMAS	$d_{0,emob}$	774 ± 35
SAXS*	$d_{3,lscat}$	-
CLS	$d_{3,St}$	911 ± 112
sp ICP-MS*	$d_{0,mass}$	-

and Table 65 show the intermethod comparison for the polystyrene particle mixture with 80 and 800 nm particles with a ratio of 2:1. For the polystyrene particle mixture with 80 and 800 nm particles with a ratio of 2:1 no validation of the bimodal distribution could be achieved with the investigated methods. The sample dispersion of particles with a high variance of the particle size is not stable over time due to accumulation. It is difficult to detect the different particle population and determine them correctly. In some rare cases participants were able to detect the 80 nm particle population but the determined percentage of 80 nm particles is not reliable and due to the rare amount of data and the unknown status of the stability of the particle dispersion no further evaluation has been done. The 800 nm could be detected in all cases. High variance of the mean and median diameter is seen in between the methods, which can be explained due to the only partly detection of the 80 nm particle fraction. The modal diameter of the 800 nm particles is in good comparison to the ones from the other methods. Only the 800 nm modal diameter is given in the figure and in the table. **Resulting change in the draft TG: Since no validation of the bimodal particle system, with particle sizes of the different populations with significant differences could be achieved, the Test Guideline will be adapted concerning bimodal particle systems. The statements from the Test Guideline were marked as a recommendation which was not validated within the ILC**.

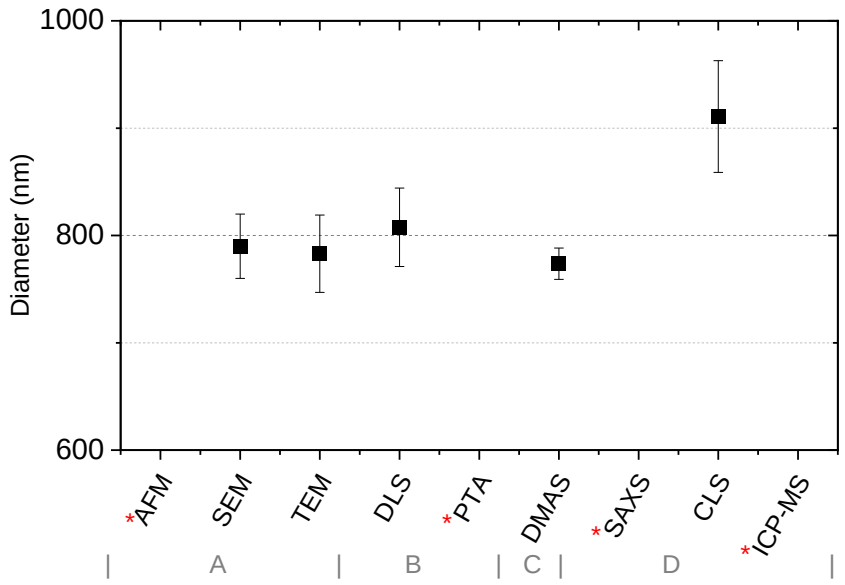

Figure 95: Intermethod comparison modal diameters of the 800 nm mode of polystyrene particles (80/800 nm). The reproducibility standard deviation (k=1) is included. Methods marked with * were not used in the ILC with this material. (equivalent circular diameter for TEM and SEM). Due to the bimodal material only the modal diameter is shown here.

Table 66. Overview of the average mean, median and modal diameters of polystyrene particles (80/800 nm) obtained by the different methods. Methods marked with * were not used in the ILC with this material. The expanded reproducibility standard deviation (k=2) is included.

Method	d	d_{modal} (nm)
AFM*	$d_{0,hgt}$	-
SEM	$d_{0,ecd}$	790 ± 60
TEM	$d_{0,ecd}$	783 ± 72
DLS	$d_{i,hyd}$	808 ± 73
PTA*	$d_{0,hyd}$	-
DMAS	$d_{0,emob}$	774 ± 35
SAXS*	$d_{3,Iscat}$	-
CLS	$d_{3,St}$	911 ± 112
sp ICP-MS*	$d_{0,mass}$	-

Silver particles

Figure 96 and Table 67 show the intermethod comparison for the silver particles. The nanomaterial includes a fraction of not intended very small particles which lead to a bimodal character. This fraction of small particles contributes to a higher uncertainty in the diameter determination. As the particles are

spherical but have an undefined size distribution the particles can be seen as a transfer material between perfect calibrating particles and real-life material. High variance of the derived diameter is in between the methods was found. DLS and PTA determine the hydrodynamic diameter, which is rather high due to the stabilizing material building the outer shell of the particles. At the moment no clear explanation is available for the high difference between SEM and TEM. The TEM measurement had to be excluded from the evaluation, due to a high uncertainty, which might arise from particle degeneration on the TEM grid or influence from radiation. Different modes are indicated in some measurements arising from the bimodal particles or can be a contribution from stabilizing material. Only for DLS a clear separation of the modes was available. For the mode diameter the results form SAXS/CLS (core material) and DMAS (outer diameter) turned out to be the most reliable results.

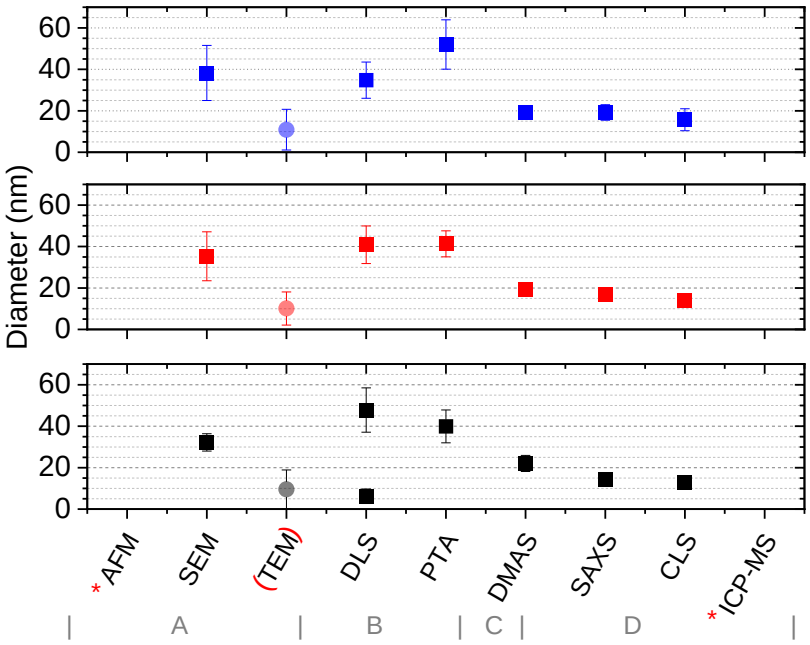

Figure 96: Intermethod comparison of mean (blue), median (red) and modal (black) diameters of silver particles. The reproducibility standard deviation (k=1) is included. Methods marked with * were not used in the ILC with this nanomaterial. Methods in brackets delivered no valid results due to an uncertainty > 50%. The results are displayed only for information (equivalent circular diameter for TEM and SEM).

Table 67. Overview of the average mean, median and modal diameters of silver particles obtained by the different methods. Methods marked with * were not used in the ILC with this nanomaterial. The expanded reproducibility standard deviation (k=2) is included.

Method	d	d_{mean} (nm)	d_{median} (nm)	d_{modal} (nm)
AFM*	$d_{0,hgt}$	-	-	-
SEM	$d_{0,ecd}$	38.3 ± 13.8	35.3 ± 11.8	32.2 ± 4.2
TEM	$d_{0,ecd}$	10.9 ± 9.8	10.1 ± 8	9.5 ± 9.4
DLS	$d_{i,hyd}$	34.8 ± 17.5	40.8 ± 18.2	6.2 ± 7 / 48 ± 21.3
PTA	$d_{0,hyd}$	52 ± 24	41.3 ± 12.6	39.9 ± 15.8
DMAS	$d_{0,emob}$	19.1 ± 3.9	19.5 ± 4.7	22 ± 7.8
SAXS	$d_{3,Iscat}$	19.2 ± 2.4	17.1 ± 2.9	14 ± 1.4

CLS	$d_{3,St}$	15.7 ± 10.6	13.8 ± 3.5	13.1 ± 3.9
sp ICP-MS*	$d_{0,mass}$	-	-	-

Zinc oxide particles

Figure 97 and Table 68 show the intermethod comparison for the zinc oxide particles. Zinc oxide was only reasonably measurable by AFM and CLS. The problems when measuring a real-life material, arising from agglomeration, had a high influence on the reported results. A very high uncertainty, over 50%, was derived for the method PTA. For the methods SEM and TEM a high uncertainty combined with the availability of only few data led to deliverables that could not be validated. Only three laboratories reported results for these particle systems and some result had to be excluded as the evaluation was not done in accordance with the Test Guideline. The values for DLS and CLS are retrieved from intensity / mass-based PSDs. Intensity/volume-based PSDs lead to higher values for the mean, median and modal diameters.

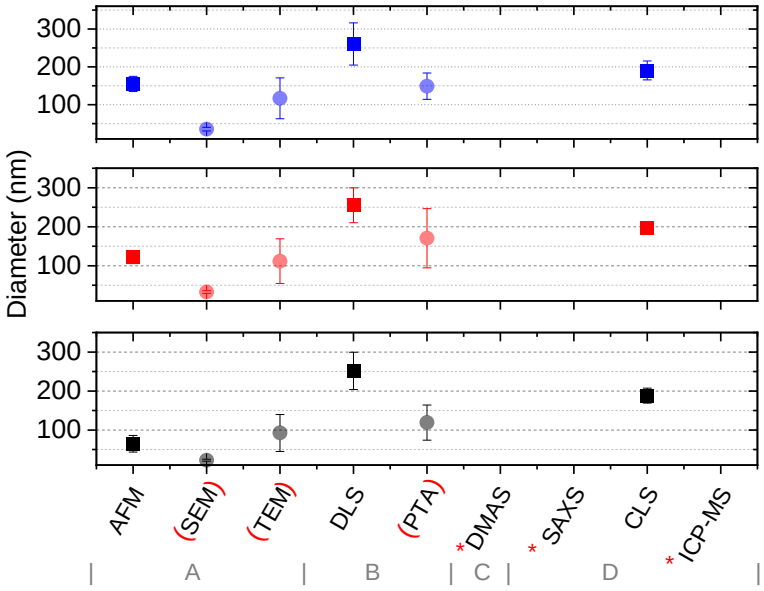

Figure 97: Intermethod comparison of mean (blue), median (red) and modal (black) diameters of zinc oxide particles Methods marked with * were not used in the ILC with this material. The reproducibility standard deviation (k=1) is included. Methods in brackets delivered no valid results due to an uncertainty > 50% or few reported results. The results are displayed only for information (equivalent circular diameter for TEM and SEM). The valid values from AFM, DLS and CLS strongly differ because of the underlying PSD. AFM is based on a number-based PSD while CLS and DLS is based on an intensity/volume-based PSD.

Table 68. Overview of the average mean, median and modal diameters of zinc oxide particles obtained by the different methods. Methods marked with * were not used in the ILC with this material. The expanded reproducibility standard deviation (k=2) is included.

Method	d	d_{mean} (nm)	d_{median} (nm)	d_{modal} (nm)
AFM	$d_{0,hgt}$	154.9 ± 40	122.2 ± 33.8	64.8 ± 41.4
SEM	$d_{0,ecd}$	No reliable validation possible		
TEM	$d_{0,ecd}$	No reliable validation possible		
DLS	$d_{i,hyd}$	260.3 ± 111,5	255,1 ± 89,4	251,6 ± 95,9
PTA	$d_{0,hyd}$	No reliable validation possible		
DMAS*	$d_{0,emob}$	-	-	-
SAXS*	$d_{3,Iscat}$	-	-	-
CLS	$d_{3,St}$	190.5 ± 50.2	196.5 ± 14.9	188.2 ± 38.3
sp ICP-MS*	$d_{0,mass}$	-	-	-

Conclusions for methods

For AFM all test materials were measured with reasonable laboratory standard deviations. The diameter of the silica particles (50 nm) could be determined with a laboratory standard deviation of 16%. For polystyrene particles (90/125 nm) the obtained laboratory standard deviation for the diameters varied between 10 to 30%. Zinc oxide could not be measured with the recommended pixel size. With the applied pixel sizes, the diameters had a laboratory standard deviation of 25-27%. The rules from the draft Test Guideline were not followed in all cases. To assure an image acquisition in a reasonable time the pixel size was chosen higher than recommended in some cases. One lab measured the silica particles with a higher pixel size. No lab measured the zinc oxide particles with recommended pixel size. Generally, the height determination is precise also at higher pixel sizes but with a higher pixel size, particles might be missed or only partly detected during the measurement. For silica, one of the labs made close-up measurements of the particles to ensure that the obtained height is not influenced by using a higher pixel size for the measurement for a statistical analysis. We regard this as a good solution.

As an outcome of this the recommended pixel size seems to be not applicable in all cases for a measurement in a reasonable time. Nevertheless, it is not intended to change the recommended pixel sizes in the Test Guideline. **Instead, it is suggested to add a second way for the determination of the particle size with AFM by using close-up measurements to ensure that no height influence is observed when measuring at a higher pixel size.** This was added to the Test Guideline.

For CLS four out of seven of the test materials were measured with reasonable reproducibility standard deviations. The diameters of the silica particles (20 and 50 nm) could be determined with a reproducibility standard deviation of 18-41% but delivered systematically to low results. Unusual high reproducibility standard deviation for this nanomaterial arises from general weak performance when measuring silica particles in this size range with CLS due to a low contrast between particles and measurement medium. The diameters of the titanium oxide particles could be determined with a reproducibility standard deviation of 16-40%. The diameters of the zinc oxide particles could be determined with a reproducibility standard deviation of 8-26% The median and modal diameters of the silver particles could be determined with a reproducibility standard deviation of 25-30% and the reproducibility standard deviation of the mean diameter is higher than 50%. The polystyrene particles (90/125 nm) and (80/800 nm) could not be validated only raw data was available, which showed too much variance. Three different measurement systems were used in this ILC. A comparability of the results for a material obtained with the different sub-methods AUC, disc CLS and cuvette CLS is not always given but the delivered results from the sub-methods agree within expanded uncertainty limits. In previous ILC it has also been proven that those sub-methods are generally good comparable with only slight differences in size determination [9]. While we see a high variance in results, the method is still within the required validation limits. **The resulting strong dependence on the measured material and used instrument is already addressed in the draft TG and thus, no further additions are needed for this method.**

For DMAS five out of six of the test materials were measured with reasonable reproducibility standard deviations. The diameters of the silica particles (20 and 50 nm) could be determined with a reproducibility standard deviation of 6-14%. The reproducibility standard deviation might be further reduced with expanded correction routines. The diameters of the titanium oxide particles could be determined with a reproducibility standard deviation of 16-18%. The diameters of the silver particles could be determined with a reproducibility standard deviation of 20-35%. For the polystyrene particles (80/800 nm) only the 800 nm particle population was detected by all labs and could be determined with a reproducibility standard deviation of 4%. The mean and median diameters of the polystyrene particles

(90/125 nm) could not be confirmed here because only few results were reported. Nevertheless, the modal diameters obtained from two laboratories are in good comparison and are well comparable to the measurement results from other methods. During the ILC some labs reported size distribution with contribution from stabilizing material. After consultation and confirmation from the participants this contribution was corrected from the background. **In the previous draft Test Guideline only the measurement of the background is advised to be done before the measurement, but no advice how background correction has to be performed is given. This was added to the draft Test Guideline**.

For DLS five out of seven of the test materials were measured with reasonable reproducibility standard deviations. The diameters of the silica particles (20 and 50 nm) could be determined with a reproducibility standard deviation of 9-19%. The diameters of the titanium oxide particles could be determined with a reproducibility standard deviation of 41-45%. The diameters of the polystyrene particles (90/125 nm) could be determined with a reproducibility standard deviation of 6-10%. For the polystyrene particles (80/800 nm) only the 800 nm particle population was detectable and could be determined with a reproducibility standard deviation of 9%. The diameters of the silver particles could be determined with a reproducibility standard deviation of 44-50%. These particles might provide a bimodal size distribution and show absorbance. Both influences the reliability of the resulting size distribution and is already stated as problematic in the Test Guideline which is supported by the resulting high reproducibility standard deviation. Also, for zinc oxide the reproducibility standard deviations of the obtained diameters are higher than 50%. Besides the wide size distribution, the dispersion quality influences a reliable determination of the size distribution using DLS. A SOP was given for the preparation of the dispersion, but a standardized dispersion process is hardly achievable due to the wide range of different sonication devices with varying energy output. For DLS, instruments with correlation analyses and frequency analyses are available. Only a rare number of participants with frequency analysis contributed to the ILC. No influence of the used instrument can be observed. Furthermore, different algorithms for data evaluation can be used. **In some cases, participants used the cumulants method for particle systems with a wide size distribution, which is not in accordance with the draft Test Guideline. Therefore, the draft Test Guideline was adapted in order to be more explicit regarding this aspect.**

For PTA two out of four of the test materials were measured with reasonable reproducibility standard deviations. The diameters of the polystyrene particles (90/125 nm) could be determined with a reproducibility standard deviation of 4-22%. The diameters of the silver particles could be determined with a reproducibility standard deviation of 30-46%. Which is rather high but still acceptable for a nanomaterial with a wide size distribution. For zinc oxide and titanium oxide a reproducibility standard deviation higher than 50% is determined. **The ILC revealed that one important point for PTA is the used version of the instrument's software. This was added in the draft Test Guideline. It is known that PTA measurement of materials with a wide size distribution is problematic. This point was already stated in the draft Test Guideline and was stressed out more in the revision based on the ILC results**.

For single particle ICP-MS only one of the test materials of the ILC was accessible for size analyses. The reproducibility standard deviations for the diameters are 30% for mean, 27% for median and **67% for the modal diameter. Although the reproducibility standard deviations for the mean and median** diameters are reasonable for a real-life material with wide size distribution, we regard this method as not evaluated from the ILC due to the reduced number of measurement data. With support of results of other ILCs good applicability is shown for gold [15] and silver particles [16]. Also, reasonable results for the analyses of titanium oxide are known [9]. **A request to the participants of the ILC was prepared to clarify if and in which way sp ICP-MS will be part of the Test Guideline. It was decided to keep the method in the draft Test Guideline but in a separate way in the appendix**.

For SEM four out of six of the test materials were measured with reasonable laboratory standard deviations. The diameter of the silica particles (20 nm) could be determined with a laboratory standard deviation of 10-12%. The diameter of the titanium oxide particles could be determined with a laboratory standard deviation of 2-22%. The diameters of the silver particles could be determined with a laboratory standard deviation of 25-36%. The diameters of the polystyrene particles (90/125 nm) could be determined with a laboratory standard deviation of 10-12%. For the PSL particles (90/125 nm) a low laboratory standard deviation is obtained but two size distributions differ from those of the other labs, which is not explainable at the moment and need further discussion with the experts. For the polystyrene particles (80/800 nm) no further evaluation of the diameters was done, as only some laboratories were able to detect 80 nm particle fraction. The modal diameter of the 800 nm particles could be derived with a low laboratory standard deviation. The material was prone to agglomeration and so no homogenous distribution of the particles on the specimen could be achieved. For zinc oxide only raw data is available that not all was derived in accordance with the Test Guideline so that no data evaluation could be done. Some laboratories submitted results from semi-automatic or automatic image evaluation. In some cases, the results were in good comparison in other they deviated and led to an exclusion of the data. The use of fully automatic image evaluation was not advised in the Test Guideline. **As a result of the ILC the draft Test Guideline was reshaped to explicitly exclude fully automated detection of particles. This may change with further technical development. As a second result from the ILC the detection of multimodal distributions was limited to comparable resolutions.**

For SAXS except of the polystyrene particles all test materials were measured with reasonable reproducibility standard deviations. The diameter of the silica particles (20 and 50 nm) could be determined with a reproducibility standard deviation of 2-3%. The diameters of the silver particles could be determined with a reproducibility standard deviation of 21-39%. For polystyrene particles (90/125 nm) only two laboratories handed in results and only one determined the mean and median diameter. The modal diameters were determined with a reproducibility standard deviation of 2%. Further evaluation has to be done for the reliable determination of the ratio of different particle population in a particle system. The results from SAXS are very reliable and good comparison of the result in between the laboratories is observed. Important for SAXS is the applied model and corrections for the data evaluation. In one case the data varied because only few of the correction steps of the raw data were performed. **Actually, the results from the ILC do support the current draft Test Guideline. All correction steps need to be applied. This was reshaped in the Test Guideline.**

For TEM four out of seven of the test materials were measured with reasonable laboratory standard deviations. The diameter of the silica particles (20 and 50 nm) could be determined with a laboratory standard deviation of 5-20%. The diameter of the titanium oxide particles could be determined with a laboratory standard deviation of 11-15%. The diameters of the polystyrene particles (90/125 nm) could be determined with a laboratory standard deviation of 7-23%. For the polystyrene particles (80/800 nm) no further evaluation of the diameters was done, as only some laboratories were able to detect 80 nm particle fraction. The modal diameter of the 800 nm particle population could be derived with low laboratory standard deviation. The material was prone to agglomeration and so no homogenous distribution of the particles on the specimen could be achieved. The diameters of the silver particles could be determined with a laboratory standard deviation higher than 50%, this is too high to be considered for a validation process of a protocol considering TEM. It is not fully clear why there is a high variance between the laboratories. Deviation from the protocol or insufficient image quality could be excluded as a cause. Degeneration of the silver particles on the TEM grid was discussed. However, TEM measurement of freshly prepared silver particles and the ones stored for several months showed no significant differences in the obtained size distribution. Degeneration of the particles would then also happen very rapidly, because of the small particle size. Further evaluation has to be done here. For zinc oxide a high variance of the obtained size distribution is seen, the derived diameters could not be used to validate the statements to this method within in the test guideline for this kind of particles. Only two laboratories handed in results for this material and one result was excluded as the data evaluation

was not in accordance to the Test Guideline. For the evaluation of the images some laboratories used automatic or semi-automatic mode. In some cases, the results were in good comparison in two other they deviated and led to an exclusion of the data. The use of automatic image evaluation was not stated in the Test Guideline. **As a result of the ILC the draft Test Guideline was reshaped to explicitly exclude fully automated detection of particles. This may change with further technical development. As a second result from the ILC the detection of multimodal distributions was limited to comparable resolutions.**

2 Fibre size determination

In the ILC on fibre length and diameter determination 13 laboratories were participating. The participating laboratories are listed in Table 69Table 69. Laboratories participating in fibre size determination listed in alphabetical order.

Institute	Abbreviation	Country Code	SEM	TEM
Federal Institute for Material Research and Testing	BAM	DE	X	X
Federal Institute of Occupational, Safety and Health (lead)	BAuA	DE	X	X
Fraunhofer Institute for Microengineering and Microsystems	IMM	DE	X	X
French Institute of Metrology	LNE	FR	X	
French National Institute for Industrial Environment and Risks	INERIS	FR	X	X
Korea Research Institute of Standards and Science	KRISS	KR	X	X
National Institute for Occupational Safety and Health	NIOSH	US	X	X
National Institute of Advanced Industrial Science and Technology	AIST	JP	X	X
National Institute of Standards and Technologies	NIST	US	X	X
National Nanotechnology Center	NANOTEC	TH		X
National Research Council of Canada	NRC CNRC	CA	X	X
Scientific and Technological Centers of the University of Barcelona and Spanish National Research Council	CCiTUB-CSIC	ES	X	X
Solvay		FR		X
Institute	**Abbreviation**	**Country Code**	**SEM**	**TEM**

For the sake of anonymity, the order of the laboratories in Table 69 does not correspond to the numbering of the results used in all subsequent paragraphs.

Table 69. Laboratories participating in fibre size determination listed in alphabetical order.

Institute	Abbreviation	Country Code	SEM	TEM
Federal Institute for Material Research and Testing	BAM	DE	X	X
Federal Institute of Occupational, Safety and Health (lead)	BAuA	DE	X	X
Fraunhofer Institute for Microengineering and Microsystems	IMM	DE	X	X
French Institute of Metrology	LNE	FR	X	
French National Institute for Industrial Environment and Risks	INERIS	FR	X	X
Korea Research Institute of Standards and Science	KRISS	KR	X	X
National Institute for Occupational Safety and Health	NIOSH	US	X	X
National Institute of Advanced Industrial Science and Technology	AIST	JP	X	X
National Institute of Standards and Technologies	NIST	US	X	X
National Nanotechnology Center	NANOTEC	TH		X
National Research Council of Canada	NRC CNRC	CA	X	X
Scientific and Technological Centers of the University of Barcelona and Spanish National Research Council	CCiTUB-CSIC	ES	X	X
Solvay		FR		X
Institute	**Abbreviation**	**Country Code**	**SEM**	**TEM**

The participants provided a total number of 55 datasets for all test materials. Subdivided into test materials and methods, the following numbers of datasets were received:

- 14 Au results (1 Dark-field scanning transmission electron microscopy (DFSTEM), 6 SEM, 7 TEM)
- 8 Ag results (8 SEM)
- 6 MWCNT results (6 SEM)
- 14 ZnO results (1 DFSTEM, 8 SEM, 5 TEM)
- 13 SiC results (1 DFSTEM, 7 SEM, 5 TEM)

Time schedule

Activity	Schedule date
Meeting on interlaboratory comparison	February 19th, 2019
Start of the interlaboratory comparison	April 9th, 2019
Completion of the interlaboratory comparison	August 10th, 2019
Discussion of results with participants	June/July 2020
Delivery of the validation report to OECD	July 2020

Study design

This interlaboratory comparison is designed to test the pairwise determination of length and diameter of fibres.

The methods that were considered in the study are Transmission Electron Microscopy (TEM) and Scanning Electron Microscopy (SEM).

Sample preparation was not assessed in this case study. All samples were prepared by the lead laboratory and were provided fully prepared to the participants.

The experimental procedure consists of two steps: Taking the images of the samples in a first step and evaluating the fibres in the images with an image analysis software in a second step.

All experimental procedures to follow were described in the document draft “TG on particle size and particle size distribution of nanomaterials” in the fibre part in subchapter “Electron Microscopy”. These experimental procedures were also described in a validation plan that was handed out to the ILC participants. The validation plan is included in the appendix paragraph 198).

Materials and test

The ILC was intended to cover materials with different properties (length, diameter, width of distribution) within the scope of the TG (fibre diameter 1 to 1000 nm, fibre length ≤ 20 µm). As for fibres no certified reference material exists, and the number of representative fibrous test materials (e.g. offered by JRC) is limited to four MWCNT materials, we chose commercially available materials to cover the full size range within the scope of the TG. We provide a list of product labellings and manufacturer names in the appendix (Table 80).

The chosen test materials (see Table 70) cover different routes of sample preparation (from aerosol and from dispersion), very different properties (e.g. light elements as carbon and heavier elements as silver) and thus cover a broad range of real life materials.

Table 70. Overview of fibrous test materials used in the interlaboratory comparison and their size related properties, with σ_{GSD} being the Geometric Standard Deviation, given by manufacturer information (*) and own pre-validation for median values (+) performed with SEM.

Test material	Au	Ag	MWCNT	ZnO	SiC
length (µm)	0.045*	0.8+	<15* 1.0+	5-50* 5.4+	50-100* 7.2+
diameter (nm)	10*	20* 25+	10-30* 30+	50-120* 90+	100-600* 140+
aspect ratio	4.5*	20+	33+	60+	51+
width of the length distribution (σ_{GSD})	1.4+	1.5+	2.3+	2.3+	3.0+
width of the diameter distribution (σ_{GSD})	1.2+	1.2+	1.4+	1.5+	1.8+

The chosen test materials cover a wide range of different sizes and therefore aspect ratios within the measurement range: The diameter of the gold nanorods is approx.10 nm (length approx. 45 nm – aspect ratio close to 3 as the lower limit for fibres), while SiC contains the widest fibres in the test with a diameter of x >300 nm (max. length >100 µm – aspect ratio > 50). Depending on the instrument in use it might be necessary to evaluate the length and the diameter separately at different resolutions.

Furthermore, the size distributions of the used test materials differ in their distribution width. SiC is the test material with the widest distribution in diameters and lengths. Using test materials with differently wide size distribution, it is possible to evaluate the widths influence on the reproducibility of the results.

The test materials cover different sample preparation qualities: Silver nanowires are short and exhibit few inter-crossings. This test material thus fulfils the criteria that enable an automated evaluation of fibre length and diameters. ZnO forms loose agglomerates and thus manual evaluation is necessary. ZnO is a test material with diameter close to 100 nm. This size value is of special interest as it provides a boundary material regarding whether it could meet the commonly used definition of a nanomaterial or not (e.g. in specific regulatory context). One of the goals of this ILC is to find out how large the uncertainties are for those boundary materials.

TEM samples for the test materials Au, Ag, ZnO, and SiC are prepared on TEM grid holders.

The test materials Au, Ag, ZnO, and SiC for SEM analysis are prepared on Si-wafer.

The MWCNT samples (Figure 130 to Figure 132) were prepared on gold coated polycarbonate filters with holes of about 0.2 µm diameter. The samples are attached to a SEM holder with copper band.

All samples were sent in twofold replication to all participants although some participants already noted that their capacity will be limited to measure a certain number of samples. In order to obtain a sufficient number of results for all samples, it was decided to define a priority list for each participant, taking into account the limits of the instruments.

Three laboratories reported the results from both methods and all test materials.

The evaluation is done by measuring pairwise the length and diameter of 200 fibres. The results are displayed as cumulative distribution functions length and diameter separately and in a plot of length versus diameter. This latter plot enables an application of different regulation (s. appendix Figure 148). From each distribution the mean, median and geometric standard deviation are evaluated. For the mean and median the uncertainties are calculated with the bootstrap method, as explained in the draft TG in paragraph “Appendix Part D”.

Evaluation of results

During the validation of the results the cumulated distribution functions (CDF) for each test material were compared in a common plot to visually assess the similarity of the obtained data. The variation of the parameters length, median and geometric standard deviation of both distributions was then assed in a statistical analysis. This statistical analysis comprised the test of the mean and median of the particle size distribution on Gaussianity and the calculation of the standard deviation for mean and median for the cleaned dataset. The standard deviations calculated in the following part of the report only refer to the between-laboratory variability. Regarding the within-laboratory variability no statements will be made since the participants were not asked to perform repeated measurements.

Further influencing factors were analysed for their statistical significance in hypothesis testing. The evaluated factors are: Influence of the pixel size, influence of the software, institute bias, comparison of the methods, and dependence of the precision on the distribution width.

Results of each test material

An overview of the results of the ILC is shown in Table 71, where given uncertainties have to be understood as **twice the standard deviation between the laboratories**. The results of all complete and valid datasets (diameter and length determination) for mean and median are summarised as length vs. diameter plots in Figure 98 and Figure 99. Please consider that both axes show the dimensions on a logarithmic scale. The figures show that the test materials under investigation cover a wide range of lengths and diameters within the range of measurements (1 nm – 1000 nm (diameter)/20 µm (length)) of the draft TG. The modal diameter and length are not given as there is no additional information value for tested fibre materials as all of them had only one mode in diameter and length.

Details of the evaluation of the results of each test material are provided in the following subsections.

Table 71. Overview of the results for the length and diameter determination. The reported uncertainty is twice the standard deviation.

Test Material	Au		Ag	MWCNT	Zn0		SiC	
method	**SEM**	**TEM**	**SEM**	**SEM**	**SEM**	**TEM**	**SEM**	**TEM**
number valid of results	**5**	**5**	**7**	**5**	**5**	**4**	**4**	**1**
mean length (nm)	59.0 ±8.7	58.6 ±8.8	686 ±202	1390 ±620	5210 ±680	3910 ±1560	11020 ±4050	10080[2]
median length (nm)	55.8 ±14.6	56.3 ±14.1	597 ±180	1020 ±430	4080 ±600	3050 ±1840	6790 ±3030	4526[2]
mean diameter (nm)	14.4 ±2.1	14.5 ±2.1	29.5 ±9.4	35.0 ±14.7	104.2 ±19.2	81.9 ±25.7	175.6 ±48.5	135.1[2]
median diameter (nm)	14.3 ±3.0	14.9 ±1.8	29.2 ±9.1	32.8 ±14.5	93.5 ±18.5	67.7 ±32.8	148.6 ±31.8	125.1[2]
width of the length distribution	1.3	1.3	1.9	2.0	2.3	2.2	2.8	4.4
width of the diameter distribution	1.2	1.2	1.2	1.4	1.5	1.6	1.9	2.3

[2] Only one TEM result for SiC met the requirement of 200 counted fibers. Therefore no uncertainties are stated.

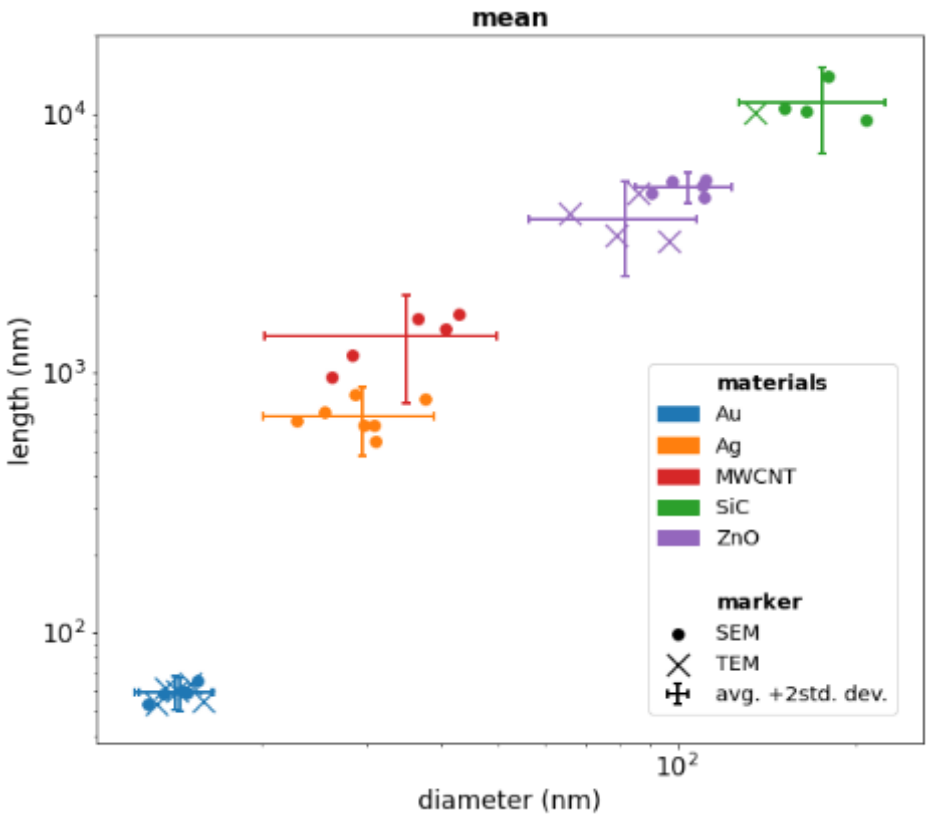

Figure 98: Mean length vs. mean diameter plot of all complete and valid measurements. Both axes show the dimensions on a logarithmic scale. For SiC, an average is only shown for SEM.

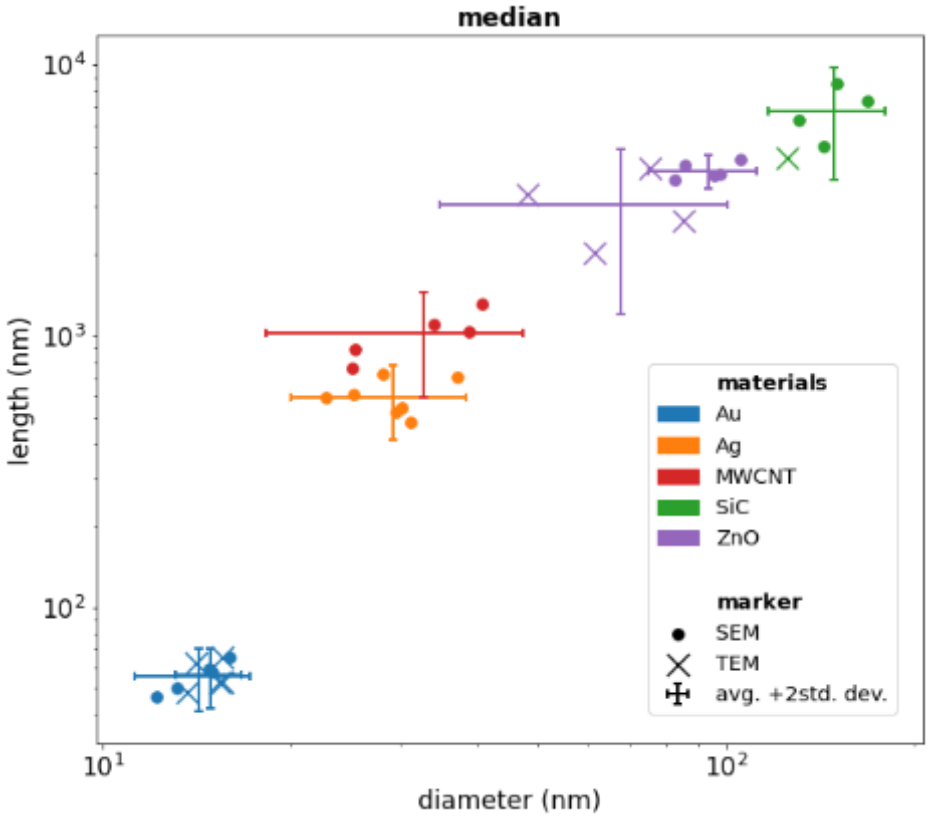

Figure 99: Median length vs. median diameter plot of all complete and valid measurements. Both axes show the dimensions on a logarithmic scale. For SiC, an average is only shown for SEM.

Silver nanowires (Ag)

The silver nanowires were considered to be the most homogeneous test material in diameter and all participants were asked to measure this test material with the highest priority. Unfortunately, it turned out during measurements performed by the ILC participants that the TEM samples of this test material were contaminated with sulphur and thus the Ag nanowires oxidised and degenerated. Consequently, we needed to dismiss the TEM samples for measurement. As the SEM samples were not contaminated, we assume that the origin of the sulphur contamination was in the batch of TEM grids used.

The test material was prepared from >20 µm long silver nanowires by applying ultrasound treatment. Ultrasound weakens the structure of the wires until they break in smaller pieces allowing to measure diameter and length pairwise at the same pixel size. In the images examples of fibres can be found that are not yet entirely broken but exhibit already a kink. This introduces some ambiguity in the evaluation when it comes to decide whether the fibre is already broken or not. We asked the participants to consider such fibres as broken, where the SEM signal shows a gap between the fragments and to measure the full length otherwise.

We received 8 SEM measurements by the participants. Examples images can be found in the appendix (Figure 149 to Figure 156). They show varying contrast as well as differences in the resolution. The pixel sizes used in image acquisition were in a range of 2.3 nm /px to 5.6 nm/ px on average. That

means that all SEM measurements were performed on average with the minimal required pixel size or better. The cumulative distribution functions of length and diameter distribution of all participants are shown in Figure 100 and Figure 101. Nevertheless, one dataset needed to be excluded from further evaluation due to deviations from the draft TG as explained in the following paragraph.

The dataset SEM 9 was acquired from images with pixel sizes varying between 1.4 and 15.6 nm. Each image had a different pixel size. Images with large pixel sizes contain much more fibres than images with small pixel sizes. The large pixel size leads to an overestimation of the diameter of the fibres. Interestingly for the Ag nanowires the usage of a larger pixel size leads to the effect of measuring longer fibres. This is due to the fact, that in this test material fibres are often broken by small gaps. Using larger pixel sizes, these gaps are blurred and fibres that are actually broken, are measured as one single fibre. The overall effect of using different pixel sizes for image acquisition is a broadening of the cumulative distribution function. Although the data acquired for Ag in this respective dataset is very close to the data of other participants, it was excluded from further analysis, because the images were acquired in deviation from the draft TG.

One of the measurements, SEM 7, was done by an auto automatic detection. In this automatic detection, the diameter was reported as the maximum of the diameter histogram generated along the fibre. Changing the evaluation mode to the one that is used in the manual detection, where the diameter is calculated as the mean value from all diameters along the fibre, the curve becomes smooth (dark green curve with legend entry SEM 7 in Figure 100-Figure 103). This measurement also yields very high values in the diameter determination. The reason for the larger diameter can be found in the image quality. The instrument in use did not allow high resolution images of the fibres, so all fibres are a little bit blurred and thus appear thicker than in images with higher resolution.

The remaining data, that was selected for further analysis is shown in Figure 102 and Figure 103. Length vs. diameter plots of all selected results can be found in the appendix (Figure 157).

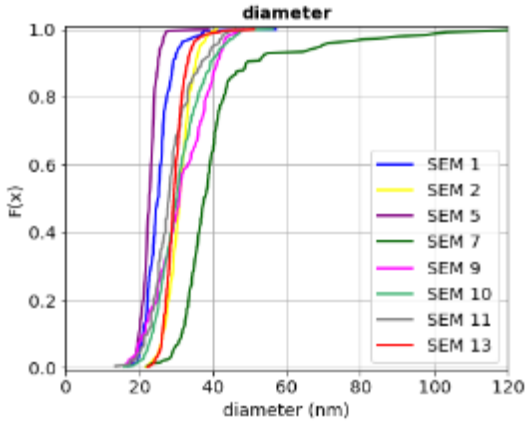

Figure 100: cumulated distribution functions of the fibre diameter for Ag nanowires. All reported SEM results are shown.

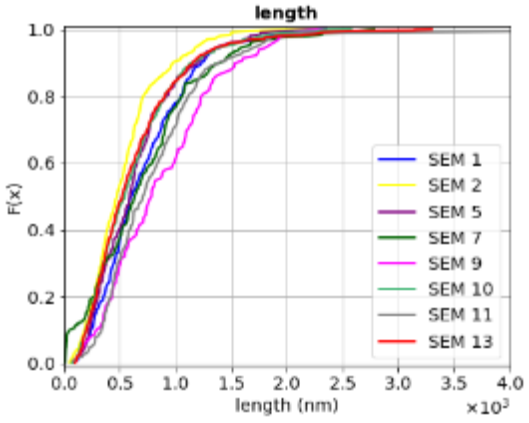

Figure 101: cumulated distribution functions of the fibre length for Ag nanowires. All reported SEM results are shown

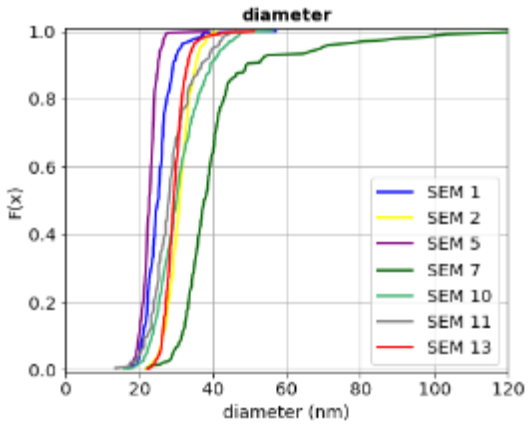

Figure 102: cumulated distribution functions of the fibre diameter for Ag nanowires. SEM results selected for further analysis are shown.

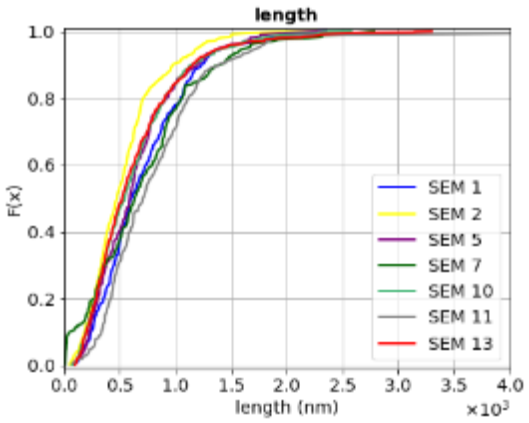

Figure 103: cumulated distribution functions of the fibre length for Ag nanowires. SEM results selected for further analysis are shown.

From the distributions of the selected datasets the mean and median values are calculated and plotted in Figure 104. The error bars are calculated using the bootstrap method.

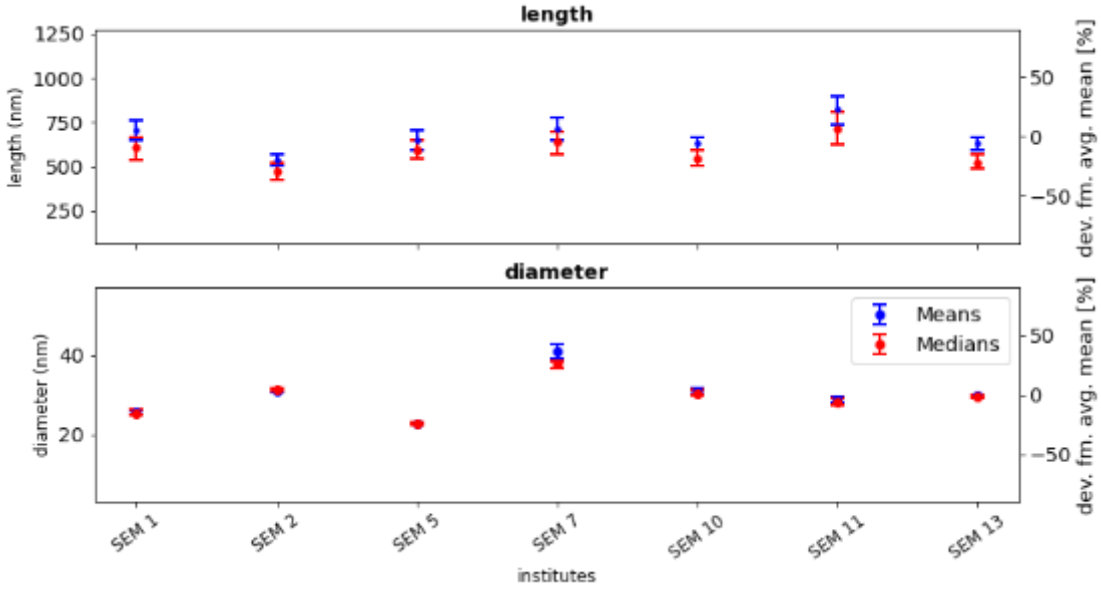

Figure 104: mean and median of length (upper subfigure) and mean and median of diameter (lower subfigure) of all selected Ag datasets.

To further evaluate the precision of the results of the interlaboratory comparison obtained on Ag nanowires, the average values of the mean and median values of all datasets were calculated as well as the between-laboratory standard deviation σ_L of the mean and median values and the relative between-laboratory standard deviation (=σ_L/average). These values are given in Table 72.

Table 72. Statistics of Ag nanowire datasets

length	**SEM**
average(**mean**(length)) (nm)	686
between-laboratory standard deviation(mean(length)) (nm)	101
relative standard deviation(mean(length))	0.15
average(**median**(length)) (nm)	597
between-laboratory standard deviation(median(length)) (nm)	90
relative between-laboratory standard deviation(median(length))	0.15
average geometric standard deviation(length)	1.88
diameter	
average(**mean**(diameter)) (nm)	29.50
between-laboratory standard deviation(mean(diameter)) (nm)	4.68
relative between-laboratory standard deviation(mean(diameter))	0.16
average(**median**(diameter)) (nm)	29.18
standard deviation(median(diameter)) (nm)	4.57
relative standard deviation(median(diameter))	0.16
average geometric standard deviation(diameter)	1.15

The standard deviation is multiplied by a factor of 2 in order to yield a coverage probability of 95%. Thus, we obtain the following results for Ag nanowires (percentages are shown in curly brackets):

- mean length: (686 ± 202 {29%}) nm, ; median length: (597 ± 180 {30%}) nm
- mean diameter: (29.5 ± 9.4 {32%}) nm; median diameter: (29.2 ± 9.1 {31%}) nm

Zinc Oxide nanowires (ZnO)

Zinc oxide is a test material, which has needlelike fibres with a wide distribution in diameters and contains fibres for which the diameter changes along the fibre length. The smallest diameters measured were about 20 nm and the largest fibres have diameters larger than 300 nm. The lengths of the fibres varies between 200 nm and >20 µm. Some of the fibres end in platelet like structures, some exhibit sharp kinks. Zinc oxide fibres tends to form loose agglomerates in which most fibres are visually be distinguished from one another.

An additional aspect contributing to a certain bias of the measured length is due to the fact that not all fibres lie flat on the surface. The resulting bias is difficult to assess. An estimation is given in paragraph 0.

14 measurements were handed in by the participants (1 DFSTEM, 8 SEM, 5 TEM). Examples images can be found in the appendix (Figure 158 to Figure 170). The pixel sizes used in image acquisition were in a range of 1.9 nm /px (for diameter measurement only) up to 133.3 nm/px.

The aspect ratio is about 50 and thus larger than some instruments can resolve at a single magnification. Therefore, with TEM 7 only the diameter was determined and in measurement of TEM 1 the diameter and length distributions were determined separately at different pixel sizes for disparate sets of fibres. Measurement TEM 8 measured the length and diameter of fibres at different resolutions pairwise by taking images with multiple resolutions of one position of the sample and by identifying each fibre at each resolution. TEM 7 was not used for the average calculation in paragraph 0 because of its missing length measurement.

The cumulative distribution functions of length and diameter distribution of all participants are shown in Figure 105 and Figure 106. 3 SEM results had to be excluded from further analysis. Each case is commented in the following two paragraphs.

The three datasets were excluded because of the insufficient pixel size. Dataset SEM 4 was measured with a pixel size of 51 nm/px and dataset SEM 3 with a pixel size of 36.6 nm, which is the maximal resolution of the instrument. In the images with the large pixel size only large fibres were visible and were counted. This leads to a strong overestimation of the diameter of the fibres and to an overestimation of the length distribution, because length and diameter of the fibres are correlated. This correlation can be estimated from the scatterplots of length vs. diameter for all selected results shown in the appendix (Figure 171 and Figure 172) for SEM and TEM, respectively.

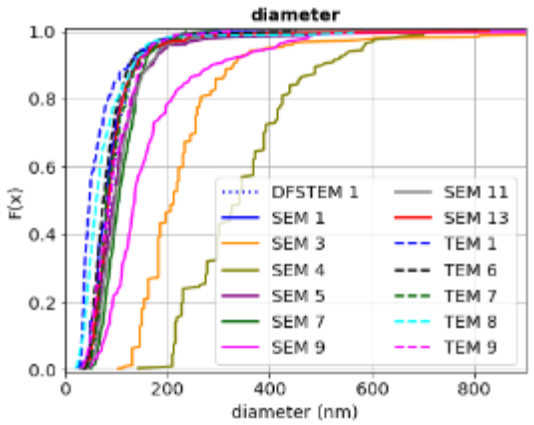

Figure 105: cumulated distribution functions of the fibre diameter for ZnO nanowires. All reported results are shown.

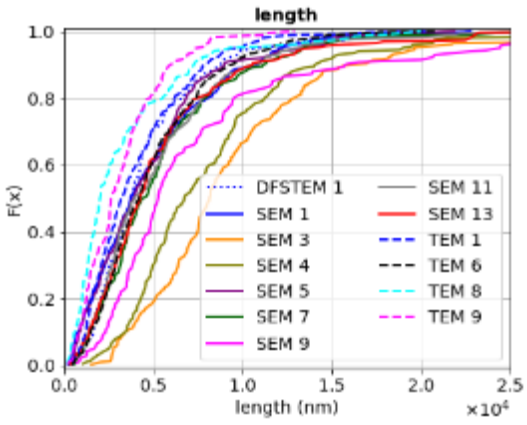

Figure 106: cumulated distribution functions of the fibre length for ZnO nanowires. All reported results are shown.

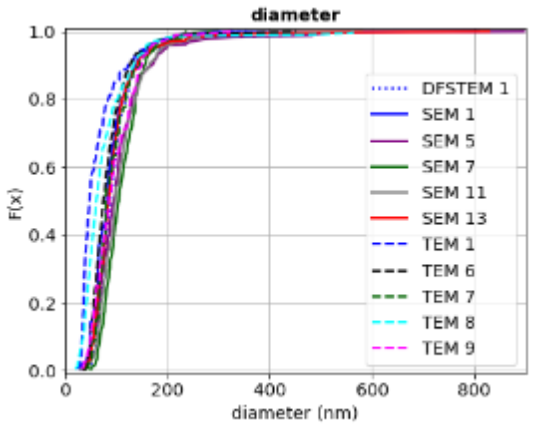

Figure 107: cumulated distribution functions of the fibre diameter for ZnO nanowires. All results selected for further analysis are shown.

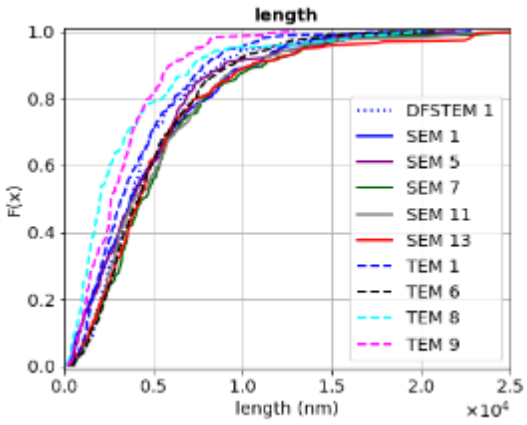

Figure 108: cumulated distribution functions of the fibre length for ZnO nanowires. All results selected for further analysis are shown.

The dataset SEM 9 was acquired from images with pixel sizes varying between 10.4 and 133.3 nm. Each image had a different pixel size. At small pixel sizes small and short fibres were measured. At high pixel sizes only the large fibres were seen and measured. This approach is problematic because each part of the distribution curve is sampled with a different weight. As a consequence, the distribution curve is broader than all other curves.

The remaining data that was selected for further analysis is shown in Figure 107 and Figure 108. The mean and median of length and diameter distributions respectively are shown in Figure 109.

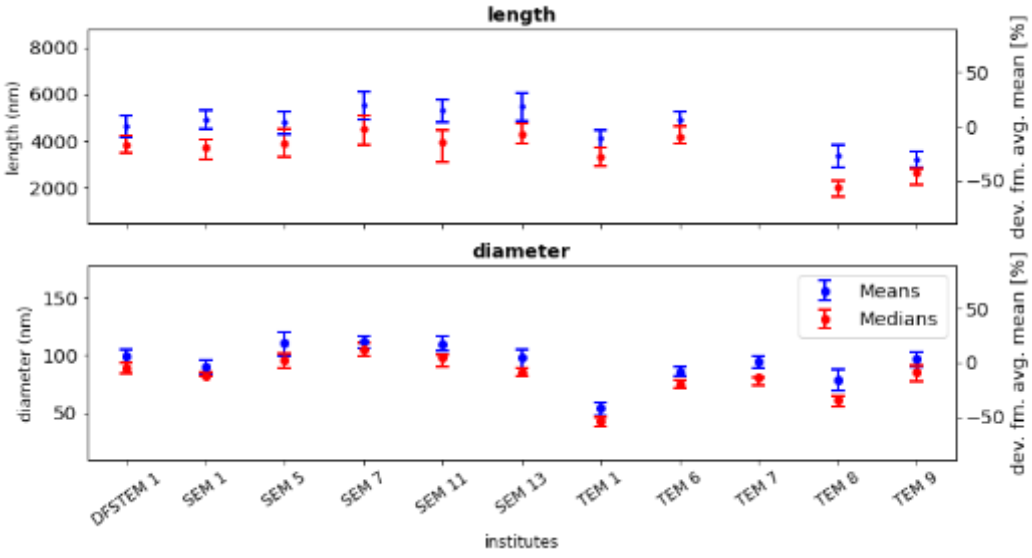

Figure 109: mean and median of length (upper subfigure) and mean and median of diameter (lower subfigure) of ZnO datasets chosen for further evaluation.

To further evaluate the precision of the results of the interlaboratory comparison obtained on ZnO nanowires, the average values of the mean and median values of the selected datasets were calculated as well as the between-laboratory standard deviation σ_L of the mean and median values and the relative between-laboratory standard deviation (=σ_L/average). These values are given in Table 73.

Table 73. Statistics of ZnO nanowire datasets

length	**SEM**	**TEM**	**DFSTEM**
average(**mean**(length)) (nm)	5210	3910	4624
between-laboratory standard deviation(mean(length)) (nm)	340	780	-
relative between-laboratory standard deviation(mean(length))	0.07	0.20	-
average(**median**(length)) (nm)	4080	3048	3825
between-laboratory standard deviation(median(length)) (nm)	300	920	-
between-laboratory relative standard deviation(median(length))	0.07	0.30	-
average geometric standard deviation(length)	2.31	2.21	2.03
diameter			
average(**mean**(diameter)) (nm)	104.19	81.85	99.56
between-laboratory standard deviation(mean(diameter)) (nm)	9.58	12.86	-
relative between-laboratory standard deviation(mean(diameter))	0.09	0.16	-
average(**median**(diameter)) (nm)	93.46	67.66	89.00
between-laboratory standard deviation(median(diameter)) (nm)	9.25	16.41	-
relative between-laboratory standard deviation(median(diameter))	0.10	0.24	-
average geometric standard deviation(diameter)	1.49	1.60	1.43

The standard deviation is multiplied by a factor of 2 in order to yield a coverage probability of 95%. Thus, the results for diameter and length of the ZnO fibres for SEM and TEM are obtained as shown in Table 74. The DFSTEM result is not included.

Table 74. mean and median results with twice the standard deviation (percentages are shown in curly brackets) for ZnO.

length (nm)	SEM	TEM
average(mean(length)) $\pm 2\sigma_L$	5210 ± 680 {13%}	3910 ± 1560 {40%}
average(median(length)) $\pm 2\sigma_L$	4080 ± 600 {15%}	3050 ± 1840 {60%}
diameter (nm)		
average(mean(diameter)) $\pm 2\sigma_L$	104.2 ± 19.2 {18%}	81.9 ± 25.7 {31%}
average(median(diameter)) $\pm 2\sigma_L$	93.5 ± 18.5{20%}	67.7 ± 32.8 {48%}

Silicon Carbide (SiC) fibres

Silicon Carbide is the test material with the widest distribution of length and diameters used in the interlaboratory comparison. The smallest fibre diameters observed were about 15 nm and the largest ones >800 nm. The length ranged from 200 nm to 160 µm. Additionally, this test material exhibits a heterogeneous morphology, fibres with zigzag contour are observed as well as fibres that look like a stack of platelets and straight fibres sometimes end in curved tails. An overview about the observed morphologies is given in Figure 110 to Figure 112.

An additional aspect contributing to a certain bias of the measured length is due to the fact that not all fibres lie flat on the surface. The resulting bias is difficult to assess. An estimation is given in paragraph 0.

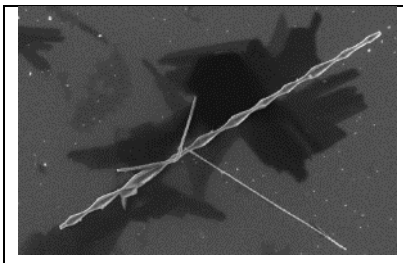

Figure 110: zigzag fibre

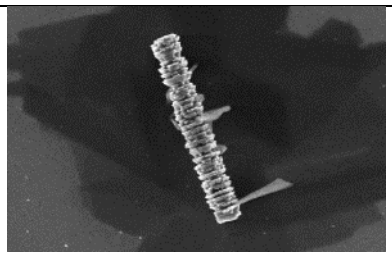

Figure 111: platelet stack

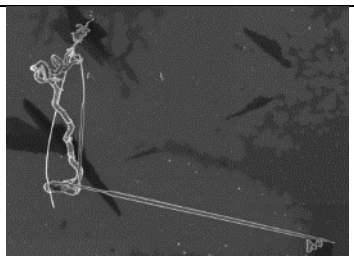

Figure 112: rigid and flexible fibre

13 measurements were handed in by the participants (1 DFSTEM, 7 SEM, 5 TEM). Examples images can be found in the appendix (Figure 173 to Figure 184). The pixel sizes used in image acquisition were in a range between 1.4 nm /px (for diameter measurement only) and 16 nm/px, for length determination up to 120 nm/px.

The aspect ratio of this test material is about 50 and thus larger than some instruments can resolve at a single magnification. Therefore, with TEM 7 only the diameter was determined and in measurement TEM 1 the diameter and length distributions were determined separately at different pixel sizes for

disparate sets of fibres. Measurement TEM 8 measured the length and diameter of fibres at different resolutions pairwise by taking images with multiple resolutions of one position of the sample and by identifying each fibre at each resolution. TEM 7 was not used for the average calculation in paragraph 0 because of its missing length measurement.

The fibres were often agglomerated or aggregated and for TEM grids it has been reported that the distribution of fibres over the grid was strongly inhomogeneous. Several participants were not able to find enough fibres to count 200 of them. DFSTEM 1 reported only 43 fibres, SEM 11 measured only the length of 93 fibres and the diameter of 132 fibres, TEM 1 reported the length of only 95 fibres and the diameter of 190 fibres, TEM 9 measured only 80 fibres, TEM 11 reported the length of only 88 fibres and the diameter of 139 fibres. Datasets with less than half of the required 200 fibres, i.e.: DFSTEM 1, length of SEM 11, TEM 1, TEM 9, TEM13 were excluded from further analysis.

Two SEM datasets were excluded because of insufficient pixel size. Dataset SEM 3 was measured with a pixel size of 36.6 nm, which is the maximal resolution of the instrument. In the images with the large pixel size only large fibres were visible and were counted. This leads to an overestimation of the diameter of the fibres and to an overestimation of the length distribution, because length and diameter of the fibres are correlated. This correlation can be estimated from the scatterplots of length vs. diameter in the appendix (Figure 185 and Figure 186) for selected results of SEM and TEM.

Dataset SEM 9 was excluded from the dataset with the same reasoning as for ZnO. Each image was taken at a different resolution with pixel sizes varying from 8.5 to 133 nm/px.

The cumulative distribution functions of length and diameter distribution of all participants are shown in Figure 113 and Figure 114.

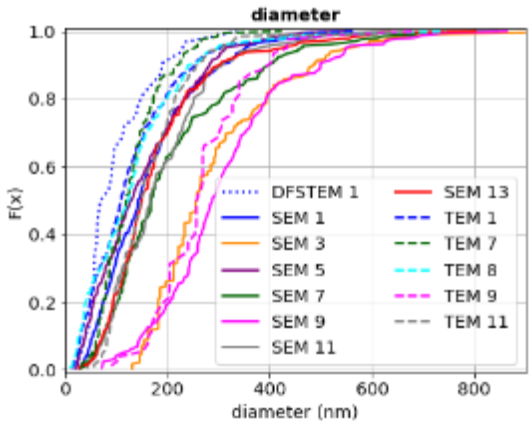

Figure 113: cumulated distribution functions of the fibre diameter for SiC fibres. All reported results are shown.

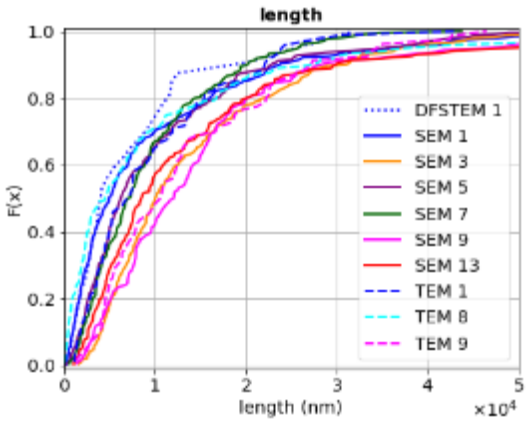

Figure 114: cumulated distribution functions of the fibre length for SiC fibres. All reported results are shown.

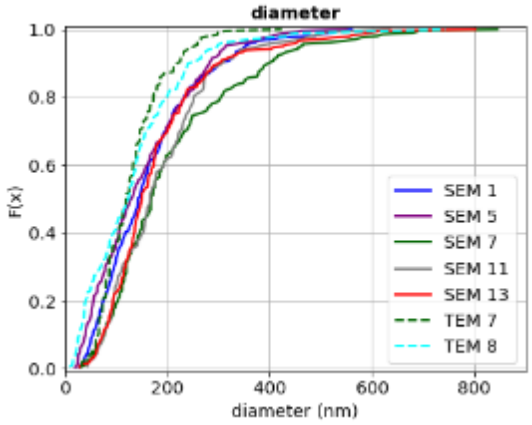

Figure 115: cumulated distribution functions of the fibre diameter for SiC fibres. All results selected for further analysis are shown.

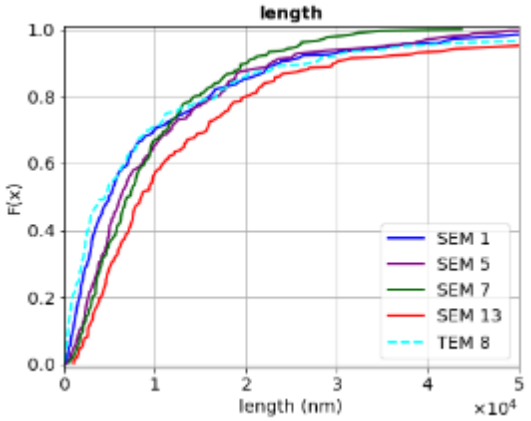

Figure 116: cumulated distribution functions of the fibre length for SiC fibres. All results selected for further analysis are shown.

The remaining data, that was selected for further analysis is shown in Figure 115 and Figure 116. The mean and median of length and diameter distributions respectively is shown in Figure 117.

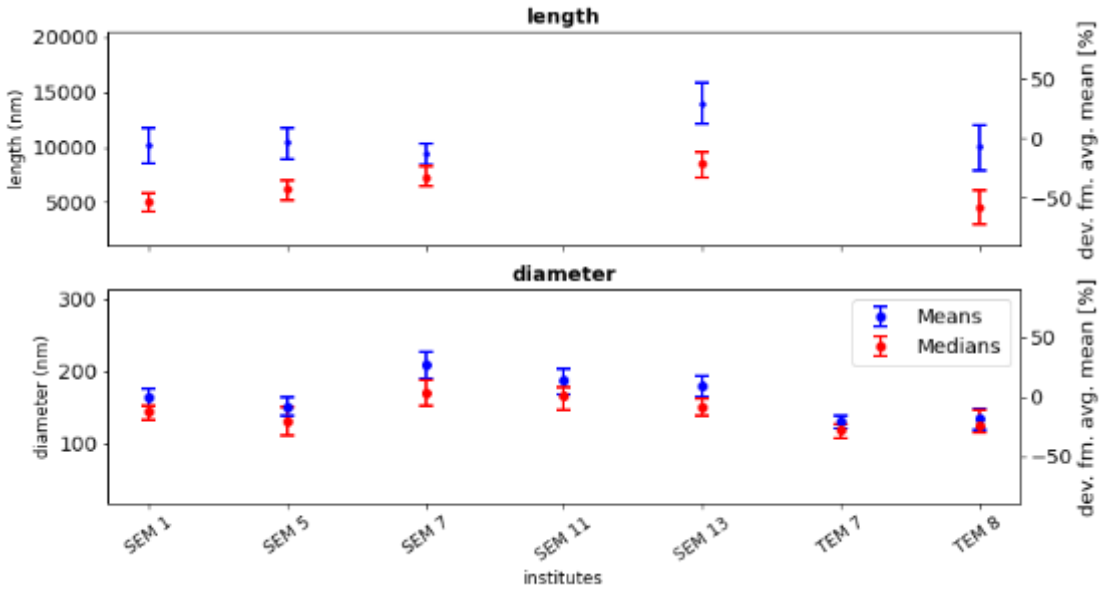

Figure 117: mean and median of length (upper subfigure) and mean and median of diameter (lower subfigure) of SiC datasets chosen for further evaluation.

To further evaluate the precision of the results of the interlaboratory comparison obtained on SiC fibres, the average values of the mean and median values of the selected datasets were calculated as well as the between-laboratory standard deviation σ_L of the mean and median values and the relative between-laboratory standard deviation (=σ_L/average). These values are given Table 75.

Table 75. Statistics of SiC nanowire datasets

length	**SEM**	**TEM**
average(**mean**(length)) (nm)	11024	10081
between-laboratory standard deviation(mean(length)) (nm)	2023	-
relative between-laboratory standard deviation(mean(length))	0.18	-
average(**median**(length)) (nm)	6789	4526
between-laboratory standard deviation(median(length)) (nm)	1513	-
relative between-laboratory standard deviation(median(length))	0.22	-
average geometric standard deviation(length)	2.77	4.43
diameter		
average(**mean**(diameter)) (nm)	175.57	135.06
between-laboratory standard deviation(mean(diameter)) (nm)	24.26	-
relative between-laboratory standard deviation(mean(diameter))	0.14	-
average(**median**(diameter)) (nm)	148.57	125.10
between-laboratory standard deviation(median(diameter)) (nm)	15.92	-
relative between-laboratory standard	0.11	-

deviation(median(diameter))		
average geometric standard deviation(diameter)	1.90	2.29

The standard deviation is multiplied by a factor of 2 in order to yield a coverage probability of 95%. Thus, the SEM results for SiC fibres are (percentages are given in curly brackets):

- mean length: (11020 ± 4050 {37%}) nm, median length: (6790 ± 3030 {45%}) nm
- mean diameter: (175.6 ± 48.5 {28%}) nm, median diameter: (148.6 ± 31.8 {21%}) nm

Gold (Au) nanorods

Gold nanorods are the test material with the smallest dimensions both in length and diameter. It is a nanomaterial at the border between fibre and particle and contains particles as well as fibres. The cumulative distribution functions of length and diameter distribution of all participants are shown in Figure 119 and Figure 120. In the data evaluation only the fibres (aspect ratio >3) were considered, all particles were disregarded. This selection is shown in Figure 118 as length vs. diameter plot. The changes of the resulting CDF are visualised with a few examples in Figure 121 and Figure 122.

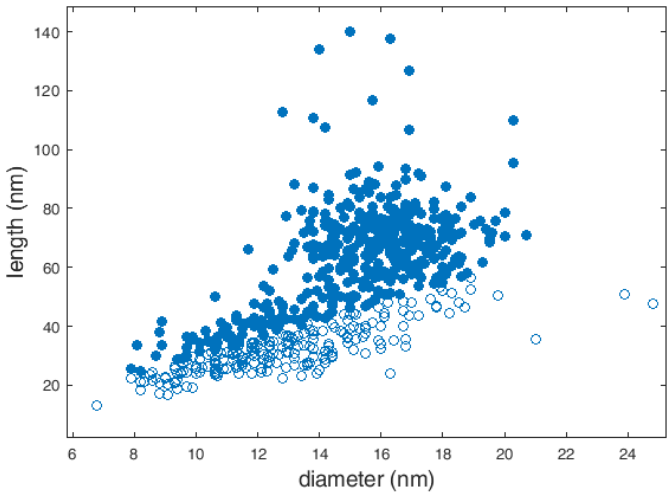

Figure 118: example scatterplot of length and diameter of all Au nanorods measured in one dataset. The open circles are nonfibrous particles with an aspect ratio <3 which are excluded from analysis.

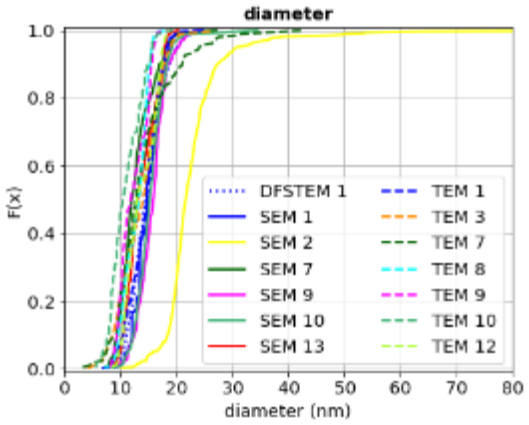

Figure 119: cumulated distribution functions of the fibre diameter for Au nanorods. All reported results are shown.

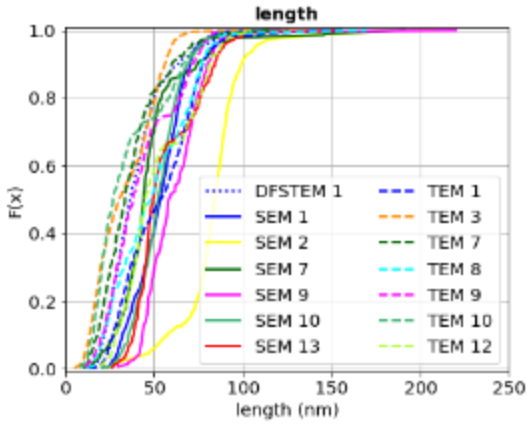

Figure 120: cumulated distribution functions of the fibre length for Au nanorods. All reported results are shown.

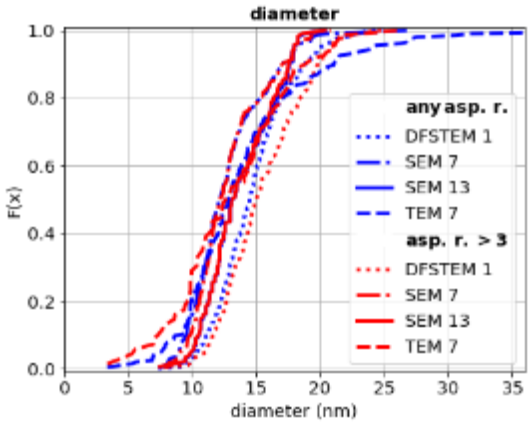

Figure 121: changes of the cumulated distribution functions of the fibre diameter due to different aspect ratios.

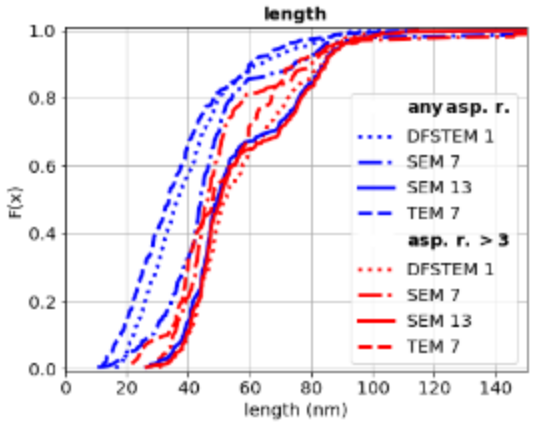

Figure 122: changes of the cumulated distribution functions of the fibre length due to different aspect ratios.

14 measurements were handed in by the participants (1 DFSTEM, 6 SEM, 7 TEM). Examples images can be found in the appendix (Figure 189 to Figure 202). The pixel sizes used in image acquisition were in a range of 0.083 nm /px, and 6.63 nm/px.

One result, SEM 2, is an outlier. In this case the image analysis has been performed semi automatically. The segmentation was done automatically and the fibres to be measured were selected manually. It seems that in the process of selecting the fibres to be measured the short fibres have been systematically neglected. The lead lab repeated the evaluation of the fibres in the first image and counted 458 fibres. The re-evaluated CDFs contain smaller particles and are in agreement with the other reported results as shown in Figure 123 and Figure 124. The result of SEM 2 has been neglected in further analysis.

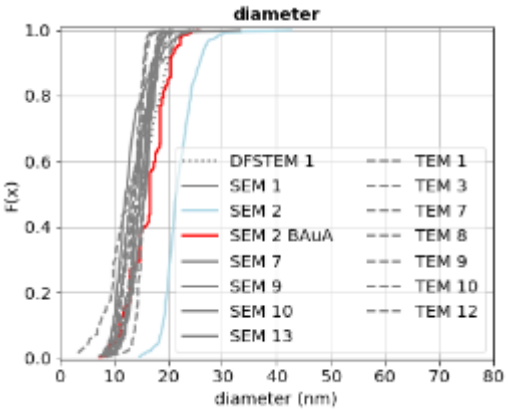

Figure 123: Comparison of reported diameters for Au nanorods of SEM 2 and re-evaluation performed by BAuA with the set of reported datasets. In the selection of fibres to measure, SEM 2 preferred large fibres over small ones.

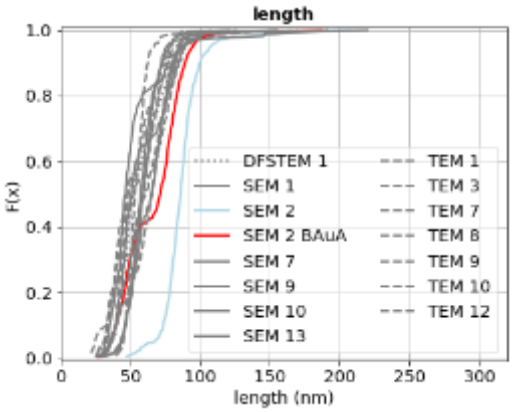

Figure 124: Comparison of reported lengths for Au nanorods of SEM 2 and re-evaluation performed by BAuA with the set of reported datasets. In the selection of fibres to measure, SEM 2 preferred large fibres over small ones.

Results that contain less than 100 counted fibres after exclusion of particles (aspect ratio ≤ 3) were neglected. This applies to datasets TEM 7 and TEM 10.

The remaining data, that was selected for further analysis is shown in

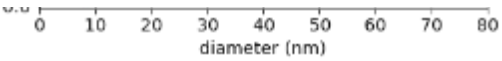

Figure 125 and Figure 127. Length vs. diameter plots of all selected results can be found in the appendix (Figure 203 and Figure 204) for SEM and TEM. The mean and median of length and diameter distributions respectively is shown in Figure 127.

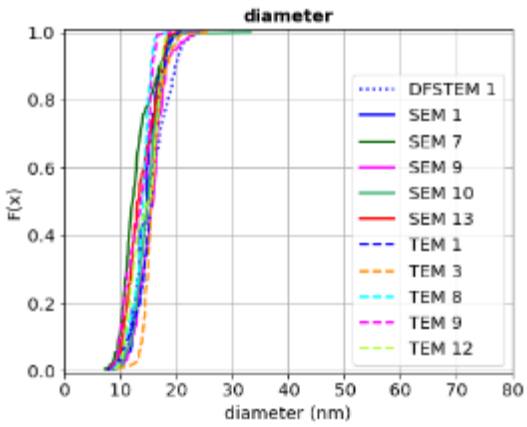

Figure 125: cumulated distribution functions of the fibre diameter for Au nanorods. All results selected for further analysis are shown.

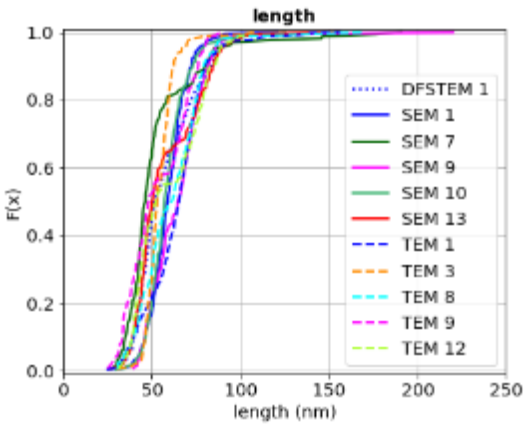

Figure 126: cumulated distribution functions of the fibre length for Au nanorods. All results selected for further analysis are shown.

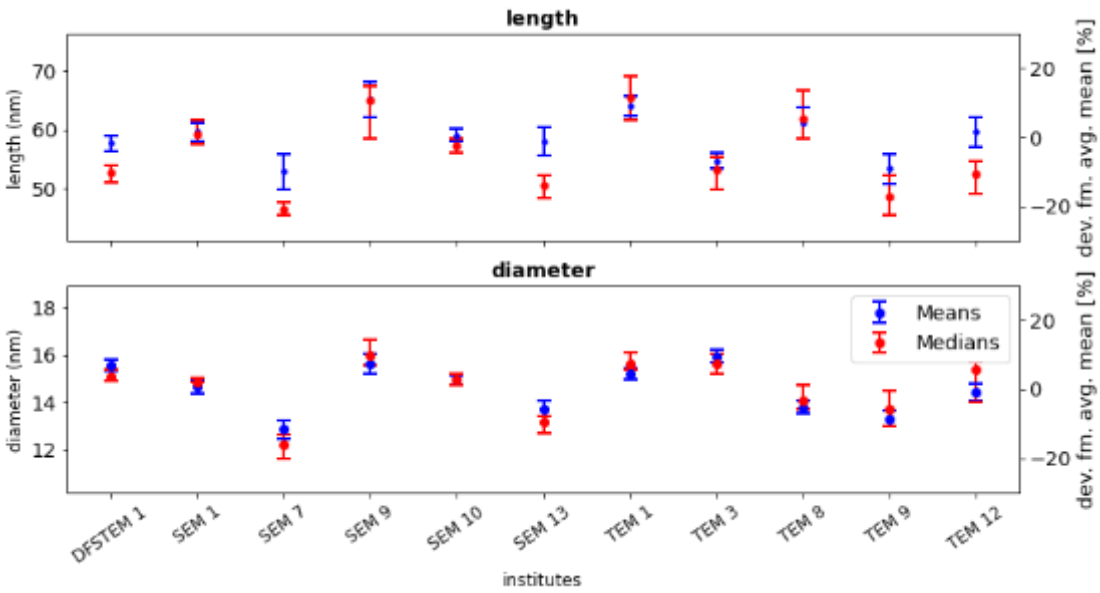

Figure 127: mean and median of length (upper subfigure) and mean and median of diameter (lower subfigure) of Au nanorod datasets chosen for further evaluation.

For the Au nanorods some institutes report a clearly bimodal length distribution, while other report a monomodal distribution. To reveal the origin of this behaviour, two sets of images (images 1 and 2, and images 17 and 18) from the lead laboratory were evaluated by two evaluators each (Figure 128 and Figure 129). Although the number of nanorods found in each set of images is >200, the distributions of nanorods differ significantly and one set of nanorod images exhibits the bimodal distribution while the

other does not. This indicated that the distribution of nanorods over the substrate is inhomogeneous and contributes largely to the observed standard deviation of the results.

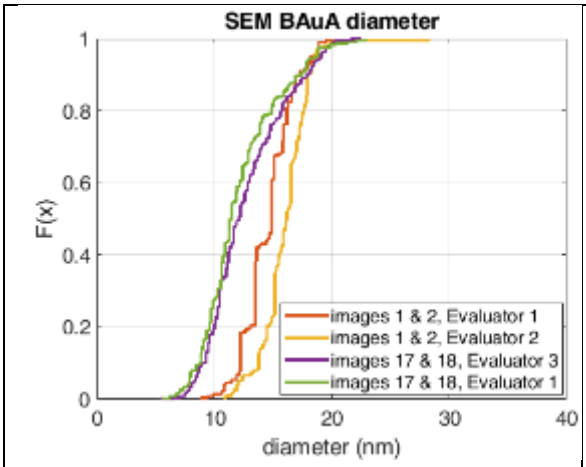

Figure 128: Influence of sample preparation on the cumulated distribution function of the fibre diameter for Au nanorods uncovered by the lead laboratory (BAuA).

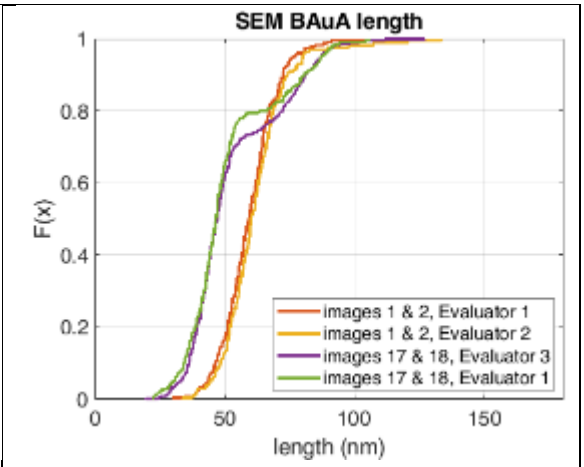

Figure 129: Influence of sample preparation on the cumulated distribution function of the fibre length for Au nanorods uncovered by the lead laboratory (BAuA).

To further evaluate the precision of the results of the interlaboratory comparison obtained on Au nanorods, the average values of the mean and median values of the selected datasets were calculated as well as the between-laboratory standard deviation σ_L of the mean and median values and the relative between-laboratory standard deviation (=σ_L/average). These values are given in Table 76.

Table 76. Statistics of Au nanorod datasets

length	**SEM**	**TEM**	**DFSTEM**
average(**mean**(length)) (nm)	59.01	58.61	57.70
between-laboratory standard deviation(mean(length)) (nm**)**	4.36	4.41	-
relative between-laboratory standard deviation(mean(length))	0.07	0.08	-
average(**median**(length)) (nm)	55.76	56.30	52.60
between-laboratory standard deviation(median(length)) (nm)	7.29	7.06	-
relative between-laboratory standard deviation(median(length))	0.13	0.13	-
average geometric standard deviation(length)	1.28	1.31	1.31
diameter			
average(**mean**(diameter)) (nm)	14.36	14.54	15.55
between-laboratory standard deviation(mean(diameter)) (nm)	1.08	1.05	-
relative between-laboratory standard deviation(mean(diameter))	0.08	0.07	-
average(**median**(diameter)) (nm)	14.25	14.88	15.10
between-laboratory standard deviation(median(diameter)) (nm)	1.50	0.91	-
relative between-laboratory standard deviation(median(diameter))	0.11	0.06	-
average geometric standard deviation(diameter)	1.19	1.17	1.23

The standard deviation is multiplied by a factor of 2 in order to yield a coverage probability of 95%. Thus, the length and diameter of the Au nanorods for SEM and TEM are obtained as shown in Table 77. The DFSTEM result is not included.

Table 77. mean and median results with twice the standard deviation (corresponding percentages are given in curly brackets) for Au nanorods.

length (nm)	**SEM**	**TEM**
average(mean(length)) $\pm 2\sigma_L$	59.0 ± 8.7 {15%}	58.6 ± 8.8 {15%}
average(median(length)) $\pm 2\sigma_L$	55.8 ± 14.6 {26%}	56.3 ± 14.1 {25%}
diameter (nm)		
average(mean(diameter)) $\pm 2\sigma_L$	14.4 ± 2.1 {15%}	14.5 ± 2.1 {14%}
average(median(diameter)) $\pm 2\sigma_L$	14.3 ± 3.0 {21%}	14.9 ± 1.8 {12%}

Multi-walled Carbon Nanotubes (MWCNT)

The multi-walled carbon nanotubes were prepared from an aerosol on a pore filter. In this case the background is very inhomogeneous. Only SEM samples were prepared and distributed among the participants of the interlaboratory comparison.

The MWCNT fibres are sometimes aggregated in a way that makes the differentiation between the individual fibres difficult. The inhomogeneous background further complicates the measurement because some fibres end in a pore and it is not clear whether the ends are still seen or hidden in the pore. Such fibres are excluded in the evaluation. Another issue is the three-dimensional structure of the highly bent fibres. Some fibres are not lying flat on the surface but instead exhibit a complicated three-dimensional structure which cannot be assessed by the two-dimensional electron microscopy images. The resulting bias is towards shorter and thicker fibres. Its magnitude cannot be assessed by a simple estimation. Examples of problematic fibres are shown in Figure 130 to Figure 132.

These difficulties make MWCNT a real-world test material with which the applicability of the draft TG to non-ideal and non-straight fibres can be assessed.

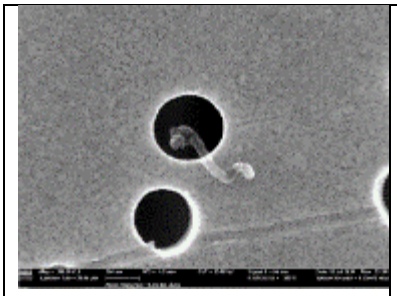

Figure 130: fibre that ends in a pore.

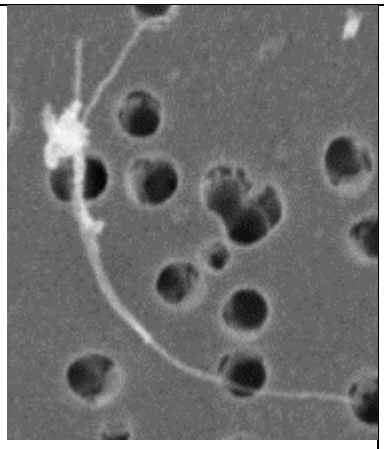

Figure 131: unclear endings due to agglomeration or fibre splitting

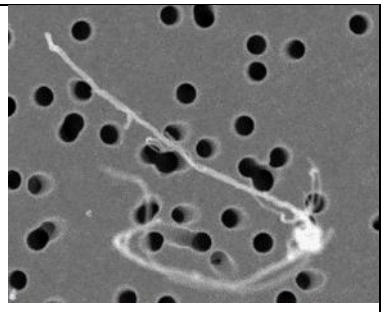

Figure 132: complex 3D structure: Fibre does not lie flat on the surface. It vanishes out of the focus of the instrument.

Six SEM measurements were handed in by the participants. Examples images can be found in the appendix (Figure 205 to Figure 210). The pixel sizes used in image acquisition were in a range of 1.12 nm /px, and 12.24 nm/px.

The cumulative distribution functions of length and diameter distribution of all participants are shown in Figure 133 and Figure 134.

Dataset SEM 9 was excluded from the analysis due to varying pixel sizes as described in paragraph 0.

The remaining data that were selected for further analysis is shown in Figure 135 and Figure 136. Length vs. diameter plots of all selected results can be found in the appendix (Figure 211). The mean and median of length and diameter distributions respectively are shown in Figure 137.

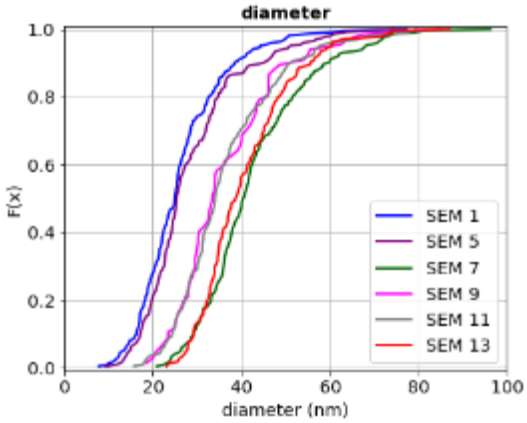

Figure 133: cumulated distribution functions of the fibre diameter for MWCNT nanowires. All reported results are shown.

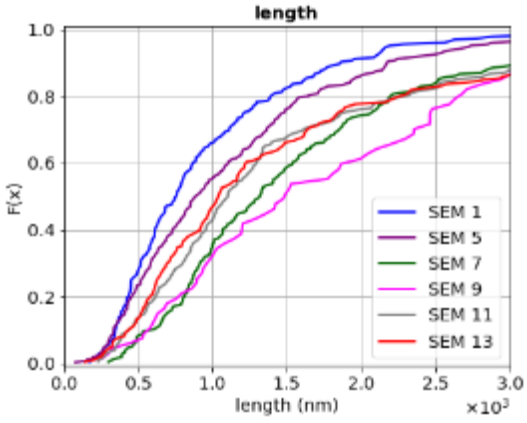

Figure 134: cumulated distribution functions of the fibre length for MWCNT nanowires. All reported results are shown.

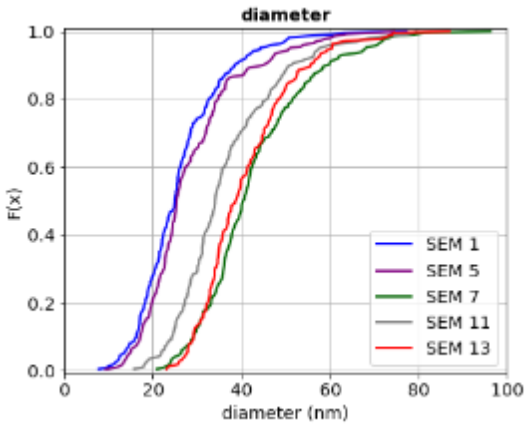

Figure 135: cumulated distribution functions of the fibre diameter for MWCNT. All results selected for further analysis are shown.

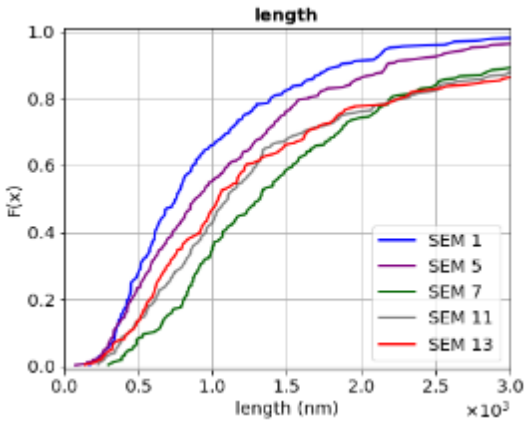

Figure 136: cumulated distribution functions of the fibre length for MWCNT. All results selected for further analysis are shown.

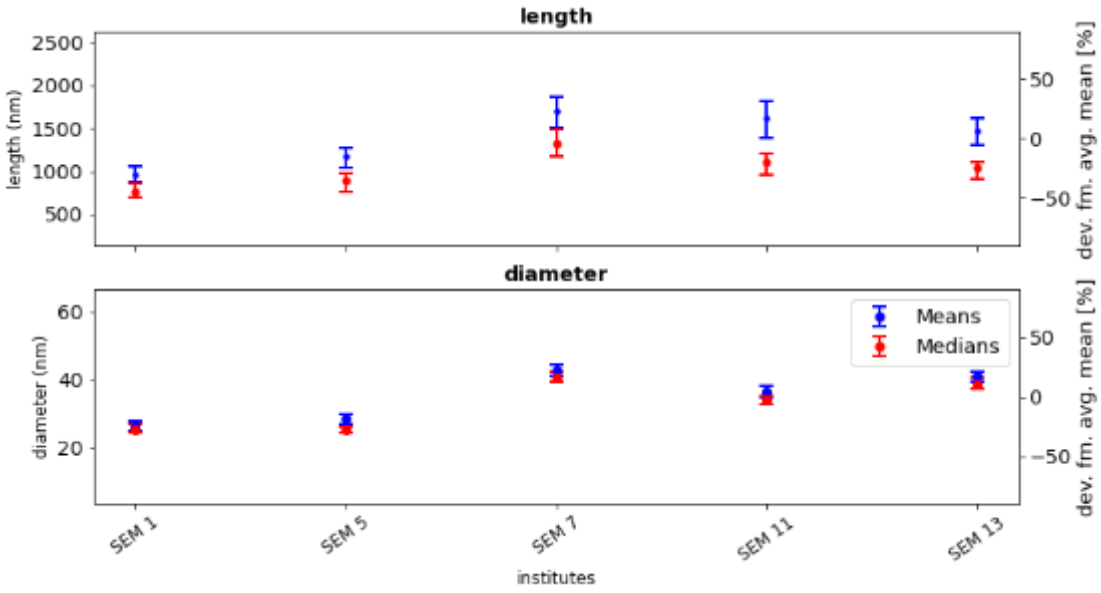

Figure 137: mean and median of length (upper subfigure) and mean and median of diameter (lower subfigure) of MWCNT datasets chosen for further evaluation.

To further evaluate the precision of the results of the interlaboratory comparison obtained on MWCNT fibres, the average values of the mean and median values of the selected datasets were calculated as well as the between-laboratory standard deviation σ_L of the mean and median values and the relative between-laboratory standard deviation (=σ_L/average). These values are given in Table 78.

Table 78. Statistics of MWCNT datasets

length	**SEM**
average(**mean**(length)) (nm)	1385
between-laboratory standard deviation(mean(length)) (nm)	309
relative between-laboratory standard deviation(mean(length))	0.22
average(**median**(length)) (nm)	1023
between-laboratory standard deviation(median(length)) (nm)	214
relative between-laboratory standard deviation(median(length))	0.21
average geometric standard deviation(length)	2.04
diameter	
average(**mean**(diameter)) (nm)	35.00
between-laboratory standard deviation(mean(diameter)) (nm)	7.36
relative between-laboratory standard deviation(mean(diameter))	0.21
average(**median**(diameter)) (nm)	32.79
between-laboratory standard deviation(median(diameter)) (nm)	7.26
relative between-laboratory standard deviation(median(diameter))	0.22
average geometric standard deviation(diameter)	1.36

The standard deviation is multiplied by a factor of 2 in order to yield a coverage probability of 95%. Thus, the results for the MWCNT fibres are (percentages are given in curly brackets):

- mean length: (1390 ± 620 {45%}) nm, median length: (1020 ± 430 {42%}) nm
- mean diameter: (35.0 ± 14.7 {42%}) nm, median diameter: (32.8 ± 14.5 {44%}) nm

Results of further statistical analysis

In this section, only the results that have been included for further statistical analysis are considered.

Comparison of TEM and SEM

It is the initial hypothesis that TEM and SEM can be used alternative to each other leading to a comparable result in determining the fibre size and size distribution. The two methods were applied to determine the fibre diameter and length of the three test materials Au, ZnO and SiC. We used the toolbox of statistical hypothesis testing to investigate the question whether the methods TEM and SEM deliver comparable results in the length and diameter measurement, respectively. First, we tested each test material with a two-tailed t-test, whether the means, medians and geometric standard deviations obtained with the two different methods are equally distributed. For Au and ZnO, a two-sample test was used. For SiC, we applied a one-sample t-test as only one result for TEM was handed in. For Au, the shortest test material in the ILC, the results of SEM and TEM were found to be comparable in size and size distribution. Significant deviations (≥95% confidence) between SEM and TEM results were found for SiC and ZnO, the two longest test materials tested in the ILC. In detail, for SiC, the mean diameter and the geometric standard deviation of diameter and length were found to be significantly different rejecting the initial hypothesis. For ZnO, the hypothesis is rejected as well, as mean diameter and length and median diameter and length were found to be of significant difference. Comparisons between SEM and TEM results are shown in Figure 138 and Figure 139.

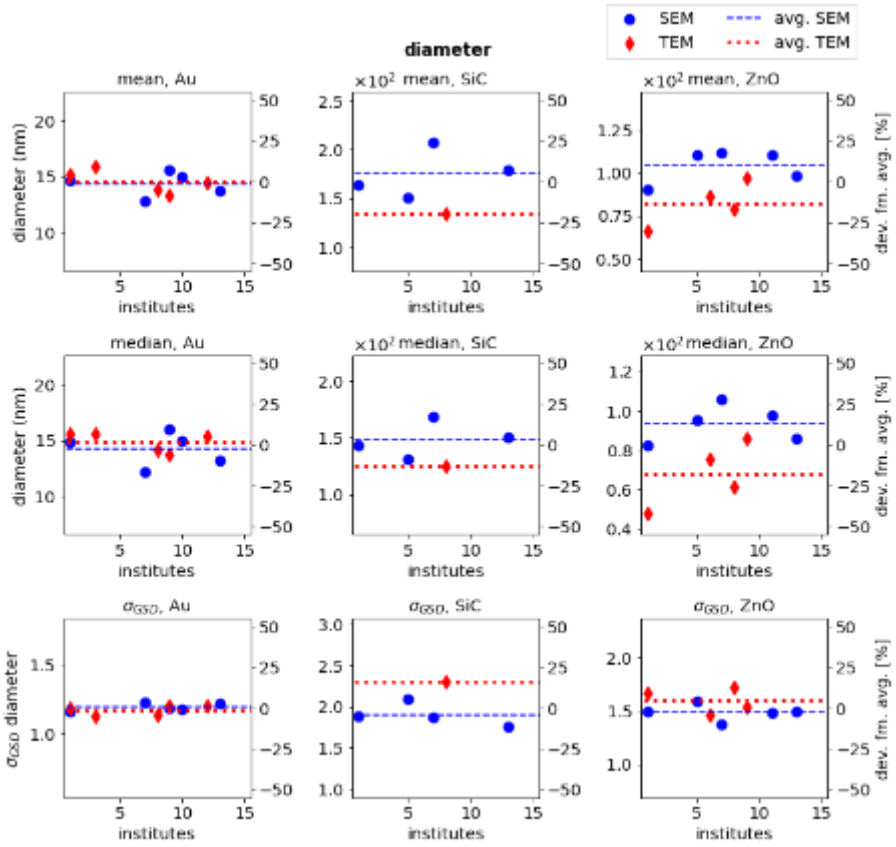

Figure 138: comparison of parameters of the diameter distribution obtained with TEM and SEM, respectively. On the left y-axes absolute values for the parameters are shown, whereas relative deviations from average are shown on the right y-axes.

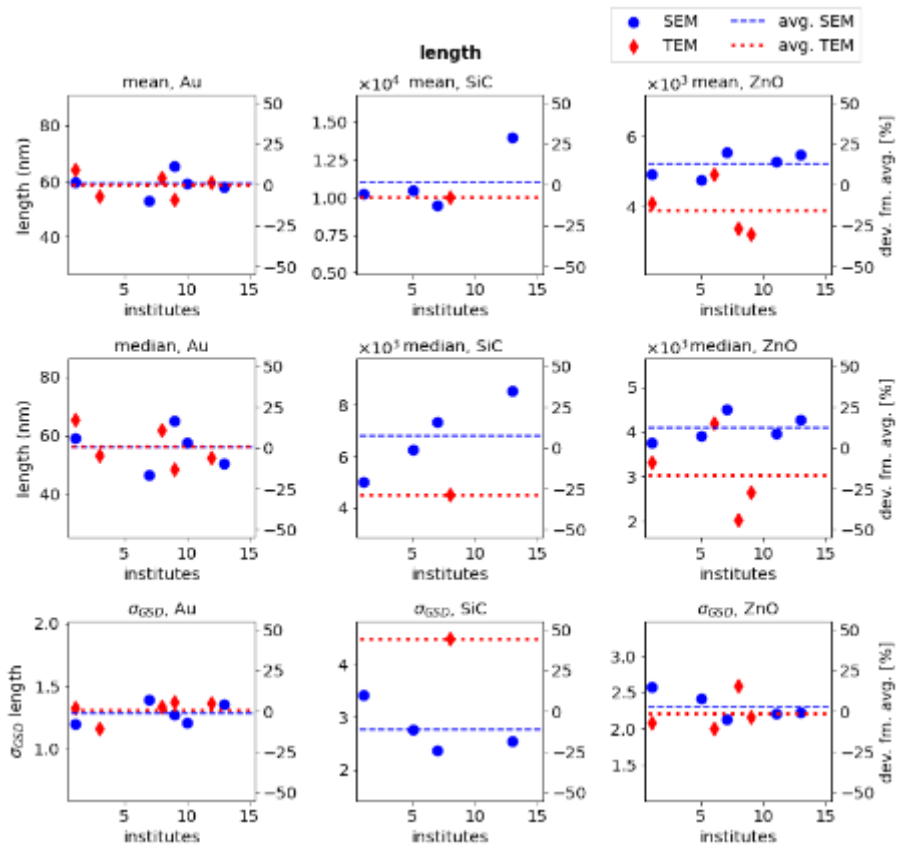

Figure 139: comparison of parameters of the length distribution obtained with TEM and SEM, respectively. On the left y-axes absolute values for the parameters are shown, whereas relative deviations from average are shown on the right y-axes.

Applying the Wilcoxon signed rank test the differences between the average values of all means, medians, geometric standard deviation for all test materials were observed to be not significant. According to this test the initial hypothesis holds. This outcome is not in contradiction with the results of the t-test. It is known that non-parametric tests, which work independently from the underlying statistic distribution of the data like the Wilcoxon-signed rank test, are less sensitive for smaller sample sizes than parametric tests such as Student‘s t-test, where specific assumptions about the data distribution should be met [22, 23].

Influence of distribution width on standard deviation of results

The test materials under investigation varied in their distribution width. Overall, the diameter distribution was narrower than the length distribution. In general, it is more error prone to determine wide length distributions than narrow length distribution, because the evaluation of the size at one single pixel size might lead the evaluator to evaluate more of either the short or the long fibres. We therefore hypothesize that the relative standard deviation obtained for each set of measurements depends on the width of the distribution. This dependence is shown in Figure 140, where the relative standard deviation is depicted as a function of the mean geometric standard deviation.

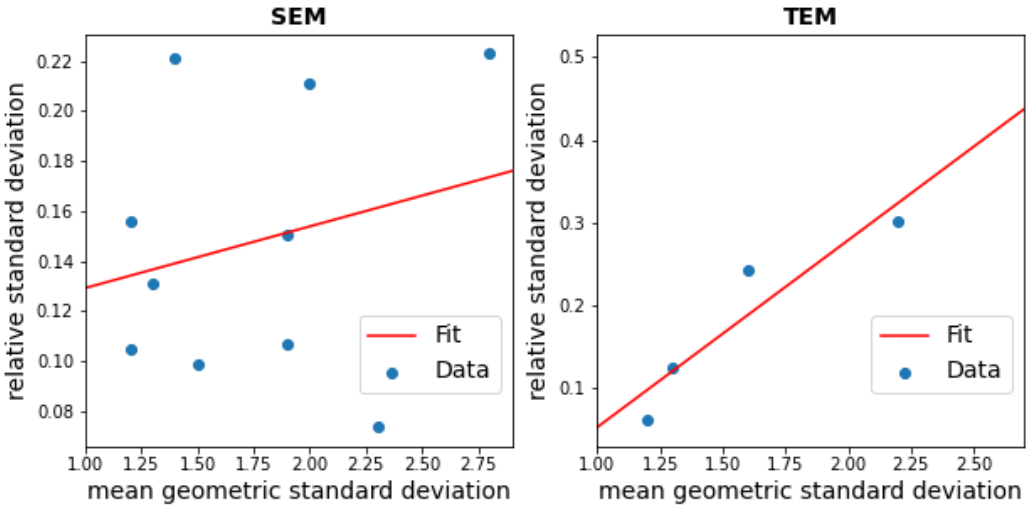

Figure 140: relative standard deviation as a function of the mean geometric standard deviation for all selected datasets. In the left plot SEM results and in the right plot TEM results are shown respectively.

For SEM, no significant dependency between the relative standard deviation and mean geometric standard deviation was found as the slope of the linear fit $m = 0.025 \pm 0.035$ turns out be zero within the uncertainty range.

For TEM, we find indeed that the relative standard deviation depends on the width of the size distribution as the slope of the linear fit $m = 0.23 \pm 0.06$ is significantly greater than zero. This will be reflected in the conclusion to limit the use of TEM and exclude this method for materials with a median length larger than 5 µm and a wide length distribution (σ_{GSD} > 1.5). Therefore, for borderline cases care has to be taken whether a potential nanomaterial is still within the limits of the draft TG or outside. A change of measurement method towards SEM will become necessary if a material falls outside of the limit.

Influence of pixel size on results

The draft TG specifies the pixel size with which a potential nanomaterial has to be measured as smaller than or equal to 4 pixel per mean diameter. We wanted to evaluate whether for the valid results a dependence of the measured size from the pixel size used for image acquisition is seen. For this, we used the fixed effect model approach and plotted the median of the measured diameters as a function of the pixel size for all test materials in Figure 141 and Figure 142 for SEM and TEM, respectively. Each test material was fitted by a linear function with the same slope but different intercepts.

For SEM, the resulting slope $m_{SEM} = 0.48$ has a 95% confidence interval of [-0.30, 1.26]. The lower bound of the 95% confidence interval is negative. Hence, no significant dependence of the median diameter from the pixel size was found.

For TEM, the resulting slope $m_{TEM} = 2.108$ is significantly greater than zero. The 95% confidence interval is all positive: [0.139, 4.078]. This means that an influence of the pixel size has been observed for TEM. As can be seen in Figure 142 this observation can be traced back to results of ZnO.

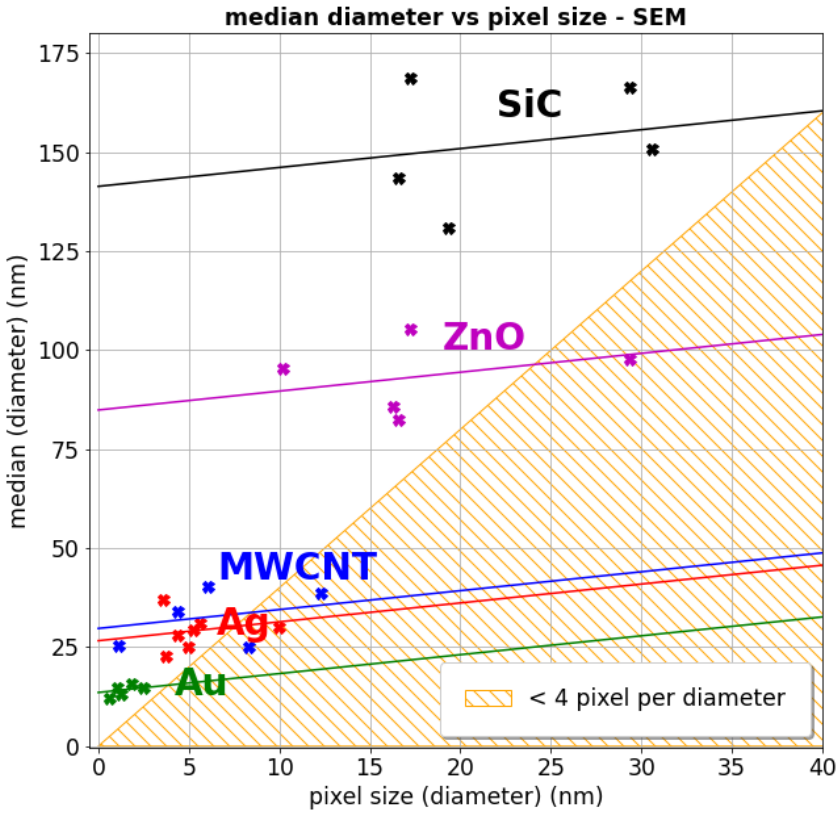

Figure 141: correlation between median of diameter and pixel size for SEM. The orange hatched area shows the region where the minimal resolution of 4 pixels defined in the Test Guideline is undercut.

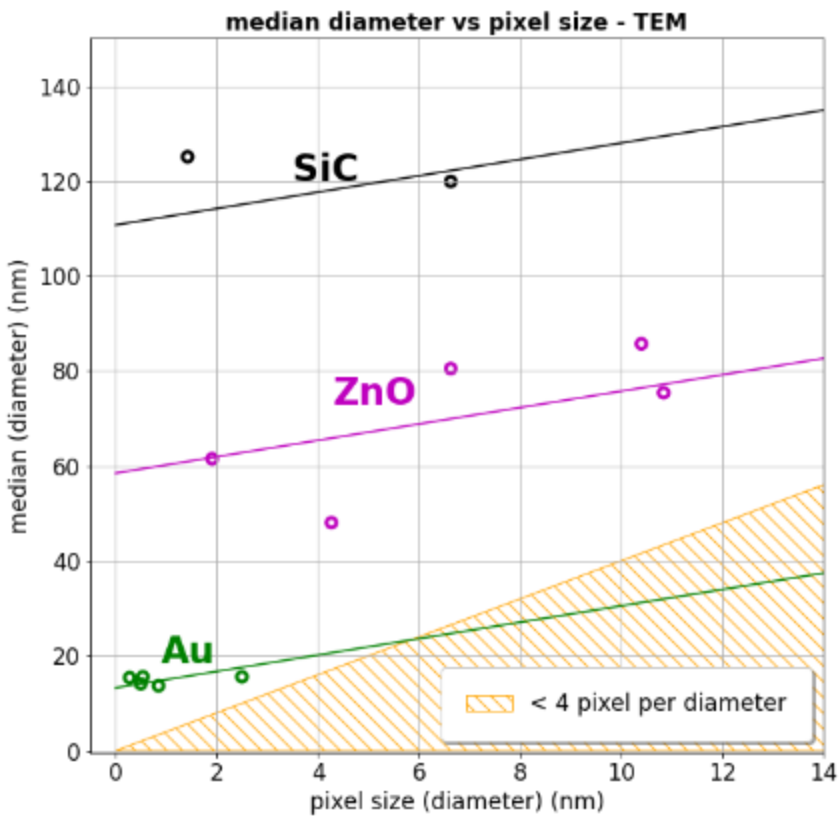

Figure 142: correlation between median of diameter and pixel size for TEM. The orange hatched area shows the region where the minimal resolution of 4 pixels defined in the Test Guideline is undercut.

Comparison of software influence

Nine different programs have been applied for the image analysis. Two softwares were applied by more than one institute, namely FibreDetect and ImageJ. In order to test the hypothesis that the software itself has an influence on the results, we applied the two-tailed Wilcoxon signed rank test. To increase the sample size, SEM and TEM results are tested together. No significant influence (confidence level < 95%) was found. The result can be made plausible by plotting the normalised median values obtained with each software by the mean value of all valid results as shown in Figure 143. No obvious trend is observed for length and diameter measurements.

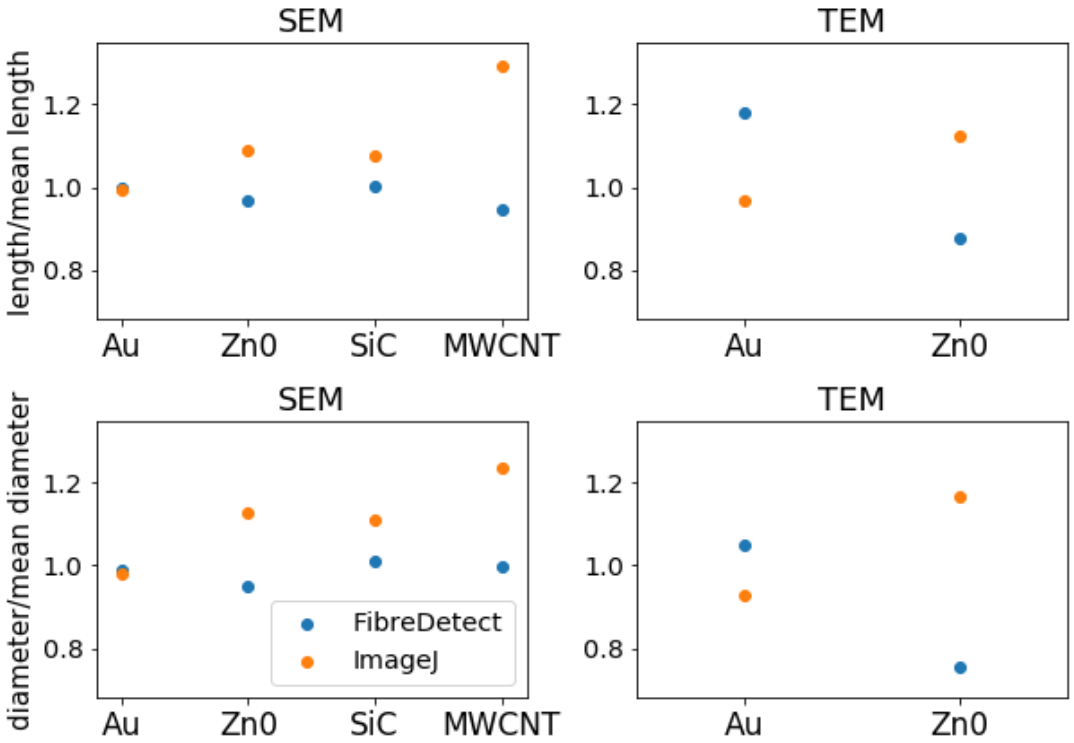

Figure 143: Software comparison. Is there a statistical significant difference between the results of FibreDetect and the results of ImageJ. The Wilcoxon signed rank test shows no significant difference: For ZnO (SEM and TEM), SiC and MWCNT the results obtained with ImageJ are higher than the FibreDetect results. On the contrary, for Au (SEM and TEM) it is the other way around.

Qualitative evaluation of institute bias

Three institutes delivered full SEM datasets for all test materials. These datasets can be used to test whether there is an institute bias among these datasets meaning that one institute has the tendency to deliver the largest results. Reasons for such an institute bias could be based on the instrument used, the pixel size chosen or the evaluator.

A Friedman test is used to test the three datasets for a rank correlation. The results show that no such correlation exists. Hence, no institute bias was found. Illustrations of the results are given in Figure 144 and Figure 145.

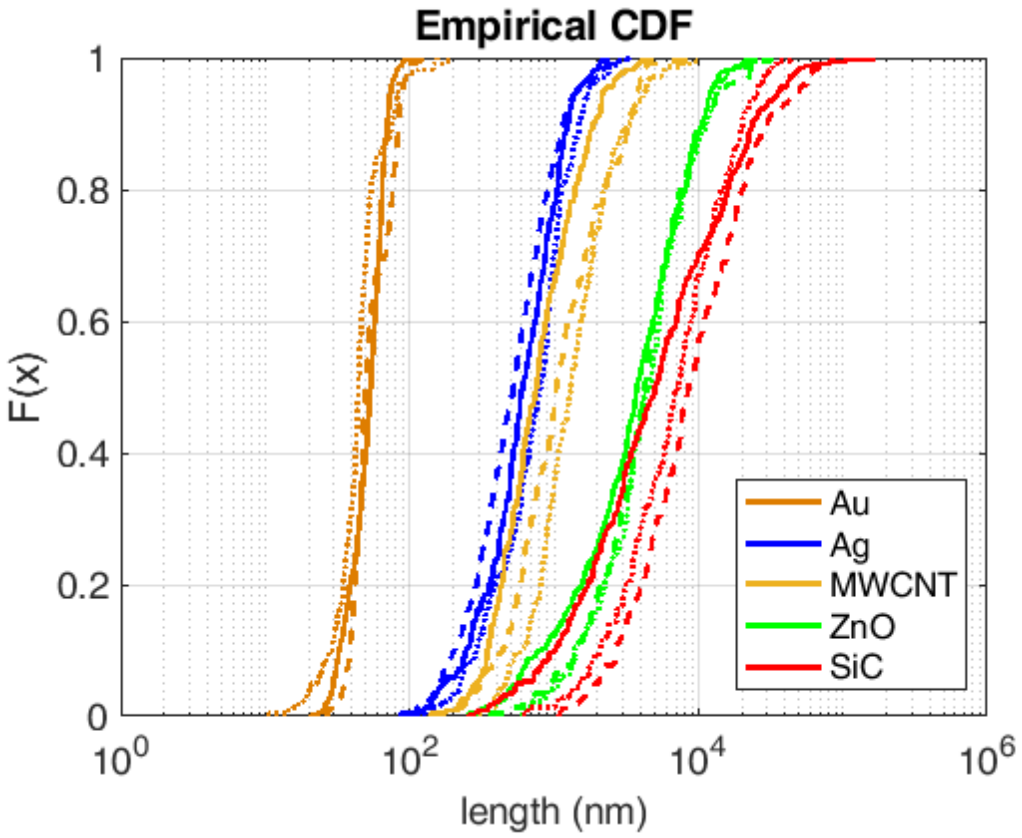

Figure 144: CDFs of the fibre length of all test materials for the three tested institutes. Each institute is marked by a different line style.

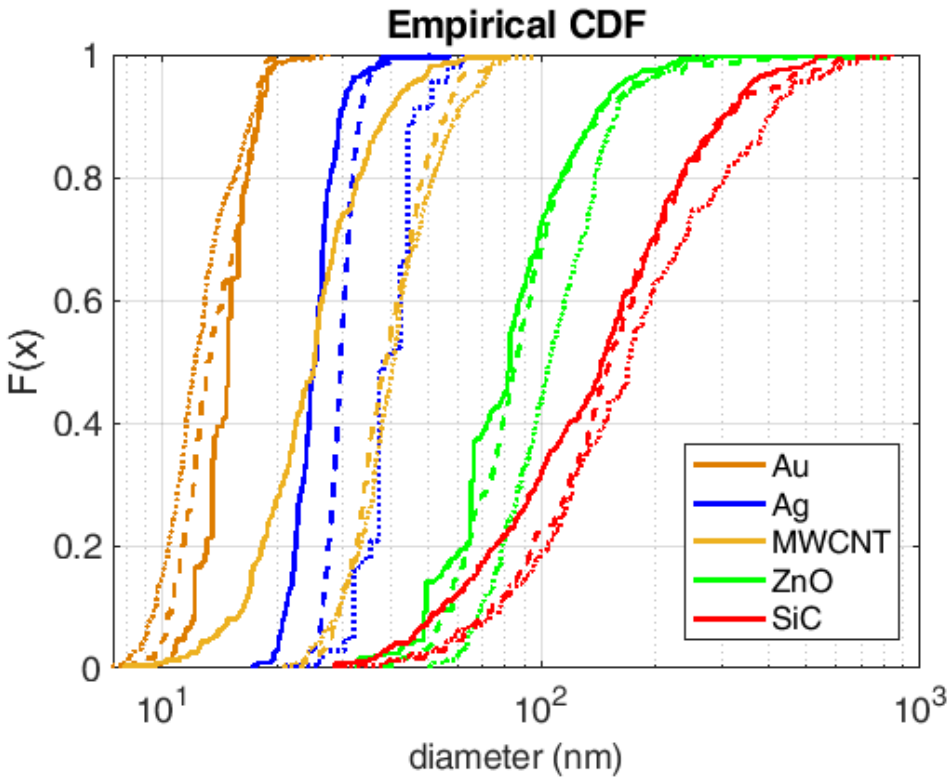

Figure 145: CDFs of the fibre diameter of all test materials for the three tested institutes. Each institute is marked by a different line style.

Evaluation of inter-evaluator contribution to the variance

In order to quantify the inter-evaluator contribution σ_{SF}^2 to the variance of the results, we asked the participants to evaluate the same SEM images of an Ag fibre sample. 7 results were handed in by the participants.

Averaging over the results, we obtain:

- mean length: 612 ± 79 nm, median length: 491 ± 53 nm
- mean diameter: 26.4 ± 5.2 nm, median diameter 26.2 ± 5.2 nm.

The stated uncertainties are twice the standard deviation $2\sigma_{SF}$.

Table 79 shows a comparison between these results and the previous results for Ag given in 0 and 0. We see that for each measurement the relative standard deviation, highlighted in grey, decreases when the same SEM images are evaluated. For diameter determination, the relative standard deviation decreases by about 40%. For length determination, the relative standard deviation decreases to less than half of its initial value. Based on these results, the inter-evaluator contribution is estimated to be $2\sigma_{SF} \leq 20\%$.

Table 79. Comparison between the results from same images and the ILC

	Ag Datasets	
length	Same images	ILC
average(**mean** length) (nm)	612	686
standard deviation(mean length) (nm)	40	101
relative standard deviation(mean(length))	0.07	0.15
average(**median**(length)) (nm)	491	597
Standard deviation(median(length)) (nm)	27	90.0
relative standard deviation(median(length))	0.06	0.15
average(geometric standard deviation(length))	2.0	1.9
diameter		
average(**mean**(diameter)) (nm)	26.4	29.5
standard deviation(mean(diameter)) (nm)	2.6	4.7
relative standard deviation(mean(diameter))	0.10	0.16
average(**median**(diameter)) (nm)	26.2	29.2
standard deviation(median(diameter)) (nm)	2.6	4.6
relative standard deviation(median(diameter))	0.10	0.16
average geometric standard deviation(diameter)	1.1	1.2

The results for the length and diameter determination are shown in Figure 146.

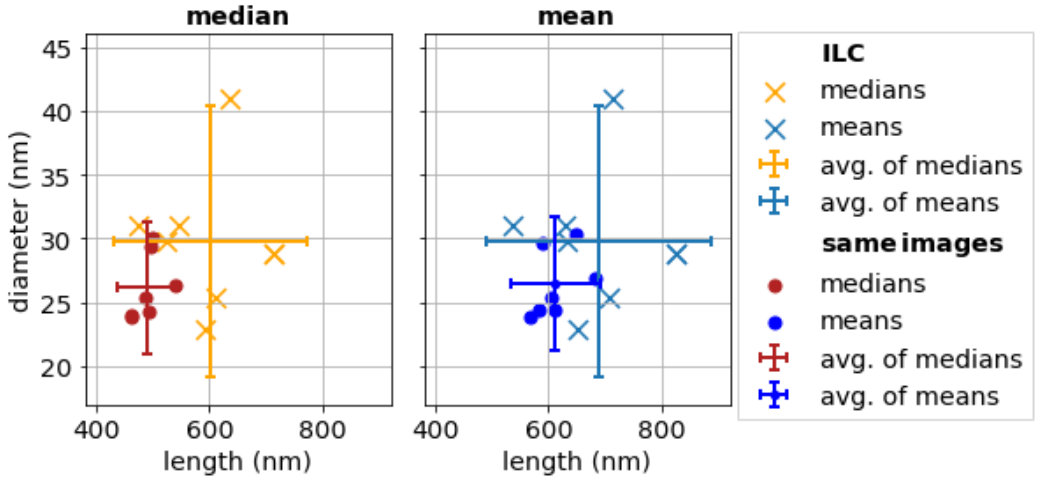

Figure 146: comparison plot between results of the evaluator bias and the ILC.

Length error estimation of upright standing fibres

The length of upright standing fibres is systematically underestimated by SEM and TEM as spatial information about the fibres is lost by a cosine projection onto the surface. We assume that the angular distribution between surface and fibre is normal distributed with a mean of 0°. Using that assumption, Figure 147 shows the mean relative error against the standard deviation of the angular distribution. The

error can be minimised using sample preparation protocols without electrostatic influence on the fibre, e.g. electrostatic precipitation. The electric charge would accumulate at either or both ends of a fibre and would highly increase the likeliness of upright standing fibres on the sample substrate.

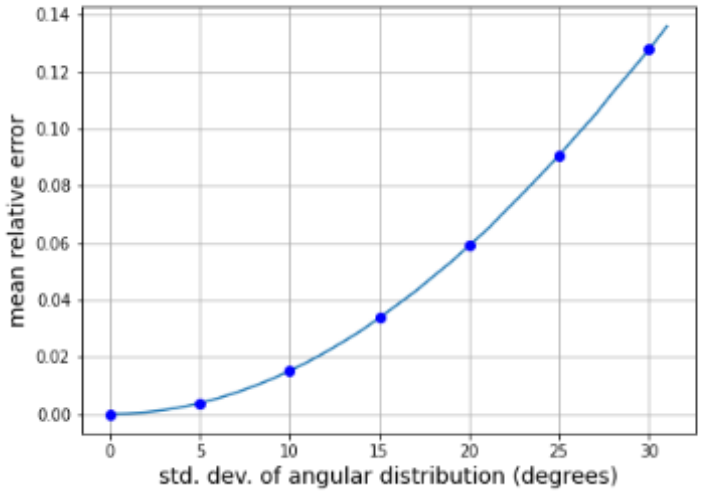

Figure 147: mean relative error against the std. dev. of the angular distribution

Summary of statistical analysis

35 SEM results from five test materials were handed in by the participants. Of these, 9 results could not be considered in the analyses. In detail, 4 results are excluded due to insufficient pixel size and 4 more due to varying pixel size in each image. One result that used an automatic segmentation is excluded because smaller fibres were systematically neglected. All in all, for each test material between four and seven valid datasets were considered for further analysis. The average of mean and median length was determined with the standard deviation between $2\sigma_L$< 16% for ZnO and $2\sigma_L$< 45% for the real-world material MWCNT. For the average of mean and median diameter, the standard deviation ranges from $2\sigma_L$< 17% for Au nanorods to $2\sigma_L$< 45% for MWCNT.

17 TEM results from three test materials were handed in by the participants. Of these, 5 results are not considered in the analyses because of insufficient numbers of counted fibres. In 2 datasets only the diameter was determined. Additionally, the TEM samples of the Ag nanowires were contaminated with sulphur and needed to be excluded from the analysis. For Au the average of mean and median length was determined with a standard deviation of $2\sigma_L$< 26% and the average of mean and median diameter with a standard deviation of $2\sigma_L$< 15%. For ZnO the average of mean and median length was determined with the standard deviation of $2\sigma_L$< 61% and the average of mean and median diameter with a standard deviation of $2\sigma_L$< 49%. For SiC only one institute was able to pairwise measure the length and diameter of 200 fibres. Therefore, no standard deviation was calculable.

3 DFSTEM results from three test materials were handed in by one participant. The result on SiC was excluded due to an insufficient number of counted fibres. The results for Au and ZnO are in accordance with SEM and TEM.

We performed multiple statistical tests to identify the influence of different factors. Student´s t-tests show significant differences between SEM and TEM results for SiC and ZnO. Furthermore, for TEM a significant correlation between the pixel size and the measured fibre diameter was found. A correlation also exists between the geometric standard deviation and the relative standard deviation. For the software used for image evaluation and the measuring institute no significant influence on the results were found.

For the evaluation of the inter-evaluator contribution to the variance the participants were asked to evaluate the same SEM images of an Ag fibre sample. 7 results were handed in by the participants. Based on these results, the inter-evaluator contribution is estimated to be $2\sigma_{SF} \leq 20\%$.

Conclusions for fibre measurements

For SEM, all test materials were measured with reasonable uncertainties. The most precise results were achieved for ZnO with twice the standard deviation $2\sigma_L$ between 14% for mean and median length, and 20% for median diameter, although it is a test material with an aspect ratio above 50 and lengths partially >20 µm. Au, the shortest test material in the test, follows with $2\sigma_L$ between 14% for mean length and 26% for median length. The highest variance was observed for MWCNT with $2\sigma_L$ around 44% for length and diameter results. It was expected to be most difficult test material in the ILC as explained in 0. In addition, the required minimal pixel size of at least ¼ of the predominant diameter was verified. Therefore, we confirm for SEM the procedure of the draft TG for the whole application range without any restrictions.

For TEM on the one hand, we have results of the Au nanorods, which are in all measured sizes almost identical to the SEM results. On the other hand, for the two longest fibre test materials ZnO and SiC with a length distribution partially above 20 µm and aspect ratios >50 the results indicated the need for careful consideration of the following issues with regard to the TEM measurements within the draft TG. For ZnO the median diameter was measured with a standard deviation of $2\sigma_L = 48\%$, the median length with $2\sigma_L = 60\%$. For SiC only one participant was able to pairwise measure the length and diameter of at least 200 fibres. These challenges are caused by technical issues, e.g. the maximum resolution of the used instrument was not sufficient. It was furthermore reported that for SiC the distribution of fibres over the TEM grids was strongly inhomogeneous which made the fibre counting more difficult. Moreover, TEM results for ZnO and SiC are significantly different to those of SEM. Additionally, for TEM a dependency of the median diameter on the pixel size caused by the ZnO results was found. Thus, the required minimal pixel size of at least ¼ of the predominant diameter could not be verified. Therefore, an addition has been made to the draft TG to limit the use of TEM and to excluded potential nanomaterials from the scope of the draft TG with a median fibre length > 5 µm and a broad length distribution ($\sigma_{GSD} > 1.5$). For fibres with an expected median length of more than 5 µm and a broad length distribution ($\sigma_{GSD} > 1.5$) it is advised to use SEM instead. Furthermore, we point out two additional observations. First, for potential nanomaterials at the border between particles and fibres it is necessary to count the particles as well, otherwise the fraction of larger fibres is overestimated as seen for Au nanorods by the result of SEM 2. A paragraph addressing this issue was added to the draft TG. Second, the sample preparation has a strong influence on the measurement result as discussed in 0. This finding confirms the statement in the chapter “Aspects of Sample Preparation” of the draft TG, where the importance of sample preparation for the outcome of the size measurement is stressed.

3 List of references

1. (OECD), O.f.E.C.-o.a.D., PHYSICAL-CHEMICAL PROPERTIES OF NANOMATERIALS: EVALUATION OF METHODS APPLIED IN THE OECD-WPMN TESTING PROGRAMME.
2. (OECD), O.f.E.C.-o.a.D., Inhalation Toxicity Testing: Expert meeting on potential revisions to OECD Test Guidelines. OECD Environment, Health and Safety Publications - Series on the Safety of Manufactured Nanomaterials, 2012. No. 35.
3. (OECD), O.f.E.C.-o.a.D., Ecotoxicology and Environmental Fate of Manufac-tured Nanomaterials: Test Guidelines. Expert Meeting Report. OECD Environment, Health and Safety Publications - Series on the Safety of Manufactured Nanomaterials, 2014. No. 40. .
4. (OECD), O.f.E.C.-o.a.D., Report of the OECD Expert Meeting on the Physical Chemical Properties of Manufactured Nanomaterials and Test Guidelines OECD Environment, Health and Safety Publications - Series on the Safety of Manufactured Nanomaterials, 2014. No. 41.
5. (OECD), O.f.E.C.-o.a.D., Genotoxicity of Manufactured Nanomaterials: Report of the OECD expert meeting. OECD Environment, Health and Safety Publications - Series on the Safety of Manufactured Nanomaterials, 2014. No. 43.
6. 6. Lamberty, A., et al., Interlaboratory comparison for the measurement of particle size and zeta potential of silica nanoparticles in an aqueous suspension. Journal of Nanoparticle Research, 2011. 13.
7. 7. Kestens, V., et al., Challenges in the size analysis of a silica nanoparticle mixture as candidate certified reference material. Journal of Nanoparticle Research, 2016. 18(6): p. 171.
8. Meli, F., et al., Traceable size determination of nanoparticles, a comparison among European metrology institutes. Measurement Science and Technology, 2012. 23(12): p. 125005.
9. Babick, F., et al., How reliably can a material be classified as a nanomaterial? Available particle-sizing techniques at work. Journal of Nanoparticle Research, 2016. 18(6): p. 158.
10. Braun, A., et al., Validation of dynamic light scattering and centrifugal liquid sedimentation methods for nanoparticle characterisation. Advanced Powder Technology, 2011. 22(6): p. 766-770.
11. Charles, M., et al., Size characterization of airborne SiO2 nanoparticles with on-line and off-line measurement techniques: An interlaboratory comparison study. Journal of Nanoparticle Research, 2013. 15: p. 1919.
12. Nickel, C., et al., Dynamic light-scattering measurement comparability of nanomaterial suspensions. Journal of Nanoparticle Research, 2014. 16.
13. Hole, P., et al., Interlaboratory comparison of size measurements on nanoparticles using nanoparticle tracking analysis (NTA). Journal of Nanoparticle Research, 2013. 15(12): p. 2101.
14. ISO/DIS 19749:(under dev), Nanotechnologies -- Measurements of particle size and shape distributions by scanning electron microscopy. under development.

15. Montoro Bustos, A.R., et al., Post hoc Interlaboratory Comparison of Single Particle ICP-MS Size Measurements of NIST Gold Nanoparticle Reference Materials. Analytical Chemistry, 2015. 87(17): p. 8809-8817.
16. Linsinger, T.P.J., R. Peters, and S. Weigel, International interlaboratory study for sizing and quantification of Ag nanoparticles in food simulants by single-particle ICPMS. Analytical and Bioanalytical Chemistry, 2014. 406(16): p. 3835-3843.
17. Rice, S., et al., Particle size distributions by transmission electron microscopy: An interlaboratory comparison case study. Metrologia, 2013. 50: p. 663.
18. ISO/DIS 21363:(under dev), Nanotechnologies -- Measurements of particle size and shape distributions by transmission electron microscopy. under development.
19. Mech, A., et al., The NanoDefine Methods Manual. Part 2: Evaluation of methods. Vol. EUR 29876 EN. 2020, Luxembourg: Publications Office of the European Union.
20. Mech, A., et al., The NanoDefine Methods Manual. Part 3: Standard Operating Procedures (SOPs). Vol. EUR 29876 EN. 2020, Luxembourg: Publications Office of the European Union.
21. Broßell, D., et al., Assessment of nanofibre dustiness by means of vibro-fluidization. Powder Technology, 2019. 342: p. 491-508.
22. Krzywinski, M. and N. Altman, Nonparametric tests. Nature Methods, 2014. 11(5): p. 467-468.
23. Siegel, S., Castellan N.J., Non-parametric Statistics for the Behavioural Sciences. 2nd ed. 1988, New York: McGraw-Hill.

4 Appendix

Information on test materials used in the ILCs

Table 80. Manufacturer's designations of test materials used in the fibre size determination.

test material	manufacturer	product labelling
Au	Sigma-Aldrich	716839
Ag	Novarials	NovaWire-Ag-A20
MWCNT	Arry International Group Ltd.	ARIGM001
SiC	ACS Material	NWSC0202
ZnO	ACS Material	NWZO01A5

Table 81. Manufacturer's designations of test materials used in the particle size determination.

test material	manufacturer	product labelling
Ag	BAM	Not purchasable
SiO_2	KRISS	CRM 301-01-002 (20 nm) and CRM 301-01-001 (50 nm)
ZnO	JRC	JRCNM62101a
PSL (90/125 nm)	Polysciences	Custom made mixture of Cat. 64009 and Cat. 64011 (1:1)
TiO_2	JRC	IRMM 388

Application of different regulations

Figure 148 shows exemplary how different regulations can be applied in a length vs. diameter plot.

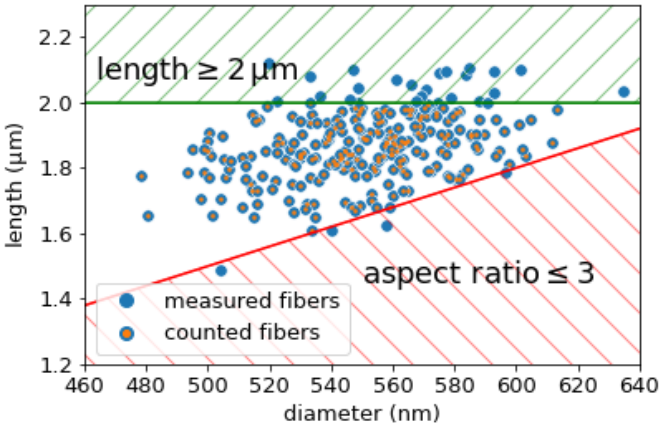

Figure 148: example of applying thresholds of different regulations in a length vs. diameter plot. The red line indicates an aspect ratio of 3. The green line shows a fictitious regulation where the maximal fibre length is set to 2 μm.

Example images (one from each institute and method)

Ag nanowires

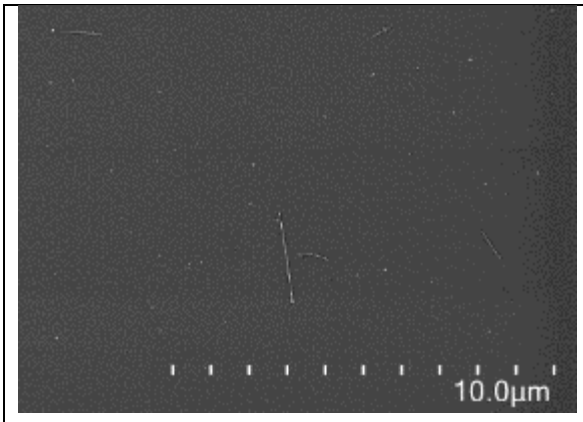

Figure 149: SEM 1, electron beam voltage: 3kV, detector: SE, pixel size 5.4 nm/px

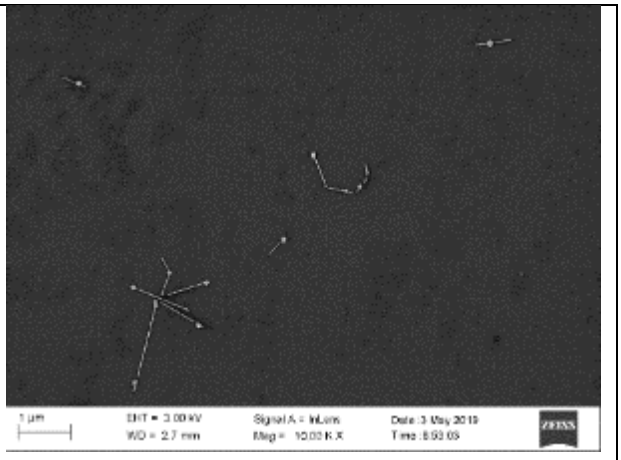

Figure 150: SEM 2, electron beam voltage: 3 kV, detector: In-lens, pixel size 5.6 nm/px

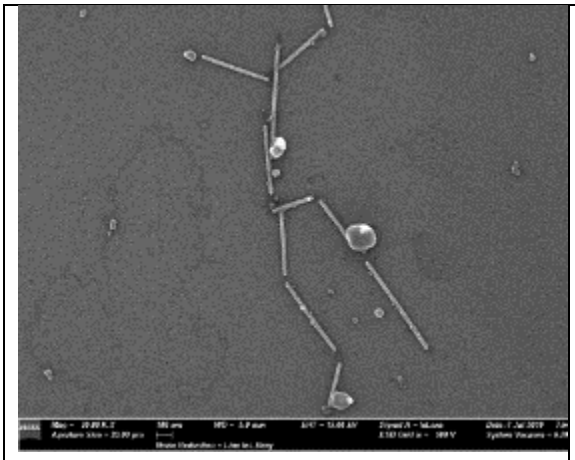

Figure 151: SEM 5, electron beam voltage: 15 kV, detector: SE, pixel size 3.7 nm/px

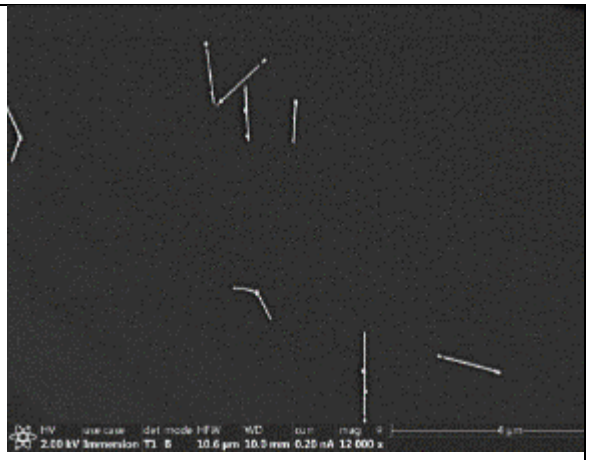

Figure 152: SEM 7, electron beam voltage 2 kV, Detector: BSE, Pixel size: 3.54 nm/ px.

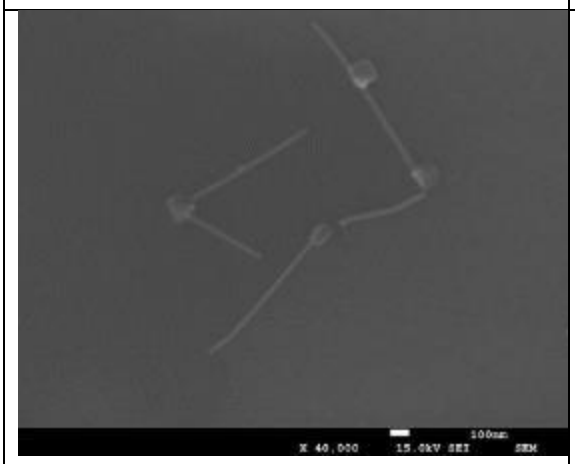

Figure 153: SEM 9, electron beam voltage: 15 kV, detector: SE, pixel size 2.3 nm/px

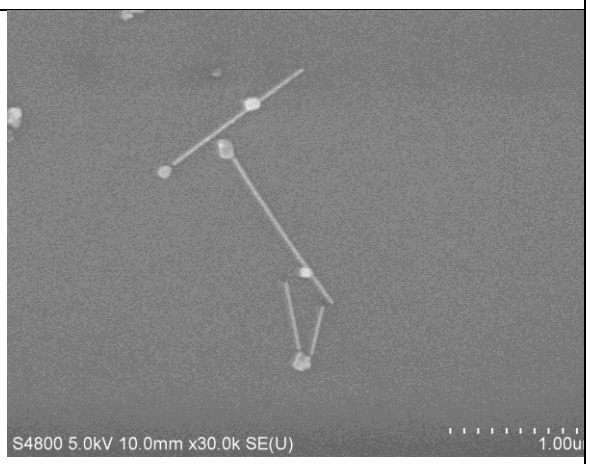

Figure 154: SEM 10, electron beam voltage: 5 kV, detector: SE, pixel size 3.6 nm/px

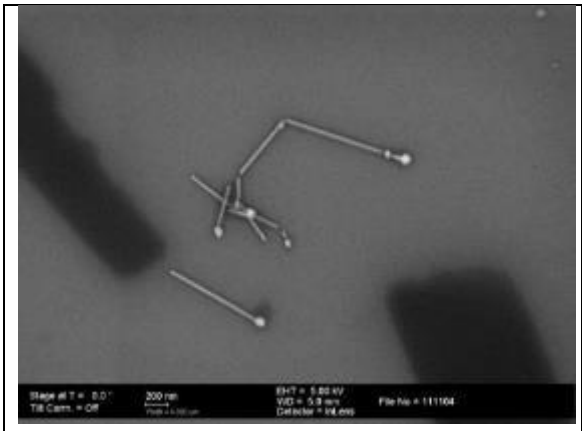

Figure 155: SEM 11, electron beam voltage 5 kV, Detector: SE, Pixel size: 4.34 nm/ px.

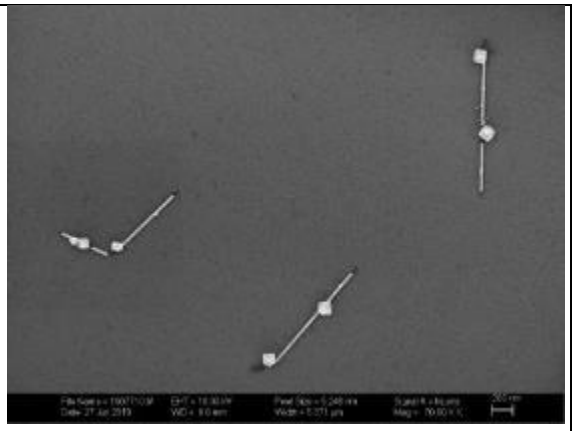

Figure 156: SEM 13, electron beam voltage: 10kV, detector: In-lens, pixel size 5.3 nm/px

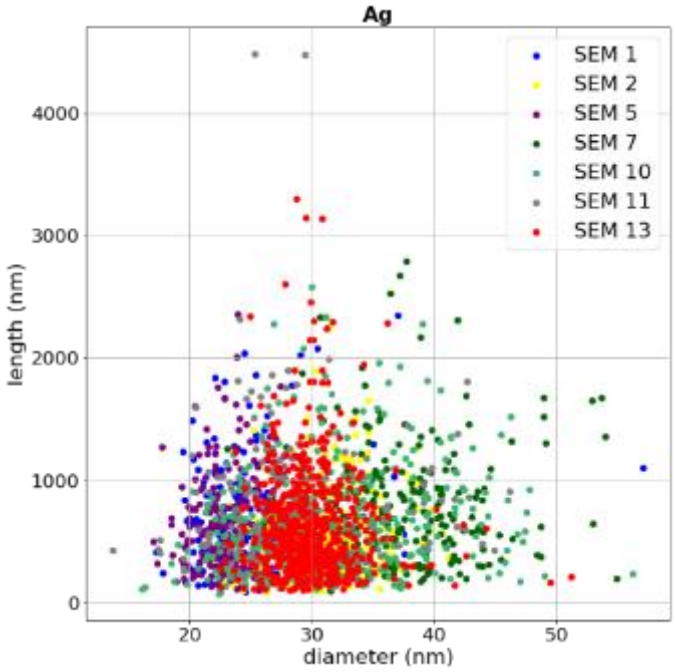

Figure 157: Scatterplot of length vs diameter for all selected results of Ag nanowires.

ZnO fibres

Figure 158: DFSTEM 1, Electron beam voltage: 30 kV, detector: dark field detector, pixel size 16.54 nm/px

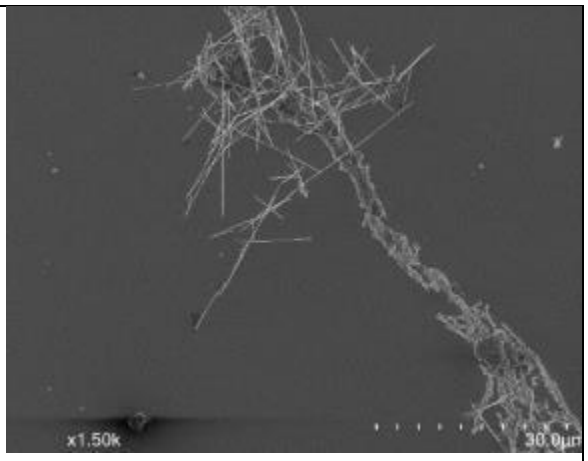

Figure 159: SEM 1: Electron beam voltage: 3 kV, detector: SE, pixel size 16.54 nm/px

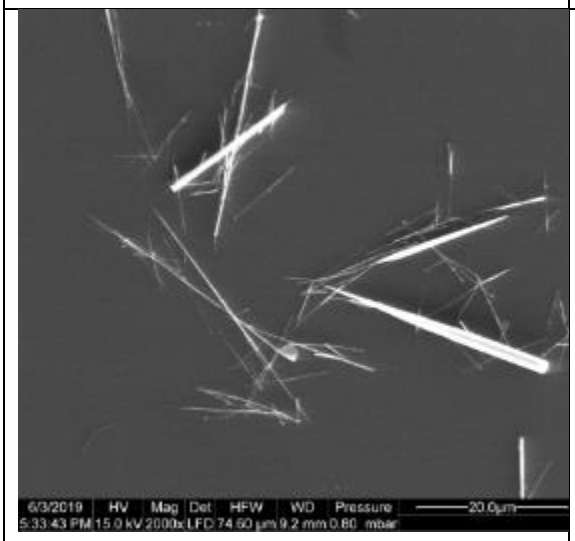

Figure 160: SEM 3, electron beam voltage: 15 kV, detector: SE detector, pixel size 36.55 nm/px

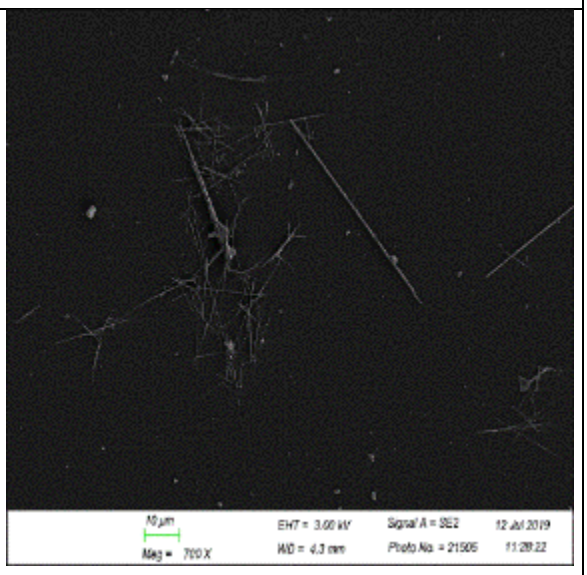

Figure 161: SEM 4, electron beam voltage: 3 kV, detector: SE detector, pixel size 51.3 nm/px

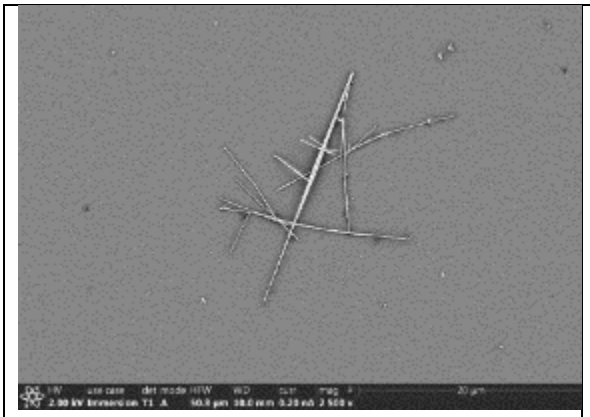

Figure 162: SEM 7, electron beam voltage: 2 kV, detector: BSE detector, pixel size 17.21 nm/px

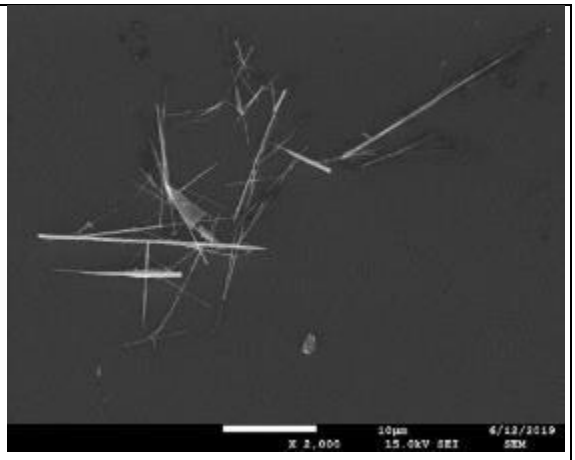

Figure 163: SEM 9, Electron beam voltage: 15 kV, detector: SE detector, pixel size: divers 10.4-133.3 nm/px

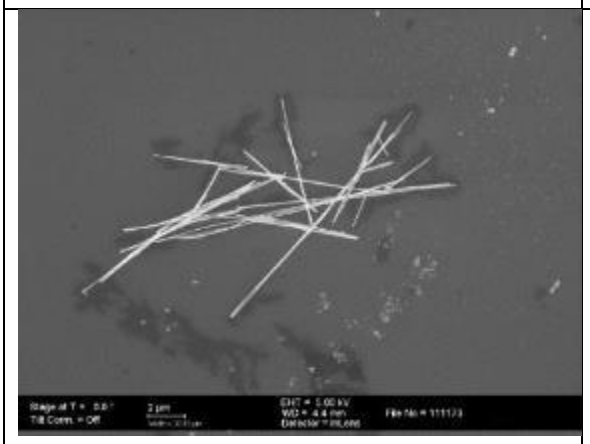

Figure 164: SEM 11, electron beam voltage: 5 kV, detector: SE, pixel size 29.3 nm nm/px

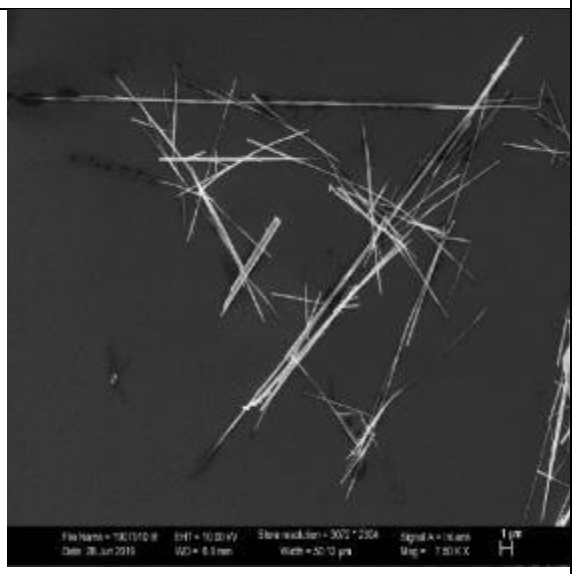

Figure 165: SEM 13, Electron beam voltage: 10 kV, detector: In lens, pixel size 16.3 nm/px

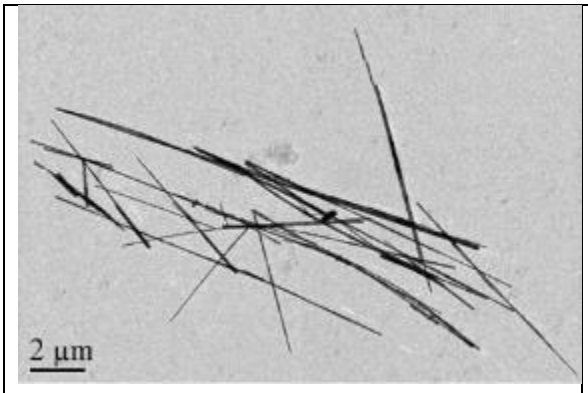

Figure 166: TEM 1, electron beam voltage: 200 kV, detector: CCD, pixel size 4.3 and 30 nm/px

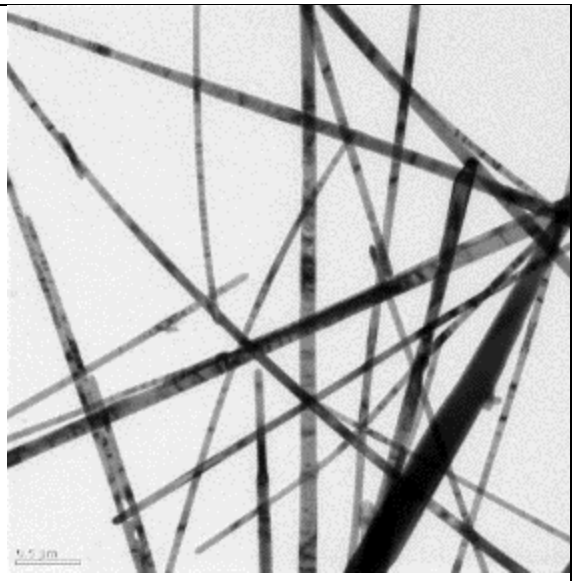

Figure 167: TEM 6, electron beam voltage: 120 kV, detector: CCD, pixel size 10.8 nm/px

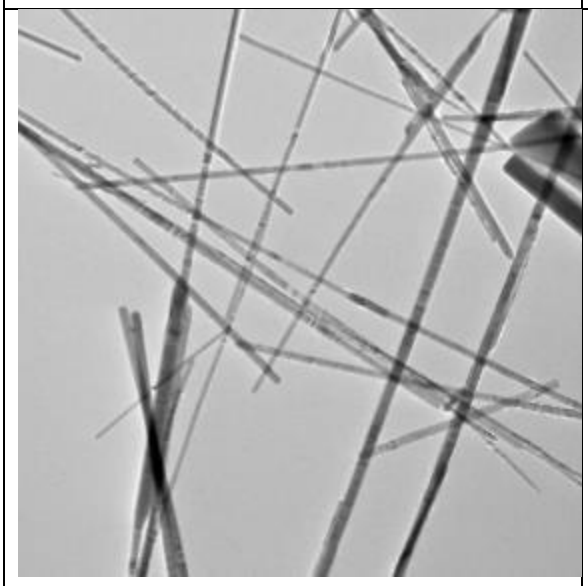

Figure 168: TEM 7, electron beam voltage: 300 kV, detector: Gatan Ultrascan, pixel size 6.63 nm/px

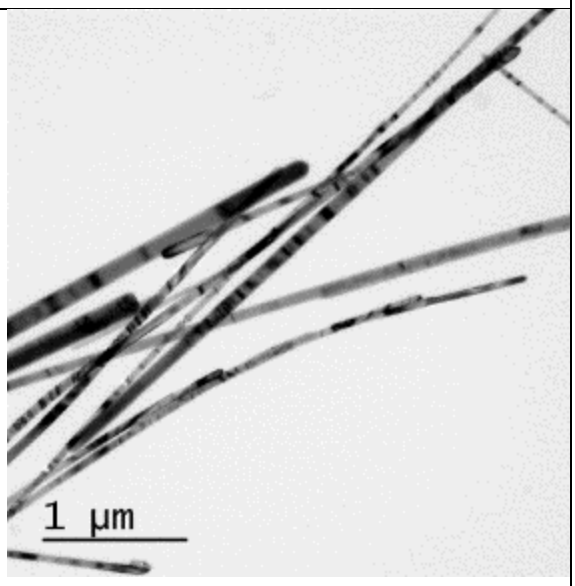

Figure 169: TEM 8, electron beam voltage: 300 kV, pixel sizes: 1.9, 18.97 nm/px

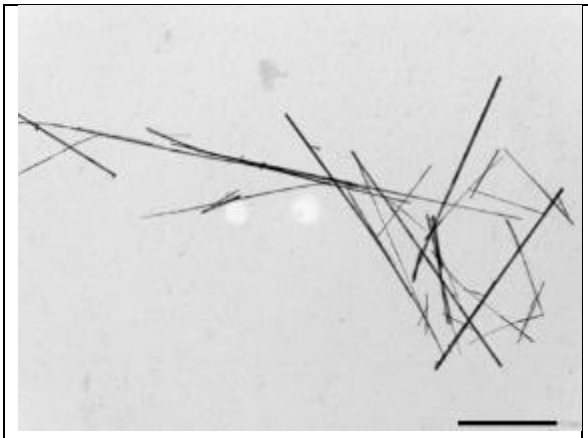

Figure 170: TEM 9, electron beam voltage: 200 kV, detector: CCD, pixel size 5.1, 10.4, and 30.3 nm/px

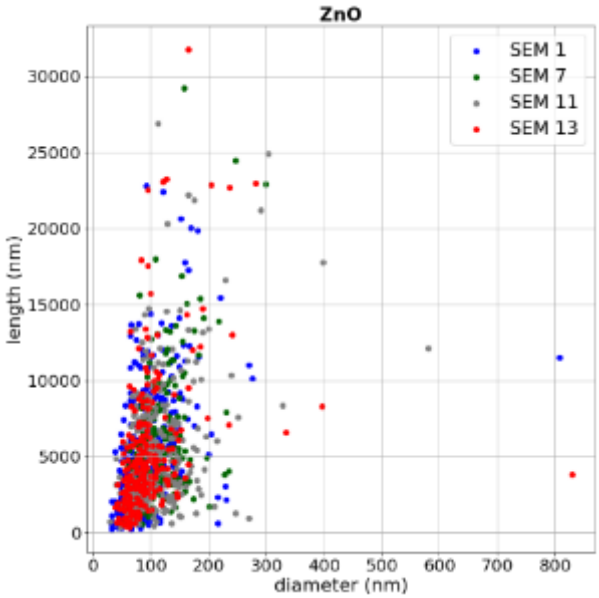

Figure 171: Scatterplot of length vs. diameter for all selected SEM results of ZnO fibres.

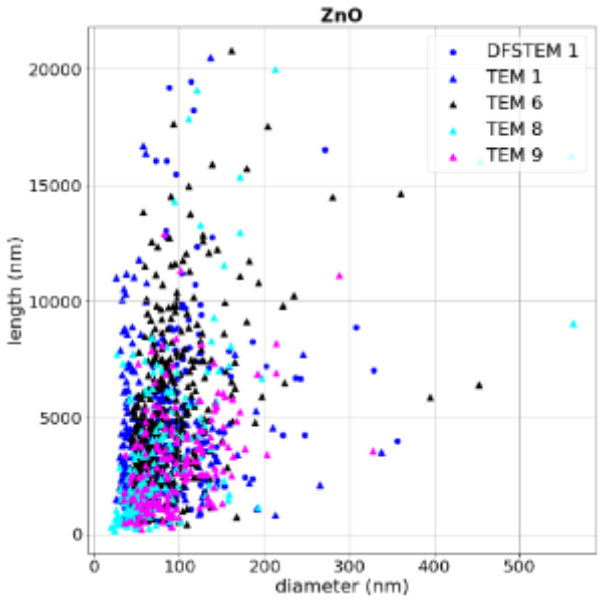

Figure 172: Scatterplot of length vs. diameter for all selected TEM and DFSTEM results of ZnO fibres.

SiC fibres

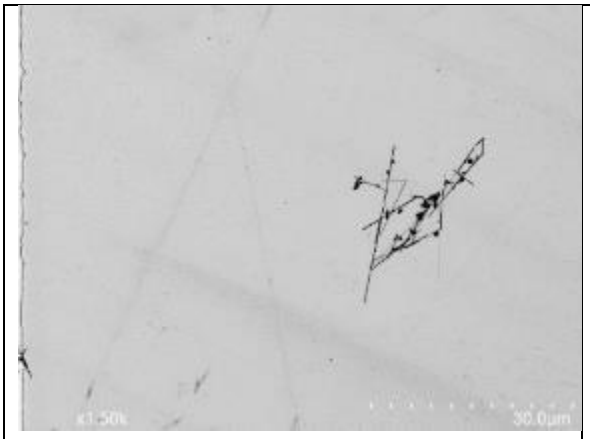

Figure 173: DFSTEM 1, electron beam voltage: 30 kV, detector: DFSTEM, pixel size 16.54 nm/px.

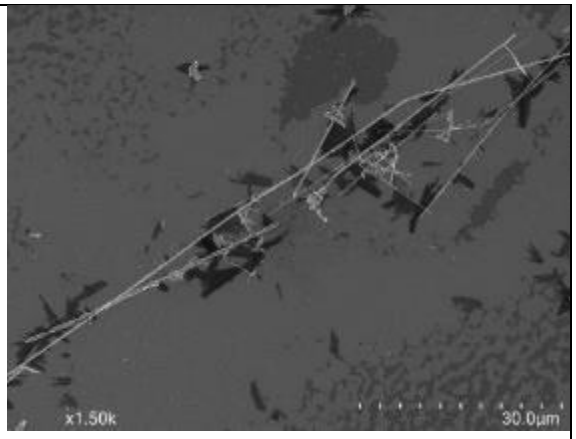

Figure 174: SEM 1, electron beam voltage: 3 kV, detector: SE, pixel size 16.54 nm/px.

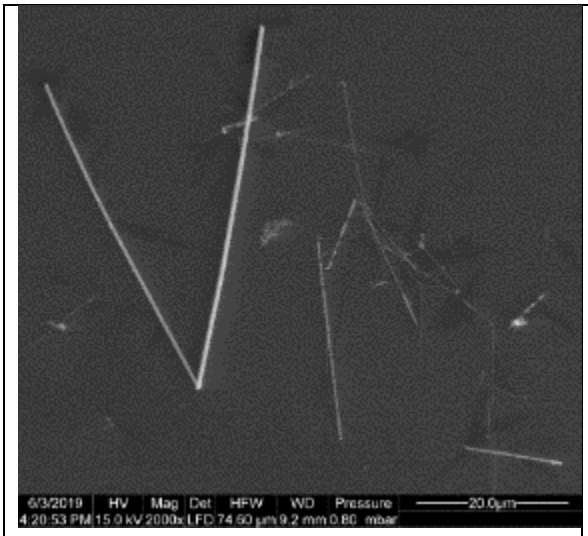

Figure 175: SEM 3, electron beam voltage: 15 kV, detector: SE, pixel size 36.5 nm/px.

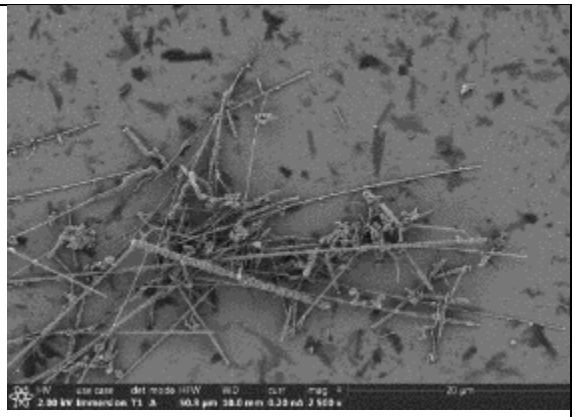

Figure 176: SEM 7, electron beam voltage: 2 kV, detector: BSE, pixel size 17.21 nm/px.

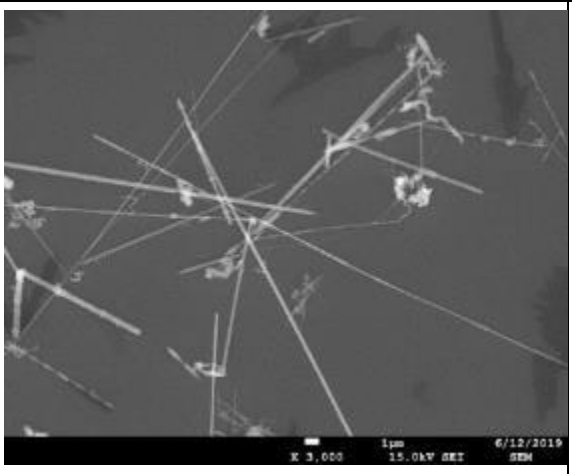

Figure 177: SEM 9, electron beam voltage: 15 kV, detector: SE, pixel size 27.8 nm/px.

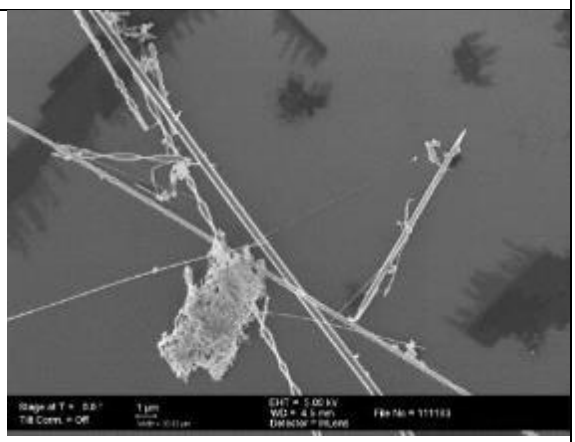

Figure 178: SEM 11, electron beam voltage: 5 kV, detector: SE, pixel size: 29.3 nm nm/px.

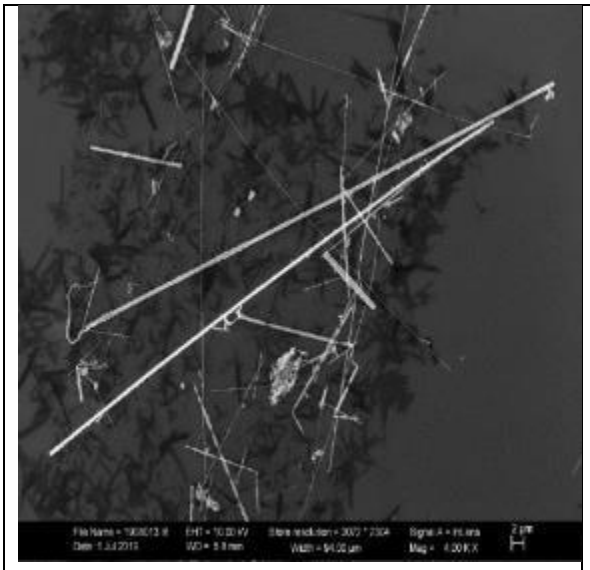

Figure 179: SEM 13, electron beam voltage: 10 kV, detector: InLens, pixel size 30.6 nm/px.

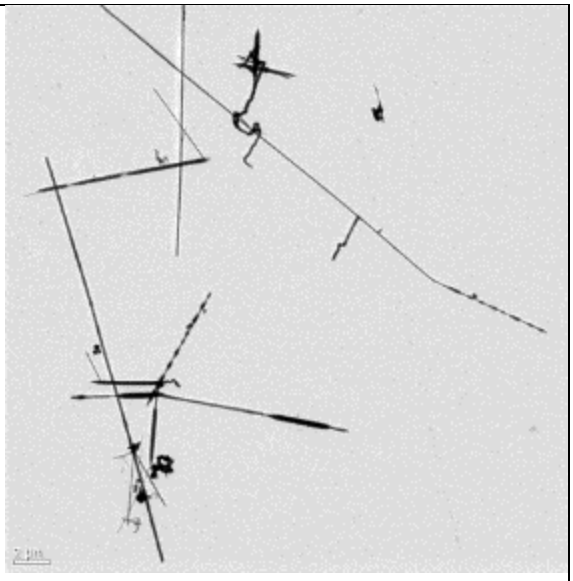

Figure 180: TEM 1, electron beam voltage: 200 kV, detector: CCD, pixel sizes: 4.3, 30, 51 nm/px.

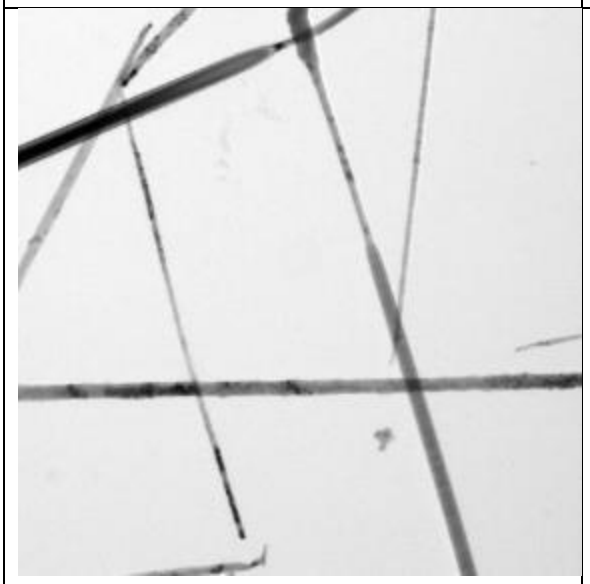

Figure 181: TEM 7, electron beam voltage: 300 kV, detector: Gatan Ultrascan, pixel size: 6.63 nm/px.

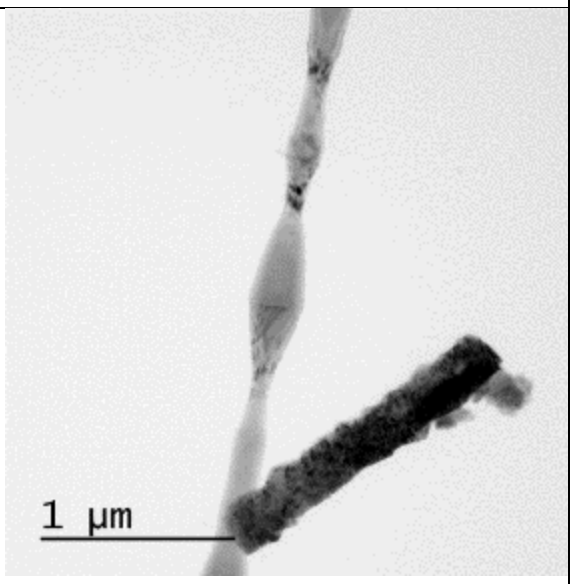

Figure 182: TEM 8, electron beam voltage: 300 kV, detector: CCD, pixel sizes: 1.4, 14.9 and 50 nm/px.

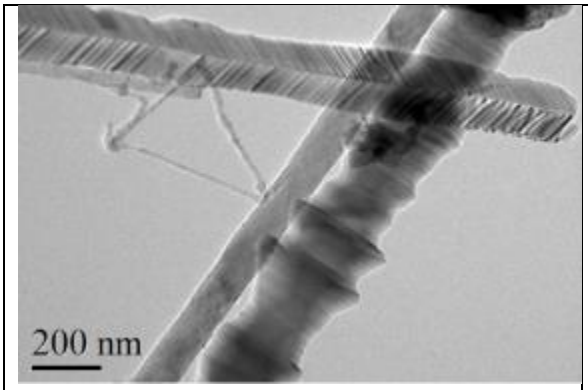

Figure 183: TEM 9, electron beam voltage: 200 kV, detector: CCD, pixel sizes: 24.1, 60, 120 nm/px.

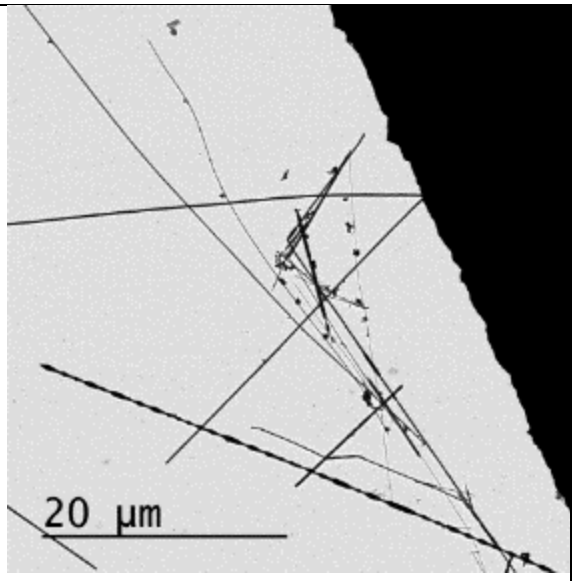

Figure 184: TEM 11, electron beam voltage: not specified, detector: not specified, pixel size: 22.7 and 14.7 nm/px.

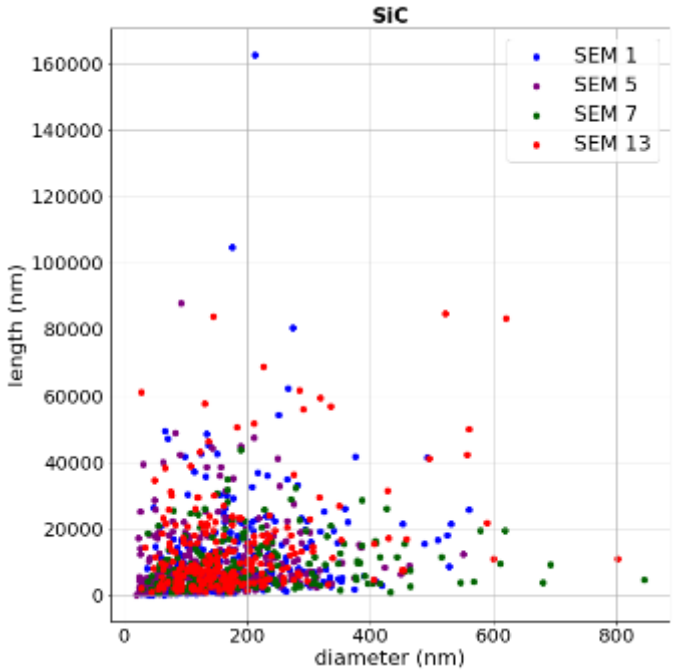

Figure 185: Scatterplot of length vs. diameter for selected SEM results of SiC fibres.

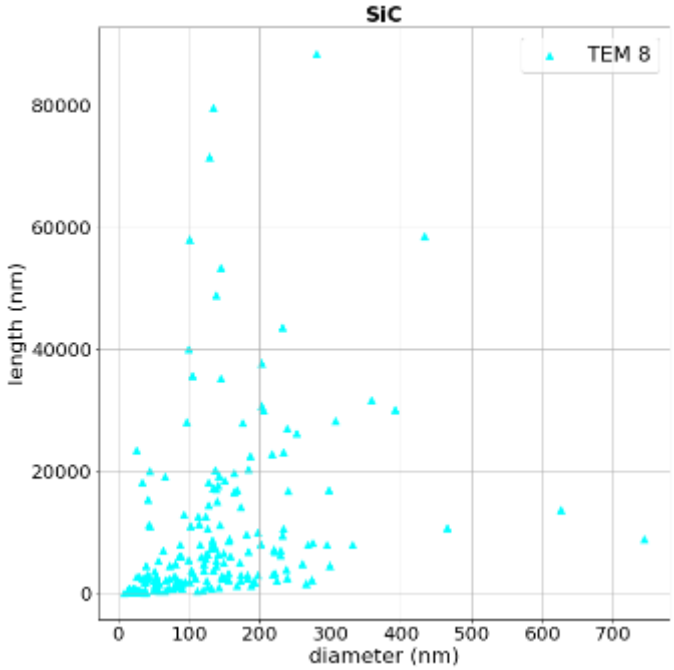

Figure 186: Scatterplot of length vs. diameter for selected TEM results of SiC fibres.

Au nanorods

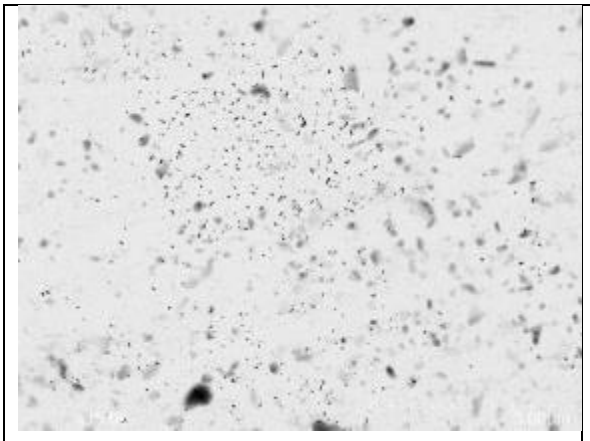

Figure 187: DFSTEM 1, electron beam voltage: 30 kV, detector: DFSTEM, pixel size: 4.96 nm/px.

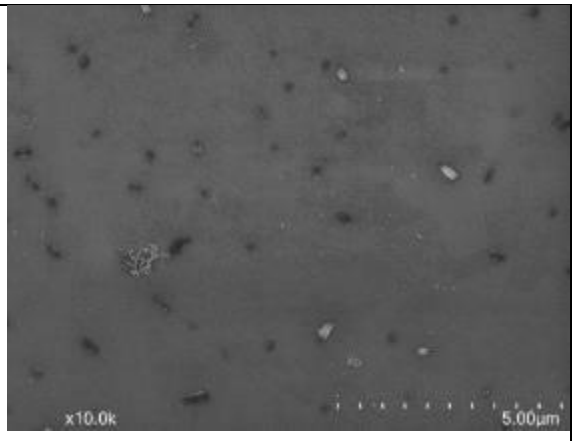

Figure 188: SEM 1, electron beam voltage: 3 kV, detector: SE, pixel size: 2.48 nm/px.

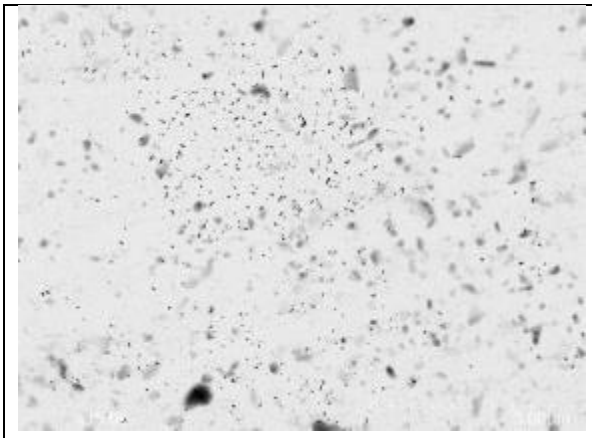

Figure 189: DFSTEM 1, electron beam voltage: 30 kV, detector: DFSTEM, pixel size: 4.96 nm/px.

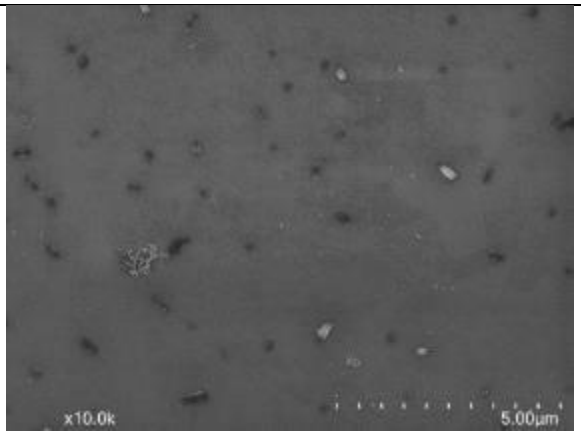

Figure 190: SEM 1, electron beam voltage: 3 kV, detector: SE, pixel size: 2.48 nm/px.

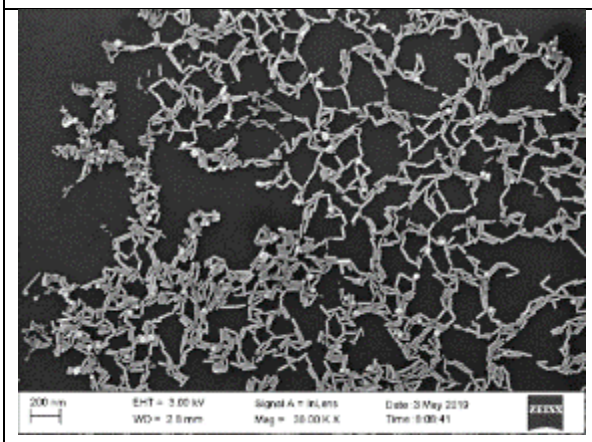

Figure 191: SEM 2, electron beam voltage: 3 kV, detector: IN-lens, pixel size: 1.86 nm/px.

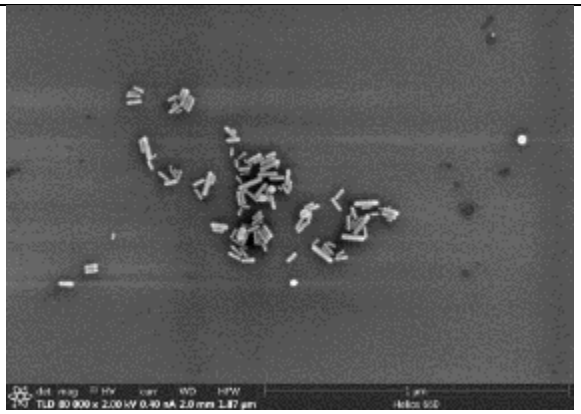

Figure 192: SEM 7, electron beam voltage: 2 kV, detector: SE, pixel size: 0.6 nm/px

Figure 193: SEM 9, electron beam voltage: 15 kV, detector: SE, pixel size: 1.85 nm/px.

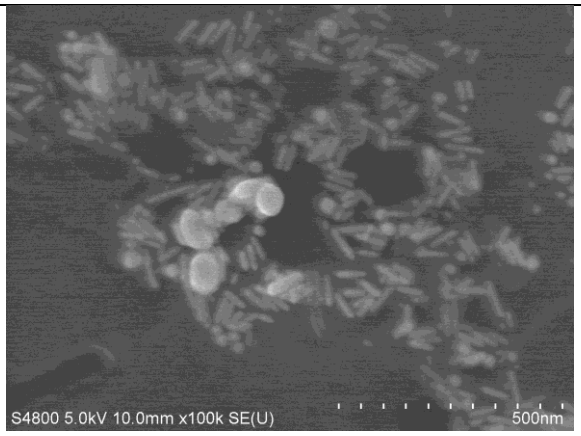

Figure 194: SEM 10, electron beam voltage: 5 kV, detector: SE, pixel size: 0.99 nm/px.

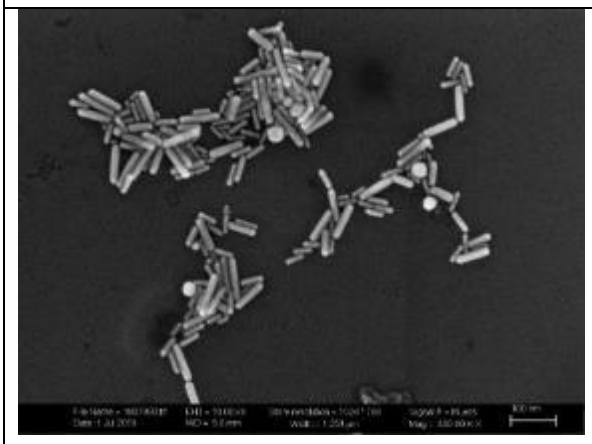

Figure 195: SEM 13, electron beam voltage: 10 kV, detector: In-lens, pixel size: 1.22 nm/px.

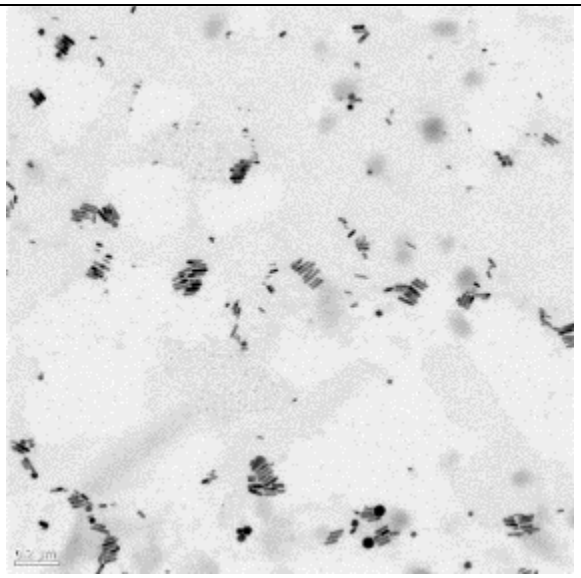

Figure 196: TEM 1, electron beam voltage: 200 kV, detector: CCD, pixel size: 2.5 nm/px.

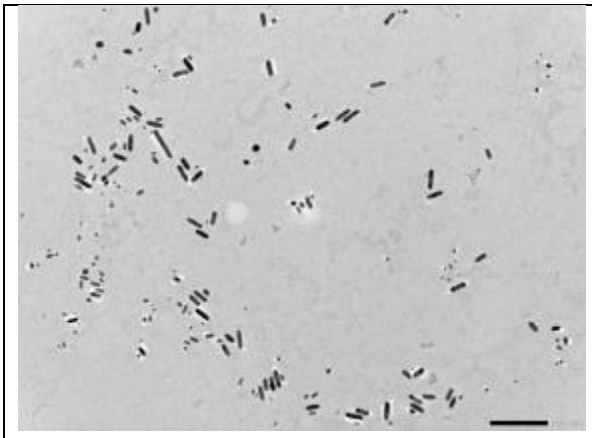

Figure 197: TEM 3, electron beam voltage: 120 kV, detector: CCD, pixel size: 0.54 nm/px.

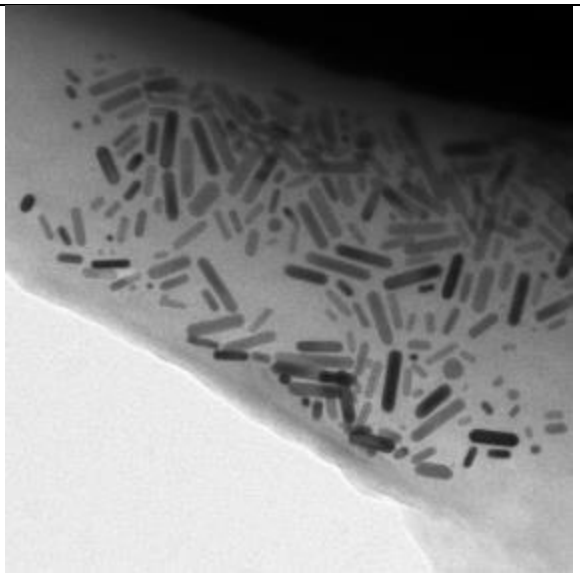

Figure 198: TEM 7, electron beam voltage: 300 kV, detector: Gatan Ultrascan, pixel size: 6.63 nm/px.

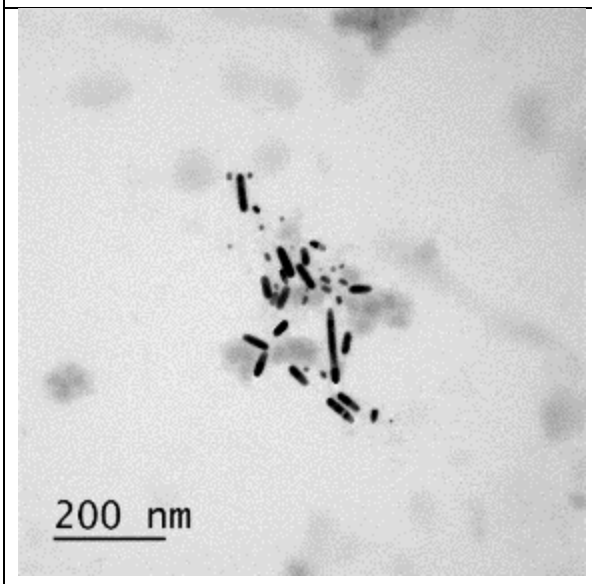

Figure 199: TEM 8, electron beam voltage: 300 kV, detector: CCD, pixel size: 0.5 nm/px.

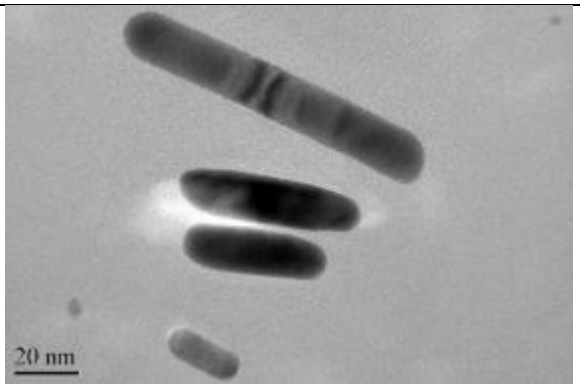

Figure 200: TEM 9, electron beam voltage: 200 kV, detector: CCD, pixel size: 0.85 and 0083 nm/px.

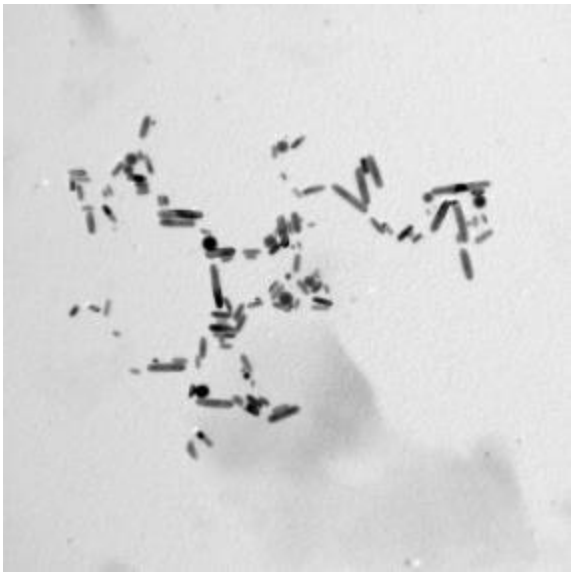

Figure 201: TEM 10, electron beam voltage: 300 kV, detector: BF, pixel size: 1.04 nm/px.

Figure 202: TEM 12, electron beam voltage: 200 kV, detector: not specified, pixel size: 0.28 nm/px.

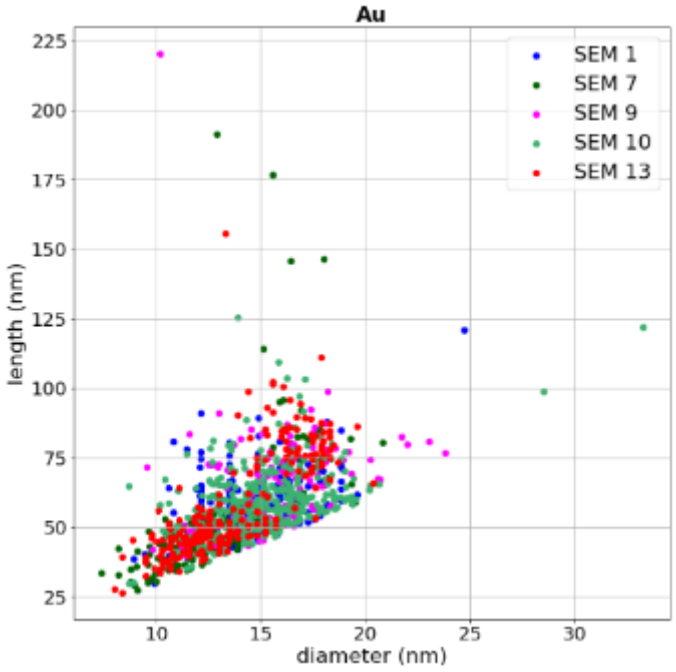

Figure 203: Scatterplot of length vs. diameter for selected SEM results of Au nanorods. The sharp lower boundary results from the evaluation of fibres with an aspect ratio of 3 only.

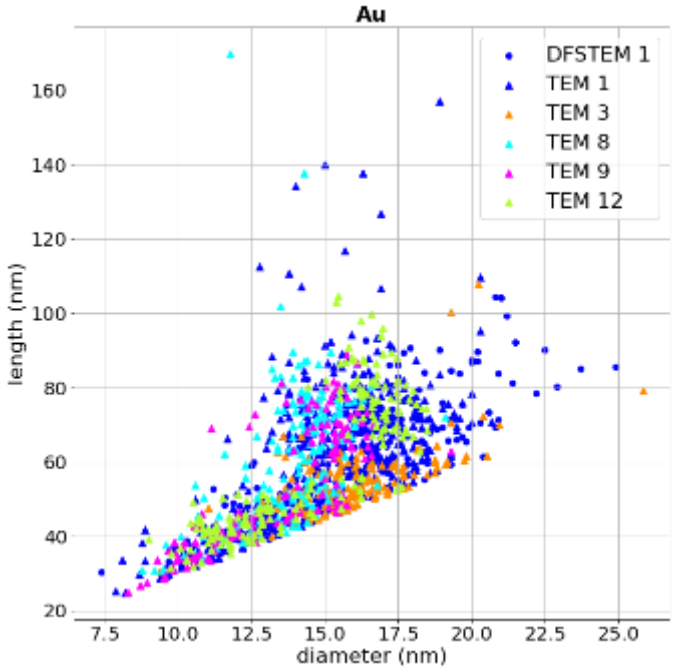

Figure 204: Scatterplot of length vs. Diameter for selected TEM and DFSTEM results of Au nanorods. The sharp lower boundary results from the evaluation of fibres with an aspect ratio of 3 only.

MWCNT

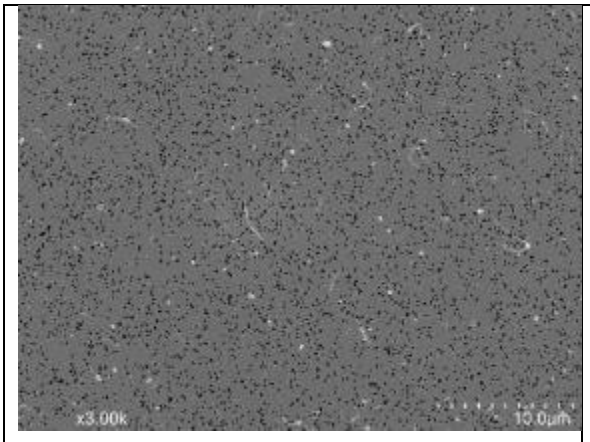

Figure 205: SEM 1, electron beam voltage: 3 kV, detector: SE, pixel size: 8.3 nm/px.

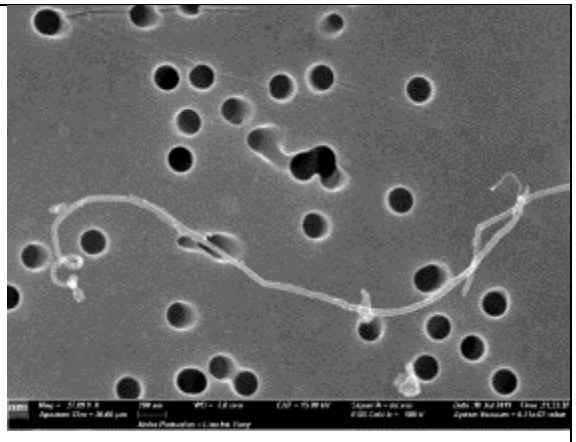

Figure 206: SEM 5, electron beam voltage: 15 kV, detector: SE, pixel size: 1.12 nm/px.

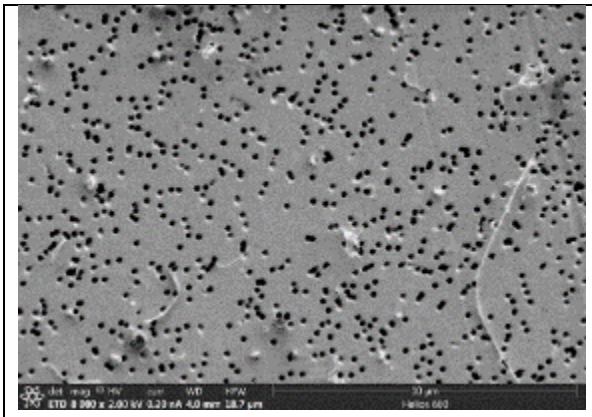

Figure 207: SEM 7, electron beam voltage: 2 kV, detector: SE, pixel size: 6.05 nm/px.

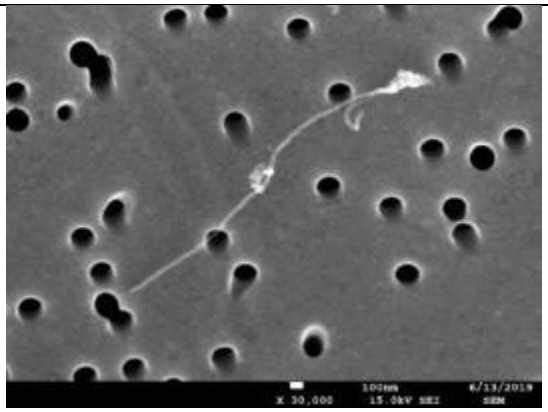

Figure 208: SEM 9, electron beam voltage: 15 kV, detector: SE, pixel size: 2.0 nm/px.

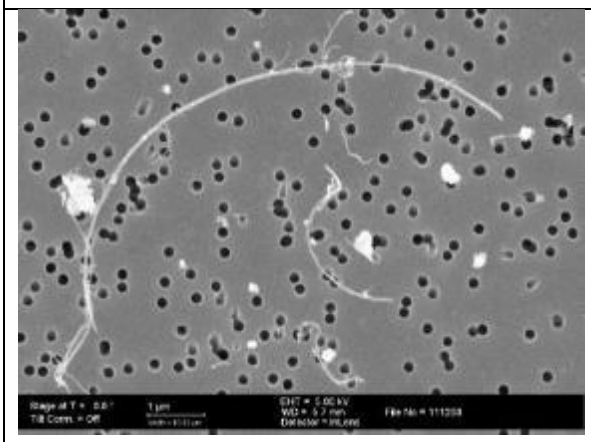

Figure 209: SEM 11, electron beam voltage: 5 kV, detector: In Lens, pixel size: 9.766 nm/px.

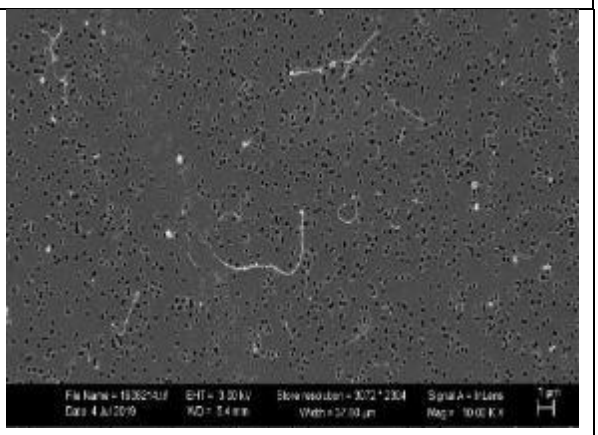

Figure 210: SEM 13, electron beam voltage: 10 kV, detector: In Lens, pixel size: 12.24 nm/px.

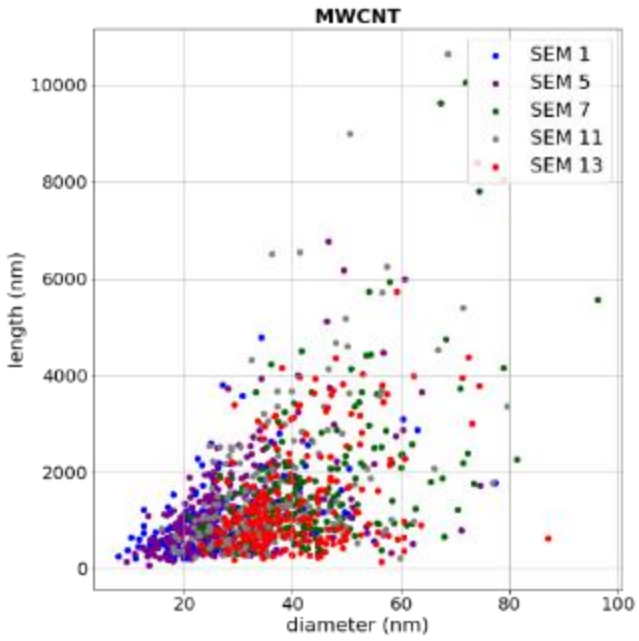

Figure 211: Scatterplot of length vs. diameter for MWCNT.

Sonication procedures for ZnO and TiO_2 particles

Table 82. Details of the sonication procedure for TiO_2 particles measured with CLS.

Lab	Concentration (mg/ml)	Sonicator brand/type	Energy output (W)	Energy input	Amplitude (%)	Cycle (%)	Pulse time (min)
01	0.1 / 0.2	Sonopuls HD 200, Fa. Bandelin	200	19.1 W	25	50	20
03	0.1 / 0.2	Hielscher Vial Tweeter UP200St	200	1.2 W/ml	75	50	20
05	0.1 / 0.2	Branson - Model SFX	550		20	50	20
07	0.1 / 0.2	Ultrasonic bath (Bransonic)	75				

Table 83. Details of the sonication procedure for ZnO particles measured with CLS.

Lab	Concentration (mg/ml)	Sonicator brand/type	Energy output (W)	Energy input	Amplitude (%)	Cycle (%)	Pulse time (min)
01	0.5 / 0.75	Sonopuls HD 200, Fa. Bandelin	200	19.1 W	25	50	20
03	1 / 2	Hielscher Vial Tweeter UP200St	200	1.2 W/ml	75	50	20
05	1 / 2	Branson - Model SFX	550		20	50	20

Table 84. Details of the sonication procedure for TiO_2 particles measured with DMAS.

Lab	Concentration (mg/ml)	Sonicator brand/type	Energy output (W)	Amplitude (%)	Cycle (%)	Pulse time (min)
01	13 / 18	Hielscher Vial Tweeter UP200St	200	75	50	15
04	6	Misonix S-4000	200	75	50	15
26	3 / 6	Branson Sonifier450	400	70	100	20

Table 85. Details of the sonication procedure for TiO_2 particles measured with DLS.

Lab	Concentration (mg/ml)	Sonicator brand/type	Energy output (W)	Energy input	Amplitude (%)	Cycle (%)	Pulse time (min)
01a	0.1 / 0.2	Sonopuls HD 200, Fa. Bandelin	200	19.1 W	25	50	20
01b	0.1 / 0.2	Hielscher Vial Tweeter UP200St	200	1.2 W/ml	75	50	20
02	0.01 / 0.1	Branson Sonifier 19mm Resonator		1.2 W/ml	36	50	
03	0.1 / 0.2	Hielscher Vial Tweeter UP200St	200	1.2 W/ml	75	50	20
07	0.1 / 0.2	Ultrasonic bath (Bransonic)	75				
15	0.1 / 0.2	Qsonica, LLC, Misonix Sonicators,XL-2000 Series	100		8		20
20	0.1 / 0.2	Vibracell VCX 750	750		60	50	
22	0.1 / 0.2	Bandelin Sonoplus HD 220/ UW 2200	200	12 W			07:40

24	0.1 / 0.2	Hielscher UP200S	200		75	50	15
25	0.1 / 0.2	Bandelin Sonoplus HD 2070	100	1.2 W/ml	40	100	
27	0.1 / 0.2	probe sonicator 3 mm,UP 200S (Hielscher) / vial sonicator	200		45 (probe) / 100 (vial)	50	20
29	0.1	Ultrasonic probe (Cole-Parmer ®)	130		75	50	10
31	0.03 / 0.06	Hielscher Probe sonicator UPS200S, 7 mm probe	200	1.1 W/ml	75	50	20
32	0.1 / 0.2	Bandelin Sonrex Digitec	650				

Table 86. Details of the sonication procedure for ZnO particles measured with DLS.

Lab	Concentration (mg/ml)	Sonicator brand/type	Energy output (W)	Energy input	Amplitude (%)	Cycle (%)	Pulse time (min)
01a	0.5 / 1	Sonopuls HD 200, Fa. Bandelin	200	19.1 W	25	50	20
01b	0.5 / 1	Hielscher Vial Tweeter UP200St	200	1.2 W/ml	75	50	20
02	0.1 / 0.5 / 1	Branson Sonifier 19mm Resonator		1.2 W/ml	36	50	
03	0.5 / 1	Hielscher Vial Tweeter UP200St	200	1.2 W/ml	75	50	20
04	0.5 / 1	Bioblock Scientific Vibracell 75043 probe-sonicator	750		40	50	
12	1 / 2	Branson Sonifier SFX 550	550	2.8 W/ml	55	50	20
13	0.5 / 1	Cole Parmer probe sonicator with 6.35 mm probe	130		50	50	6
15	0.5 / 1	Qsonica, LLC, Misonix Sonicators,XL-2000 Series	100		8		20
19	0.5 / 1	Branson Sonifier450	400		70	100	20
20	0.5 / 1	Vibracell VCX 750	750		60	50	
22	1 / 2	Bandelin Sonoplus HD 220/ UW 2200	200	12 W			07:40
24	0.5 / 1	Hielscher UP200S	200		75	50	15
25	0.5 / 1	Bandelin Sonoplus HD 2070	100	1.2 W/ml	40	100	
27	0.5 / 1	Probe sonicator 3 mm,UP 200S (Hielscher) / vial sonicator	200		45 (probe) / 100 (vial)	50	20
28	0.5 / 1	UP400S (Hielscher) probe sonicator	400		75	50	30
29	0.5	Ultrasonic probe (Cole-Parmer ®)	130		75	50	10
31	0.2 / 0.5	Hielscher Probe sonicator UPS200S, 7 mm probe	200	1.1 W/ml	75	50	20

Table 87. Details of the sonication procedure for TiO_2 particles measured with PTA.

Lab	Sonicator brand/type	Energy output (W)	Energy input	Amplitude (%)	Cycle (%)	Pulse time (min)
01	Hielscher Vial Tweeter UP200St	200	1.2 W/ml	75	50	15
02	Branson SONIFIER 450 D	400	1.2 W/ml	36	50	
15	Qsonica, LLC, Misonix Sonicators,XL-2000 Series	100		8		20
22	Bandelin Sonoplus HD 220/ UW	200	12 W			07:40

	2200					
24	Hielscher UP200S	200		75	50	15
30	LabSonic P	400	7.32 W	40		20

Table 88. Details of the sonication procedure for ZnO particles measured with PTA.

Lab	Sonicator brand/type	Energy output (W)	Energy input	Amplitude (%)	Cycle (%)	Pulse time (min)
01	Hielscher Vial Tweeter UP200St	200	1.2 W/ml	75	50	15
02	Branson SONIFIER 450 D	400	1.2 W/ml	36	50	
22	Bandelin Sonoplus HD 220/ UW 2200	200	12 W	-	-	07:40
24	Hielscher UP200S	200		75	50	15
30	LabSonic P	400	7.32 W	40		20

Table 89. Details of the sonication procedure for TiO_2 particles measured with sp ICP-MS.

Lab	Concentration	Sonicator brand/type	Energy output (W)	Energy input	Amplitude (%)	Cycle (%)	Pulse time (min)
04	800/1600 ppt	Qsonica S-4000	600		70	50	
05	2/5 ppb	BRANSON Sonifier 550D	550		30	50	20
22	100/500 ppt	Bandelin Sonoplus HD 220/ UW 2200	200	12 W			07:40
25	100/500 ng/L	Bandelin Sonoplus HD 2070	100	1.2 W/ml	40	100	

Annex A. Questions raised and answered during the interlaboratory comparison

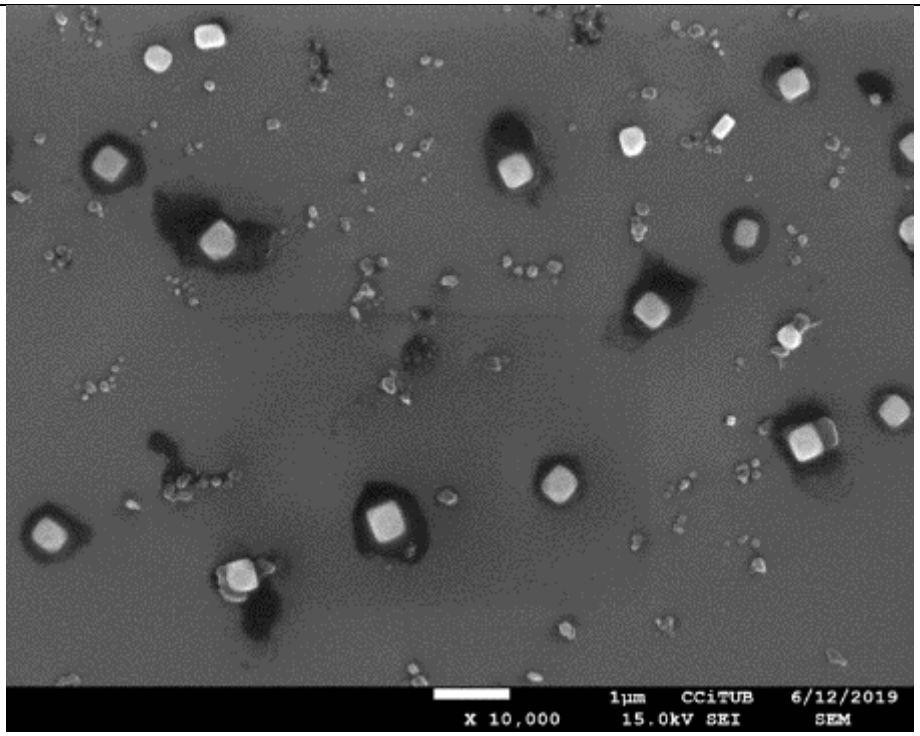

Figure 212: example SEM image of the Au nanorod sample that exhibits squared particles.

Question: In the Au nanorod sample, squared particles are found. Are those supposed to be counted? (s. Figure 212)

Answer: No, they are no fibres and are not the intended nanomaterial.

Question: In the Ag nanowires sample (s. Figure 213) the fibres exhibit kinks and small gaps. How is the length of such fibres to be evaluated?

Answer: The fibre ends if no connection between neighbouring fibres is seen. Thus, a fibre might extend over a kink or might end in the middle of two segments lying in a straight line. Correction: This was the initial answer to the question. We later decided to exclude the Ag Nano wires to be measured in TEM from the ILC because of sulphur contamination to the prepared TEM samples, see also next question.

Figure 213: Example TEM image of deteriorated Ag nanowires sample.

Question: The Ag sample on the TEM grid (s. Figure 213) seems to be deteriorated. Is the morphology in correct?

Answer: No. The TEM samples are indeed deteriorated and are excluded from the interlaboratory comparison.

Annex B. Inter-laboratory validation plan of the test guideline on particle size and size distribution of nanomaterials - Fibres

Safety indications:

The prepared samples contain fibres with lengths >5 µm and diameter <3µm that are respirable and can possibly cause adverse health effects. All samples have to be handled with care. We recommend using personal safety equipment, i.e. gloves, safety goggles and mask, to protect skin and lungs from contact with the material.

Introduction

The present document aims at providing assistance to the independent laboratories participating in the interlaboratory comparison test to validate the applicability of the experimental routines currently included in the draft OECD Test Guideline to determine the particle size and size distributions of particles and fibres. The validity of the Test Guideline is evaluated in separate interlaboratory comparisons for particles and fibres, respectively.

Scope of the interlaboratory comparison

Interlaboratory comparisons which evaluate the length and diameter of fibres are scarce. This interlaboratory comparison is the first one to test the pairwise determination of length and diameter of fibres.

In an intra-laboratory prevalidation we estimated the uncertainties for repeatability and reproducibility for the evaluation routine described in the draft Test Guideline. The international, inter-laboratory comparison is done to assess the influence of different technical specifications and the comparability of the methods Scanning Electron Microscopy (SEM) and Transmission Electron Microscopy (TEM). We decided to perform the test on four samples to possibly obtain information about the influence of the width of the size distribution on the reproducibility. Furthermore, we would like to encourage the participants to use the automated image evaluation software provided by BAuA, or alternative automated evaluation routines. This would allow comparing results from an automatic image evaluation and visual image evaluation.

As described in the draft Test Guideline the evaluator represents another source of uncertainty in the process of sample evaluation. We therefore will, towards the end of the round robin test, distribute a small number of SEM images taken by one or more participant to the other participants to be reevaluated. Form this reevaluation results the evaluator related uncertainty can be obtained.

We expect that some participants will need to use different resolutions to determine the diameter and length distribution, given the differences in available instruments. The results of this methods will be evaluated for comparability, as well.

Materials, reagents and analysis

The materials are distributed as prepared samples in order to exclude errors resulting from sample preparation, which is not part of the test guideline. Thus, the requirements in materials, reagents and means of analysis are minimal:

- Transmission Electron Microscope (TEM) and/or
- Scanning Electron Microscope (SEM)
- Calibration grid
- Tweezers
- Personal safety equipment: gloves, safety goggles and mask.
- Software routine for the evaluation of the images[3].

Rationale for the choice of test materials in the interlaboratory comparison:

The chosen materials (s. Tab. 1) cover different routes of sample preparation (from aerosol and from dispersion), very different materials (light elements as Carbon and heavier elements as Silver) and thus cover a broad range of real-life materials.

The chosen materials cover a wide range of different sizes within the measurement range: The diameter of the gold nanorods is approx.10 nm (length approx. 45 nm), while SiC contains the widest fibres in the test with a diameter of x>300 nm (max. length l_{max}>100 µm).

Furthermore, the size distributions of the used materials are differently wide. SiC is the material with the widest distribution in diameters and lengths. For a wide size distribution, the amount of fibres evaluated (N = 200) is considered to be low. Using materials with differently wide size distribution, it is possible to evaluate this influence on the reproducibility of the results. Depending on the instrument in use it might be necessary to evaluate the length and the diameter separately at different resolutions.

The materials cover different sample preparation qualities: Silver nanowires are short and exhibit few intercrossings. This material thus fulfils the criteria that enable an automated evaluation of fibre length and diameters. ZnO forms loose agglomerates and thus visual evaluation is necessary.

MWCNT and ZnO are both materials with diameter close to 100 nm. This size is of special interest in different nanomaterial-specific regulations. One of the goals of this round robin is to find out how large the uncertainties are for materials close to a regulatory limit.

Table. 1: Overview of fibrous materials used in the interlaboratory comparison and their size related properties

Material	Au	Ag	MWCNT	ZnO	SiC
Label	012	003	013	008	009
Length /µm	0.045	0.8	1.0	5.4	7.2
Diameter /nm	10	25	90	117	140
Aspect ratio	4.5	20	33	60	51
Width of the length distribution σ_{GSD}	1.4	1.5	2.3	2.3	3.0

[3] An editor software can be provided by BAuA that supports the visual evaluation of SEM and TEM images and that also allows for automatic evaluation of samples with best preparation quality. Participants interested in trying out or using this editor software, please contact BAuA.

Experimental procedures

The samples are delivered in a prepared state. The experimental procedures are described the section "Description of the Methods, Fibres: Electron microscopy".

a. Deviating from the protocol please count the number and measure the length and width of fibres that extend over the upper or the left edges of the image. Please mark those fibres in the evaluation. 200 fibres should be measured that do not cross the edge of an image.

Evaluation and representation of obtained results, test report

The evaluation of the test results is described in the section "Data evaluation and error calculation" and the data to be reported is listed in the section "test report" in the draft Test Guideline. Additionally, we would like the participants to provide the following information:

a) The size of both sides of the acquired image in pix x pix.

b) The number and length and diameters of fibres that extend over the upper or left edge of the acquired and evaluated images.

c) All images should be uploaded to the BSCW server <Link censored> in the following folder:

Fibres/<Method>/<Institute-name>/.

Please create a folder for each sample labelled with the sample name e.g. Fibres/Scanning Electron Microscopy/BAuA/TGP_2019_01_03_003_01/ You'll receive an email with an invitation to the bscw.bund.de server shortly.

The mean and median values of the length and diameter distribution are to be calculated for the fibres fully contained in the image, only.

Examples of the graphical representation of typical results for a fibre material are given in Fig. 1 and Fig. 2.

An excel file for guidance on the reporting "Reporting_sheet_fibres_excel.xlsx" is provided.

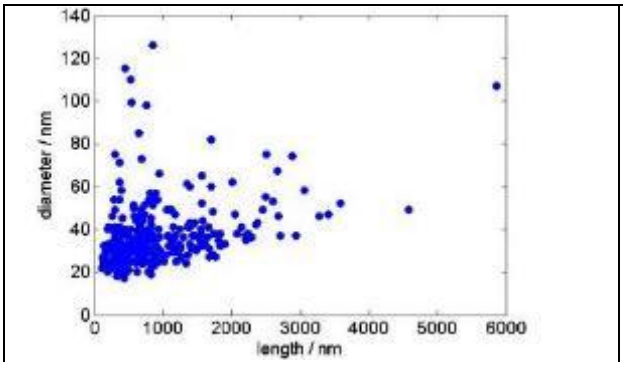

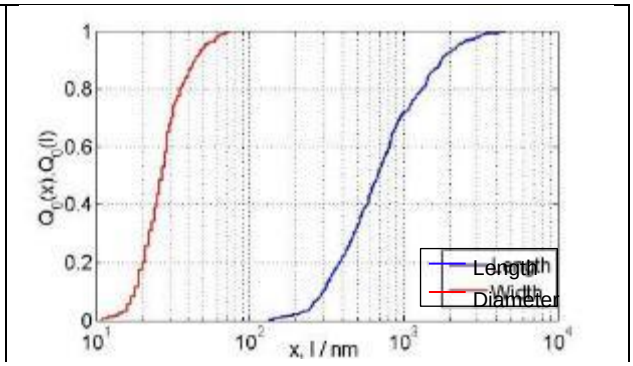

Fig. 1: representation of the results of all pairs of length and diameter for all evaluated fibres.	Fig. 2: graphical representation of the cumulative distribution of length and diameter. The scale of the x axis may be logarithmic, but does not have to be.

Validation of the results from the participating laboratories

For each material the mean and median values and their corresponding bootstrap errors are compared to evaluate the interlaboratory and intermethod variability and estimate the precision of the method described in the test guideline.

From the results of the interlaboratory comparison the different contributions to the uncertainty as well as the total error of the measurement is to be estimated.

Annex: Examples of the samples, additional information for sample preparation

Au nanorods 012

The Au nanorods samples exhibit some clearly spherical, non-rodlike particles. They are not to be measured. Furthermore, some of the rods might have an aspect ratio below 3. Those rods need to be measured, counted and evaluated. This is a borderline material between a particulate and a fibrous material and we will test whether the instructions given in the test guideline are sufficient to treat such a borderline case.

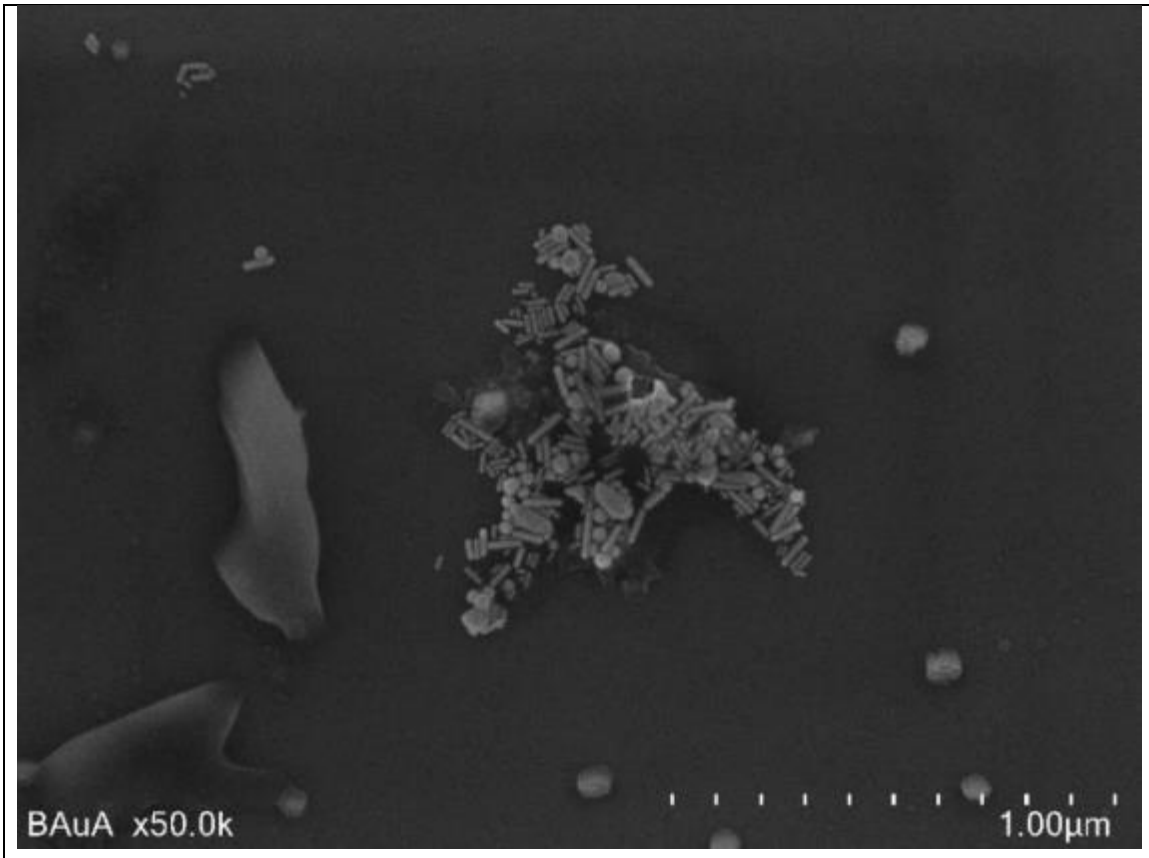

Ag Nanowires (Ultrasound treated) 003

The Ag Nanowires samples is considered as an ideal test material, because the fibres are well dispersed, they exhibit an aspect ratio low enough to be imaged with many instruments and the fibres are mostly straight or weakly bent. Every participant is asked to measure this material with the highest priority.

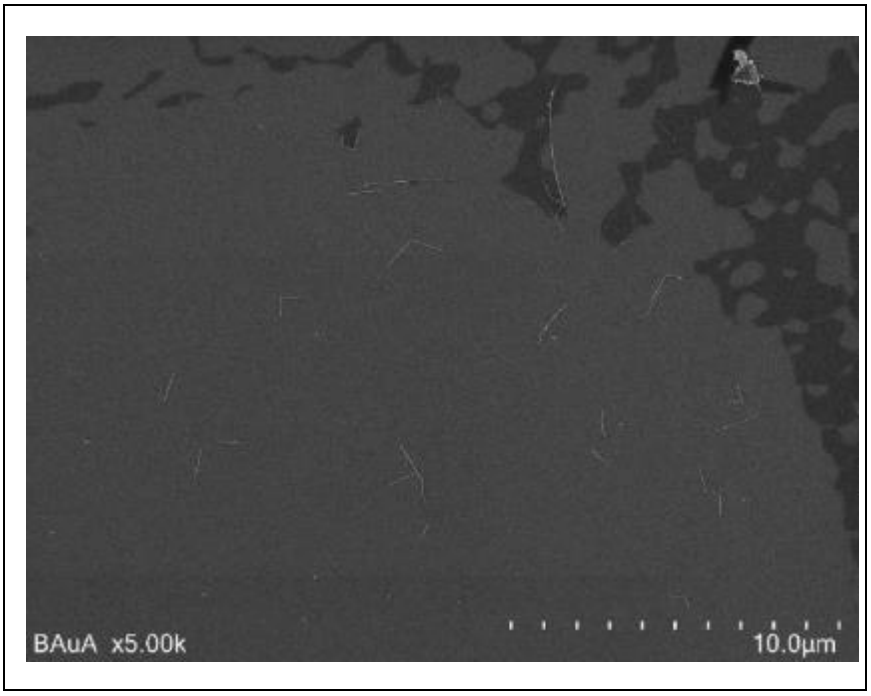

Special cases:

Some Ag fibres exhibit sharp kinks, as shown in Fig.3. Shall these fibres be counted as one or two?

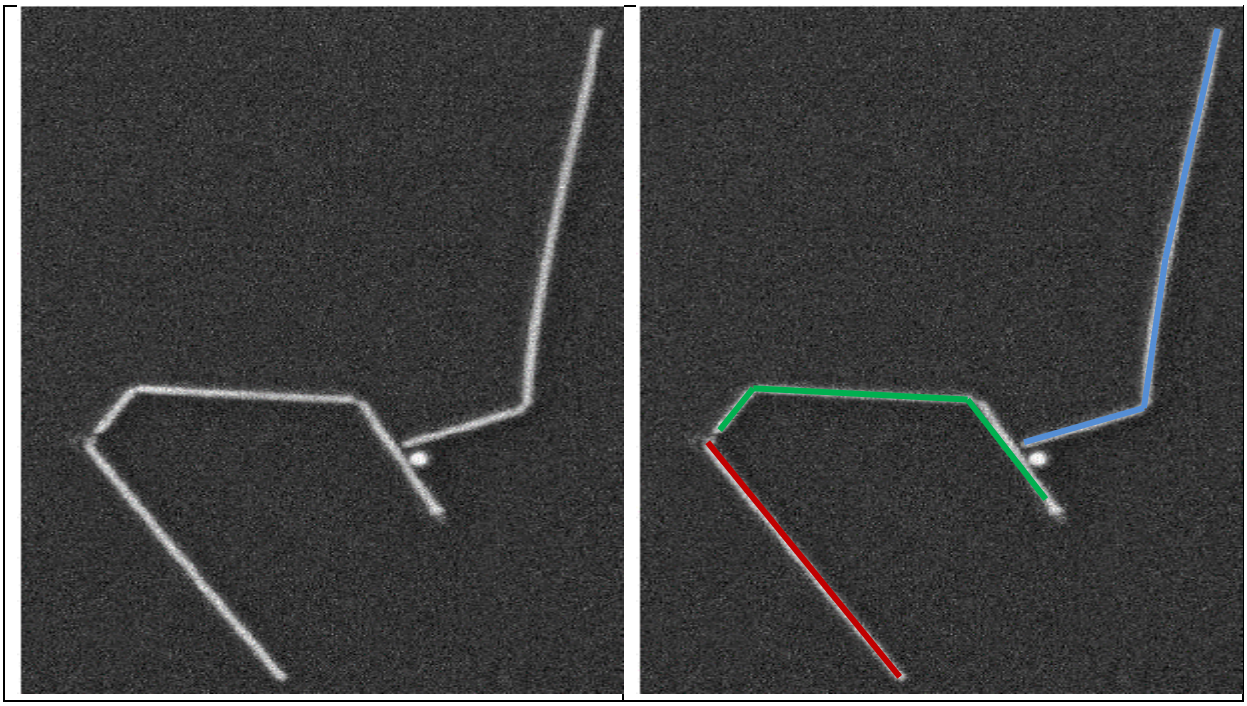

Fig. 3: How to count fibres that exhibit sharp kinks.

Fibres should be counted as one as long as no interruption between the fibres is visible. In this example we would recommend to count three fibres (marked in red, green and blue in the right image). Keep in mind that there is no right or wrong, and that the uncertainty introduced by the subjectivity of the

evaluation will be evaluated in the second step of the interlaboratory comparison, when images from one lab will be send to another lab for evaluation.

ZnO 008

The ZnO material exhibits aggregates of many fibres. The fibres are straight and for many fibres in an aggregate it is possible to find both ends and identify the course of the fibre. Make sure that you mark the fibres that you already counted!

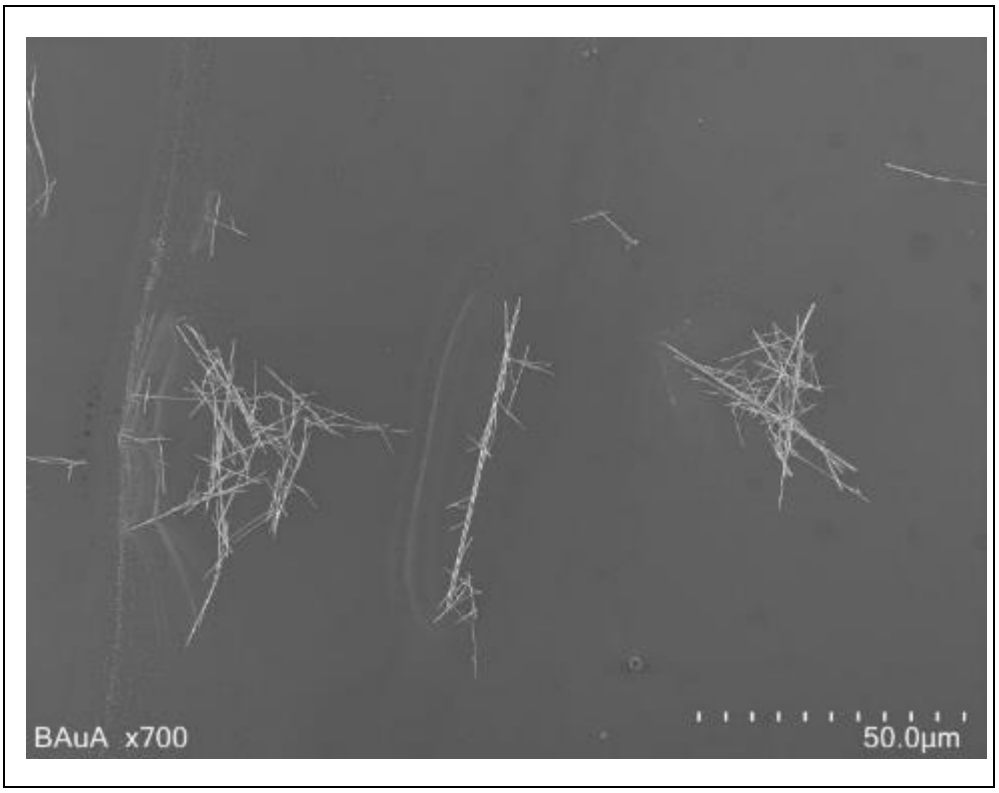

SiC 009

The SiC material is very inhomogeneous. Very thin and very thick fibres occur as well as fibres with a substructure varying in diameter along their course. Also, some very long fibres are incurred in this sample. It is possible that with some instruments it is difficult to image the whole length of the fibres while fulfilling the condition of imaging the diameter with 4 pixels. In those cases a separate measurement of length and diameter distributions might be necessary as described in the test guideline.

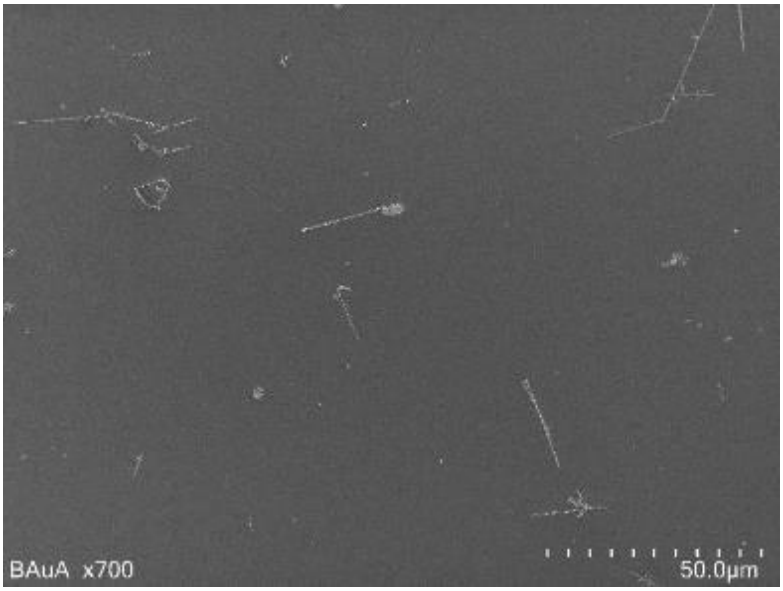

Multi walled carbon nanotube (MWCNT) 013

Please note that the MWCNT sample was prepared on gold coated polycarbonate filters with pores of about 180-200 nm diameter. The sample is attached to a REM holder with copper band. It needs to be carefully removed and attached to another REM holder before imaging. In case the filter does not detach from the copper band by gently tearing on the filter using tweezers, you can use scissors to cut the sample from the copper band.

In the evaluation of the length and diameters of fibres of the MWCNT material please exclude fibres that end inside a filter pore and which ends are thus not visible. If a fibre is branched, please measure the longest continuous path as the length of the fibre. Please note that some fibres exhibit weak contrast and neat image evaluation at high zoom levels are required to identify all fibres.

For MWCNT samples you don't need to measure fibres extending over the edge of the image.

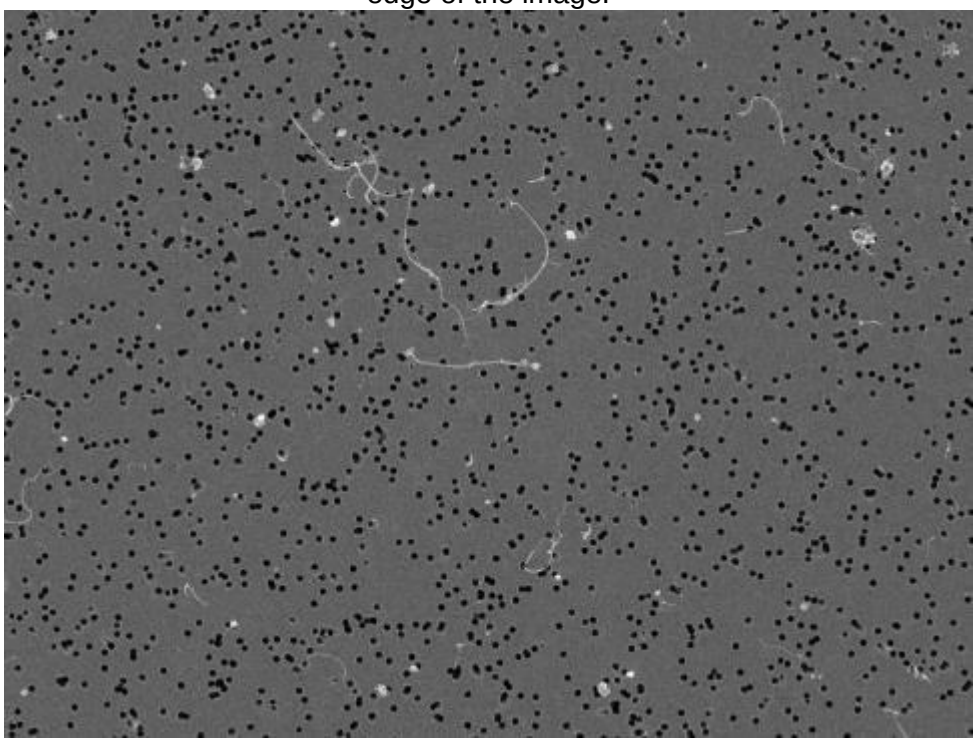

- **Special cases for MWCNT fibres:**

What to do with fibres that end in a filter pore?

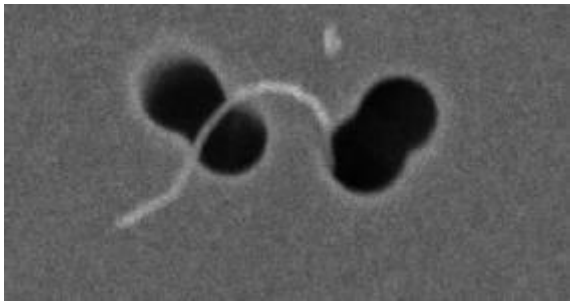

Fibre ends in a hole. Don't measure it.

- **What if a fibre ends in a particle?**

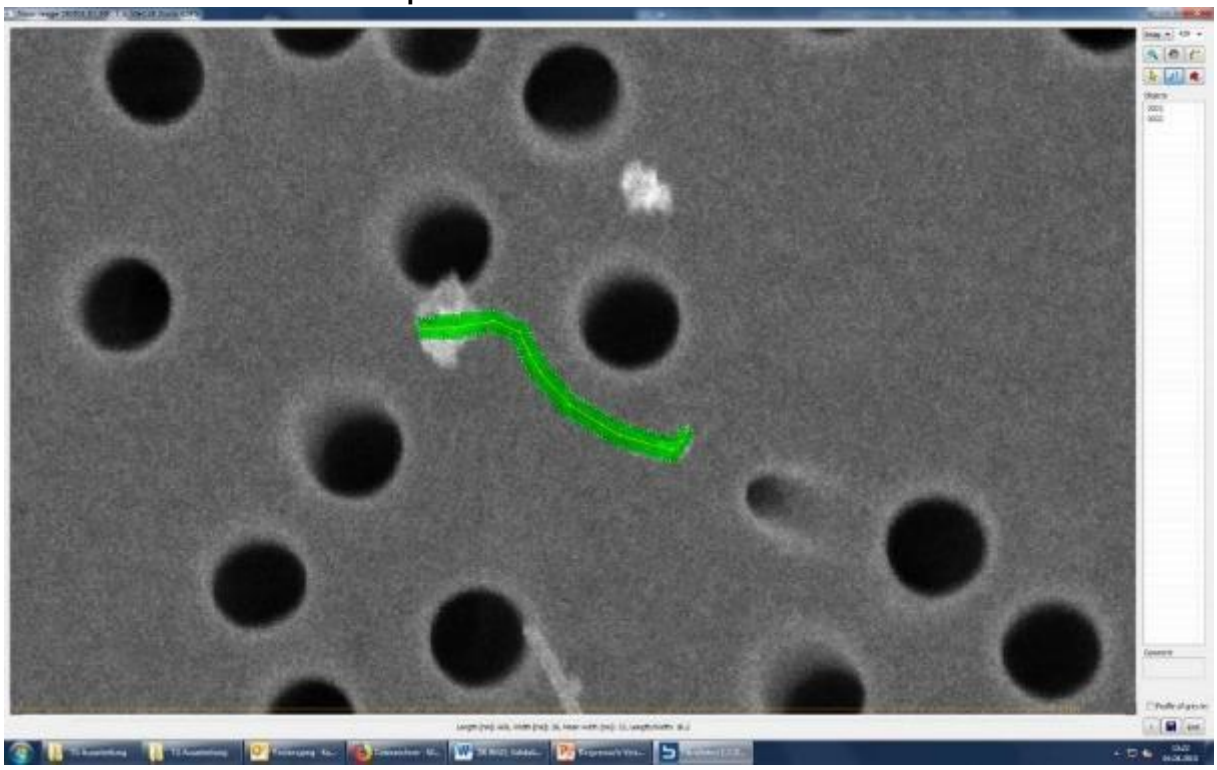

Fibre ends in a particle. Measure the longest length, unless it is clearly visible where the particle starts and where the fibre ends.

- **Fibre goes through a particle:**

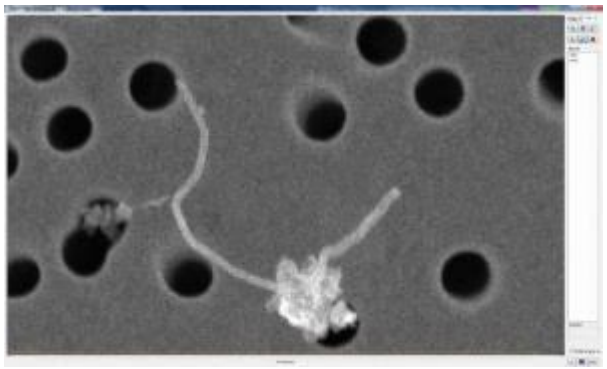

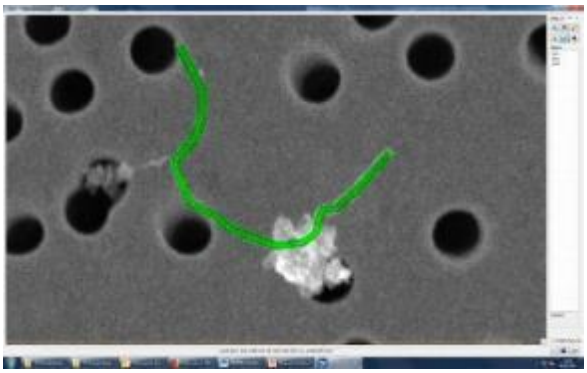

Although you cannot really see the exact course of the particle, it is okay to estimate the course through/behind the particle and measure the fibre.

- **How to deal with fibre agglomerates:**

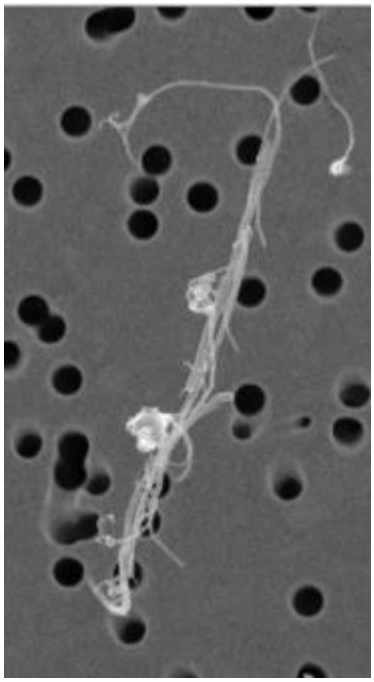

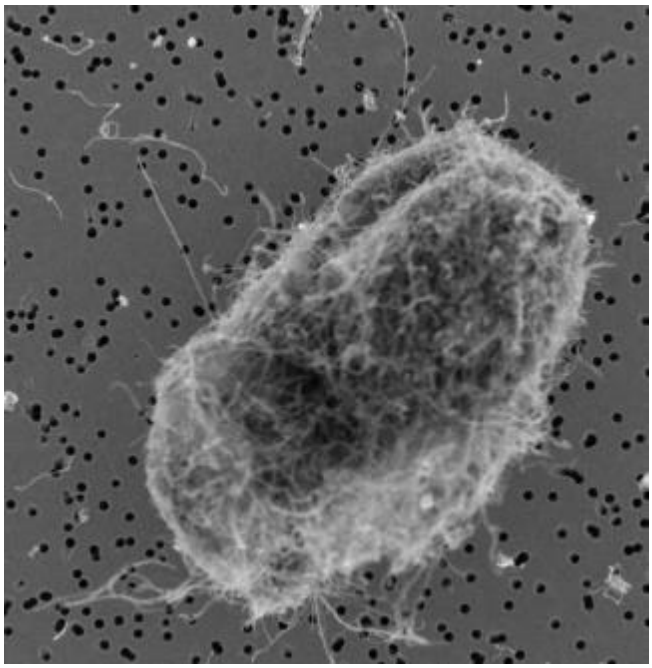

In the cases presented in the table it is not clear which fibre takes which route and which fibre ends belong together. Therefore, these aggregates have to be excluded from analysis. These images are examples of agglomerates with non-evaluable fibres. Thus, the corresponding image is to be counted as an image containing non-evaluable agglomerates.

Another example:

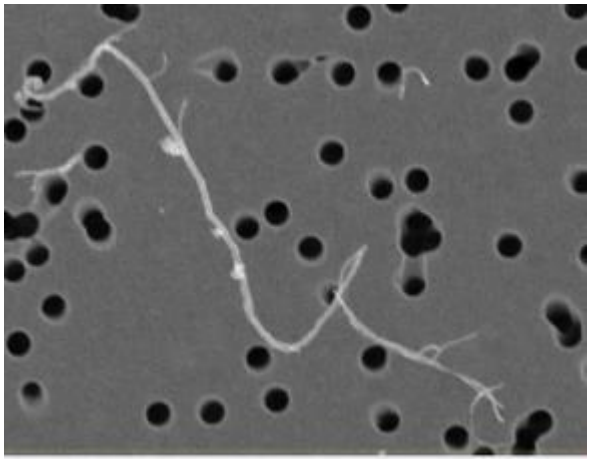

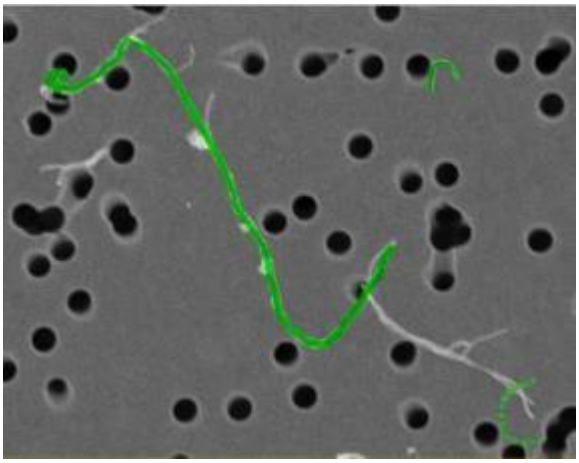

In this fibrous agglomerate several fibres can be traced individually. All others have to be ignored.

- **How to deal with clearly 3 dimensional objects (e.g. spiral like)?**

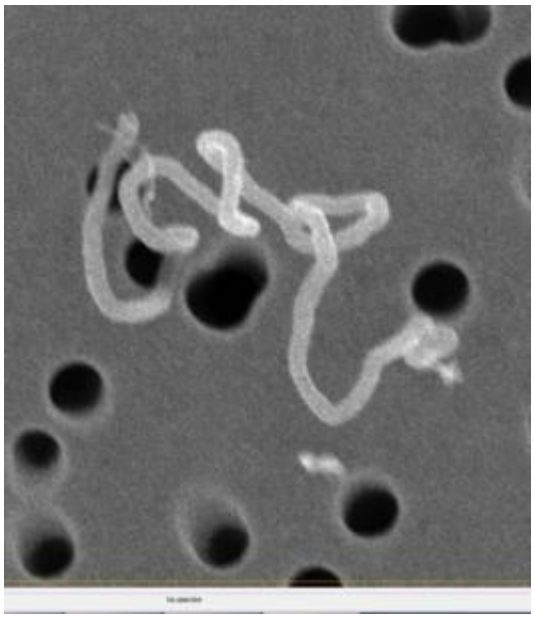

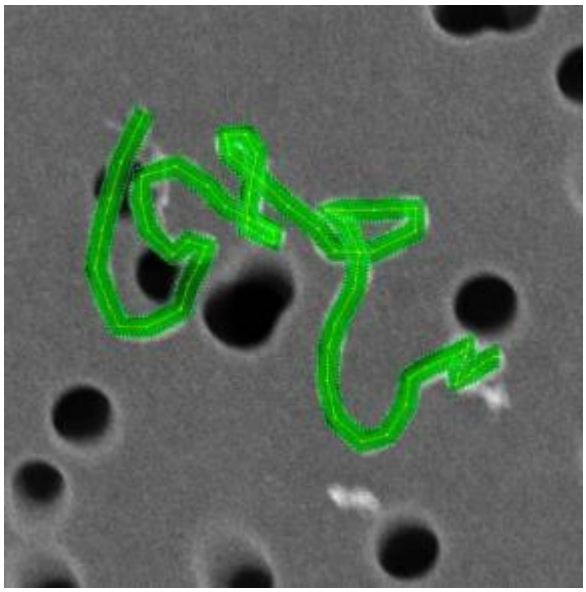

Track the course as neatly as possible. The measurement of the length will be shorter than the object is, because of lack of 3D information. But we cannot avoid this.

Second example:

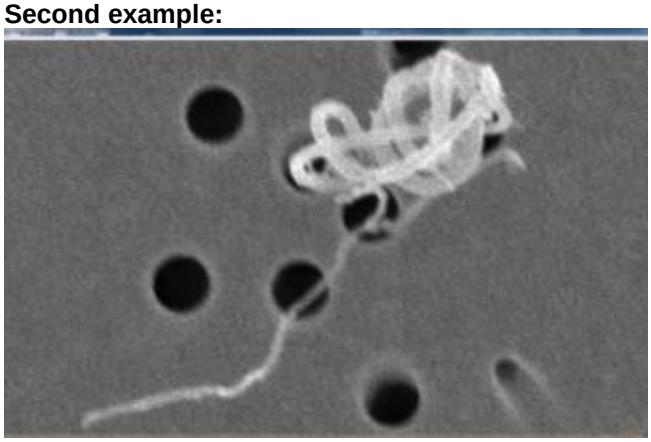

The course of this spiral like object cannot be tracked. This fibre has to be excluded from analysis. You might find that the lower fibre is a separate object and you can trace it from end to end. Then you can mark and measure it.

FAQ answered in the telephone conferences:

How are the different classes of sample preparation defined?

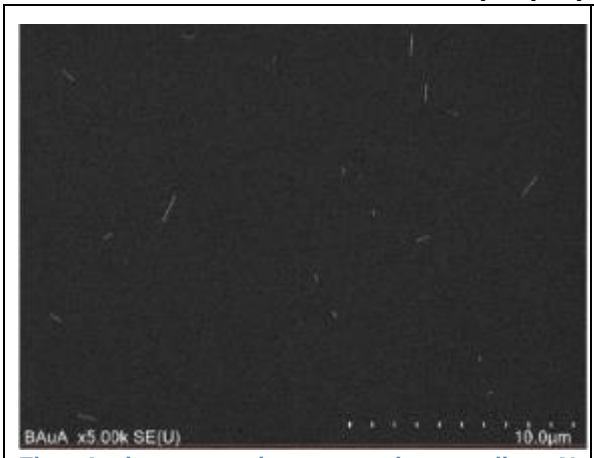

Fig. 4: best sample preparation quality; No intercrossings, almost no impurities-> automated evaluation possible

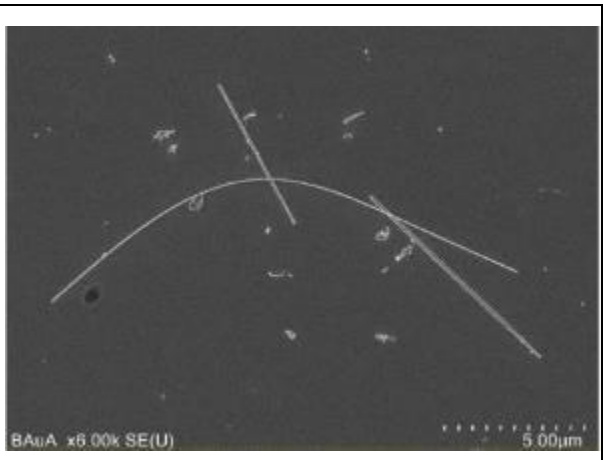

Fig. 5: acceptable sample preparation quality, some intercrossings, some impurities, agglomerates.-> visual evaluation possible

Fig. 6: acceptable sample preparation, although heavily aggregated, it is possible to evaluate the course of most of the fibres and measure their diameter and length.

Fig. 7: Fair sample quality: aspect ratio too large for pairwise length and diameter determination at one magnification

How to choose the appropriate resolution?

- Estimate the prominent width of the fibres, from an overview picture.
- Measure this width (several times at different fibres to get a good estimate)
- The pixel size for imaging should be ≤ 1/4th of that width!

How to evaluate the images?

- Two-step procedure recommended:
  1. Image acquisition
  2. Image evaluation using an image evaluation software (e.g. ImageJ, GIMP, FibreDetect (available from BAuA),…)

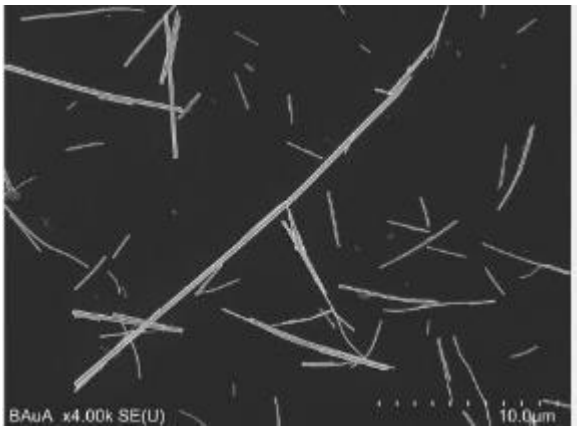

Fig. 8: aquired image, not yet evaluated.

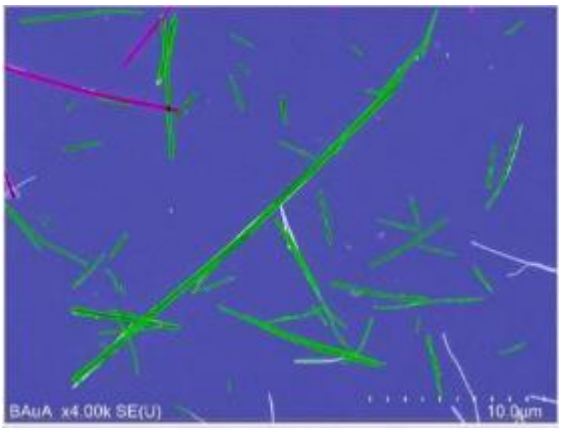

Fig. 9: evaluated fibres are marked in green. Partial fibres at upper and left side of the image are marked in pink.

All fibres, of which both ends and the course are visible, are to be measured.

- Please zoom in until you can see the individual pixels when measuring the fibre width – otherwise the subjective error will be large and the result of the width will depend on the zoom you used.
- The length of the fibre is evaluated by tracing the course of the central line of the image of the fibre and determining its length.
- Mark the fibre that you already measured, to avoid double measurement or ignorance of measureable fibres.
- Measure the diameter at least at three positions of the fibres and take the mean value as final diameter. (Using the software FibreDetect, the diameter will be evaluated at each position along the fibre and the mean value is calculated.)
- Make sure that the length and diameter of each fibre is saved as a pair of values!
- At the end of each image evaluation: Write down whether the image contained non-evaluable aggregates/agglomerates.
- Tip: count all fibres that do not cross an edge of an image first. Then count the fibres crossing at two sides of the image. The partial fibres have to be marked. Please count 200 fibres that do not cross an edge.
- Fibres longer than 20 µm can be counted as 20 µm long.
- Fibres longer than 20 µm that cross the side of an image do not need to be marked as partial

Why to count 200 fibres?

- The bootstrap error of the median stabilizes at N=200.

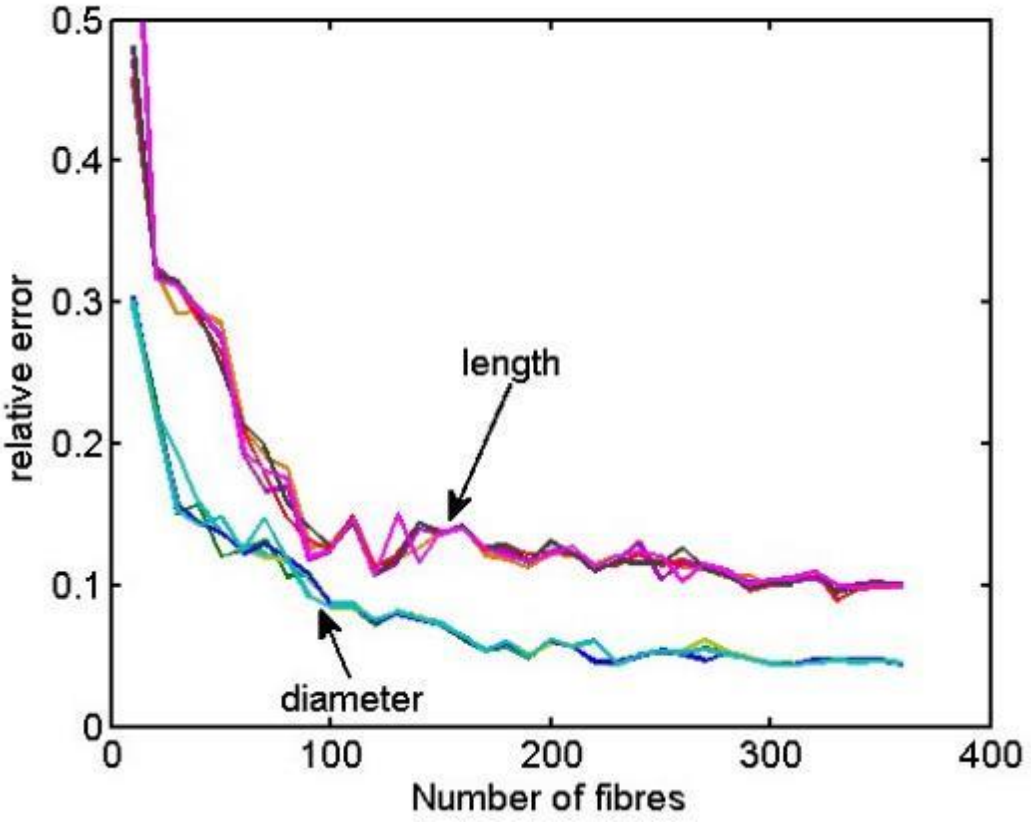

Fig. 10: bootstrap error of a length and diameter distribution as a function of measured fibres.

How to report results?

– The results should be reported as a table containing for each fibre the values of diameter and length as well as a comment in case the fibre crosses the upper or left edge of the image. An example of a reporting sheet and how this list might look like is given in the Reporting file: “Reporting_sheet_fibers_excel.xlsx”.

Annex C. Inter-laboratory validation plan of the test guideline on particle size and size distribution of manufactured nanomaterials – Particles

Distribution:

The samples are distributed as powder (ZnO, TiO_2) and particle dispersion (Ag, PSL, SiO_2) in original vials. The protocol for preparation of dispersions from the powder is given in this document. To eliminate influences from sample preparation the samples for SEM, TEM and AFM are sent out prepared on TEM-grid (carbon film on copper grid) or silicon wafer.

Characterization data:

NM 110: http://publications.jrc.ec.europa.eu/repository/handle/JRC64075

Safety indications:

In general, when handling nanomaterial protective clothing and gloves have to be worn. All samples have to be handled with care. Further information on handling the material are to be taken from the materials safety sheets. The safe handling of the used instruments is described by the manufacturer.

Introduction

The present document aims at providing assistance to the independent laboratories participating in the round robin test to validate the applicability of the experimental routines currently included in the draft OECD test guideline to determine the particle size and size distributions of particles and fibres. The validity of the test guideline is evaluated in separate round robin tests for particles and fibres, respectively.

Scope of the round robin test

To determine the particle size distribution of a material, many different methods are available. Based on ENV/JM/MONO(2016)7 we have chosen nine methods that have a large range of applicability, a high availability or are common to use to determine a particle size distribution. Each method is applicable to a certain range of materials. In this round robin we intend to test the validity of the methods and comparability of the measurement results by using a broad range of materials (c.f. rationale for the choice of particle test materials).

Materials, reagents and analysis

The materials are distributed as powders, dispersion or readily prepared, depending on the material and used method. In order to minimize errors due to sample preparation, the sample preparation protocols for all materials and methods are given.

All materials, reagents and instruments that are necessary to prepare the sample are listed in the experimental procedures. Materials and reagent needed to perform the measurements are listed in the test guideline.

Rationale for the choice of particle test materials in the round robin

The materials are chosen to cover a broad range of sizes within the range of validity of the test guideline of 1-1000 nm. The materials contain ideal spherical particles as well as more irregularly shaped real-world materials. The physico-chemical properties of the materials vary in a wider range (density, scattering, atomic number, refractive index). Thus, not all materials can be measured with every method. A matrix of which material is measured with which method in this interlaboratory comparison is given in the table below.

Method	Ag 17 nm	SiO_2 20 nm	SiO_2 50 nm	ZnO ~100 nm	PSL Mix 90/125 nm	TiO_2 ~250 nm	PSL Mix 80/800 nm
DLS	X	X	X	X	X	X	
CLS	X	X*	X*	X	X	X	X
PTA	X			X	X	X	
SAXS	X	X	X		X		
sp ICP-MS						X	
AFM			X	X	X		
TEM	X	X	X	X	X	X	X
SEM	X	X		X	X	X	X
DMAS	X	X	X		X	X	X

General dispersion protocol and information about the materials

Guidance on the preparation of stock dispersions and general information about the test materials are given in the following paragraphs.

Please note that the stated time spans for sonication are given as an orientation. The actually needed time span depends on the power output of the used instrument. A SOP for the calibration of a sonication device is given here: https://doi.org/10.6028/NIST.SP.1200-2. The specific power absorbed under the described conditions is ~1.2 W/mL. If there is no possibility to calibrate the device, it is recommended to make test measurement (e.g. DLS) in between the sonication process, to test if the obtained sizes differ or not. The samples should be sonicated as long as is needed to receive a stable size. The here given sizes of a material depend on electron microscopic analysis, so note that the particles size with DLS might differ significantly (e.g. mean diameter for DLS ZnO approx. 160 nm, TiO_2 approx. 300 nm)

NM 110 ZnO

The material is distributed in powder form.

Refractive index: 2.03
Density: 5.61 g/cm^3
Preparation of stock dispersion:
Instruments:

- Probe sonicator or vial sonicator
- Analytical balance (precision 0.1 mg)
- Ultrasonic bath sonicator and/or
- Vortex-mixer

Materials and chemicals

- Glass vial in appropriate dimensions to use with probe sonicator
- 2ml plastic microcentrifuge tubes for the use of vial-sonicator
- Sodium hexametaphosphate (SHMP) CAS No. 10124-56-8, extra pure
- Water ultrahigh purity
- ZnO NM 110 (distributed)
- Pipette
- Spatula
- weighting boats/papers or similar

Dispersion procedure

- Solution of surfactant is prepared (2mg/ml): 100 mg of SHMP are weighed and put in a vial. 50 mL of Water are added. Use only after complete solution of the material and homogenize before use.
- Dispersion: 40 mg of ZnO are weighed and put in a vial. 20 ml of SHMP solution (2mg/ml) are added.
- Sonication:
    - Probe sonicator: The dispersion is placed in the probe sonicator. The probe head should be immersed to a depth of approximately 1 cm. The vial should not be touched by the probe head. Throughout the sonication process the vial is cooled with an ice water bath. The sample should be sonicated with 75% amplitude and 50% cylce for 20 minutes (Hielscher Probe sonicator UPS200S, 7 mm probe).
    - Vial sonicator: 2 ml of the dispersion (to be shaken before use) are filled in a plastic microcentrifuge vial and the closed vial is placed in the vial sonicator. The sample should be treated for 15 minutes at 75% amplitude with a cycle time of 50%.

IRMM 388 coated TiO_2

The material is distributed in powder form.

Refractive index: 2.61

Density: 4.23 g/cm^3

Preparation of stock dispersion:

Instruments:

- Probe sonicator or vial sonicator
- Analytical balance (precision 0.1 mg)
- Ultrasonic bath sonicator and/or
- Vortex-mixer

Materials and chemicals

- Glass vial in appropriate dimensions to use with probe sonicator.
- 2ml plastic microcentrifuge tubes for the use of vial-sonicator
- NaOH (0.1 M)
- Water ultrahigh purity
- TiO2 IRMM 388 (distributed)
- Pipette
- Spatula
- weighting boats/papers or similar

Dispersion procedure

- NaOH-Solution is prepared: 40 mL of Water are given in a vial and 350 µl of 0.1 M NaOH are added. Homogenize before use.
- Dispersion: 10 mg of TiO2 are weighed and put in a vial. 20 ml of NaOH solution are added. In the case of DMAS a higher concentration is needed, weight 120 mg TiO2 and add 20 ml of NaOH solution.
- Sonication:
    - Probe sonicator: The dispersion is placed in the probe sonicator. The probe head should be immersed to a depth of approximately 1 cm. The vial should not be touched by the probe head. Throughout the sonication process the vial is cooled with an ice water bath. The sample should be sonicated with 75% amplitude and 50% cylce for 20 minutes (Hielscher Probe sonicator UPS200S, 7 mm probe).
    - Vial sonicator: 2 ml of the dispersion (to be shaken before use) are filled in a plastic microcentrifuge vial and the closed vial is placed in the vial sonicator. The sample should be treated for 15 minutes at 75% amplitude with a cycle time of 50 %.

301-04-001 SiO_2 / 301-04-002 SiO_2

Dispersion of SiO_2 in DI water with a concentration of 10 mg/ml. Before use the dispersion has to be shaken.

Refractive index: 1.46

Density: 2.19 g/cm^3

Ag-NP

Dispersion of Ag in DI water with stabilizer with a concentration of 100 µg/ml. As stabilizer 4% (w/w) polyoxyethylene glycerol trioleate (TAGAT™ TO), 4% (w/w) polyoxyethylene (20) sorbitan mono-laurate (TWEEN-20™) and 7.5% (w/w) ammonium nitrate are added. Before use the dispersion has to be shaken.

Refractive index: 0.135

Density: 10.49 g/cm^3

PSL (bimodal mixtures)

Dispersion of Polystyrene in DI water with stabilizer with a concentration of 10 mg/ml. As stabilizer 0.1% sodium dodecyl sulfate (SDS) and 0.05% NaN_3 are added. Before use the dispersion has to be shaken.

Refractive index: 1.59

Density: 1.04 g/cm^3

Experimental procedures

Guidance on sample preparation for the respective methods is given in the following paragraphs.

Electron Microscopy

Materials and instruments

- Transmission electron microscope and/or
- Scanning electron microscope
- Calibration grid
- Tweezers
- Software for the evaluation of the images

For TEM the samples are prepared on a TEM grid (copper mesh with carbon film). Samples for SEM are prepared on a silicon wafer. Preparation has been done by spin-coating or by drop deposition of the material dispersion. The wafer have not been coated with a conductive material after sample deposition, but normally there shouldn´t be a problem with charging of the material. Samples are fragile - handle with care.

For the implementation of the test, data evaluation and reporting the respective paragraphs of the test guideline should be followed. Please use also the distributed excel sheet as guidance for reporting of data.

The number of counted particles depends on the width of the size distribution. In the following table the number of particles to be counted are listed:

Material	Particle number
SiO_2	>300
Ag	>700
ZnO	>700
TiO_2	>700
PSL	>700

Please determine from a particle (o):
- Minimum Feret diameter
- Maximum Feret diameter
- Area equivalent diameter

Do not count (x):
- Particles that overlap the image edge
- Particles you cannot separate clearly

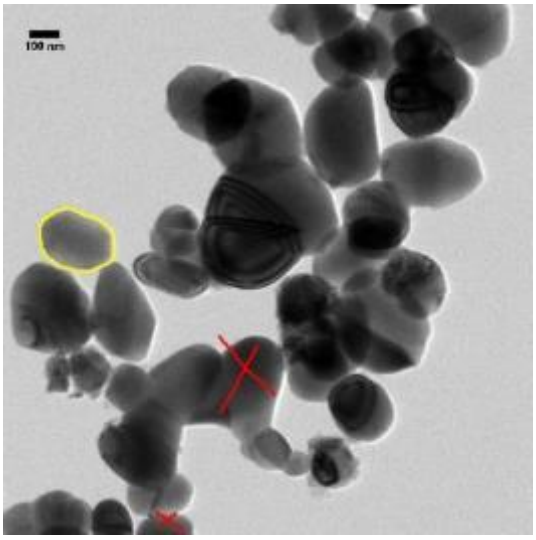

Dynamic Light Scattering

Materials and instruments

- Dynamic light scattering instrument
- Cuvette (if needed)
- Pipettes
- Water ultrahigh purity
- SHMP-solution (from dispersion procedure ZnO)
- NaOH-solution (from dispersion procedure TiO_2)

For the measurement with DLS the dispersion of the respective material should be diluted to the following concentrations.

Material	1. Concentration	2. Concentration	Diluent
SiO_2	10 mg/ml	5 mg/ml	Water
Ag	100 µg/ml	50 µg/ml	Water
ZnO	1 mg/ml	0.5 mg/ml	SHMP solution
TiO_2	0.2 mg/ml	0.1 mg/ml	NaOH solution
PSL	1 mg/ml	0.5 mg/ml	Water

After dilution to the desired concentration, the dispersion should be vortexed or shaken to ensure homogenization. For each material both concentrations are to be measured. The dispersion has to be

freshly prepared for the measurement. The particles might sedimentate or agglomerate, especially ZnO and TiO_2, if the time spans between preparation of the dispersion and measurement are too long (>30 min). For redispersion the sample can be treated in an ultrasonic bath for 10 minutes. For the implementation of the test, data evaluation and reporting the respective paragraphs of the test guideline should be followed. Please use also the distributed excel sheet as guidance for reporting of data.

Centrifugal Liquid Sedimentation

Materials and instruments

- Centrifugal liquid sedimentation instrument or analytical ultracentrifuge
- Pipettes
- Cuvette (if needed)
- Sucrose (for disc-CLS)
- Dodecane or similar capping agent
- Water ultrahigh purity
- SHMP-solution (from dispersion procedure ZnO)
- NaOH-solution (from dispersion procedure TiO_2)

Disc-CLS

For the use of disc-CLS a gradient has to be prepared. Establishment of the gradient should be done in accordance to the manufacturer recommendations. A sucrose gradient should be prepared in in accordance to the given concentration in the following dispersion. For example, for an 8-24wt% gradient with a total volume of 14.4 ml 9 subsamples of 1.6 ml sucrose solution with increasing concentrations are prepared. The subsamples are injected stepwise in the rotating disc starting with the highest concentration. Then 0.5 ml of dodecane are injected as capping agent. After preparation of the gradient 30 minutes should be waited to let the gradient stabilize before starting the measurement.

For the measurement the use of 22000 rpm is suggested. Lower rpm will result in longer measurement times. If the instrument only supports lower rpm than 22000, use the highest possible. For the measurement with CLS the dispersion of the respective material should be diluted to the following concentrations.

Material	1. Concentration	2. Concentration	Diluent	Gradient
SiO_2	10 mg/ml	5 mg/ml	Water	0-8wt%
Ag	100 µg/ml	50 µg/ml	Water	8-24wt%
ZnO	2 mg/ml	1 mg/ml	SHMP-solution	8-24wt%
TiO_2	0.2 mg/ml	0.1 mg/ml	NaOH-solution	8-24wt%
PSL	5 mg/ml	2 mg/ml	Water	8-24wt% (with 0.1wt% SDS)

After dilution to the desired concentration the dispersion should be vortexed or shaken to ensure homogenization. For each material both concentrations are to be measured. The dispersion has to be freshly prepared for the measurement. The particles might sedimentate or agglomerate, especially ZnO and TiO_2, if the time spans between preparation of dispersion and measurement are too long (>30 min).

For redispersion the samples can be treated in an ultrasonic bath for 10 minutes. For the implementation of the test, data evaluation and reporting the respective paragraphs of the test guideline should be followed. Please use also the distributed excel sheet as guidance for reporting of data.

Cuvette-CLS /Analytical Ultracentrifuge

For the measurement with CLS/AUC the dispersion of the respective material should be diluted to the following concentrations. The following measurement conditions are recommended for measurement with a fixed speed: 4000 rpm, 25 °C, measurement intervals: 10x 1s, 30x 3s, 120x 5s, 60x 10s, 60x 50s, 60x 150s, 100x 300s

For measurement with ramped speed option it is recommended to follow the here given protocol: https: https://doi.org/10.1016/j.impact.2017.12.005

Material	1. Concentration	2. Concentration	Diluent
SiO2	10 mg/ml	5 mg/ml	Water
Ag	100 µg/ml	50 µg/ml	Water
ZnO	2 mg/ml	1 mg/ml	SHMP solution
TiO2	0.2 mg/ml	0.1 mg/ml	NaOH solution
PSL	2 mg/ml	1 mg/ml	Water

After dilution to the desired concentration the dispersion should be vortexed or shaken to ensure homogenization. For each material both concentrations are to be measured. The dispersion has to be freshly prepared for the measurement. The particles might sedimentate or agglomerate, especially ZnO and TiO_2, if the time spans between preparation of dispersion and measurement are too long (>30 min). For redispersion the samples can be treated in an ultrasonic bath for 10 minutes. For the implementation of the test, data evaluation and reporting the respective paragraphs of the test guideline should be followed. Please use also the distributed excel sheet as guidance for reporting of data.

Differential Mobility Analysis System

Materials and instruments

- Differential mobility analysis system
- Electrospray aerosol generator and/or
- Atomizer with dryer
- Pipettes
- Water ultrahigh purity (bidest water)
- Buffer solution (NH_4Ac/NH_3-buffer pH 8) (electrospray)
- NaOH-solution (from dispersion procedure TiO_2)

For the measurement with DMAS the dispersion of the respective material needs to be aerosolized. For this purpose, an electrospray aerosol generator or an atomizer can be used. The therefore needed concentration of the dispersion depends on the from the aerosol generator generated droplet size. The droplet size varies between the generation methods and the used instrument. The following listed concentration are only suggestions based on own measurements and need to be adjusted to the used

instrument. Typical electrospray aerosol generators have an upper limit below 100 nm. For this reason, the suggestions are only given for applicable materials.

Material	1. Concentration Electrospray	2. Concentration Electrospray	Diluent	1. Concentration Atomizer	2. Concentration Atomizer	Diluent
SiO_2	1 mg/ml	0.5 mg/ml	Buffer	0.1 mg/ml	0.05 mg/ml	Water
Ag	100 µg/ml	50 µg/ml	Buffer			
TiO_2				6 mg/ml	3 mg/ml	NaOH solution
PSL				0.1 mg/ml	0.05 mg/ml	Water

It is recommended to use a NH_4Ac/NH_3-buffer (pH 8) as diluent for the use of the electrospray aerosol generator. The buffer solution should be prepared as followed:

- Dissolve 0.77 g of NH_4Ac in 500 mL ultrapure water
- Add approximately 0.75 mL of 1 M NH_3 aqueous solution to reach pH 8. The pH should be measured while adding the NH_3.

After dilution to the desired concentration the dispersion should be vortexed or shaken to ensure homogenization. For each material both concentrations are to be measured. The dispersion has to be freshly prepared for the measurement. The particles might sedimentate or agglomerate, especially TiO_2, if the time spans between preparation of dispersion and measurement are too long (>30 min). For redispersion the samples can be treated in an ultrasonic bath for 10 minutes. For the implementation of the test, data evaluation (paragraph 81) – 100)) and reporting (paragraph 183)) the respective paragraphs of the test guideline should be followed. Please use also the distributed excel sheet as guidance for reporting of data.

Particle Tracking Analysis

Materials and instruments

- Particle tracking analysis system
- Pipettes
- Water ultrahigh purity
- SHMP-solution (from dispersion procedure ZnO)
- NaOH-solution (from dispersion procedure TiO2)

For the measurement with PTA the dispersion of the respective material should be diluted to a concentrations of 10^6 to 10^9 particles/ml. After dilution to the desired concentration the dispersion should be vortexed or shaken to ensure homogenization. For each material both concentrations are to be measured. The dispersion has to be freshly prepared for the measurement. The particles might sedimentate or agglomerate, especially ZnO and TiO_2, if the time spans between preparation of dispersion and measurement are too long (>30 min). For redispersion the samples can be treated in an ultrasonic bath for 10 minutes. For the implementation of the test, data evaluation and reporting the respective paragraphs of the test guideline should be followed. Please use also the distributed excel sheet as guidance for reporting of data.

Small Angle X-ray Scattering

Materials and instruments

- Small angle X-ray scattering instrument
- Pipettes
- Water ultrahigh purity

For the measurement with SAXS the dispersion of the respective material should be diluted to the following concentrations.

Material	1. Concentration	2. Concentration	Diluent
SiO_2	10 mg/ml	5 mg/ml	Water
Ag	100 µg/ml	50 µg/ml	Water
PSL	1 mg/ml	0.5 mg/ml	Water

After dilution to the desired concentration the dispersion should be vortexed or shaken to ensure homogenization. For each material both concentrations are to be measured. The dispersion has to be freshly prepared for the measurement. The particles might sedimentate or agglomerate if the time spans between preparation of dispersion and measurement are too long (>30 min). For redispersion the samples can be treated in an ultrasonic bath for 10 minutes. For the implementation of the test, data evaluation and reporting the respective paragraphs of the test guideline should be followed. Please use also the distributed excel sheet as guidance for reporting of data.

Single particle Inductively Coupled Plasma – Mass Spectrometry

Materials and instruments

- Single particle ICP-MS instrument
- Pipettes

– Au-NP (60 nm) or other suitable standard of known size

– Ionic standard of titanium

– Water ultrahigh purity

– Dispersion of TiO2

– NaOH-solution (from dispersion procedure TiO2)

– Nitric acid solution (3%)

For the determination of linearity response different dilutions of the ionic standard are prepared. Dilute the ionic standard to concentrations of 0, 0.5, 1, 2, 5, 10 and 20 µg Ti/L.

The dispersion of TiO_2 should be diluted to concentration of 100 and 500 ng/L. It is recommended to stepwise dilute the stock dispersion to the desired concentration and vortex or shake the in between received dilutions. Both concentrations are to be measured. After dilution to the desired concentration the dispersion should be vortexed or shaken to ensure homogenization. For each material both concentrations are to be measured. The dispersion has to be freshly prepared for the measurement. The particles might sedimentate or agglomerate if the time span between preparation of dispersion and measurement are too long (>30 min). For redispersion the samples can be treated in an ultrasonic bath for 10 minutes. For the implementation of the test, data evaluation and reporting the respective

paragraphs of the test guideline should be followed. Please use also the distributed excel sheet as guidance for reporting of data.

Atomic Force Microscopy

Materials and instruments

- Atomic force microscope (Tip <10 nm)
- Tweezers
- Software for the evaluation of the images

Samples for AFM are prepared on a silicon wafer. Samples are fragile - handle with care. For the implementation of the test, data evaluation and reporting the respective paragraphs of the test guideline should be followed. Please use also the distributed excel sheet as guidance for reporting of data.

The number of counted particles depends on the width of the size distribution. In the following table the number of particles to be counted and the recommended pixel size are listed:

Material	Particle number	Pixel size
SiO_2	>300	3
ZnO	>700	4
PSL	>700	5

Evaluation and representation of obtained results, test report

The evaluation of the test results is described in the section “Data evaluation and error calculation”.

The evaluation of the test results is described in the section “test report” in the test guideline. The items specific for each method have to be considered and included in the respective test report. The specific paragraphs for each method are given in the experimental procedures. A full uncertainty calculation of the measurement in accordance ISO principles (Guide to the Expression of Uncertainty in Measurement, ISO, Geneva, 1993, ISBN 92-67-10188-9) should be done and reported.

As guidance an excel sheet will be provided for the reporting of data.

For the upload of data, a BSCW server is installed, where every institute has access to an own folder in the respective section. You should have got an invitation to bscw.bund.de server. If not, please contact us.

You can create your own folder for each sample and upload the data there. Please use the sample name as folder denomination.

Validation of the results from the participating laboratories

The reported particle size distributions and the mean, median and modal values of the particle size for each material are compared between the laboratories. The goal of the test guideline is a comparability between different methods. This implies a comparability between different laboratories for the results of the same methods. In addition to the overall results, also the limits of the test guideline are evaluated. The limits of validity will be determined by the results of the round robin test.

Different contributions to the uncertainty are a further subject of evaluation. Depending on the results of the round robin test the typical uncertainty contributions will be mentioned in the TG and thus contribute to the total error of a method.